DEVELOPMENT OF NEW ANTI-BIOADHESIVE SURFACES FOR SPECIFIC NEURODEGENERATIVE AGENTS

Tjaša Vrlinič

Doctoral Dissertation
Jožef Stefan International Postgraduate School and Université du Maine, France
Ljubljana, Slovenia, July 2011

Evaluation Board:

Ass. Prof. Uroš Cvelbar, Chairman, Institut "Jožef Stefan", Jamova 39, Ljubljana, Slovenia

Ass. Prof. Janez Kovač, Member, Institut "Jožef Stefan", Jamova 39, Ljubljana, Slovenia

Dr. Karin Anselme, Member, Institut de Chimie des Surfaces et Interfaces, CNRS,
15 r Jean Starcky, 68057 Mulhouse, France

MEDNARODNA PODIPLOMSKA ŠOLA JOŽEFA STEFANA
JOŽEF STEFAN INTERNATIONAL POSTGRADUATE SCHOOL

Tjaša Vrlinič

DEVELOPMENT OF NEW ANTI-BIOADHESIVE SURFACES FOR SPECIFIC NEURODEGENERATIVE AGENTS

Doctoral Dissertation

PRIPRAVA NOVIH NEADHEZIVNIH MATERIALOV ZA POTREBE SPECIFIČNIH RAZISKAV S PODROČJA NEURODEGENERATIVNIH BOLEZNI

Doktorska disertacija

Supervisor: Prof. Dr. Miran Mozetič and Dr. Fabienne Poncin- Epaillard

Ljubljana, Slovenia, October 2011

Index

Abstract

The research work presented in this thesis considers the development of new biocompatible surfaces that are able to control the adhesion of specific proteins responsible for the development of neurodegenerative diseases such as Creutzfeldt–Jakob, Alzheimer, Parkinson and Lewis body disease. Our approach was focused on problems prior to the detection step, which were never considered before, particularly on the improvement of Eppendorf tubes that are used for the storage of body fluids like cerebrospinal fluid and blood. Namely these tubes made of polypropylene induce high depletion of biological material, in some cases even over 70%, resulting in a low concentration of these biomarkers for the further immunoenzymatic detection.

With the purpose to reduce the adhesion, two courses of treatments were anticipated. The first one consists of surface modification by highly reactive fluorine plasma treatment and the second one incorporates development of new hydrophilic surfaces by coupling two techniques: plasma activation and subsequent grafting of polymer-surfactant complexes. With the latter approach, an original way of surface modification has been attained that permits controlled configuration of nanostructured surfaces. All steps of surface modifications were well characterized by different physicochemical methods. The surface hydrophilic/hydrophobic character was determined by measurements of polar and apolar surface energy, surface charge by magnitude of zeta potential, surface chemistry was evaluated by x-ray photoelectron spectroscopy (XPS), while the surface roughness and topography were monitored by atomic force microscopy (AFM). The interactions between functional groups of treated supports and proteins were interpreted referring to different models of adhesion established for a range of pH values close to the classical biological protocols.

Finally, in order to validate the non-adhesive properties of newly developed Eppendorf tubes, immunoenzymatic analyses were carried out in hospital centres of partners that were participating to the project STREP NEUROSCREEN n° LSHB-CT-2006-03 7719 (Centre de Recherche sur les Protéines Prion; Liege (ULG), Hospices Civils de Lyon (CHUL) and Lancaster University (L-UNI)).

In-vitro analyses have shown that these tubes lead to a decrease of antigen adsorption up to 100%. Obtained results are contributing importantly to the neurodegenerative protein standardisation, sampling, storage and more importantly to ambitious plans in early detection of neurodegenerative diseases.

Povzetek

V predstavljenem raziskovalnem delu obravnavamo razvoj novih biokompatibilnih površin s katerimi lahko omejimo adhezijo snovi, ki povzročajo razvoj nevrodegenerativnih bolezni kot so Creutzfeldt-Jakobova, Alzheimerjeva, Parkinsonova in Lewisova bolezen. Predvsem smo se posvetili izboljšavi ravnanja z vzorci pred detekcijo, posebej izboljšavi epruvet tipa Eppendorf, ki jih uporabljamo za sharanjevanje telesnih tekočin, na primer cerebrospinalne tekočine in krvi. Na stene teh epruvet, izdelanih iz polipropilena, se oprime znatna količina genetskega materiala, ki včasih doseže tudi 70 % razpoložljive snovi. To povzroči močno znižanje koncentracije patogenov pri sledeči imunoencimatski detekciji.

Da bi zmanjšali adhezijo nevrodegenerativnih proteinov na površino materialov, smo razvili dve metodi modifikacije teh površin. Pri prvi površino obdelamo z visoko reaktivno fluorovo plazmo, pri drugi pa tvorimo novo hidrofilno površino s pomočjo aktivacije osnovne površine s plazmo, ki ji sledi nanos polimernih materialov. Pri drugem pristopu smo razvili nov način modifikacije površine z uporabo kompleksnih raztopin polimerov in površinsko aktivnih snovi. Tako smo omogočili kontrolirano konfiguracijo nanostrukturiranih površin. Vse stopnje modifikacij smo karakterizirali z različnimi fizikalno-kemijskimi metodami. Hidrofilnost oziroma hidrofobnost površin smo določili z merjenjem polarne in nepolarne površinske energije, površinski naboj pa z merjenjem zeta potenciala. Kemijske lastnosti površin smo opazovali z rentgensko fotoelektronsko spektroskopijo, hrapavost in topografijo površin pa z mikroskopom na atomsko silo. Interakcije med funkcionalnimi skupinami modificiranih materialov s patogenimi agenti smo obravnavali glede na različne modele ahezije, pri pH vrednostih ki odgovarjajo klasičnim biološkim protokolom.

Nazadnje smo z imunoencimatskimi analizami dokazali, da novo razvite površine epruvet Eppendorf zmanjšajo, včasih tudi preprečijo, adhezijo nevrodegenerativnih povzročiteljev. Analize so opravili v bolnišničnih centrih partnerjev pri projektu STREP NEUROSREEN n° LSHB-CT-2006-03 7719 (Centre de Recherche sur les Protéines Prion; Liege (ULG), Hospices Civils de Lyon (CHUL) and Lancaster University (L-UNI)).

In-vitro analize so pokazale, da se je po primerni obdelavi površin adsorpcija antigenov zmanjšala tudi do 100 %. Pridobljeni rezultati pomembno prispevajo k boljši standardizaciji ter shranjevanju proteinov, in s tem povezanim ambicijoznimi plani za zgodnjo detekcijo nevrodegenerativnih bolezni.

Abbreviations

α-syn	=	alpha synuclein
AA	=	amino acid
Aβ-42	=	beta-amyloid-42 peptide
AFM	=	atomic force microscopy
CSF	=	cerebrospinal fluid
ATPR	=	atom transfer radical polymerization
BSA	=	bovine serum albumin
CAC	=	critical aggregation concentration
CHAPS	=	(3-[(3-Cholamidopropyl)dimethylammonio]-1-propanesulfonate)
CMC	=	critical micelle concentration
CTAB	=	cetyl trimethylammonium bromide
CVD	=	chemical vapor deposition
CytC	=	cytochrome c
DC	=	direct current
DNA	=	deoxyribonucleic acid
DODAB	=	dioctadecyldimethylammonium bromide
ECM	=	extracellular matrix
ELISA	=	enzyme-linked immunosorbent assay
HA	=	hydroxylapatite
HDPE	=	high density polyethylene
LCST	=	lower critical solution temperature
LS	=	light scattering
Lyz	=	lysozyme
MIX I	=	poly(N-isopropylacrylamide) + cetyl trimethylammonium bromide
MIX II	=	poly(N-isopropylacrylamide) + polyoxyethylene (20) sorbitan monolaurate
MW	=	microwave
NMP	=	nitroxide mediated polymerization
NVP	=	N-vinyl pyrrolidone
OES	=	optical emission spectroscopy
PA	=	polyamide

PAAc	=	poly(acrylic acid)
PAAm	=	polyacrylamide
PBS	=	phosphate buffered saline
PE	=	polyethylene
PEEK	=	polyether ether ketone
PEG	=	polyethylene glycol
PEI	=	polyethyleneimine
PEO	=	polyethylene oxide
PEPVD	=	plasma-enhanced chemical vapor deposition
PET	=	poly(ethylene terephthalate)
PFOS	=	perfluorooctanesulfonate
PHEMA	=	poly(2-hydroxyethyl methacrylate)
PLGA	=	poly(lactic-co-glycolic acid)
PMMA	=	poly(methacrylic acid)
PMOXA	=	poly(2- methyl-2-oxazoline)
PNIPAM	=	poly(N-isopropylacrylamide)
POEGMA	=	poly(oligoethylene glycol) methacrylate
PP	=	polypropylene
PrPc	=	cellular prion protein
$PrPrec_{hum}$	=	recombinant human prion protein
PrPsc	=	scrapie prion protein
PS	=	polystyrene
PTFE	=	polytetrafluoroethylene
PVC	=	polyvinyl chloride
PVD	=	physical vapor deposition
QCM	=	quartz crystal microbalance
RAFT	=	reversible addition−fragmentation chain transfer polymerization
RF	=	radio frequency
RNA	=	ribonucleic acid
SAM	=	self assembled monolayer
SANS	=	small-angle neutron scattering
SDS	=	sodium dodecyl sulfate
SPR	=	surface plasmon resonance
ssDNA	=	single-stranded DNA molecule
TauPHF	=	hyperphosphorylated tau protein
Taurec	=	recombinant tau protein
Tween 20®	=	polyoxyethylene (20) sorbitan monolaurate
XPS	=	x-ray photoelectron spectroscopy

1 Introduction

Nowadays, neurodegenerative diseases like Creutzfeld Jacob, Alzheimer, Parkinson and Lewis body disease touch a large number of elderly population. These diseases develop as a result of progressive loss of structure and function of neurons, by formation of insoluble protein aggregates that appear in the patient's brain [1]. An enormous research is devoted to their early detection and potential curing [2, 3]. Even though, the clinic symptoms allow their identification, only *post-mortem* analyses give a certain diagnostic so far. The clinical signs appear at very late stage of the disease, where it is already impossible to efficiently inhibit their progress.

The presence of these diseases is monitored by the concentration of biomarkers, specific to each disease [4]. They can be found in different body fluids like blood and cerebrospinal fluid (CSF). Actually, in early stages of the disease, the concentration of pathogenic agents is too low to be detected by standard immunoenzymatic methods used for their identification. The attempts for early stage diagnostic of these agents were made as well with different physiochemical methods. For example, an optical test with interior laser ophthalmoscope was developed, which seems to be able to detect a presence of amyloid beta proteins that are found in all Alzheimer's patients in the lens of the eye [5]. As well new brain-imaging methods were developed in which the radioactive dye is injected in the blood system and travels to the brain, where it attaches to the amyloid plaques [6].

On the other hand, the efficiency of immunoenzymatic detection can be improved through different ways as well. A very promising method of detection was developed [7], where the system based on enzymatic test was replaced by the DNA marker, which allowed an amplification of the signal by real time polymerase chain reaction (RT-PCR). The efficiency of ELISA test itself can be improved by development of antibodies with better recognition of infectious agents, they can be concentrated with a help of nano-beads and with improved attachment of detection antibodies (homogeneity, orientation) on the strips used for ELISA tests [8,9]. There exist an alternative (complementary) way, namely we can react also in the early stage, before the detection, by preventing the adsorption of these pathogenic agents on the sampling tubes, keeping their concentration intact.

The control of protein adhesion for various applications has been researched for several decades [10]. Nevertheless, the problematic of neurodegenerative deterioration for either detection or standardisation was first considered under the European project Neuroscreen n° LSHB-CT-2006-03 7719. It has been realised, that there was a great loss of biological material on the inner walls of sampling tubes with time, leading to the dubitable titration values.

The example of Aβ-42 storage in different sampling tubes (performed by CHUL (Hospices Civils de Lyon)) can be seen in Table 1. The CSF was disseminated in four different commercial tubes that are used regularly in hospital laboratories and stocked at 4ºC for 24 (48) h. After this time the ELISA tests were performed for Aβ-42 peptide.

Table 1: Titration results for Aβ-42 peptide stored in different untreated tubes at 4ºC for 24 (48) h.

Time of storage/ Tube	24 h	48 h
PP blue	- 36 %	- 60 %
PP green	- 38 %	- 42 %
PP red	- 34 %	- 60 %
PS	- 55 %	/

The obtained results have shown an important loss of peptide after just 24 h of storage and it kept decreasing with time. As well the tubes did not have the same response. Similar was noticed for other proteins. The variations between the tubes were reported to be up to 25% for Tau, pTau181 and up to 65% for the Aβ-42 peptide [11]. These results indicate important information, namely it was observed that patients were diagnosed for Alzheimer disease when the analyses were made immediately after the sampling. However, in just six hours the amount of specific proteins adsorbed on the sampling tubes was so important, that the identification of the disease was already negative. Moreover, the loss reported here is solely due to the adsorption that occurred during the storage, without considering the adsorption that takes place during sampling, purification and aliquoting.

Next to the native forms of these proteins that are found in cerebrospinal fluid, we have also worked with recombinant forms in PBS buffer, which are used as model proteins for standardisation. Analogously to proteins in matrix, they disclose very high adsorption on the tubes, resulting in a false standardisation.

Therefore the key solution to these problems would be an appropriate modification of the inner walls of sampling and storage tubes that could prevent the adsorption of these specific proteins, which is also the subject of presented work. The coatings used for modifications should have several properties: they need to be biocompatible, non-adhesive and stable under various experimental conditions (T, ionic strength, pH).

The thesis is structured in five chapters. The first chapter presents the state of the art in the field of biocompatible materials, low pressure “cold” plasmas, different grafting techniques and protein-surface interactions, with the main focus on the development of non-adhesive surfaces. From this review it will become clear that there exist numerous ways to modify the surface and that so far no general rule for production of anti-fouling surfaces exist. In the second chapter experimental work is exposed, with detailed protocols for each method used. The results and the discussion are presented in the third and fourth chapter. The third chapter offers an insight into material modification and its detailed characterisation, whereas the fourth chapter presents the results of *in vitro* responses of degenerative agents towards the new surfaces. The last chapter (Chapter 5) presents the conclusions made according to the results obtained form surface analyses and biological validation tests.

1.1 Design of novel biomaterials

1.1.1 What are biomaterials?

Biomaterials are defined as materials that constitute parts of medical implants, extracorporeal devices and disposables that have been used in medicine, surgery, dentistry and veterinary medicine, as well as in every aspect of patient health care [12]. These materials should be able to support or replace natural function. By the European directive No.93/42/CEE from June 14th 1993 the biomaterials are divided in four main categories: a) medical devices, b) apparatus for in vitro diagnostics, c) implants and prostheses and d) hybrid organs. They are used in many different domains like cardiology, orthodontics, bone reconstructions, orthopedics, plastic reconstructions and analytic substrates (Figure 1, Table 2) [13].

Figure 1: Examples of biomaterial utilization a) knee arthroplasty b) cosmetic dentistry, c) angioplasty and d) biomedical diagnostics.

There are several types of materials such as metals, composites, natural and synthetic polymers that can be used as biomaterials for different applications (Table 2). These materials satisfy the requirements for biomedical applications in many parameters, especially from mechanical point of view, however their surfaces are often not compatible with living tissues and organisms to which they are exposed [14,15]. Major risks that need to be avoided are immunological or inflammatory reactions; there should be no change of plasma enzymes and proteins when they are in contact with living material inside or outside the human body, absence of toxic and carcinogenic products, no deterioration of tissue and materials and absence of immune factors responsible for thrombosis and obstructing the flow of blood through the circulatory system [16].

Materials taking into consideration above mentioned statements can be referred to as “biocompatible” materials. Enormous amounts of studies are dedicated to the research of new biocompatible materials due to the increasing number of artificial substitutes every year. Nevertheless, the biocompatibility is and stays a very complex phenomenon, which is still not completely understood due to the lack of knowledge of *in vivo* conditions. A caution should be taken in defining a biomaterial as biocompatible, since the applications of these materials are specific. A biomaterial that is biocompatible or suitable for one application may not be biocompatible in another [17].

Table 2: Materials frequently used as biomaterials and their application fields [18].

MATERIAL	Type	Application fields
METAL	Steel	Hip replacement, cardiovascular stents, dentistry
	Ti and Ti alloys	Hip replacement, knee implants, cardiovascular stents, dental implants
	Ag, Au	Antibacterial deposition on cardiovascular prostheses, dental implants
	Ceramic	Bone reconstruction, orthopedics, cardiovascular valves
	hydroxyapatite	Ophthalmology, bone reconstructions
NATURAL POLYMERS	Polysaccharides (cellulose, alginate, chitosan, starch)	Membranes, ophthalmology, adhesive bandage, plating
	Proteins and glycoprotein (collagen, gelatin, fibrinogen, heparin)	Ligaments, soft tissues, tendons, surgical suture, deposition on artificial cornea, cardiovascular stick, bone reconstruction stick, plating of cardiovascular prostheses
SYNTHETIC POLYMERS	HDPE	Tubing, catheters, bone reconstruction
	Poly (acrylates)	Ophthalmology, Orthodontics, Orthopedics
	PTFE	Cardiovascular prosthesis, chirurgical tools
	PEEK	Orthopedics
	PET	Cardiovascular prostheses, tendons and ligaments, analysis substrates,
	PVC	Medical devices
	PP, PS	Analysis substrates, pipettes, storage tubes
ELASTOMERS	Silicone	Orthopedics, gastric rings, probes and catheters
	Polyurethane	Probes and catheters, orthopedics, tubes, Gloves, operating fields.

1.1.2 Fundamental interactions between surfaces and biomolecules

Depending on the application, attachment of biomolecules to the material is either favoured or needs to be prevented. The adhesion of various microorganisms or proteins can occur on most of the surfaces, including metals and alloys, glass, polymer materials with hydrophilic character or most inert hydrophobic surfaces like PTFE [19]. There is a limited knowledge on what is going on the interface of living and non-living matter. The exact mechanism of adsorption to surfaces is not completely understood yet and remains a key question in many studies [20].

For certain biomaterials like contact lenses, biosensors, microfluidic devices, patterned supports for tissue engineering, analytic or storage materials, various devices in contact

with blood (vascular grafts, catheters and dialysers) it is very important to avoid the unspecific protein adsorption. Proteins naturally adsorb on the foreign surfaces and significantly modify their characteristics. For example the adsorption of blood proteins to devices like vascular grafts triggers the thrombosis and consequently the clothing of vessel [21].

The proteins can be adsorbed through many different mechanisms due to their complex nature; therefore the control of their adsorption is very difficult to achieve [22]. It was proposed that the low adhesion materials should be either super hydrophilic or super hydrophobic in order to be protein repellent [23]. The creation of surfaces with hydrophilic surfaces is thought to strongly adsorb water. This high content of water present on the surface should provide minimal surface tension in contact with biological containing liquids due to its similarity. On the other hand extremely hydrophobic surfaces would repel the water and by this keeping the minimal contact of liquid containing bio-molecules with the surface [18].

Coating of surfaces with non- charged hydrophilic polymers like Polyethylene glycol (PEG), Poly(methyl methacrylate) (PMMA), Poly(ethylene oxide) (PEO) have been found to reduce the protein and cell adsorption due to the elimination of electrostatic forces and the hydrophobic interactions between surface and proteins in solutions [24-26]. These kinds of coatings showed very promising results for the devices that are used in short to medium time use (dialysis), however the performance of grafted implant surfaces (cardiovascular grafts) in longer times still remains questionable due to their loss of performance. For example hydrophobically modified polymers exhibit little interaction with blood platelets and therefore they are often used for different application where the thrombosis effects need to be reduced (polyester terephtalate (Dacron) grafts- synthetic material used to replace normal body tissues) [27]. The non-fouling surfaces and protein surface interactions will be examined more in details in the chapter 1.4.

For certain materials it is important that they present antibacterial properties, because the bacteria’s and cells compete for the adhesion to the implants and tissues. The bacterial attachment is mainly driven through the adhesion of microorganisms on surfaces with subsequent colonization of exposed surface. Two main paths are taken in order to avoid the bacterial adhesion. First is through development of surfaces with antimicrobial properties through implementation of ions like Cu or Ar [28] or through coating of material with non- fouling surface layers like PEO [29].

For various implant materials the growth of cells on the surface needs to be promoted. The growing of cells is favoured on the surfaces that exhibit moderate energy and contain polar functional groups. Various oxygen deposited films exhibit rapid cell growth while nitrogen containing species exhibit high affinity for serum fibronectin and moderate influence on cell growth [30]. Another approach that is often used for implant devices is the immobilization of biological molecules like collagen or fibronectin. In natural environment cells grow on the extra cellular matrix (ECM) consisted of different proteins and polysaccharides. Therefore the modification of synthetic materials is directed in the creating of surfaces having similar composition as ECM [31].

Another problem with implantable materials is the releasing of toxic components to the system (Ni from NiTi alloys, polymer with the catalyst residues, etc...). Modification of these surfaces with plasma has shown to be satisfactory in preventing the leakage of toxic materials to the blood. In addition these coatings are able to prevent the corrosion of implants [32]. So called slippery surfaces are prepared normally by using the extremely hydrophilic glycoprotein’s that are able to produce very viscous substances. These kinds of surfaces are used for devices in order to have less painful insertion, precise operation and protection of the tissue for injuries [33]. Flexible polymer materials are needed for the artificial ligaments, inter vertebral discs and tendons where strong adhesion to the bones

is needed. These are usually phosphate based graft chains that are able to form strong bonds with Hydroxylapatite (HA) that is the main inorganic component of bone tissues [34].

In detection diagnostics techniques, biochips or other analytic supports can be functionalized for highly specific antigen recognition with low non-specific interactions. For example the polystyrene support was treated by gamma irradiation, coated with allyldextran, followed by $NaIO_4$ chemistry in order to functionalize the dextran layer. In the next step streptavidin or neutravidin was coupled. This kind of surface shows extremely high hydrophilicity with low non- specific interactions and high binding to biotin-modified antibody or antigen [35]. On the other hand the grafting of physiologically active surfaces like polyacrylamide (PAAm,) or poly (acrylic acid) (PAAc) have drawn much attention for specific binding of biologically active molecules like DNA and pathogenic proteins from the blood. These kinds of surfaces can be also referred to as immuno adsorbant surfaces [36].

The development of stimuli-responsive polymers is another broad area that is attracting much interest in the last years. These materials are able to respond to external stimuli such as temperature, pH, light, electric field, chemicals and ionic strength. The responses are shown as dramatic changes in shape, surface characteristics, solubility, formation of an intricate molecular self-assembly or a sol-gel transition. Applications of stimuli-responsive or so called ‘smart’ polymers are found often in delivery of therapeutics, tissue engineering, bioseparations and sensors [37, 38]. Coatings that are most usually used as stimuli-responsive polymers are Poly (N-isopropylacrylamide) (PNIPAM) and PNIPAM based copolymers, poly (ethylene glycol) (PEG)–poly (lactic-co-glycolic acid) (PLGA) copolymers, Poly(acrylic acid) (PAAc), Poly(methacrylic acid) (PMAA) and poly(ethylene imine) (PEI) [39].

1.1.3 Techniques for modification of biomaterials

In order to develop an appropriate material for specific applications their surfaces need to be modified/functionalized by either physical or chemical modification and in some cases the combination of both methods can be applied. The methods based on physisorption of macromolecules have a deficiency; the layers formed on the surface of the substrate are bonded solely through relatively weak forces, like electrostatic, hydrogen and van der Walls bonds. For many biomedical applications, materials with long- term survival and stable coatings with no depletion are necessary. For this reason the use of physisorbed layers for *in-vivo* and *in-vitro* conditions is limited and the chemical methods for covalent binding of materials are favoured.

There exist many methods to introduce the functional groups to the surface: the conventional wet chemical treatments, UV treatments, ozone treatments and ionization radiation treatments (plasmas, ion beams and laser) [40]. Wet chemical treatments are often employed due to their easy accessibility. However these techniques have often various limitations like:

- the modification is not limited to the surface of the material and the molecules can penetrate through the material,
- the homogeneity of modification is not adequate,
- they are unfriendly to the environment and user,
- their long-lasting performance is questionable.

The use of non-equilibrium plasmas for surface modifications is a good alternative to classical organic chemistry reactions. These kinds of modifications are relatively easy and quick, the use of toxic solvents is avoided and under soft plasma conditions the ablation of material is negligible. The plasma can be used either to incorporate in the surface various functional groups or for growing of thin films through polymerization of monomers. The thickness of the thin polymerized films can be relatively good controlled by adjusting the time of deposition. In this case the negative point the method is that the coatings are not very strongly attached to the surface and the chemical composition of the polymeric chain is rather hard to control [41].

On the other way the non-depositing gases like O_2, N_2, CO_2, CF_4, He, Ar can be used for introduction of polar or non-polar functional groups like hydroxyl, carbonyl, amine and fluorinated groups to the surface. The wettability and reactivity of such surfaces towards an environment in which they are exposed to are modified. For example the surfaces with grafted apolar (fluorine) functional groups affect greatly the non- adhesion of several bio molecules [42]. On the contrary, the polar and hydrophilic surfaces exhibit higher tendency for the various molecules and play significant role in cell adhesion and cell growth mechanism. They can also be used directly for protein or enzyme immobilization. This kind of material functionalization can be also categorized as single step modifications and will be discussed further in chapter 1.2. Furthermore, these reactive groups formed on the surface can be served for covalent grafting of specific molecule as shown in Figure 2 [43]. The introduction of graft chains can be achieved through various mechanisms: ionic mechanisms, coordination mechanism and free radical mechanisms, chemical grafting or radiation induced grafting. The grafting mechanisms, or so called two step processes, will be discussed more in detail in chapter 1.3.

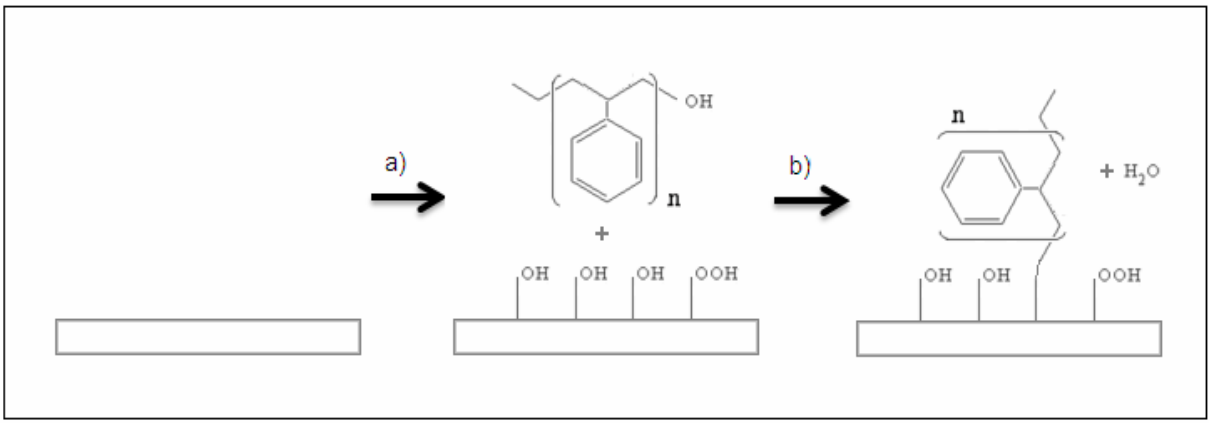

Figure 2: Schematic figure of a) oxygen containing plasma functionalization of material through one step mechanism and b) subsequent grafting of hydroxyl terminated polystyrene (PS-OH) on activated surface; two step mechanism.

There are several advantages of surfaces with graft polymer chains towards the ones formed through single step modifications. First, the stability of these layers is much higher due to the covalent boding to the substrate and second there is no or minimal ageing effect of grafted materials, which is especially problematic for hydrophilically modified surfaces. Finally, the nano (micro)-sized layers have controlled chemical composition, hydrophilic/ hydrophobic balance, roughness and topography. Last, there is a wide variety of functional groups that can be introduced to the surface, which allows adjusting the surface of material for numerous applications.

1.2 Biomaterial elaboration through one step plasma functionalization

The surface properties of materials are ruled by the nature of the material itself. Often, these properties are not satisfactory for certain applications and they need to be modified. In order to improve the biocompatibility and biofunctionality of materials the surface energy, functional groups, topography and morphology need to be changed. This can be done through different treatments, but plasma modification seems to be most appropriate one, as it enables a quick and uniform modification of the surface of the material, leaving its bulk properties intact.

Basically, RF gas plasma treatments can be used for three different types of polymer surface modifications. Firstly, the surface of the material can be modified by plasma functionalization and/or plasma etching. With this kind of treatment, besides changing the surface chemistry through introduction of specific chemical groups, the surface structure (morphology, topography, roughness) can also be affected. Secondly it can be used for plasma polymerization of monomer precursor. In this case plasma acts as an initiator by forming free radicals in the monomer gas and on the surface of the substrate. As a result a thin film is deposited on the surface of the substrate. Finally the surface chemistry of a polymer can be changed by plasma immobilization of various molecules with functional end groups onto the surface by plasma activation of the material with polar or inert gasses.

1.2.1 Plasma state

Plasma describes the state of a (partially) ionized gas and is sometimes referred to as the fourth state of matter. Plasmas are generated by applying either high temperatures or strong electric or magnetic fields to gas. In the first case we are talking about thermo dynamical equilibrium plasmas or »hot plasmas«, whereas in the second case it is called non- equilibrium or »cold« plasmas.

Creating low temperature plasma is usually done by applying an electric field to gas. This can be done with different type of discharges, like direct current (DC) glow discharge, radio frequency (RF), micro wave (MW), DC discharge with a hot cathode or combined discharges. The free electrons in these discharges are accelerated by the electric field and collide with neutral gas molecules or atoms. Due to these collisions, metastable species, positive ions, electrons and free radicals are generated [44]. Collisions can be elastic, inelastic or superelastic. Elastic collisions of electrons with a molecule cause a slight increase in the kinetic energy of the molecule and do not lead to creation of plasma radicals. However, at inelastic collisions, the energy is transferred to dissociation, ionization and excitation of molecules and creation of new particles, called radicals. Radicals can be rotationally, vibrationally and electronically excited molecules, atoms and ions. Probability for a certain collision depends on the available energy and on the scattering cross-section. In general, the most important is the available energy of an electron, which has to exceed the threshold for the reaction. With increasing the electron energy, probability for reaction usually increases, reaches a maximum and then starts decreasing with further increase of electron energy. The lowest energy threshold is for the excitation of rotational states, of the order of magnitude 0.01 eV, for vibrational is 0.1 eV and for the excitation of electronic states it is in the order of few eV, which is also characteristic dissociation energy. The energy required for ionization usually exceeds 10

eV, because we need sufficient energy to remove the electron from the attractive forces of the core [45].

If the energy of the electron is too small to dissociate or ionize the molecule, excitation to different rotational and vibrational states may occur. Probability of reaching a certain state is also determined by quantum nature of the particles [46]. Excited states can decay by electrical dipole radiation. Whereas when an excited radical is relaxed to its lower or ground state, it emits a quantum of electromagnetic wave (photon). The characteristic life expectancy of an excited state depends on the type of excitation and the type of molecule, usually the order of magnitude is around 1 μs. However, if the transitions with dipole radiation are forbidden, the life expectancy of excited species increases up to 1s or more. These are so called metastable states, which can decay only by quadropole or higher multipole radiation. There is a higher possibility that metastable excited states decay by collisions with other particles in the gas or on the chamber walls. Many other particles including ions and neutral atoms in the ground state relax mainly on the walls of a discharge chamber. Charged particles are lost on surfaces, where they neutralize with a high probability, while neutral particles recombine on the walls of reactor chamber with a probability that depends mainly on the characteristics of the wall material [47].

1.2.1.1 Non-equilibrium “cold” plasma

Special case of thermodynamically non-equilibrium plasma used for polymer functionalization is low pressure weakly ionized plasma. This kind of plasma has special properties; the degree of ionization is very small and consequently the density of charged particles is low, and at the same time the degree of dissociation is high. Beside the molecules of the source gas, the most numerous species are free radicals. As such, they are the dominant species which means that they define the characteristics of the plasma. These free radicals are chemically much more reactive than the original gas. The chemical reactions are the same as they are in the source gas, but the potential barrier for reactions has been lowered considerably by dissociating the molecules of the source gas. Therefore, free atoms are able to react with substrates already at room temperature [48, 49]. This is of a great importance concerning the fact that we want to functionalize just the surface of materials, without changing its bulk properties that depend on the temperature.

1.2.2 Plasma-surface interactions

Plasma is a highly reactive environment of reactive species with a wide range of internal energies. Consequently, these active species have different effects on the materials exposed to plasma phase as shown in Figure 3. Chemical bonds between atoms in a solid material have a typical binding energy of 3-5 eV, so accelerated ions, vacuum UV radiation and radicals have sufficient energy to break any chemical bond [50].

The ion bombardment of the material exposed to plasma causes sputtering of the surface atoms and further ions can chemically react with the surface. The combination of both results in an anisotropic-reactive ion etching [51]. The energetic UV radiation from the plasma has several effects on organic materials. The VUV radiation can cause photoionization, while UV radiation causes dissociation of bonds, yielding free radicals and may excite specific groups. This can lead to chain scissions, rearrangements or even

elimination of specific functional groups. The radicals created on the surface can further crosslink, can react with species from the plasma phase or can react with oxygen when exposed to air afterwards [52].

The radicals colliding with the surface of the substrate can be incorporated at the surface (e.g. by radical-radical recombination), can abstract hydrogen or other atoms like fluorine from the surface or can induce polymerization and crosslinking on the surface [53]. The interaction of neutral species with the surface is largely dependant on their chemical reactivity. During plasma processes, a competition between modification, degradation process (sputtering or chemical etching) and a (re)deposition process exists. The overall effect of the plasma process is determined by the sort of the gas used; type of plasma discharge, nature of the substrate and to a less extent by other conditions such as pressure and substrate temperature [54].

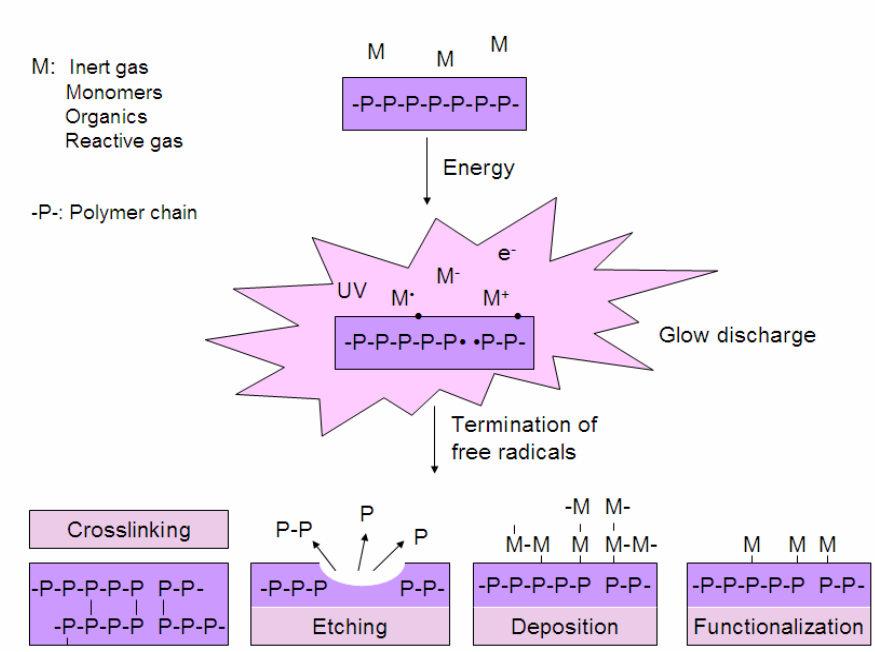

Figure 3: Schematic presentation of plasma surface interactions; P= polymer chain and M= gas.

The mechanisms involved in plasma treatment of polymer materials are not yet completely understood. The main drawback of plasma techniques is the difficulty to achieve a good understanding of the interactions between plasma species and treated surfaces. We have to consider many factors depending on both generation of active species in the gas phase and their interaction with the treated material. Furthermore it needs to be mentioned that the degradation of the surface leads to formation of molecular fragments that are volatilised from the substrate to the plasma phase and consequently change the plasma chemistry [55].

Finally, we need to considerate that polymer surfaces are dynamic systems which will interact with their surroundings. Majority of plasma treatment (excluding fluorinated gasses) yields polar groups at the surface. Upon storage in the air or vacuum which are considered to be hydrophobic media, the surface reorganizes in this way that the polar groups are buried in deeper surface layers. This lowers the surface free energy and is thermodynamically favourable The rearrangement is kinetically controlled and happens typically in order of minutes, hours and has an influence on some phenomena like adhesion, wettability and availability of functional groups for coupling. This is also referring as an ageing of the material [56].

1.2.3 Applications of low pressure non-equilibrium plasmas

Plasma processes have been developed to attain specific surface properties of biomaterials, like promotion of adhesion, functionalization of the surface, enhanced surface wettability and spreading, improvement of biocompatibility, molecular immobilization, non-fouling coatings, barrier surface coatings, reduced surface friction, etc [57].

Depending on the application an appropriate plasma treatment needs to be chosen. In order to improve the adhesion for example, strong interfacial forces are required; therefore plasma treatment that renders chemically active functional groups, such as amines, carboxyl, and hydroxyl groups are employed. Further, if the free radicals on the surface are required or if performance of the polymers should be enhanced (like hardness, chemical resistance) surface crosslinking and activation with noble gasses is employed. In all above mentioned cases, the surface energy of material increases due to the formation of polar functional groups (Figure 4). On the other hand, the surface energy can be decreased by using fluorine-rich plasmas. These plasmas enable incorporation of fluorine functional groups on the polymer surface yielding the material highly hydrophobic [58].

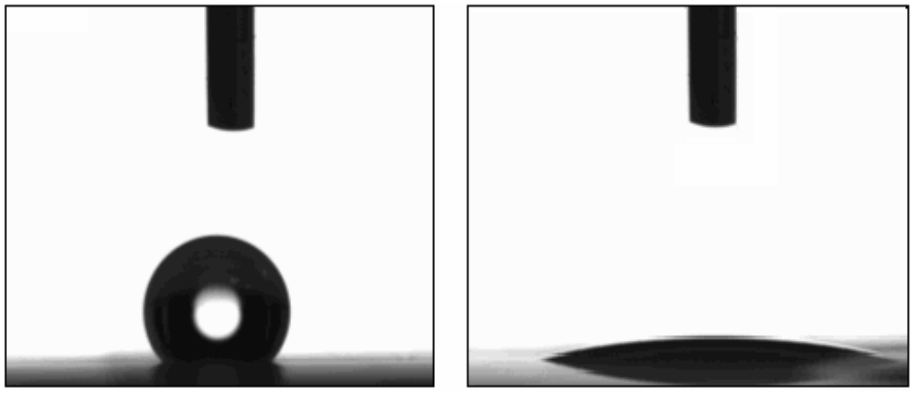

a) b)

Figure 4: Picture of a) Hydrophobic surface and b) hydrophilic surface.

1.2.3.1 Development of (super) hydrophobic surfaces

The process of hydrophobization of polymeric materials has been known for decades. Hydrophobic surface is obtained quite easily by deposition of “Teflon” - like layers on the substrate. They can be attained in various ways: by conventional immersion, spin coating methods and by different sputtering techniques. As PTFE is not soluble in any organic or inorganic solvent, layers formed by immersion and spin coating are not very uniform, stable and do not express well enough the hydrophobic character [59].

In recent years the synthesis of hydrophobic surfaces through deposition of fluorocarbon films is often observed. The depositions can be achieved either by chemical methods like chemical vapour deposition (CVD), physical methods like physical vapour deposition PVD, plasma enhanced physical vapour deposition (PEPVD) or by deposition of fluorinated silane in the form of self assembled monolayers (SAM-s) [60]. Classically, such coatings reflect only moderate hydrophobicity, which means that the contact angle is usually less than 120 °.

To build up more hydrophobic (superhydrophobic) material, it is necessary to texture

the surface [61]. The superhydrophobic surfaces are characterised by the water contact angles superior to 150º. In the nature we can observe this phenomenon as a so-called "Lotus effect". A characteristic of the surface of a lotus leaf is that it is at the same time superhydrophobic and self-cleaning. In general, lotus effect is achieved when two conditions meet: the surface must be covered with material that has a low surface energy and the material must have a fine structure. Namely rough structure allows the capture of the air bubble in the area between the liquid and substrate and thus prevents their contact. Ultrahydrophobic synthetic materials have appeared only recently. These surfaces are still little known in the field of bioadhesion and present a great potential in this area [62]. Their synthesis for the industrial purposes leads often to various defects of material like mechanical fragility and opacity. These deficiencies are directly correlated with the roughness and the structuring that is needed to obtain ultrahydrophobic character. Therefore the compromise between the surface energy, mechanical and optical properties of the material needs to be achieved.

Conventional methods for the synthesis of structured material is the surface-etching either by chemical way with HF, XeF_2 for example or by reactive plasma ion etching. In the next step the coatings with hydrophobic properties are applied to these surfaces. Compared with conventional immersion methods, more hydrophobic surfaces are obtained on the account of structuration, however the satisfactory adhesion of these layers remains unsolved [63]. Other methods that are often used are micro(nano)-lithography (either through etching of silicon and deposition of thin apolar layers or through masks made of colloidal particles), transfer moulding of a pattern etched on silicon in the PDMS matrix and the blend of polymers with their demixing properties that lead to different geometries. All these methods lead to materials with typical surface roughness of few hundred nanometres to several micrometers [64].

An alternative approach is the functionalization or deposition of highly fluorinated thin films on organic or inorganic substrates by means of cold plasma. In this case we need to use non- polar gasses like CF_4, SF_6 or their mixture with hydrogen and/or noble gasses [65]. CF_4 is one of the most widely used components of feed gas mixtures employed for a variety of plasma-assisted material processing applications. CF_4 molecules can undergo bond scission and ionization in the presence of an alternating electromagnetic field. The electron impact studies showed the appearance of many ground and electronically excited species in fluorine gas discharges, which can interact with each other or with the substrate. In spite of wide variety of species present in the plasma phase, there are only few that are involved in functionalization of the surface. These are mainly F atoms, with smaller concentration of CF_3, CF_2 and CF radicals respectively [66]. The fluorine atoms are also known to be an etching agents, therefore the modification of surface with CF_4 plasma was proposed to be the sum of two mechanisms: degradation and fluorination. These two mechanisms appear to be competitive and parallel at the same time [67].

The roughness of the surfaces obtained with plasma etching is usually much lower than with other methods, from few nanometres up to few hundreds of nanometres. Therefore the ultrahydrophobic character can be obtained in a wide range of surface roughness. For this reason it was suggested that the topography of the surface (surface features) have a larger effect on the superhydrophobic character than the roughness value itself (Figure 5). By changing the experimental conditions or addition of a foreign gas to fluorocarbon feed it is possible to change continuously the relative importance of the active species and therefore the etching or polymerizing capacity of discharges. On generally, higher that F/C ratio is, the more the discharge is suitable for etching and less for polymerization process [69]. The parameter has been originally formulated by Coburn and Winters [70] for Si and SiO_2 etching essentially to characterize the stoichiometry of the active species.

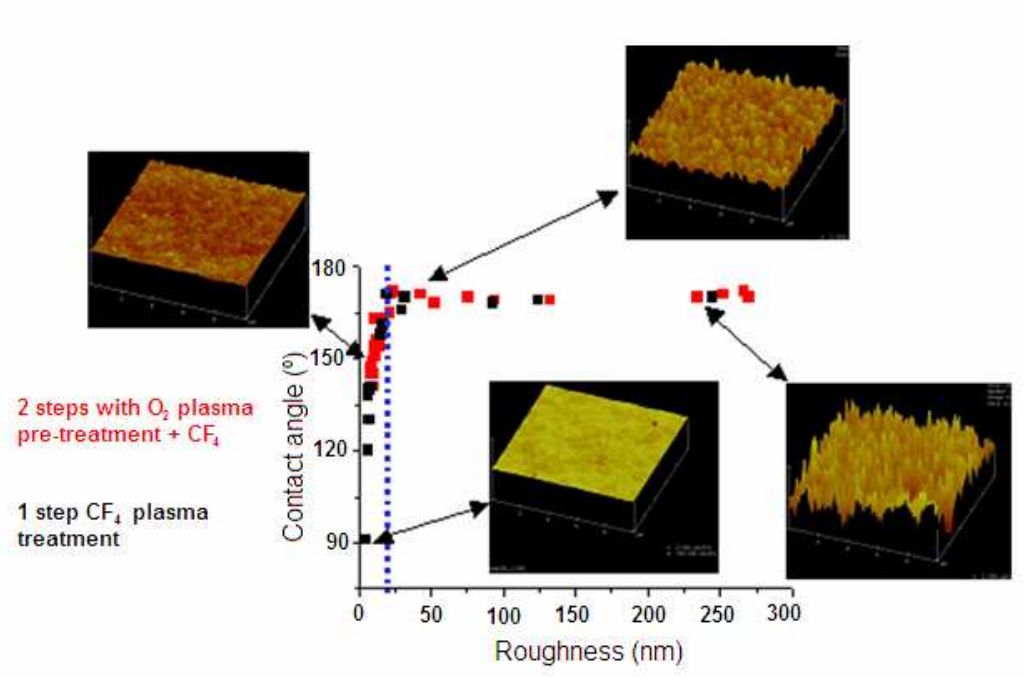

Figure 5: Ultrahydrophobic surfaces obtained with one step CF_4 plasma treatment (black points) and two step treatments with O_2 and CF_4 plasma (red points) [68].

Addition of reducing gas such as hydrogen reduces the etching activity of the discharge. In fact, hydrogen reacts with F atoms leading to unreactive HF, so the recombination process of CF_x and F is reduced and CF_x density increases, which are the building blocks for polymerization. On the other hand the addition of oxygen increases the etching properties of the discharge system. Oxygen reacts selectively with radicals, leading to less reactive CO, CO_2 and COF_2 species and this means that F atoms are no longer recombined and their relative density increases [71].

1.2.3.2 Development of (super) hydrophilic surfaces

Many polymer materials are rather hydrophobic due to a lack of polar functional groups, resulting in a high surface energy and unsatisfactory adhesion of different coatings (often in aqueous solution). In order to increase the surface free energy of the material, or in other words make it hydrophilic, we need to activate the material by introducing polar functional groups at the surface [72]. The switch between hydrophilic and superhydrophilic (super wetting regime) will depend strongly on the roughness factor. [73]. Terms superhydrophilicity and superwetting were introduced a few years after the term superhydrophobicity to describe the complete spreading of water or liquid on substrates.

A wide spectrum of functionalization techniques is available to render surface hydrophilic like physical deposition/ adsorption, chemical modification, grafting and plasma techniques. Polymer surfaces can be modified by physical adsorption of amphiphilic molecules. Sol-gel method (wet-chemical technique or chemical solution deposition) methods are used primarily in the synthesis of materials and ceramics engineering. Precursor molecules in this case determine the type of reaction. Precursor (salt) can be deposited on the substrate and forms a film (with "dip coating" or "spin coating" technique). However, in order to obtain a stable surface the molecules should be irreversibly adsorbed (covalently bonded) and this presents a large problem in majority of

the adsorption techniques. Other chemical processes that are widely used are chemical vapour (CVD) and physical vapour (PVD) deposition techniques [74]. On the other hand polymer surfaces can be chemically modified by liquid or gas phase reactions. Often strong oxidizing acids (e.g. permanganate, chromic acid, fuming nitric acid, perchloric acid, sulphuric acid) are used to introduce different functional groups like carbonyl, carboxylic or sulfonate groups to the surface. Also some other techniques like flame and thermal treatments can be used that introduce radicals to the surface and cause chain scissions. The radicals introduced to the surface react subsequently with oxygen and/or nitrogen leading to hydroxyl, carbonyl, amide and carboxylic acid groups [75]. Furthermore ion beams, laser treatments that combine UV in thermal effect, gamma irradiation, ozone, mechano -chemical activation techniques are used to induce chemical (create free radicals or peroxides) and morphological changes at polymer surface [76].

Treatment of polymer surfaces by exposing them to plasmas containing reactive or inert gases has been often used to improve the adhesion properties of material. Generally oxygen plasma treatments lead to introduction of oxygen containing groups like carboxyl, carboxyl, peroxide and hydroxyl groups. In the oxygen plasmas at the same time etching and functionalization of the surface occurs. The neutral O atoms react with carbon atoms on the surface and form small volatile products like CO and CO_2 that are pumped from the system, living free radicals on the surface [77]. The carboxylic groups may be also introduced to the substrate by treating them with CO_2 or CO plasmas. In this case, next to the groups formed with oxygen plasma, new functional groups like esters, aldehydes and ketons appear [78]. If the treatment of the surface by O_2 and CO_2 plasmas is compared, the O_2 plasmas introduce much faster the functional groups, while CO_2 plasmas produce much less damage (etching) of the material. The carboxylated surfaces can be produced as well by plasma polymerization of monomers like acrylic or propanoic acid, while the high amount of the hydroxyl groups on the surface can be obtained by plasma polymerization of methanol, ethanol, allyl alcohol and methylbutylnol monomers [79].

Nitrogen, ammonia and N_2/H_2 plasmas introduce primary, secondary and tertiary amines on the surface and as well the amides. Beside the nitrogen containing functional groups, there is always observed a presence of oxygen containing functional groups on the surface due to the post oxidation reactions with free radicals incorporated in the surface and the presence of residual impurities (e.g. water vapour) in the discharge chamber. Different nitrogen containing plasmas will produce different nitrogen functional groups. When NH_3 plasma is used it is possible to create a relatively high amount of primary amino groups, which is not the case for pure N_2 plasma [80]. An alternative way to introduce amine groups on the surfaces is through plasma polymerization of amine based monomers like allylamine, ethylenediamine and diaminocyclohexane [81].

Polymers treated with Ar or He plasma will not lead to incorporation of new functionalities onto the polymer surface, but to the creation of free radicals on it. These free radicals can react with oxygen when exposed to the air and form crosslinks and unsaturated bonds due to the chain scissions. Besides the activating advantage of this kind of treatment inert plasmas are often used for cleaning of the surfaces before exposing them to another gas or material [82]. One of the slight limitations of plasma technologies is the diversity of the functional groups produced by the multitudes of chemical reactions that happen in the plasma phase. Nevertheless, it can be concluded that plasma based techniques are very efficient methods for modification of different materials that can be used for various applications.

1.3 Biomaterial elaboration through two-step treatment: Surface activation and polymer grafting

There are several ways that thin films can be deposited on the surface of a substrate like spin coating, precipitation, polymer adsorption and chemical grafting. The grafting techniques have few advantages towards the classical surface functionalization in the meaning that the introduction of graft chains is rather easy and well controllable, there is a large spectrum of functional groups that can be inserted on the surface which can be served to control the surface properties like adhesion, wettability, biocompatibility and as well for multi-functional stimuli responses. Furthermore the covalent attachment of graft chains to the surface avoids their depletion and by this gain long term chemical stability [83].

The conformation of grafted polymer chains will depend on many factors. Firstly on the grafting technique used that can influence the grafting thickness and density, secondly on the building blocks used for grafting and thirdly the environmental conditions like quality of the solvent, pH, T and salt concentrations [84].

1.3.1 Grafting of polymer brushes

1.3.1.1 “Grafting to” and “grafting from” methods

The grafting methods are generally divided to “grafting to” and “grafting from” techniques. The main difference between them is how the molecules in question are attached to the surface of the material as shown in Figure 6.

In the “grafting to” method the polymer chains are simply attached to the given surface via chemical reaction between the surface functional groups of the material and the end functionalized group of the polymer backbone [85]. Effective anchoring of polymers can be performed only if appropriate reactive groups are located on the surface of the substrate. The way the surface will be modified depends also on the reactivity of functional groups in the polymer chains. First surfaces are functionalized by different chemical or physical treatments like UV, flame, ion beam treatment, gamma irradiation, plasma treatment or by strong oxidizing acids. These kinds of treatment usually lead to formation of oxygen, nitrogen or sulphur containing functional groups on the surface of the material.

In the next step the functional molecules containing desired properties are attached to the activated substrate. In the case when modifying molecules do not posses befitting end functionalized groups able of coupling with the substrate, they need to be synthesized by different polymerization reactions. Commonly used methods are living anionic or cationic polymerizations, radical group transfer and ring opening polymerizations [86].

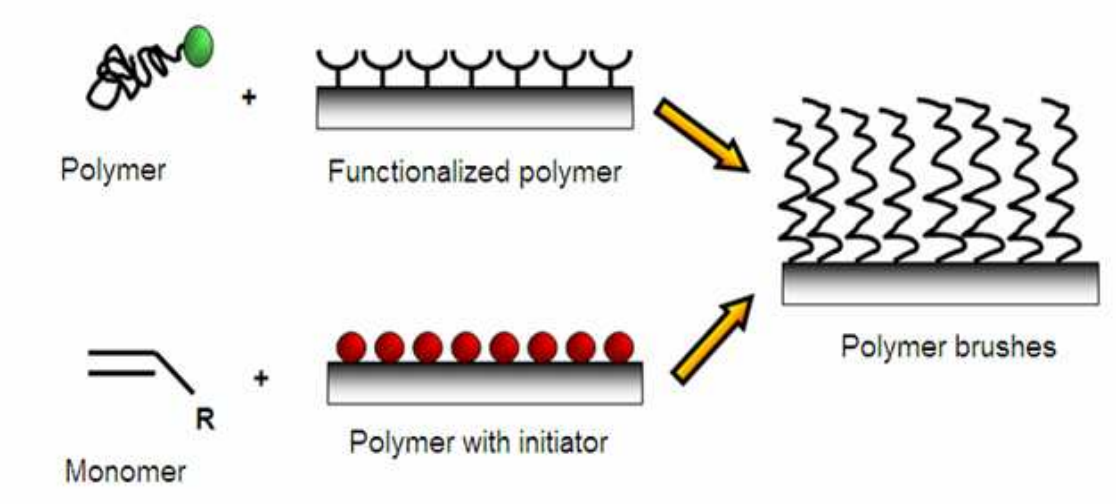

Figure 6: Comparison between “grafting to” (up) and “grafting from” (down) method.

The advantage of such functionalization is that the molecular weight and chain length of the polymer are well defined. The negative point of this approach is the lower grafting density of the surface due to the steric hindrance and overlapping of the pre-adsorbed polymer molecules on the surface. Additionally the chain thickness is pre- defined with length of grafted molecules and can not be freely adjusted [87].

For these reasons, an alternative “grafting from” method is often employed. “Grafting from” or so called surface initiated polymerization (SIP) is based on formation of thin films through polymerization of monomers from surface bound polymerization initiators. The choice of initiator that will be introduced on the substrate must be appropriate for the method of polymerization that will be used afterwards. In the case of conventional radical polymerizations (RAFT, ATRP) initiators like peroxide, azo- initiators or photo initiators are used. As the chains are growing form the surface and the diffusion particles are monomers, the initiators are easily accessible and therefore high density polymer brushes can be formed [88].

1.3.1.2 Homopolymer brushes

There are different scenarios that can happen when the polymer chains are grafted to the surface. Many factors can influence the conformation of the anchored chains on the polymer substrate, like quality of the solvent (pH, T°C, salt concentration), type of polymers (monomers), identity and quantity of the functional groups, etc [89].

Polymer molecules used for grafting can be constituted from single or several end grafted functional groups. In a good solvent single reactive side chains groups form brushes, while multiple reactive sites form rather loops and tails at the surface of a grafted material (Figure 7).

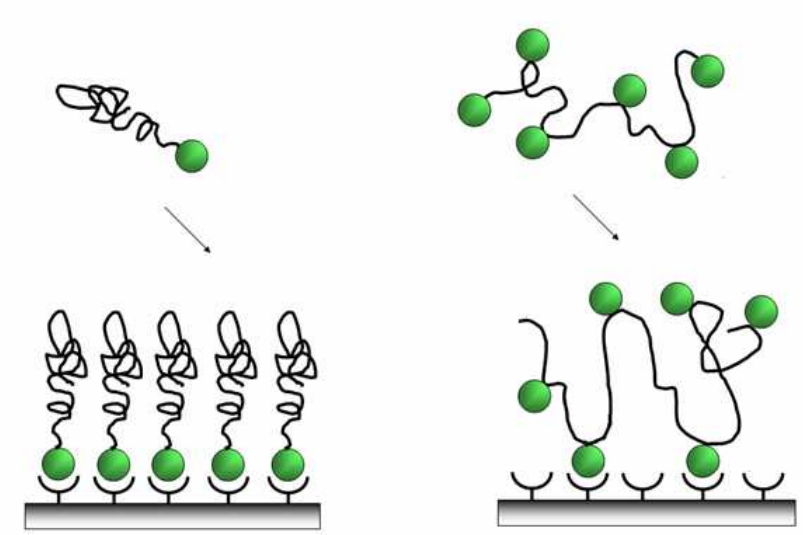

a) b)

Figure 7: Scheme of polymer grafting for a) single activated end- groups b) multiple activated side groups.

Furthermore, the density of polymer chains and the quality of the solvent will influence on the way the chains will graft to the surface (Figure 8). In the diluted regime the polymer chains adopt one of the extreme conformations; either they appear as a mushroom like structures in a good solvent or as a pancake like structures in a bad solvent. Namely, when there are only few long chains attached to the surface under good solvent conditions, they behave similarly to the free chains in the solution (expanded coils).

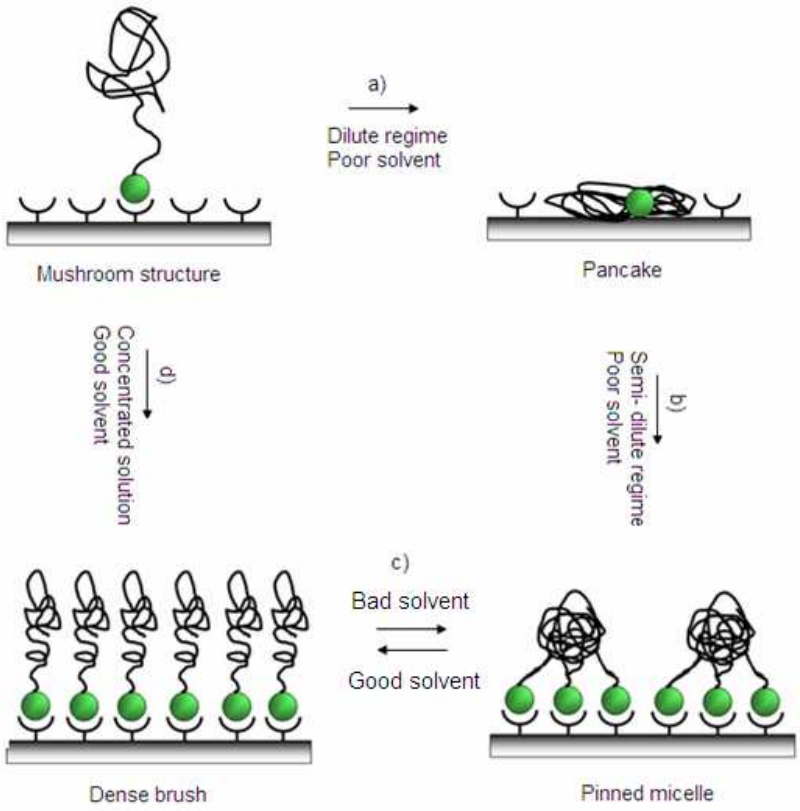

Figure 8: Conformation of polymer chains as a function of solvent quality and grafting density

Another important factor is that there is no or weak affinity of polymers towards the surface. Under good solvent conditions polymer tries to maximize the number of contacts with the solvent and at the same time keep the chain stretching at minimum. On the other hand, if an attractive interaction exists between surface and polymer, it tends to maximize its interaction by flattening on the surface. When the solvent is poor, polymer tries to minimize the contact with the solvent and forms individual collapsed globules. Accordingly, polymers in a good solvent will occupy a larger surface area than in a poor solvent, thus higher degree of polymer adsorption is found from poor solvents. With further increase of grafting density the semi- diluted regime is obtained and chains begin to interact with each other and form surface bound aggregates of different shapes and sizes, so called pinned micelles. Additional increase of grafting density forces the chains to stretch normal to the substrate due to the increase of osmotic pressure among the chains, which results in construction of polymer brushes [90].

An immense research is being dedicated to the study of adaptive polymer brushes. These materials are able to change their conformation with small changes in surrounding environment, such as light, T°C, pH and salt concentration (Figure 9) [91,92].

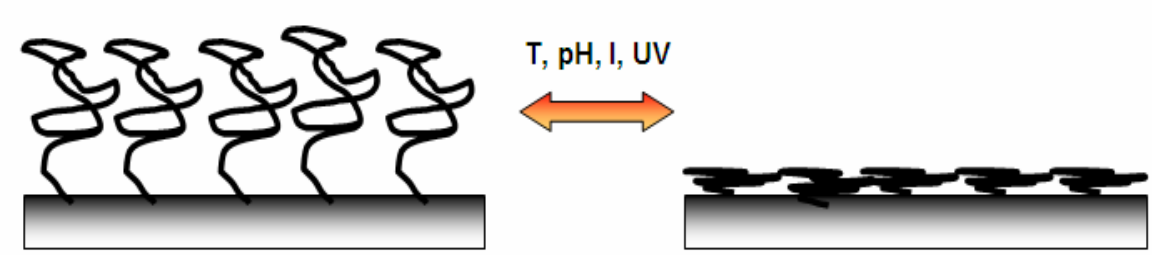

Figure 9: Reversible collapse of polymer brush chains under external stimulus.

The photo responsive-layers are based on incorporation of photo active groups like azo-benzene chromophore on the surface of a substrate, that are able to react with incoming UV light. This light source changes the conformation of –N=N- group from *trans* to *cis* isomers which as a consequence causes collapse of the chains towards the surface. The response of polymers to temperature is frequently caused by hydrogen bonding groups in the polymer backbone. Usually below the lower critical solution temperature (LCST) the polymer is completely miscible with water, but when the temperature is increased the phase separation occurs and compact globules are formed. One of the most used polymers in thermo adaptive studies is PNIPAM, due to the fact that his LCST is close to the human body temperature [93]. Another class of stimuli-responsive polymers are polyelectrolytes. Their form is almost exclusively dominated by electrostatic reactions. They can go under abrupt changes under pH, salt concentrations or electric field alteration. Frequently polyacrylic acid based polymers are selected for this purpose [94].

1.3.1.3 Mixed polymer and copolymer brushes

Further research in developing the adaptive surfaces was through grafting of mixed polymer brushes. The field of research is relatively new; it dates to the end of 1990's. Each component of the nanostructured heterogeneous layer in these systems has its role. Besides the importance of functional groups for the specific behaviour, the morphology of

the surface can be influenced through various ratios of functionalities and solvent properties (Figure 10) [95].

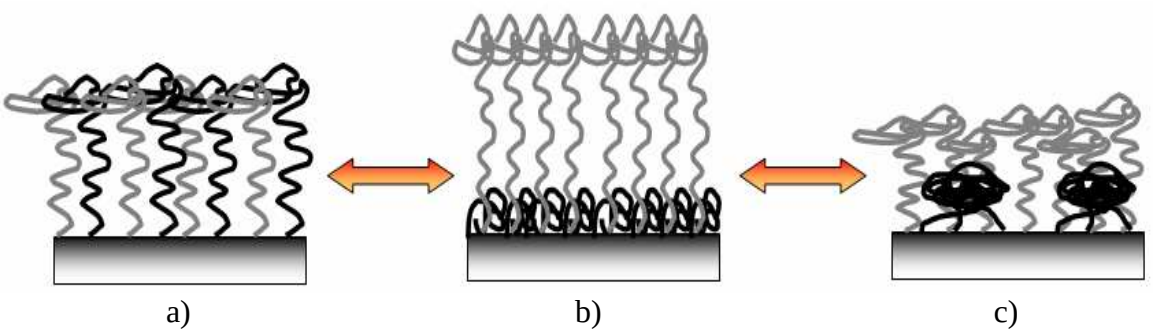

Figure 10: Scheme of mixed polymer brushes grafted on the surface under a) non-selective solvent, b) solvent selective for green chains and c) solvent poor for black chains.

In the first case both polymers are present on the surface and surface properties are governed by both polymers (Figure 10.a). In selective solvent the unfavourable polymer chains form clusters near the substrate, while the chains facilitating this solvent remain at the top layer and determine the properties of the film (Figure 10.b). The Figure 10.c is presenting the situation where the solvent is poor for black chains. In this case the surface morphology is affected by formation of pinned micelles on the surface.

The methods for synthesis of mixed brushes are composed of two steps. First is the insertion of appropriate initiator to the surface that is able to induce the polymerization of both components. In the next step the surface is subjected to a monomer solution of first component and after certain time the substrate is exposed to a second solution of monomer. The ratio of components is controlled by time of grafting reaction for each. All the classic ways of polymerization can be used; however lately there is more and more tendency in using atom transfer radical polymerization (ATRP) due to better molecular weight control and lower polydispersity [96].

An interesting work was done by Motornov et al. [97]. They have grafted mixed polymer brushes through grafting of polystyrene in the first step and poly(2-vinylpyridine) in the second step to Si wafers and polyamide (PA) substrates. On the PA fabric the switching behaviour was much more pronounced than on Si wafer. The wettability changed from extremely hydrophilic state to superhydrophobic state (150°) under external stimuli.

Similar behaviour as for mixed brushes can be observed for block-copolymer brushes grafted on the surface of the substrate. The great interest in this kind of materials is raised from the fact that the building blocks of di or tri-copolymers are usually immiscible functional groups, which as a consequence allows them to self-assemble in well organized nanoscale periodic structures. Typically these are spherical, cylindrical or lamellar forms, depending on the composition of the copolymers [98].

The applications of above described multi-component materials are broad. They can be used for changeable biomaterials, surface pattering, magnetic and optical materials, templates for the fabrication of information storage devices, nanowires, nanomembranes, imaging technologies, etc.

1.3.2 Grafting of surfactants

The adsorption of surfactants is mainly determined by two factors: the first one is the interaction of the surfactant with the surface and the second one is the hydrophilicity /hydrophobicity. In other words, the hydrophobic chains are not soluble in water and therefore they prefer to adsorb to the surface. The increase of the adsorption is also increased with the augmentation of critical packing parameter (CPP). The CPP is demonstrating how tightly surfactants are able to pack at the surface of a substrate. This parameter depends on the balance between hydrophobic and hydrophilic moieties. In aqueous solutions the high packaging is rather unfavourable and can be artificially increased in several ways. In order to benefit from the fact that hydrophobic interactions are leading to higher adsorption, longer and branched or multiple hydrocarbon chains can be used. Additionally the inclusion of salts reduces the repulsive electrostatic forces between surface and surfactant, leading to smaller effective cross-sectional area per surfactant. For this reason neutral surfactants adsorb much stronger than for example anionic surfactants.

The adsorption of surfactants on non-polar surfaces is shown in Figure 11. The hydrophobic chains of surfactant interact with the surface, while its hydrophilic moieties stay in the contact with the solution. The adsorption free energy of surfactants at the hydrophobic surfaces is very similar to the micellization free energy of surfactant and in this way the structure on the surface appears like micelles.

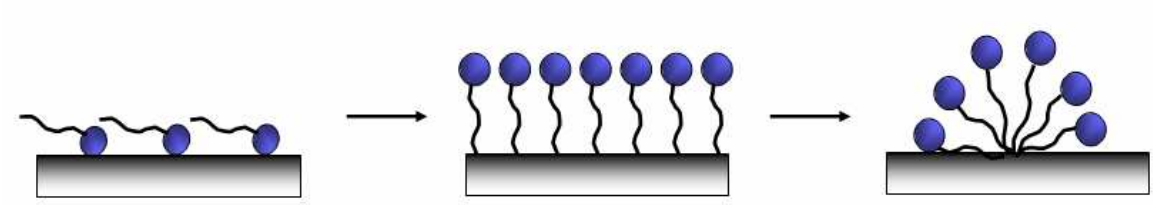

Figure 11: Adsorption of surfactants on non- polar surfaces.

Contrary, on polar surfaces surfactants adsorb with their polar component while the apolar tail stays in the solution. This is only possible in a very low surfactant concentration due to the fact that it is energetically unfavourable to have insoluble chains in the solution.

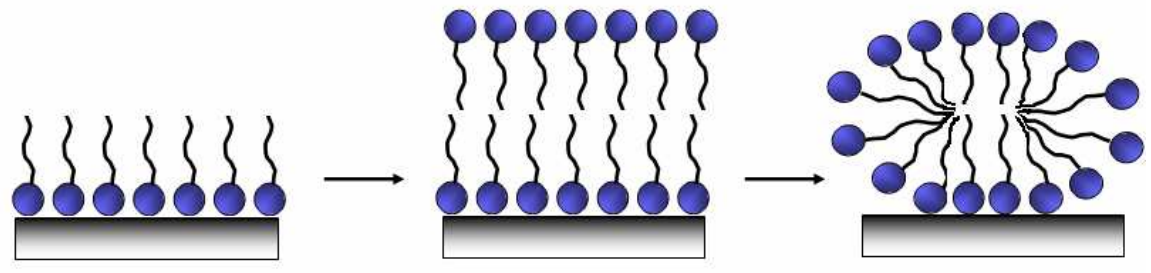

Figure 12: Adsorption of surfactants on polar surfaces.

Therefore with the increase of surfactant concentration the hydrophobic parts of surfactants in the solution will further adsorb and form bilayers with pre-adsorbed surfactants as shown in Figure 12. The bilayers are formed when there is extremely strong interaction between surfactant head group and surface. If the interaction strength is

moderate, rather micelles or similar aggregates will form. In the case of surfactant adsorption to polar surfaces, micellization occurs considerably bellow the critical micelle concentration (CMC) of surfactants (ionic and non-ionic) due to the surface induced self-assembly [99].

Modification of surfaces with surfactants is often used in different biochemical and biomedical fields. These surfaces can be applied for separation membranes, capillary electrophoresis, as blocking agents in ELISA (Enzyme-Linked ImmunoSorbent Assay) tests or for different surface chemistries where the non-specific adsorption of molecules needs to be inhibited and at the same time the immobilization of specific agents (antibodies, drugs, cells) has to be enhanced [100].

Surfactants can be basically divided into anionic (SDS-sodium dodecyl sulfate, PFOS-perfluorooctanesulfonate), cationic (DODAB-Dioctadecyldimethylammonium bromide, CTAB-hexadecyl trimethyl ammonium bromide) and zwitterionic or amphoteric (betains, sulfobetains, CHAPS (3-[(3-Cholamidopropyl)dimethylammonio]-1-propanesulfonate)) and non- ionic surfactants (Triton, Polysorbats). Non-ionic surfactants possess non-dissociable head groups, such as alcohol, phenol, ether, ester or amide. A majority of these surfactants are made hydrophilic by the presence of polyethylene glycol chain and are referred to as polymeric surfactants or surface active polymers. There exist two main types of polymeric surfactants in so called “block” or “graft” configurations. The most used block polymer surfactants are copolymers between ethylene-oxide and propylene-oxide. The polyethylene oxide (PEO) is known and one of the most used surfactants for creation of non-fouling surfaces that will be discussed further in the 1.4 chapter. There exist many different studies on attachment of PEO to various surfaces (PP, PE, PET, PTFE, silica). The simple physical adsorption resulted in formation of unstable layers with a high tendency to desorbe from the surface. The effect was specially pronounced for the layer molecular weight PEO surfactants [101].

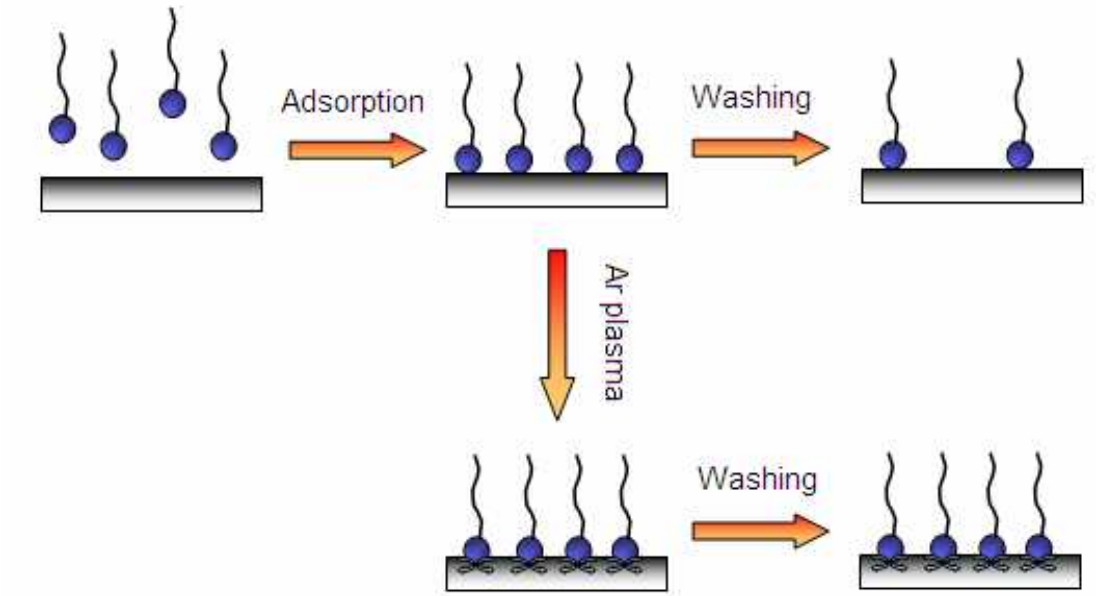

Figure 13: Scheme of Argon plasma treatment for the immobilization of surfactants.

The most veritable tool seems to be the utilization of specific irradiation techniques. An interesting way of surfactant immobilization was presented by the group of Sheu [102]. They have immobilized poly (ethylene oxide) PEO surfactants on hydrophobic surfaces using the CASING (crosslinking by activated species of inert gasses) technique. Low density polyethylene (LDPE) was first coated with the PEO and than the surface was crosslinked by argon plasma treatment (Figure 13). They have seen that there was no depletion of the

surface after washing it in the case of Ar plasma crosslinked surface, while the surfactants on the surface deposited with solely physical adsorption showed the change of surface properties. Since than, several surfactants and their di- triblock copolymers were grafted to polymeric and non-polymeric supports by CASING method.

1.3.3 Grafting of particular thermo-sensitive polymer: PNIPAM

Poly (N-isopropylacrylamide) (PNIPAM) is nowadays one of the main representatives of thermo-responsive polymers. Considerable amount of work on reversible phase transitions of this polymer started with Tanaka et al. [103]. In the Figure 14 is shown an exponential increase of publications considering PNIPAM and PNIPAM based co-polymers [104].

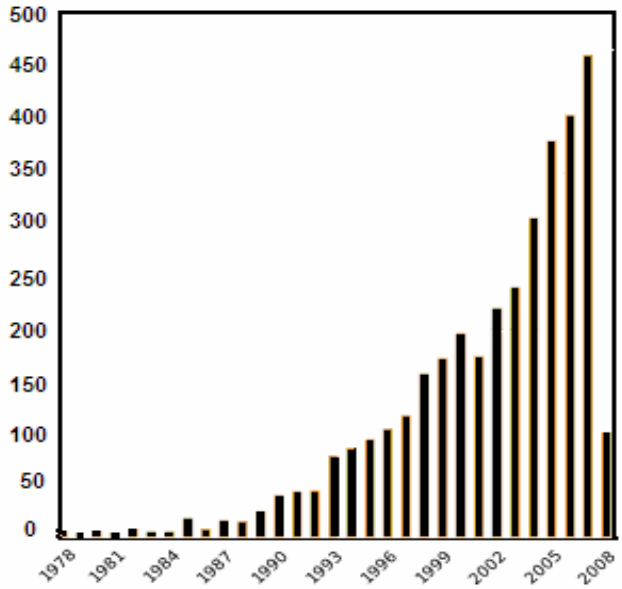

Figure 14: Annual evolution of the amount of academic references about PNIPAM indexed in the CAS online database.

The interest of PNIPAM is its low critical solution temperature (LCST) at 32°C, which is close to body temperature and because of this unique property it is potential candidate for several bio- medical applications. At temperatures below the LCST, PNIPAM is completely dissolved in water and forms extended structures with a random coil conformation. The hydration of chains is enabled by the hydrogen bond formation between secondary amide hydrogen N-H and carbonyl C=O groups with surrounding water molecules. Nonetheless, when the temperature is increased the hydrophobic interactions predominate and polymer collapses into globular structures, leading its precipitation out of water (Figure 15). This transition effect is the result of temperature induced entropy gain from the dehydration of amide moieties and is completely reversible [105].

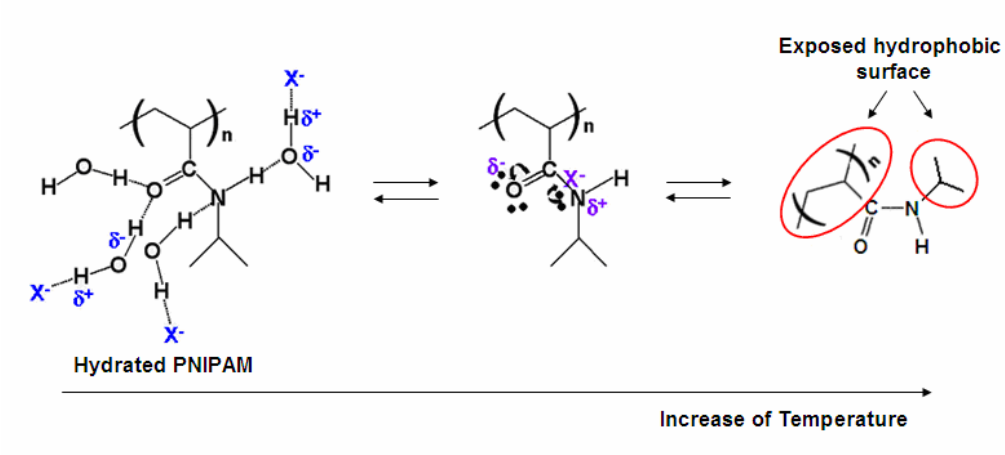

Figure 15: Reversible transition of PNIPAM chains with temperature.

The behaviour of PNIPAM in water phase is extensively studied under various external conditions (T, ionic strength, salt, presence of ions). The interest is in the research of the protein folding that seems to have similar conformation changes at the LSCT as PNIPAM. The phenomena of undesired protein folding are known to cause various fatal disorders, like accumulation of amyloid plaques and consequent development of Alzheimer disease [106]. Wu et al. [107] were the first ones that observed a stable single chain to single globule transition in extremely diluted PNIPAM solutions by DLS measurements. They have found out that chain density in the globule state is slightly lower than predicted on the basis of a space-filling model, meaning that there is still some water present in the fully collapsed state; the radius of gyration (Rg) decreased from 127 to 17.9 nm with temperature change. The measurement with a small increase of temperature displayed the two intermediate (crumpled coil and the molten globule) states between the formations of collapsed globule from extended random coil that can be seen in Figure 16.

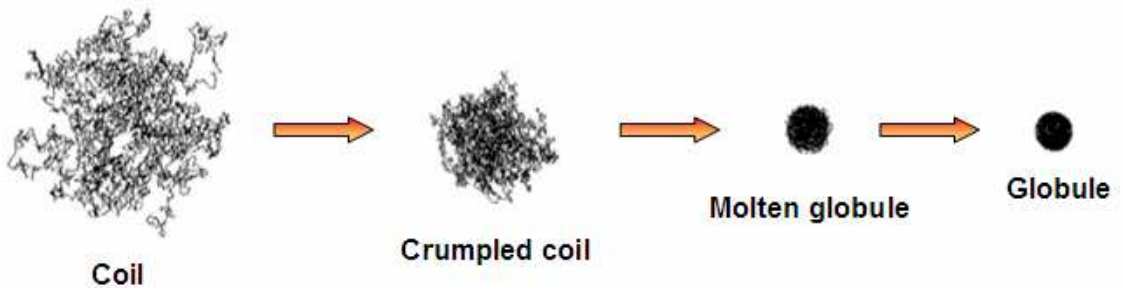

Figure 16: Transition of PNIPAM single chain in water to single globule state through intermediated with increase in temperature.

Upon the adsorption of PNIPAM to the surface, new properties and behaviour can be induced. Halperin [108] made a model of phase behaviour of end- grafted polymers exhibiting LCST on the Gennes n-cluster model. He predicted the transition depends on grafting density and on the molar mass of the chains. This was confirmed by many authors, observing that reversible transition between from hydrophilic to hydrophobic states was much more pronounced with longer chains and higher grafting densities. In some cases the transition was negligible or could not be even observed [109].

Immobilization of PNIPAM layers on surfaces can be achieved by many techniques, such as plasma polymerization, photoinitiated polymerization, atom- transferred radical polymerization (ATPR), reversible additional fragmentation transfer polymerization

(RAFT), nitroxide mediated radical polymerization (NMP), polymerizations on self assembled monolayer (SAM) modified surfaces, covalent grafting by ultraviolet and electron beam irradiation and plasma – induced grafting via plasma activation or peroxide radicals methods [110]. These various techniques were successfully employed for modification of diverse polymeric (PP, PE, PEO, PS, PTFE, PET) [111] and non-polymeric (Au, Si wafers, glass, hydroxyapatite) [112] substrates. These materials can be in the form of films, nanoparticles, membranes or any other kinds of supports.

Validations of temperature induced phase transitions of PNIPAM modified supports can be monitored by different approaches. Most common and available is the measurement of contact angle, where the character changes from hydrophilic below the LCST to hydrophobic above the LCST. The values of contact angles are reported to be from 40° to 65° at lower temperature and raised up to 90° at elevated temperature [113]. The angle 90° corresponds to alkyne/ alkene/ alkane surface energy, which implies that the hydrophobic parts of PNIPAM are completely exposed to the surface [114]. Other methods that were used to measure the transition of PNIPAM are atomic force microscopy (AFM) analyses, ellipsometry, surface plasmon resonance (SPR), quartz crystal microbalance (QCM) or light scattering (LS) and small angle neutron scattering (SANS) methods for nanoparticles and nanobeads [115].

An interesting experiment was done where PNIPAM was grafted on PEO pre-deposited Si wafers. First the poly (ethylene oxide) deposition was performed with continuous-wave plasma polymerization. After PEO layers were activated with argon plasma in the same reactor. The activated samples were removed from the reactor for 5 min and immersed into aqueous monomer solution of NIPAM where the polymerization took place [116]. Surprising results were obtain by continues and pulsed plasma polymerizations. The thermo-responsive behaviour of PNIPAM was retained even in the case when continues mode of polymerization was used, however only under very low discharge power. In the pulsed mode the time on of duty cycles governed the hydrophilicity of the surface polymer layer [117]. PNIPAM is often co-polymerized as well with different segments possessing specific properties. This can be various pH, salt, conductivity responsive materials like polyacrylic acid (PAA), acrylamide, N-*tert* butyl-acrylamide, etc [118]. Introduction of additives to the PNIPAM backbone can also change the LCST of the polymer. By these modifications, better control of parameters can be achieved, that are especially important for the *in-vivo* applications.

As it was mentioned above, the principle domain of PNIPAM employment is in bio medical applications, due to the reversible transition of polymer chains that occurs close to the body temperature. This property makes PNIPAM a promising candidate in many applications like temperature responsive membranes, temperature responsive chromatography, immuno-tests, controlled drug and growth factor release, tissue engineering, control of the attachment and the detachment of cells, the recovery of cultured cells and bio- fouling releasing coatings [119]. PNIPAM can be also coupled with various biological molecules (DNA, protein, antibodies) and can be used for the purification of the proteins and enzymes. For example the immunology tests are made by coupling an antibody to PNIPAM molecule and making it thermo-sensitive. The antibody reacts specifically with the searched antigen and in the next step the labelled detection antibody is coupled. When the temperature is increased they precipitate and interact with each other and by this increasing the signal. As the signal is multiplied, lower levels of proteins can be detected [120].

The growth of cells on PNIPAM is enhanced above the LSCT temperature (human body temperature), where the polymer possesses hydrophobic properties. The cells attach to the surface and proliferate. As the growth support is cooled down, the cells are reversibly released from the surface, without any conformational or functional changes

[121]. The same can be applied for reversible attachment and purification of the proteins (Figure 17). The controlled capture and release of several proteins, microorganisms and cells on PNIPAM prepared with different grafting techniques are reported by different authors [122,123]. They have managed to reversibly (de) adsorb various commercial proteins like avidin, BSA, HSA, myoglobin, cyt-C and lysozyme.

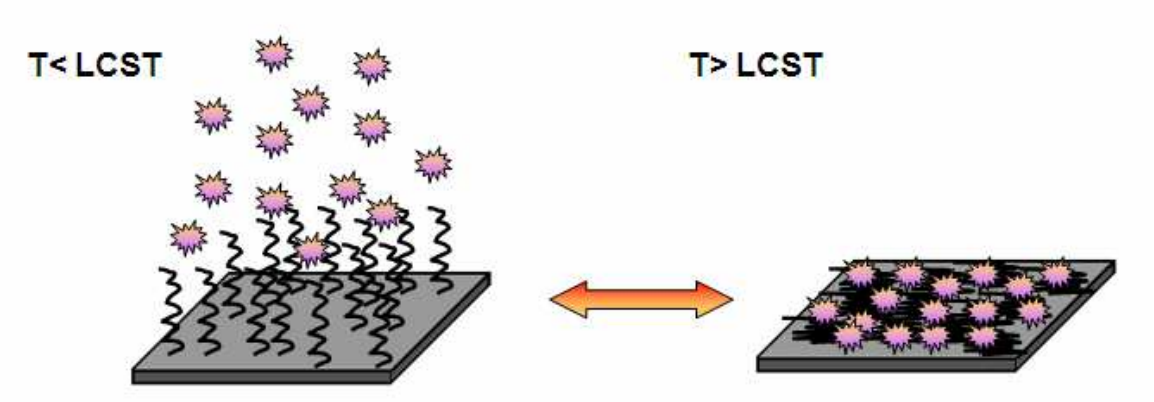

Figure 17: Reversible attachment and detachment of proteins on PNIPAM grafted substrate with the control of temperature below and above the LCST.

1.4 Proteins and surfaces

The study of protein surface interactions gained a lot of interest in the past few decades because these interactions are fundamentally responsible for biocompatibility of the materials. The biological cascade of undesirable reactions like bacterial adhesion or thrombogenesis can be triggered by the deposition of proteins on the surface of the material. This spontaneous adsorption will occur characteristically in order of seconds or minutes since the foreign surface is introduced into the protein solution. For this reason, it is rarely a problem to achieve the adsorption of proteins to the surface, but rather how to prevent it. Proteins are very complex in nature and the number of factors influence their adsorption, and consequently the prediction of interactions between proteins and surfaces remains an extremely challenging problem. Although the mechanisms of adsorption are not fully understood, there are few physicochemical characteristics that are known to influence these phenomena [124]:

a) type of protein (size, stability, concentration, functionalities and protein-protein interactions),
b) surface free energy (hydrophilic/ hydrophobic balance/ polarity),
c) surface charge and related electrostatic interactions,
d) type, thickness, density, adhesion and mobility of surface functional groups,
e) micro and nanotopography features and roughness,
f) time dependant unfolding,
g) Vromans effect,
h) Biological surrounding: pH, salts, temperature, etc.

1.4.1 Protein-surface interactions

The thermodynamic principles governing the adsorption involve number of enthalpic and entropic terms that are either favouring or resisting the adsorption:

$$\Delta_{ads}G = \Delta_{ads}H - T\Delta_{ads}S < 0$$

G, H, S and T stand for the Gibbs energy, enthalpy, entropy and temperature of the system, while Δ_{ads} indicates change in thermodynamic functions of state resulting from the adsorption process. The enthalpy part involves intermolecular forces such as van der Waals forces, Coulomb forces, Lewis acid-base forces whereas the entropy part is based on hydrophobic interactions, conformational entropy and restricted mobility. The adsorption will occur when the change in Gibbs (G) energy becomes negative and will be a net result between attractive and repulsive interactions between the surface of the material, protein molecules and the solvent (Figure 18).

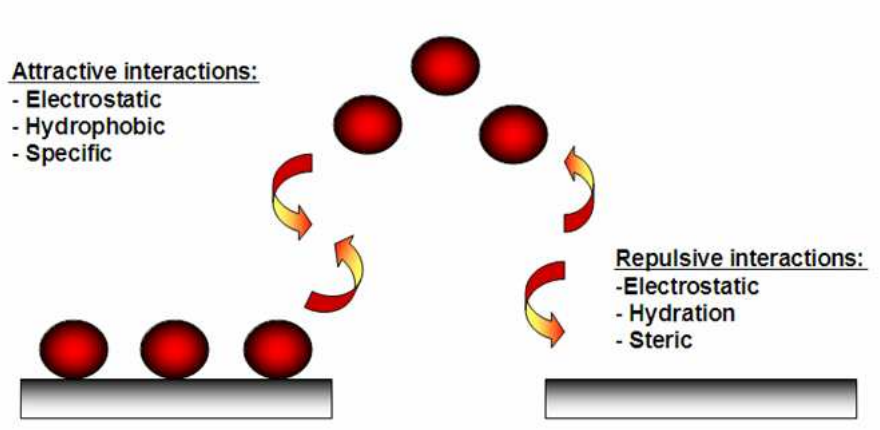

Figure 18: Scheme of attractive and repulsive forces governing the adsorption of the protein.

In general protein adsorption is believed to occur through several equilibrium states. First the proteins are transported towards the surface where they reach an energetic boundary layer, attach to the surface which can be followed by some structural rearrangements of the protein or they can be detached and transported away from the surface. The simplified scheme is shown in Figure 19. During the adsorption step, protein may rapidly unfold on the surface in order to adapt its energy to the new environment; all the proteins will actually partially unfold upon adsorption. The adsorption it self happens in microseconds to milliseconds, while relaxation demands much longer periods, from hours to days. In the case of very strong surface-protein affinity, non-equilibrium states can be retained or in other words they irreversibly adsorb to the surface [125].

The first layer of proteins can be adsorbed reversibly or irreversibly, while the second layer tends to adsorb reversibly due to little or no affinity among the proteins. Most authors are explaining that this phenomenon is probably mainly due to the retention of hydrated water by the protein molecules, preventing close interactions in the solution [126]. The reversible adsorption is often observed with smaller molecules, while the adsorption of big molecules like random polymer coils is rarely reversible. This behaviour arises from the fact that they posses many active sites that are able to adhere to the surface and even if it will loose contact at one point it will be still attached through many other segments. Proteins are polymers as well, however contrary to free polymer chains they form highly regular compact states with little flexibility. When they come into contact with the surface they do not unfold completely like polymers, therefore their detachment

becomes feasible due to much lower number of contacts with the surface [125]. Most of the surfaces (substrates and protein) are heterogeneous in charge, in H-bond affinities and hydrophobicity. This means that the proteins will react with surfaces in different ways and the orientation of the proteins on the surfaces will be affected. The adsorption of proteins will be also influenced by pre-adsorbed molecules in the nearby sites, either by geometrical or repulsive forces. Also the higher will be the bulk concentration the greater amount of protein will adsorb [127].

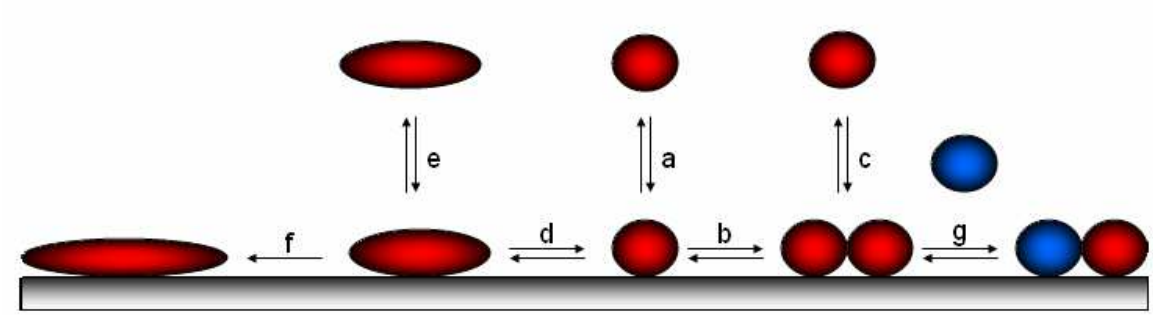

Figure 19: Adsorption paths of protein to the surface; a) protein adsorption- desorption, b) lateral mobility, c) dissociation of a protein attached to another protein, d) reversible denaturation and changes in protein conformation, e) dissociation of the altered protein, f) denaturation and irreversible adsorption and g) exchange of proteins from solution.

Another important factor is protein conformational stability in native state, the relative amounts of α-helixes and β-sheets, the overall hydrophobicity and electrical charge under working conditions. If the protein is weakly stable it will be preferably adsorbed to the surface because of the conformational contribution through adsorption in increase of entropy. Proteins are just conditionally stable under best solvent conditions and even a small change in pH, TºC, addition of denaturants will affect their stability. This is exactly what happens when a solid surface is exposed to the aqueous protein solution, the equilibrium is broken. Therefore proteins with low stability will adsorb and release their native structures. Adsorption is driven by the increase in the conformational entropy of the protein. The hard proteins go through minor conformational changes under the conditions that they are adsorbed to the hydrophilic surfaces [128]. It can be said that how the surface will be covered depends on many factors such as physical and chemical structure of the protein and the surface, thermodynamics of interactions and kinetics of mass transport. Because the adsorption is influenced by so many parallel and consecutive steps there are many new microenvironments that can be created and the adsorption becomes history dependant, leading to possible different results in the same systems [129].

1.4.1.1 Protein structure and properties

Proteins are linear polymers formed by linking the α-carboxyl group of one amino acid to the α-amino group of another acid with a peptide bond. These peptide residues are forming the (- NH- CHR- CO-) where R is standing for the various side functional groups-amino acids. These side groups are constructed from up to 20 various amino acids, which can be polar, apolar or charged. This is called primary structure of the protein, demonstrating the amino acid sequence (Figure 20.a). Primary structure spontaneously

folds to very regular secondary structures presented by alpha helixes or beta sheets. The coiled α-structure is stabilized by intrachain hydrogen bonds between NH and CO groups, while β-sheets are stabilized by hydrogen bonding between polypeptide strands. The next step is folding of secondary structures into tertiary structures where it comes to spatial arrangement of amino acids that are far apart in the sequence (Figure 20.b). This folding to tertiary structures enables the creation of active sites that are able to perform biological functions. Last conformation is called quaternary structure that occurs in some cases where multiple stand proteins (tertiary subunits) aggregate and form oligomeric proteins (Figure 20.c) [130].

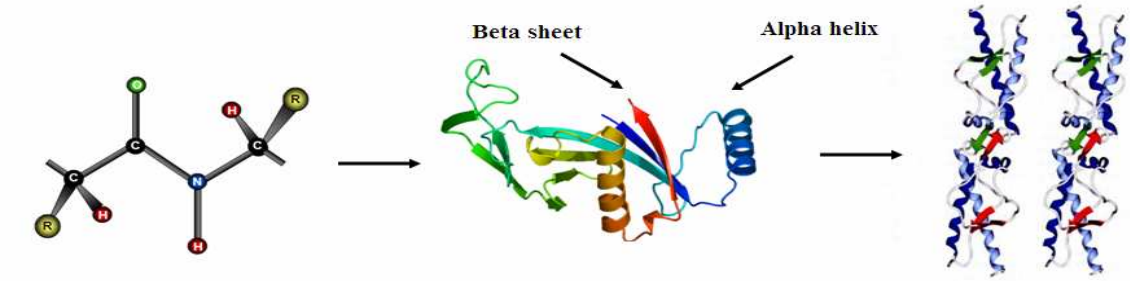

a b c

Figure 20: Structure of protein; a) primary structure (peptide bond), b) tertiary structure (composed of secondary structure presenting α-helixes and β-sheets), c) quaternary structure (aggregation of subunits formed in tertiary structure).

In general proteins fold into globular or fibrous forms. Globular proteins are compactly folded, while the filamentous are elongated. This fact will influence their stability and consequently the degree of conformational changes upon their adsorption on the solid surfaces [131]. The folding to tertiary and quaternary structures is governed by hydrophobic effect, where the free energy in the aqueous solution is decreased by burring of non-polar functional groups inside the protein. For this reason the proteins are generally constructed so that the hydrophobic part presents the core of the protein, while polar residues stay on the surface in contact with the solvent. However, in most of cases the protein surface is composed of polar and apolar parts (amphiphilic), where hydrophobic patches present one third of the surface coverage and polar parts between 25- 50%.

Furthermore, within the same protein the side chains can be acidic or/ and basic making the polypeptide amphoteric. The overall surface charge of the protein will depend on the pH of the solution and will have zero net charge at its isoelectric (pI) point. Usually 15 to 40% of protein surface is charged [132]. The non uniform distribution of amino acid residues on the exterior of the protein molecules, the overall geometrical asymmetry of proteins, and the existence of patches at the protein surfaces with different properties makes the proteins extremely surface active as demonstrated on the Figure 21. The favoured bonding of certain types of residues will also influence the orientation of the biomolecules, which is important for immunological reactions [127,133].

Protein aggregation can occur at all steps in the manufacturing process (cell culture, purification and formulation), storage, distribution and handling of products. It results from various kinds of stress such as agitation and exposure to extremes of pH, temperature, ionic strength, or various interfaces (e.g., air–liquid interface). High protein concentrations (as in the case of some monoclonal antibody formulations) can further increase the likelihood of aggregation.

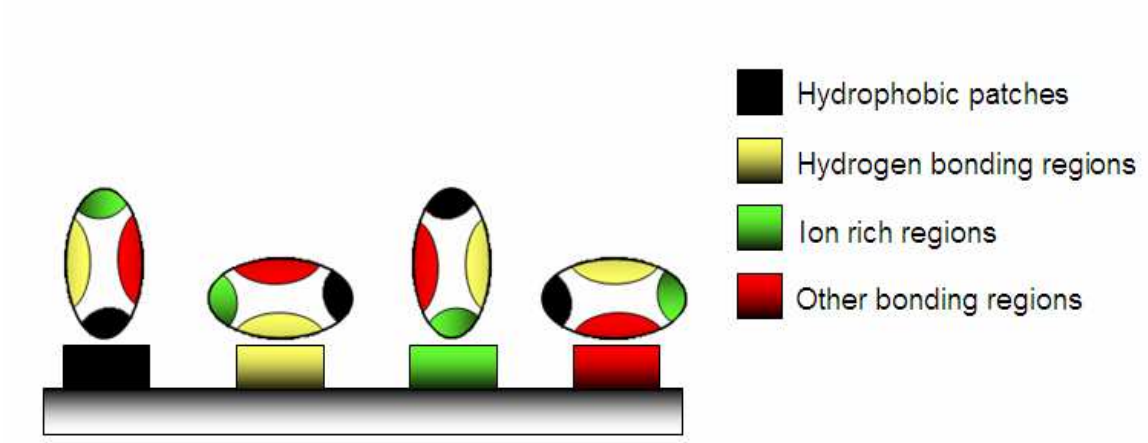

Figure 21: Demonstration of possible routes for protein adsorption reactions.

The protein folding and unfolding is “all or non” process that results from a cooperative transition. If there is one part of the protein that will be unstable under exposed conditions (temperature, high solute concentrations, pH extremes, mechanical forces and presence of denaturants) the interaction between this disrupted part and the rest of the protein will be destabilised. Thus conditions that lead to disruption of any part of a protein structure will likely to unravel protein completely. Inappropriate protein conformation can result in pathological conditions and is associated with various prion related neurodegenerative diseases, like Creutzfeld–Jakob disease, bovine spongiform encephalopathy and amyloid related neurodegenerative illnesses such as Alzheimer disease, Huntington’s disease and Parkinson disease. The appearance of these diseases is assigned to multimerisation of misfolded proteins into insoluble, extra cellular aggregates and/or intracellular inclusions [134].

1.4.1.2 Influence of surface hydrophobicity and hydrophilicity on adsorption

When a solid material is exposed to the protein solution they will tend to adsorb and saturate the surface. In the case of hydrophobic surface the proteins adsorb through different hydrophobic patches on the protein surface. In the next step the protein will want to unfold on this surface by spreading its hydrophobic core on the substrate in order to reduce the net hydrophobic surface area of the system in the solvent.

The unfolding of protein is accompanied by the release of water molecules from the interface leading to an entropy gain of the system. On the other side hydrophilic surfaces want to interact with the polar and charged functional groups of the protein surface, however in this case proteins have much lower tendency to irreversibly unfold on the surface [135]. In both cases the changes in the state of hydration have a large impact. Namely the water molecules in the solution are strongly bonded to the proteins and surfaces through electrostatic interactions including hydrogen bonding, rendering the polar groups solvable in water. If the surface of a protein and support are both polar their hydration is favourable. In this case it is possible that there is some water retained between the surface of substrate and the protein molecule which will prevent or diminish the adsorption (Figure 22) [136].

With polar surfaces it is very important to know the difference between “hard” and structurally unstable “soft” proteins. The “hard” proteins will adsorb on them only if they are electrostatically attracted, while “soft” proteins go through abrupt changes resulting in

the increase of conformational entropy large enough to cause their adsorption to otherwise electrostatically repellent surfaces [137]. As it was reported the adsorption of proteins on hydrophilic surfaces is mainly due to the Coulomb forces, therefore the design of non- fouling material is often based on polar and non-charged surfaces [138]. Generally it is observed on hydrophilic surfaces that the thickness of a monolayer obtained by ellipsometry, light scattering, viscosimetry, scanning probe microscopy or the surface force techniques corresponds to the diameter of native protein [139].

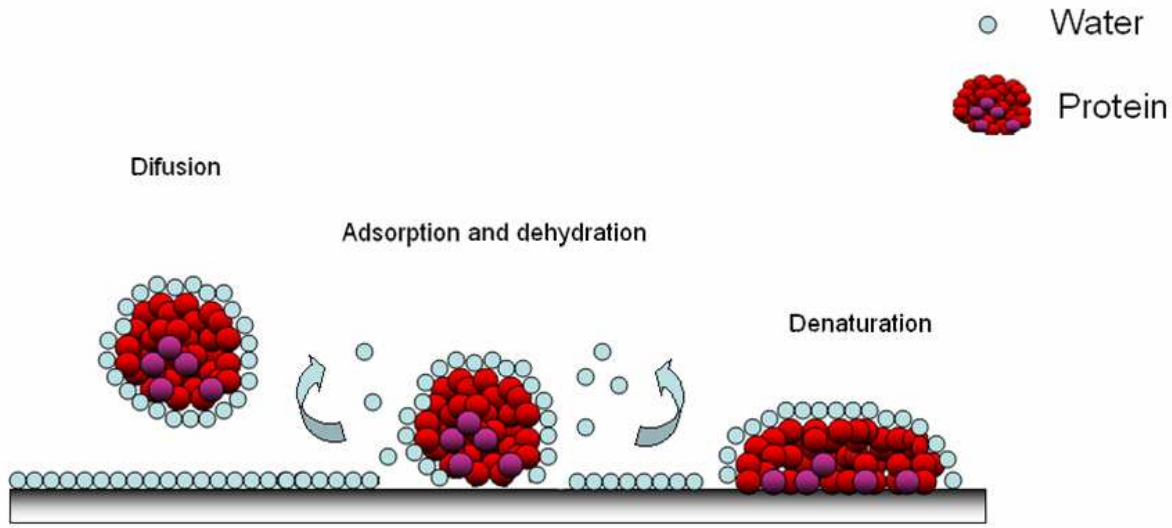

Figure 22: Adsorption of protein on a polymer surface; the diffusion of hydrated protein toward the surface, adsorption and dehydration and relaxation of protein and its denaturation.

Apolar groups on the contrary, do not have possibility for such favourable hydration interactions and are expelled from aqueous environment. The presence of apolar patches on the protein surface leads first to the dehydration and consequent protein adsorption that is accompanied by the release of hydrophilically bound water molecules from the interface, leading to an entropy gain of the system. The protein can relax upon the adsorption if long enough time of contact is provided; therefore it is possible that the proteins will aggregate on the surface. However this aggregation on the surfaces usually stops with the growing of the second layer, because there are not as much conformational changes of proteins that are adsorbed to irreversibly changed first protein layer. The growth of third layer will be prevented due to the low affinity of proteins among them selves, probably due to the thin hydration layer around their surface [140]. For example it is a general rule that proteins adsorb stronger and in higher quantities on hydrophobic surfaces, but it was reported as well that in solutions with high concentration of proteins, where that the mass transport is much higher than the rate of protein spreading and reorientation on the surface, adsorption was lowered on hydrophobic surfaces. For hydrophilic surfaces quite opposite effect was noticed; they can adsorb in higher amounts than on the hydrophobic surfaces [141].

1.4.1.3 Influence of charge on adsorption

Generally both molecular surface and protein are electrically charged. In aqueous medium they are surrounded by counter ions that neutralize the surface charge. These charge–charge interactions between the surface and the protein result in an electric field overlap. Electrical double layers will enhance the electrostatic interactions if the protein and the

surface have opposite charge or repulsion if the charge is the same. Maximal adsorption occurs when the charge density of the protein matches exactly to the one of the surface which results in a zero net charge at the contact region. Figure 23 is showing charge distribution for the system before and after adsorption [142]. The adsorption (to lower extent) can be observed as well on the surfaces that contain the same charge as protein. This indicates that global electrostatic forces without a doubt affect adsorption but do not necessarily dominate it [143].

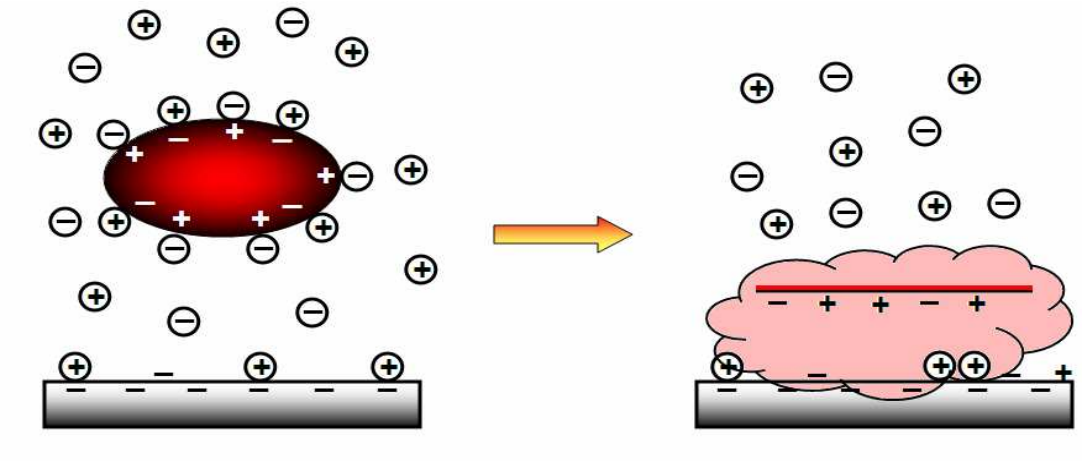

a) b)

Figure 23: Schematic presentation of charge distribution a) before and b) after the adsorption; +/- charge of the protein and substrate surface, ⊕/⊖ charge of electrolyte ions.

The electrostatic interactions will be strongly influenced by pH and ionic strength of the solution. At low ionic strength cationic proteins bind to anionic surfaces and reversibly. The major driving force for this event is the combination of ion- ion enthalpic interactions accompanied by entropy gain for released counter ions and water molecules. However these interactions are greatly diminished at physiological conditions, due to the weaker electrostatic interactions, shielding of protein ionic groups and greater stability of proteins [144].

For most of proteins the adsorption is maximal at their isoelectric points, because here the protein-solvent interactions become less favourable and protein-protein interactions more favourable, due to the zero net charge between them. At the pH far from pI of proteins the formation of double layers is very likely to be retained, due to the electrostatic repulsions as the charge on protein surfaces becomes more important. On the other hand the proteins are most stable at its pI and therefore high (low) pH solutions may lead to their denaturation and increased adsorption due to the lost of stability [145].

1.4.1.4 Influence of surface topography and roughness on adsorption

Current trends in research of biomaterials include the research of surfaces with topological features at nano-scale, up to 100 nm. The effects of micro scale topography on cellular responses are rather well explored *in vitro* from physico-chemical and biological aspects [146,147]. Recently few studies appeared that revealed the influence of nano-topography on protein adhesion and consequently altered cellular responses [148].

The reports how surface topography influences the protein adsorption are non-consistent. One of the reasons is the different nanoscale features that can be created on the

surface which will affect the amount and conformation of the adsorbed proteins. The characteristics of topographic features include roughness, curvature and specific geometrical features. Dynamic interactions between nanoscale surfaces and proteins are complex due to the combination of attractive and repulsive forces that are governed by local changes in surface properties, including its chemistry. Local wettability of the surface is also modulated and this may induce the different degrees of geometrical packaging of the proteins [149]. The overall effect of surface roughness from different reports available is not clear at this moment. Some reports suggest that the amount of proteins adsorbed is not (or very moderately) affected by the surface roughness and there was no conformational changes of proteins [150]; on the other side few reports reveal high augmentation of proteins adsorbed and abrupt changes in their conformations upon adsorption [149]. It was stated as well that proteins with dimension in the same order as the surface roughness are not conformationally altered by the surface and proteins with dimensions much smaller or much larger change upon adsorption [151]. Cai et al. [152] investigated the adsorption of proteins to surfaces with different roughness. They found no linear relationship between the surface roughness and protein adsorption. Other study of topography influence on adsorption of A and F-actin was performed by Galli [153]. They have seen that more F-actin adsorbed on the flat silicon surface comparing to the nanometer groove structure due to the inclination of F-actin on these features. On the other hand for globular A-actin there were no differences of adsorption behaviour or activity observed on different surface topographies.

The study of nano-topography influence on protein adsorption is still under development and a limited knowledge is known about this topic. It can be said for sure that nano-topography can have significant influence on the protein adhesion, where their size and shape play an important role. Furthermore the same nanostructures appear to have different influence on different proteins. In general, introduction of tailored nano-topographies in biomedical devices presents an attractive route to improve their performance for various applications. As all biomolecules possess three dimensional conformations and are not just planar the insertion of topography on the material surface enables “mimicking” their natural environment.

1.4.1.5 Protein adsorption from multi-component solutions

In complexes biological medium like blood, plasma, cerebrospinal fluid (CSF) or other body liquids, there exists a wide variety of different proteins. As a consequence, these proteins compete among them selves for the adsorption to the exposed surface. An important factor is a mass transfer towards the surface which depends on the concentration of individual protein in the solution and is inversely related to its molar molecular weight. Namely the more concentrated and smaller proteins arrive first to the surface and can be later replaced by larger proteins under the condition that they are able to form stronger interactions with the surfaces [154]. This effect is referred to as Vroman effect and was first described by Vroman and Adams [155] (Figure 24) for fibrinogen adsorption from blood and plasma. They have noticed when the artificial material was exposed to biological liquid, a rapid adsorption of albumin occurred, which was later replaced by higher molecular weight proteins like fibrinogen and kininogen.

However, this is true in the case of protein interaction with hydrophilic surfaces as there are weak conformation changes of protein under the adsorption, while for the hydrophobic surfaces the adsorption is often irreversible and the protein can not be replaced by another. As well, higher stability protein will be desorbed more easily as their

relaxation on the surfaces is much lower than in the case of “soft” proteins [156]. Therefore the adsorption of proteins from multi- component solutions will be dependant on time, concentration, type of protein and the surface. Depending on these conditions, the surface will be composed of higher degree of certain protein on account of decreased adsorption of others regarding to the bulk solution, even though it is present in much smaller concentrations [157].

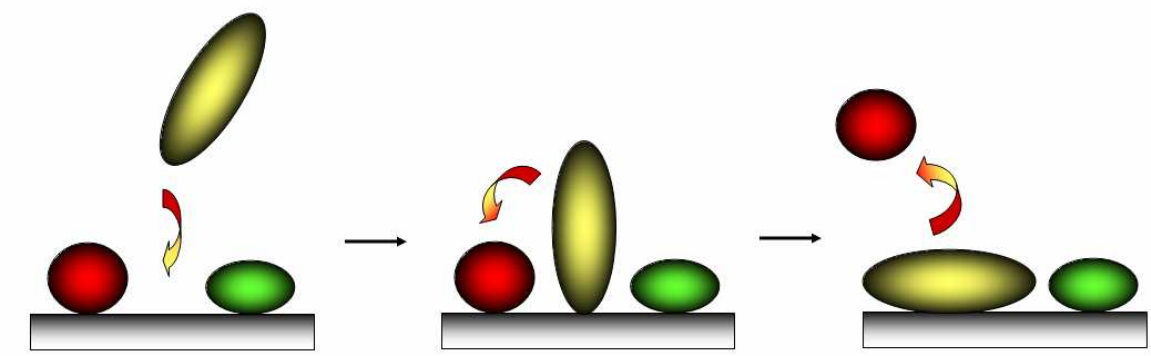

Figure 24: Illustration of the Vroman effect; replacement of protein adsorbed on the surface by higher molecular weight protein exhibiting stronger binding affinities for the surface.

1.4.2 Protein resistant surfaces

The adsorption of proteins can be diminished by either thermodynamic or kinetic control. Thermodynamic control refers to the alteration of the interaction potential between protein and the surface by eliminating the attractive interactions between them. Kinetic control can be achieved through slowing down the rate of protein adsorption by high potential barriers for the interaction, for example by introduction of long range repulsive forces through polymer grafting [158]. The efficiency of the polymer brushes to prevent the adsorption of the proteins was studied theoretically by Halperin, Jeon and Szleifer [159]. Halperin proposed that the adsorption will depend on the grafting density of polymer and that there are three possible situations of attachment that need to be avoided:

a) adsorption of protein to the outer edge of the brush due to the protein- brush interaction via Van der Waals or electrical double layer attraction,
b) adsorption of proteins upon compression of polymer film for large proteins
c) adsorption to the surface due to the diffusion of proteins through the brushes to the substrate as shown on Figure 25.

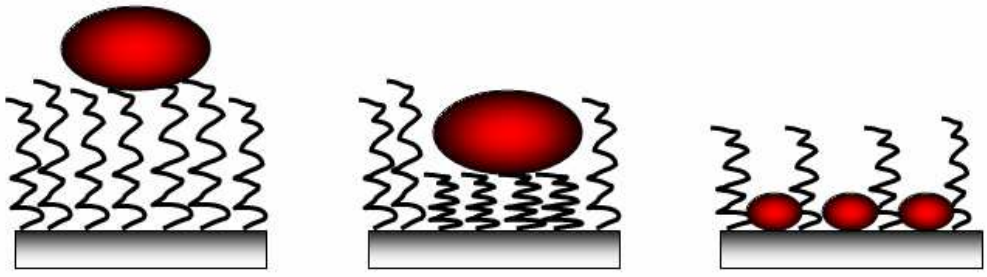

a) b) c)

Figure 25: Modes of protein adsorption on polymer brushes: a) adsorption at the edge of

the brush, b) compressive mechanism and c) invasive mechanism.

Accordingly to thermodynamic equation ($\Delta_{ads}G = \Delta_{ads}H - T\Delta_{ads}S < 0$), the functional groups on the surface should be lower in enthalpy when bound to the water than when bound to protein. Considering entropy the functional groups must be able to maintain the higher state of system entropy when bonded to water, than when bonded to proteins to reduce the restriction in the configuration state [160]. Also for this reason most of the non-fouling surfaces are based on synthesis of grafted surfaces with highly hydrophilic functional groups. These are in most cases neutral polymers like poly(ethylene glycol) (PEG) or poly(ethylene oxide) (PEO), polysaccharides (derivates of cellulose, dextran, agarose and hyaluronic acids), poly(acrylamide) (PAAm), poly(2-hydroxyethyl methacrylate) (PHEMA), N-vinyl pyrrolidone (NVP) and poly(2-methyl-2-oxazoline) (PMOXA) or zwitterionic polymers like phosphoryl choline [161,162].

There has been a great amount of studies and coatings proposed, however the highest amount of attention was given to the study of PEG and PEO and their di or tri- blocks (PEO-PPO-PEO, PLL-PEG) copolymer coatings [163]. Highly resistant protein behaviour of these polymers is prescribed to the several factors: high hydrophilicity (internal and external), high excluded volume, steric repulsion of the proteins due to the flexible chains, favourable enthalpy for the interactions of polymer chains with water comparing to the protein. Studies of oligo (ethylene glycol) (OEG) SAM-s layers showed that the density and length of the chains have a great influence on non-adsorption of proteins. Most of the reports are showing best results with long and highly dense graft chains, however some authors obtained very efficient resistance also with short densely grafted (1nm) PEO and PEG chains, indicating that the chain length does not seems to be a predominant factor leading to protein resistant surfaces. As well it was shown by some groups that too long OEG chains were not as performing when the grafting density was too high due to the limited mobility of chains [164].

Introduction of high density hydrophilic PEG chains through the side chains (poly (oligoethylene glycol) methacrylate (POEGMA) showed high protein resistance for various proteins due to the extremely good inter hydration of the chains (Figure 26). [165].

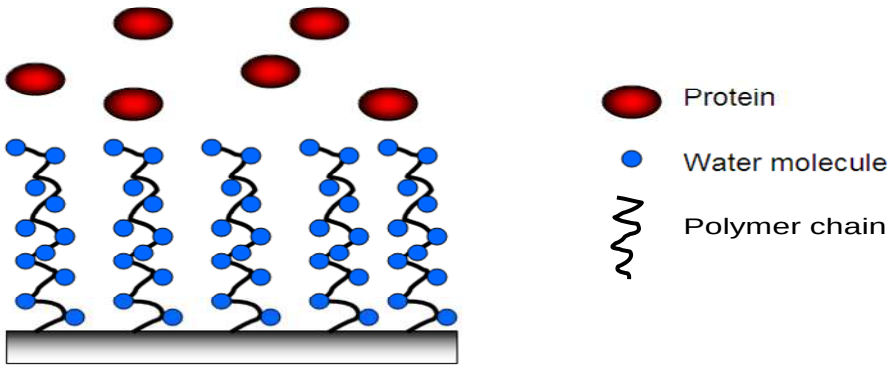

Figure 26: Scheme of protein repellent polymer grafted surface with extremely hydrated chains.

Another study [166] was made where they have modified 48 SAM layers by different functional groups and systematically studied the adsorption of lysozyme and fibrinogen as a function of surface coatings. They have stated that the surface in order to be non-fouling should be hydrophilic, possesses hydrogen bond acceptors, should not posses H bond donors and finally should be neutrally charged. The absence of hydrogen bond donor can

not be followed as a general rule, because as mentioned above oligo glycols contain these groups that are known to be highly non-adhesive. Another treatment that was found to exhibit no or negligible adsorption of various proteins like BSA, HAS, Lyz, Cyt C, fibrinogen and myoglobin is poly (N-isopropylacrylamide) PNIPAM grafted layers under its LCST. When the temperature increases above the LCST they adhere to the dehydrated PNIPAM surfaces and their affinity can be rather reversibly controlled by change of temperature. The detachment reported varied between 60 % and 100%, where 100% corresponds to complete detachment of proteins [167,168]. These reversible behaviour of protein adsorption on the PNIPAM and PNIPAM based grafted surfaces is often used for purification of proteins and nucleic acids (DNA, ssDNA and RNA), membrane modifications and gene delivery vectors [169].

1.4.3 Physicochemical properties of specific proteins: prion protein, Tau and α-synuclein

Prion protein related illnesses include diseases like fatal familial insomnia, Gerstmann-Sträussler- Scheinker syndrome and Creutzfeld-Jakob disease (CJD). Different forms of prion proteins can exist in the nervous system. The normal cellular form (PrP^{C}) and infectious form of prion protein (PrP^{Sc}) called as well scrapie prion protein. The mechanism of transformation is not yet completely understood, but is believed that the PrP^{sc} induces further misfolding of normal cellular protein. These misfolded forms accumulate in the brain and destroy the nerve cells. The cellular and infectious forms differ just in their conformation; the normal cellular PrP^{c} has alpha helix content around 42% and negligible beta character 3%, while the infectious form possesses 43% of beta rich sheets, while the amount of alpha helixes diminishes to 30% (Figure 27) [170].

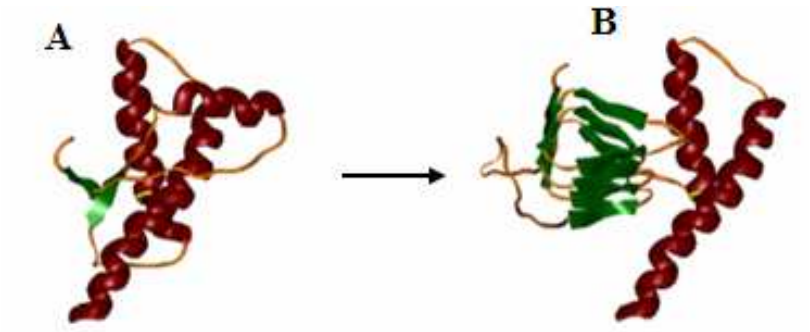

Figure 27: Three dimensional structure of Pr^{Pc} (A) and a model proposed for PrP^{sc} (B).

Another protein involved in development of neurodegenerative diseases is α-synuclein. Soluble α-synuclein can aggregate and form insoluble fibrils referred to as Lewy bodies and enhances the evolution of pathological diseases like multiple system atrophy, dementia with Lewy bodies and Parkinson's disease. Synucleins are relatively unstable proteins, composed of α-helixes and beta sheets in equilibrium (Figure 28). When this equilibrium is interrupted, there is a strong increase in beta sheets, suggesting that this could be responsible for aggregation and fibrillization of α-syn. The primary structure of α-syn is divided into three main domains: residues from 1-60 (N-terminal region) that is dominated by α-helix sequence, 61-95 residues (central region) consisted of hydrophobic parts involved in protein aggregation and 96- 140 residues (C-terminal region) without special conformation structures that is highly acidic and rich with proline [171].

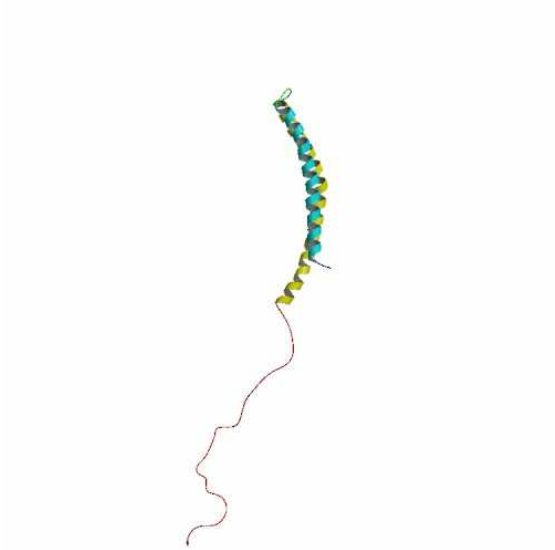

Figure 28: Three dimensional structure of α-synuclein.

Tau protein is a soluble microtubule associated protein that is found mostly in neuronal cells. The role of Tau protein is to stabilize the microtubules and when this stabilization is defected the Tau proteins aggregate in human brain and form neurofibrillary tangles (NFTs). These tangles are formed by hyper phosphorylation of Tau protein (pTau) and self- assembly of paired helical filaments (PHF). The most known "Tauopathy" nowadays is Alzheimer's disease. Tau protein exist in six isoforms, distinguished by number of binding domains, making their size vary between 352 and 441 amino acids. Next to the abnormal levels of pTau found in the cerebrospinal fluid (CSF) of patients with Alzheimer's disease, there is also subtype of amyloid beta peptide (Aβ-42) that is used for diagnostic purposes [172]. Some basic characteristics of studied proteins are gathered in Table 3.

Table 3: Basic properties of representative proteins. Hyl –hydrophilic, Hyb- hydrophobic.

Proteins/ properties	**Prion protein**			**α- syn**		**Tau protein**			**AB**
	PrP^{rec}	PrP^{c}	PrP^{sc}	α^{rec}	α^{oligo}	Tau^{rec}	pTau	Tau^{PHF}	Ab42
pI	9.8	5.8-6.5	4.6	4.7	4.6-5.1	4.7-6.9		5.5-6.5	5.5
Size (AA)	218	231		140		441			
form					filament		filament	filament	
Hydrophobicity	Hyl		Hyb	Hyl					Hyb

2 Experimental part

This chapter is describing methods used for development of non-adhesive surfaces towards the specific neurodegenerative agents and their characterisation. In the first part polypropylene plates were modified in weakly ionized, low-pressure radio frequency (RF) plasma of tetrafluoromethane (CF_4) and helium. Helium plasma activated supports were coated with a thin layer of polymer or mixtures polymer-surfactant. Various surface analyzing techniques were employed to study the characteristics of modified polymers. Plasma phase was monitored by optical emission spectroscopy (OES) and actinometry measurements. The wettability of samples was measured by contact angle method, chemical composition by X-ray photoelectron spectroscopy (XPS) and surface morphology by atomic force microscopy (AFM). In the second part the optimally prepared samples were exposed to various protein solutions and their interaction was followed by XPS analyses and confocal microscopy. Finally the third part of this chapter presents the protocols for immunodetection of the neurodegenerative agents (recombinant and in cerebrospinal fluid- CSF) stored in treated Eppendorf tubes by Enzyme-linked immunosorbent assay (ELISA) tests. The plan of experimental work is presented in Figure 29.

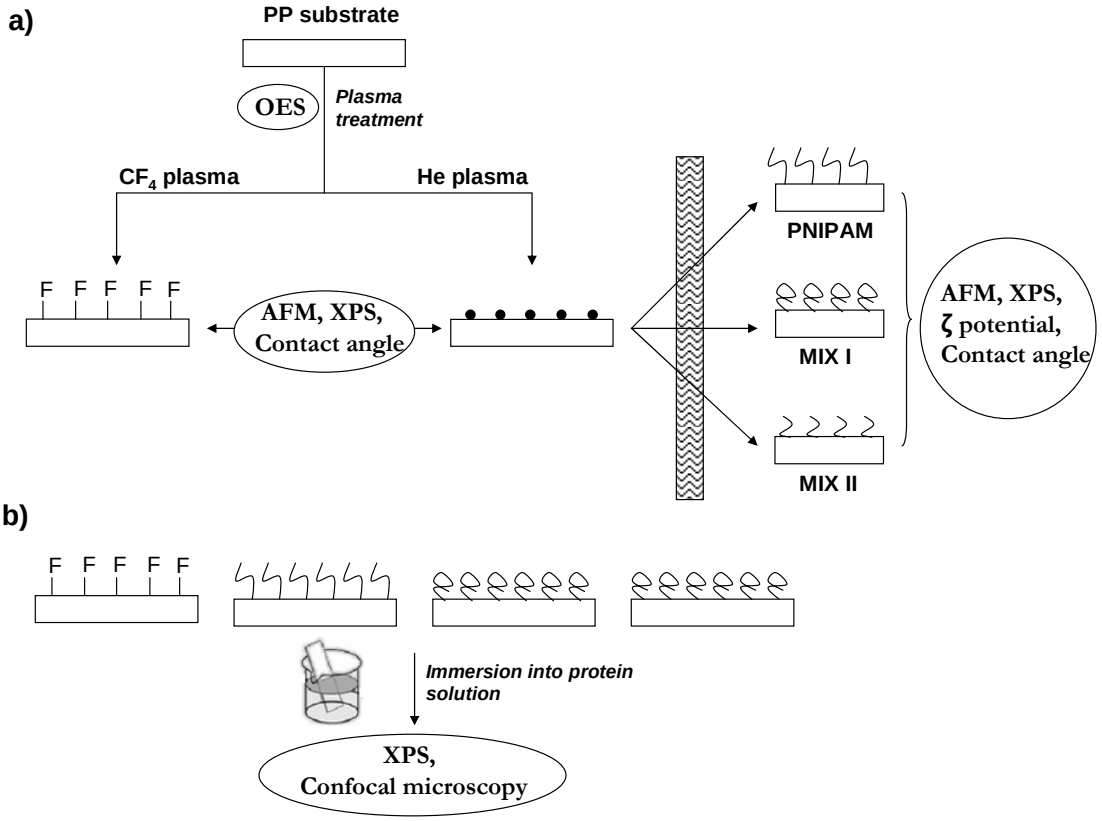

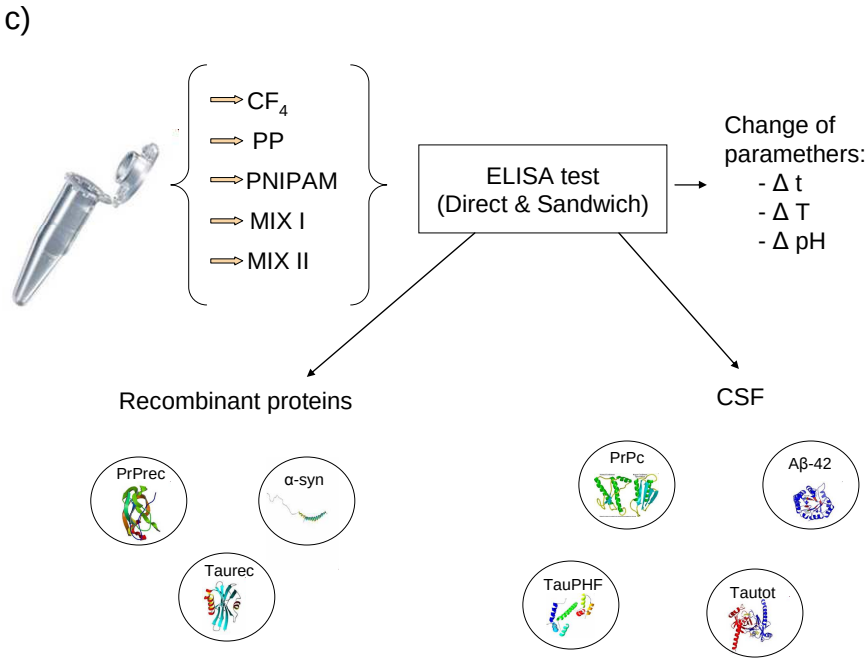

Figure 29: Outlined plan of experimental work; a) substrate functionalization, b) protein coating and c) biological validation of Eppendorf tubes.

2.1 Functionalization of supports

2.1.1 Plasma treatment

Plasma treatment experiments have been performed in the discharge chamber shown in Figure 30. The chamber is made from stainless steel and has inner dimensions 28.5x13.8x 23.5 cm^3. The flat rectangular electrode is powered by a RF generator via a matching network. The RF generator operates at the industrial frequency of 13.56 MHz and the output power up to 120 W. The system is pumped with a turbomolecular pump with the nominal pumping speed of 900 m^3h^{-1}backed by a two stage oil rotary pump with the nominal pumping speed of 25 m^3h^{-1}. Pressure is measured with a baratron attached to the discharge chamber. The ultimate pressure in the system is about 1×10^{-5} mbar. Gases are leaked in the system through flow meters. The experiments were realized by optimization of the following treatment parameters:

- discharge power (P, W)
- gas flow (Φ, sccm)
- time of treatment (t, min)
- type of gas

The experiments of plasma treatment were performed as follows. The polypropylene supports and Eppendorf tubes (both produced by EUDICA, Annecy) were washed in ethanol solution under ultrasound for 15 min and dried over night under laminar flow. Cleaned samples were mounted onto the bottom of the discharge chamber. The chamber was closed and pumped by the rotary pump until the pressure around 1×10^{-2} mbar was obtained. Afterwards the turbomolecular pump was turned on and the pressure dropped significantly until it reached the pressure of 1×10^{-5} mbar, typically after 30 min of pumping. Either

tetrafluormethane or helium gases were then introduced into the discharge chamber. The discharge was created at the power between 10 and 100 W, whereas the time of treatment varied between 0 min and 10 min for CF_4 treatment and between 0 min to 3 min for helium plasma activation. The flow of CF_4 gas was varied form 10 sccm to 40 sccm and the flow of helium gas from 15 sccm to 90 sccm. After the treatment the discharge power was cut off and the reactor chamber was set back to the atmospheric pressure. The samples were taken out from the discharge chamber for further treatments and analyses.

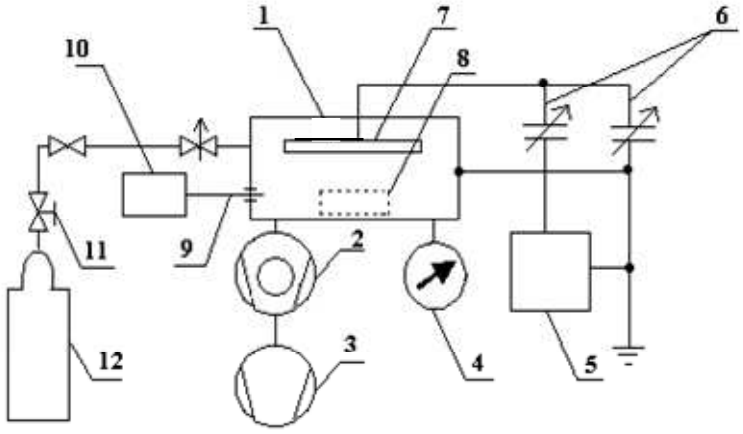

Figure 30: The experimental setup. 1 – discharge chamber, 2 – turbomolecular pump, 3 – rotary pump, 4 – vacuum gauge, 5 – RF generator, 6 – matching network, 7 – powered electrode, 8 – sample, 9 – optical fiber, 10 – optical spectrometer, 11- high pressure valve, 12 – gas flask.

2.1.2 Preparation of immersion solutions

Three different types of aqueous solutions containing polymer and polymer/surfactant mixture were prepared for the immersion of the helium plasma activated samples. Commercial poly(N-isopropylacrylamide) (PNIPAM) with M= 20000-25000g/mol was provided from Sigma Aldrich. The crystals were diluted in distilled water and agitated with magnetic stirrer for 3 h at room temperature (RT) until they completely dissolved. The concentration of PNIPAM solution was adjusted between 0.001 g/L and 10 g/L.

The second solution is a mixture of PNIPAM and hexadecyl-trimethyl-ammonium bromide (CTAB, Sigma Aldrich). CTAB is a surfactant molecule with molecular weight of 364.45 g/mol and critical micelle concentration (CMC) equal to 1 mM. The CTAB powder was diluted in distilled water under ultrasound for 1h at 40ºC. For classical grafting tests CTAB was prepared at the c= 1 mM and added to PNIPAM solution with c= 0.5 g/L at the volume ratio V_{CTAB}/V_{PNIPAM}= 1:1. This mixture was stirred for at least one hour before using at room temperature. From now on it will be referred to as MIX I.

The third solution is composed of PNIPAM and polyoxyethylene (POE 20) sorbitan monolaurate or commercially known under the name Tween 20®. Tween 20® (M= 1227.54g/mol, CMC= 8.04×10^{-5}) was provided from Sigma Aldrich and diluted in the distilled water to the concentration of 50 µl/L, or 0.05% at room temperature. Afterwards PNIPAM at the c= 0.5 g/L was heated up to 28ºC and the Tween 20® solution was added in $V_{Tween\ 20}/V_{PNIPAM}$= 1:1. The solution was agitated with magnetic stirrer for 2 h at elevated temperature of 40ºC and used hot for further grafting. The increase of temperature for this

mixture is needed due to the low affinity of neutral polymers toward the neutral surfactants. Namely the increase of temperature will induce the reorientation of PNIPAM chains and consequently the self assembly based on hydrophobic interactions can occur. A name MIX II was applied to this mixture.

For the study of polymer to surfactant ratio the solutions were prepared at $n_{polymer}/n_{surfactant}$= 1/5, 1/10, 1/50, 1/100 and 1/1000 for MIX I and 1/5, 1/10, 1/25, 1/50 and 1/500 molar ratio for MIX II. The molecular formulas of PNIPAM, CTAB and Tween 20® are presented in Figure 31.

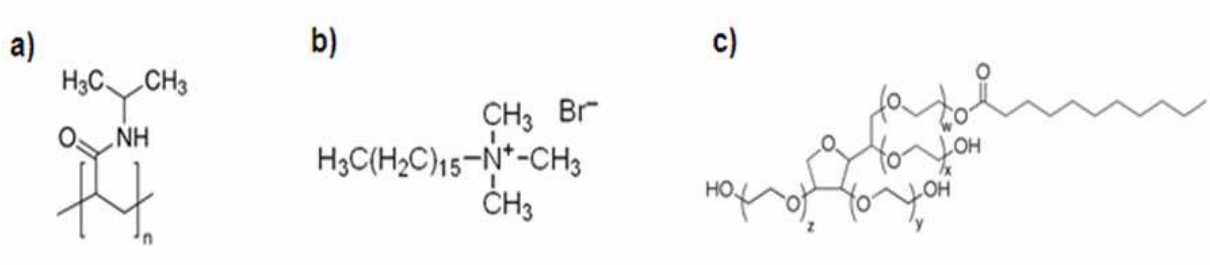

Figure 31: Molecular formulas of a) poly(N-isopropylacrylamide), b) hexadecyl-trimethyl-ammonium bromide and c) polyoxyethylene (POE 20) sorbitan monolaurate.

2.1.3 Surface grafting

The helium plasma activated samples were taken from discharge chamber and immediately immersed into PNIPAM, MIX I and MIX II solutions. Typical time between the exposure of samples to air and their immersion was well below 30 s.

In order to optimize the grafting parameters of PNIPAM, the helium activation conditions were fixed to P= 75 W, Φ= 30 sccm and t= 3 min, whereas the immersion was done in solutions with different PNIPAM concentrations between 0.001 g/L and 10 g/L for 2 h. After that time the samples were taken out of solution and immersed into distilled water for a short duration (around 5 seconds) and dried under laminar flow at room temperature over night. In the next step the solution concentration was fixed at 2 g/ L and the time of dipping varied from 5 min to 300 min for the same plasma parameters. Finally the study of plasma treatment time on grafting of PNIPAM was done. The helium plasma was created at P= 75 W and Φ= 30 sccm, while the time of treatment varied between 0 and 180 s. The solution concentration was fixed at 0.5 g/L and the time of immersion to 2 h.

The grafting of MIX I was performed after 60 s of helium plasma activation at P= 75 W and Φ= 30 sccm, whereas the time of the immersion was pre-determined to 5 h. In the first part of the experiments the influence of polymer and surfactant concentration on the grafting were studied. Concentration of PNIPAM (C_p) was fixed at 0.5 g/L and concentration of CTAB (C_c) was changed between 0.1 and 2 mM or the concentration of CTAB was fixed at 1mM and concentration of PNIPAM changed between 0.02 and 2 g/L. Likewise for PNIPAM, the influence of plasma treatment time (0 s to 180 s) on surface modification was studied. The variations between the polymer and surfactant concentrations were done with a purpose to observe at which conditions it would be possible to obtain structured mixed micelles like suggested in Figure 32.

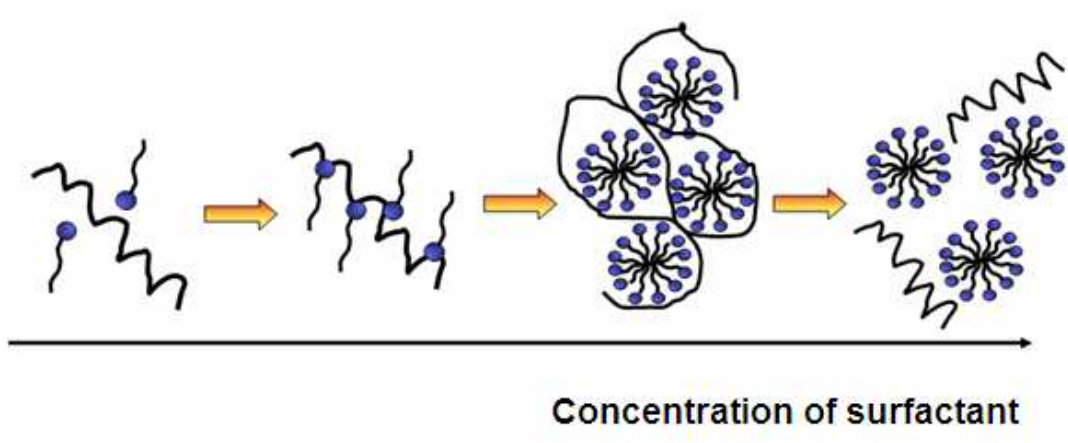

Figure 32: Influence of surfactant addition on self- assembly of protein and surfactant and formation of mixed micelles.

Similarly to PNIPAM and MIX I, MIX II was grafted to helium activated samples after 180 s of activation at P= 75 W and Φ= 30 sccm. The dipping in the solutions with different concentration ratios between PNIPAM and Tween 20® lasted 5 h at the temperature of 28ºC. The concentration of PNIPAM (C_p) was fixed at 0.5 g/L and the mass fraction of Tween 20® (W_T) varied between 0.01% and 0.1%. After that the concentration of Tween20® was fixed at 0.05% and concentration of PNIPAM changed between 0.02 and 2 g/L. In the following step the activation of PP plates with helium plasma was varied between 0 s and 180 s, before the immersion. All substrates grafted with MIX II were rinsed with warm water and dried at elevated temperature (T=40ºC).

2.2 Characterisation of plasma by optical emission spectroscopy (OES)

Optical emission spectroscopy was used for *in-situ* diagnostics of excited species present in the plasma discharge as a function of discharge parameters. In this work an optical emission spectroscopy of CF_4 and He plasma was performed by using JOBIN YVON TRIAX 320 monochromator with a focal length of 32 cm. The photons are detected with a CCD camera with a spectral response in the range from 180 to 1000 nm. The spectrometer is equipped with two high resolution diffraction gratings (1200 grooves/mm, 0.05 mm), where the first one is centred at 250 nm and used mainly for the measurements in the UV region (180 nm to 400 nm) an the second one is centred at 500 nm, used for measuring in the visible and near IR region (400 nm to 1000 nm). Plasma glow luminescence is detected through an optical window linked by an optical fibre to the input of JOBIN YVON HR 320 spectrometer. Signal is then amplified by HAMAMATSU R928 photomultiplier and processed by the software (version 3.2, JOBIN YVON). The spectrometer is linked to the controller Spectralink JOBIN YVON to control and to process data.

Quantitative analyses of the species concentration in the initial state were evaluated by actinometrical measurements, where 2% of Ar gas was added to the feed gas of the plasma. The principle of the method is described in the following lines. The electron impact excitation reaction of the ground state is $e^{-}* + X \rightarrow X* + e^{-}$, where X is the species of interest. Excitation is followed by emission of photon: $X* \rightarrow X + h\nu$. The emission from the

excited state can be expressed as:

$$I_i = \Gamma_i k_i [e^-][i] \quad (1)$$

where I_i is the intensity of the emission from species i (either X or actinometric gas), $[e^-]$ is the electron density, [i] is the concentration of species I, k_i is the excitation efficiency of species I and Γ_i is the branching ratio for emission relative to all other de- excitation paths. The excitation efficiency is a function of the electron energy distribution and the excitation cross section:

$$k_i = \int_0^\infty \nu(\varepsilon)\sigma_i(\varepsilon) f(\varepsilon) d\varepsilon \quad (2)$$

where ε is the electron energy, ν(ε) is the electron velocity, $\sigma_i(\varepsilon)$ is the collision cross section for the excitation of I, and f(ε) is the electron energy distribution. Actinometry accounts for changes in electron density by scaling the emission intensities of X with the emission intensities of inert gas atoms as follows:

$$\frac{I_x}{I_{Act}} = \frac{\Gamma_x k_x [e^-][X]}{\Gamma_{Act} k_{Act} [e^-][Act]} \quad (3)$$

Typically, the electron- impact excitation cross sections are chosen in the way that the excitation energy thresholds are comparable and in this case the same group of electrons is responsible for excitation of both species. With these conditions met, the relative concentration of reactive species can be determined from the ratio of emission intensities:

$$[X] \propto \frac{I_x}{I_{Act}} [Act] \quad (4)$$

The use of this technique involves ensuring that the addition of actinometer (noble gas) does not change the characteristics of plasma.

2.3 Surface characterisation

2.3.1 Surface grafting

The contact angle method was used to determine the surface energy components of solid plates and their acid-base character. The measurements were performed with RAME HART goniometer (model 100-00-230) equipped with:

- A sample holder
- An optical fiber illuminator (Green light source)
- A rotating protractor combined to an optical magnification of x 23
- A micro-syringe

In our study the surface energy of the samples was calculated from the contact angle measurements of three different liquids (ultrapure milliQ water, diiodomethane and glycerol, using the Fowkes and Owens-Wendt method:

$$\gamma_l (1+\cos\Theta) = 2 (\gamma_s^d \gamma_l^d)^{1/2} \quad \text{and} \quad \gamma_l (1+\cos\Theta) = 2 (\gamma_s^d \gamma_l^d)^{1/2} + 2 (\gamma_s^p \gamma_l^p)^{1/2} \qquad (5)$$

where γ stands for surface energy, Θ for contact angle and the indexes s and l indicate the solid and liquid respectively. The exponents d and p present dispersive and polar components of the surface energy. The surface energies of different liquids are gathered in Table 4.

Table 4: Surface energies of different liquids used for contact angle measurements.

Liquid	γ_l (mJ/m^2)	γ_l^d (mJ/m^2)	γ_l^p (mJ/m^2)
Water	72.8	21.8	51.0
Diiodomethane	50.8	49.5	26.4
Glycerol	63.4	37	1.3

Several drops of water (3μL), diiodomethane (1.5 μL) and glycerol (1μL) were deposited on treated and untreated surfaces in order to improve the accuracy of the results. Moreover the same treatments were done and measured numerous times. The average error for most of the measurements was below ± 2º.

2.3.2 X-ray photoelectron spectroscopy (XPS)

The surface of the samples was analysed with XPS instrument TFA XPS Physical Electronics. Typical time between the samples preparation and analyses was around 14 days. The pressure in the XPS analysis chamber was about 6×10^{-10} mbar. The samples were excited with X-rays over a 400-μm spot area with monochromatic Al $K_{\alpha 1,2}$ radiation at 1486.6 eV. The photoelectrons were detected with a hemispherical analyzer positioned at 45° with respect to the normal to the sample surface. The energy resolution was about 0.6 eV. Survey-scan spectra were made at a pass energy of 187.85 eV, while the form of the C1s peak was analyzed at a pass energy of 23.5 eV and a 0.1-eV step. Since the samples are insulators, we used an additional electron gun to allow the surface neutralization during the measurements. The spectra were fitted using MultiPak v7.3.1 software from Physical Electronics, which was supplied with the spectrometer. The curves were fitted with symmetrical Gauss-Lorentz functions.

2.3.3 Zeta potential measurements

The measurements of zeta potential were done by the ZetaCAD provided by CAD instrument. The buffer solutions for the ζ(pH) measurements were prepared in ultra pure milliQ water with addition of NaCl prior to any change in pH. In order to avoid the excessive amount of ions on the electrodes and their saturation the NaCl solution was prepared at the concentration of 1.7×10^{-3} M. In the next step the solution pH was adjusted by addition of either NaOH or HCl until the pH= 3, 4, 5.5, 7.4 and 9.6 were reached. The pH of the solutions was measured by pH meter HI-8014 from HANNA Instruments. The electrolytes were introduced in the cell at constant temperature of 25ºC and sent in between the samples at pre- determined pressure that remained the same for all measurements. For each sample the liquid passed from one cell to another and back until

the potential stabilized, on average after 5 cycles. The example of obtained curve can be seen in Figure 33 for MIX I sample at pH= 5.5.

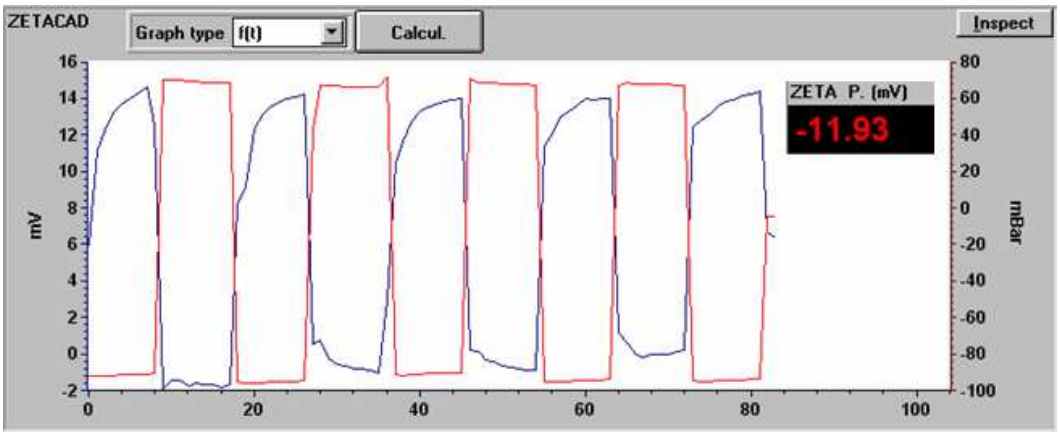

Figure 33: Zeta potential measurement of MIX I treatment at pH= 5.5.

In the next phase the potential was calculated with ZetaCAD software where the conductivity needed to be artificially corrected with a proper value measured with a conductivity meter. Between each change of solution with different pH, the instrument was rinsed with ultra pure milliQ water, where 3 cycles between the cells were done. In order to eliminate the effect of hysteresis the measurements were always performed from the lowest pH=3 to the highest pH=9.4 and backwards. For each sample the experiment was repeated three times, therefore the results represent the average of six measurements for each pH.

2.3.4 Atomic force spectroscopy (AFM)

Surface morphology and roughness was observed by atomic force microscopy. The imaging was done with AFM (Solver PRO, NT-MDT, Russia) in the tapping mode in air. The samples were scanned with standard Si cantilever with a constant force of 10 N/m and the resonance frequency of 170 kHz. All measurements were done typically after 2 weeks of treatment on areas 10×10 μm^2 and 5×5 μm^2. The average surface roughness (Sa) was calculated from images made of areas measuring 5×5 μm^2. To obtain representative results average surface roughness was obtained from 5 different areas.

2.3.5 Confocal microscopy

The imaging of protein coated samples was performed by confocal microscopy, type Leica TCS-SP2 (Leica Microsystems Heidelberg, Germany). The protein solutions of $PrPrec_{hum}$, Tau_{rec} and α-syn were prepared at the c= 50 ng/mL in PBS buffer solution at pH=7.4. Each protein solution was stained with Rhodamine at the volume concentration 0.5 %. In parallel a blank suspension of buffer solution and rhodamine was prepared with absence of proteins (at the same rhodamine concentration). The concentration of rhodamine was determined from several preliminary tests with a purpose to obtain optimal conditions with lowest background caused by rhodamine interaction with the surface. These tests were done on highly repellent and highly attractive surfaces for chosen proteins in order to optimise the concentrations used. Prepared solutions were

smeared over the untreated and treated samples and left for 2 h. After that time, samples were quickly splashed with distilled water and dried under laminar flow over night. These supports were after attached to microscopy slides and analysed by confocal microscopy.

2.4 Biological validation of Eppendorf tubes by ELISA tests

The untreated, CF_4, PNIPAM, MIX I and MIX II treated tubes were stored under nitrogen atmosphere and tested for their storage capabilities by Enzyme-linked immunosorbent assay (ELISA) tests on several proteins. The tests were performed approximately one week after preparation of the tubes. Nonetheless, a separate test was made with tubes developed and stored for 6 months in order to assure that the efficiency of tubes remained unchanged.

The ELISA test involves chromogenic reporters that indicate the presence of antigen by observable colour change that is monitored by a spectrophotometer. The principles of direct and "Sandwich" ELISA test are shown in Figure 34.

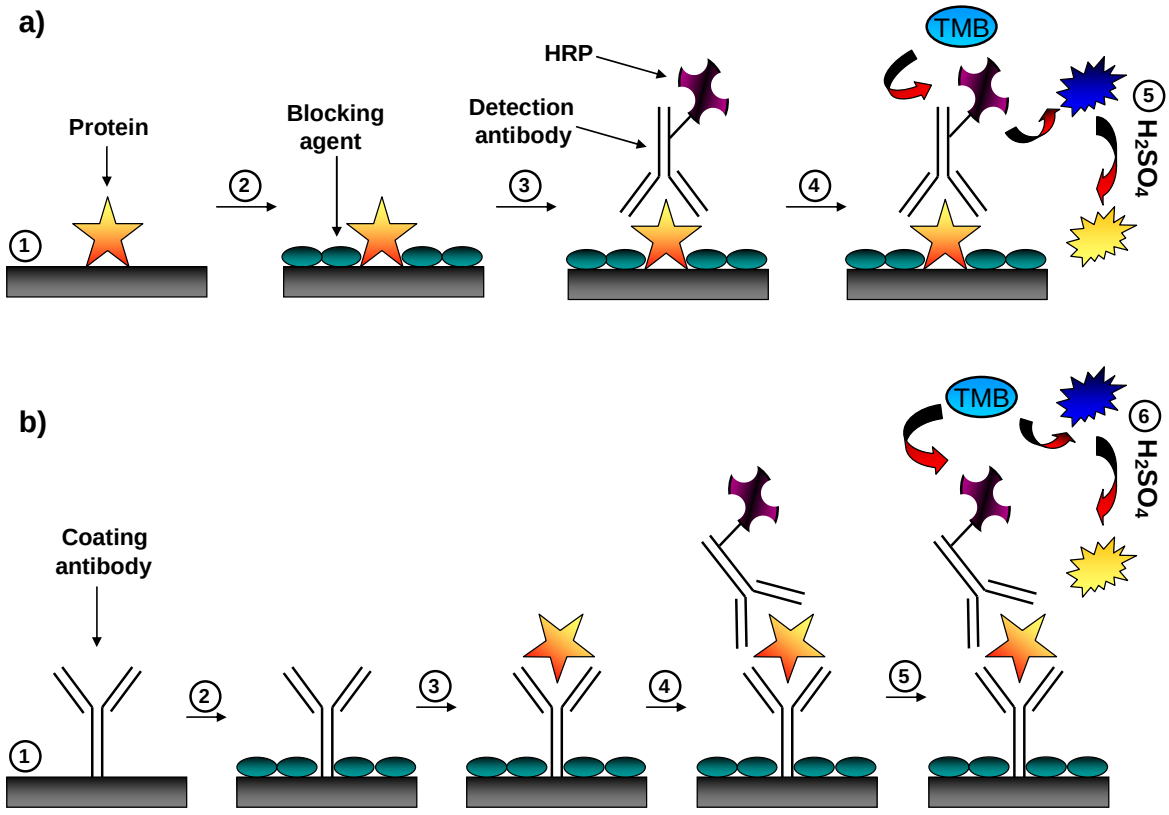

Figure 34: Scheme of a) direct and b) "Sandwich" ELISA test.

In the direct ELISA test the antigen solution was stored in the Eppendorf tubes at specific experimental conditions (temperature, time and pH). In the next step tubes were purged and washed with buffer solution in order to remove the antigen that did not attach to the surface of the tubes. This supernatant that was removed from the tubes is directly deposited to the pre- coated and blocked strips (prepared a day before) used for complementary "sandwich" ELISA test (Figure 34.b, third step). Tubes are then exposed to a solution that is containing

blocking agents (BSA, gelatine, Tween, Casein) until the surface is saturated. This is followed by a washing step and addition of the detection antibody coupled with an enzyme, like for example horseradish peroxidase (HRP), which is used to amplify a signal and increase the sensibility of a target molecule. The unfixed HRP is then washed with the buffer solution and 3,3',5,5'-tetramethylbenzidine (TMB) is added. TMB forms a blue product when it reacts with the peroxidase. Further addition of sulphuric acid stops the reaction and turns TMB yellow. This colour is at the end read with the spectrophotometer at 450 nm. Therefore the optical density measurements obtained by direct ELISA tests will be proportional to the amount of protein adsorbed on tubes. On the other hand "sandwich" ELISA (Figure 34.b) will give the complementary information about how much of the protein remained in the solution. For this reason it is important to analyse the supernatant from the same tube on which the direct ELISA was performed. The detailed protocols for each protein will be given in the next subchapters.

2.4.1 ELISA protocols for detection of different neurodegenerative agents

2.4.1.1 Direct and "sandwich" ELISA protocol for detection of $PrPrec_{hum}$

DIRECT ELISA TEST:

- Coating of 50 μL of $PrPrec_{hum}$ in differently treated Eppendorf tubes; the protein was diluted to the c= 1μg/mL in PBS buffer at pH= 7.4. The time and temperature of coating depended on the experiment and will be specified before each results report, standard study was done at 4ºC and t= 24 h
- Washing of the tubes with PBS (250 μL) five times and saturation of the surface with 3% BSA, V= 50 μL. Saturation was done at 37ºC for 1h.
- Washing of the tubes with PBS (5 times, 250 μL) and addition of the biotinylated antibody 7F4- biot (V= 50 μL, c= 1 μg/mL) for 1h at 37ºC
- Washing of the tubes with PBS (5 times, 250 μL) and addition of streptavidin coupled with HRP (V=50 μL, 1/7500 dilution in PBS) for 30 min at 25 ºC
- Washing of the tubes with PBS (5 times, 250 μL) and addition of TMB (V=50 μL, 1/10 dilution in TMB dilution solution) for 30 min at 25 ºC in the dark
- Stopping of the reaction by addition of H_2SO_4 (V=50 μL, c= 1N)
- Transfer of the solution form tubes to polycarbonate reading plates and analysis with spectrophotometer at 450 nm

"SANDWICH" ELISA TEST:

- Coating of detection strips with 50 μL of detection antibody Saf 32. Ab was diluted in the carbonate buffer (pH= 9.4) to the c= 10μg/mL during the night at 4ºC
- Washing of the strips with PBS (200 μL) five times and saturation of the surface with 3% BSA, V= 50 μL. Saturation was done at 37ºC for 1 h
- Washing of the strips with PBS (5 times, 200 μL) and addition of the $PrPrec_{hum}$ that was stored in differently treated tubes (V= = 50 μL, c= 1 μg/mL) for 1 h at 37ºC

- Washing of the strips with PBS (5 times, 200 µL) and addition of the biotinylated antibody 7F4- biot (V= 50 µL, c= 1 µg/mL) for 1 h at 37ºC
- Washing of the strips with PBS (5 times, 200 µL) and addition of streptavidin coupled with HRP (V=50 µL, 1/7500 dilution in PBS) for 30 min at 25 ºC
- Washing of the strips with PBS (5 times, 200 µL) and addition of TMB (V=50 µL, 1/10 dilution in TMB dilution solution) for 30 min at 25 ºC in the dark
- Stopping of the reaction by addition of H_2SO_4 (V=50 µL, c= 1N)
- Transfer of the solution form the strips to the reading plates and analysis with spectrophotometer at 450 nm

2.4.1.2 "Sandwich" ELISA protocol for detection of PrPc from CSF

- Coating of cerebrospinal fluid of a patient number 0106730 in differently treated Eppendorf tubes for 24 h at 4°C, V= 50 µL
- Coating of capture antibody 3F3 (Kit Roboscreen) at 37°C for 2h in PBS (pH= 7.4) on untreated PP (Neuroscreen) strips; (V= 50 µL, c= 10µg/mL)
- Washing of strips with PBS (5 times, V= 200 µL) and saturation with PBS- BSA (3%) at 37 °C for 1 h, V= 50 µL
- Washing of strips with PBS (5 times, V= 200 µL) and coating with the CSF from the tubes (stored for 24 h under point 1) at 37 °C for 1 h, V= 50 µL
- Washing of strips with PBS (5 times, V= 200 µL) and coating with the detection antibody 15F5-HRP (Roboscreen Kit) at 37°C for 1h; (V= 50 µL, c= 1/10)
- Washing of strips with PBS (5 times, V= 200 µ L) and addition of TMB solution (75µL TMB, 45 µL peroxidase solution, 3 mL staining buffer; Roboscreen Kit) at RT in the dark for 30 min; (V= 50 µL)
- Addition of H_2SO_4 (V= 50 µL, c= 2N) and plate reading at 450 nm

2.4.1.3 "Sandwich" ELISA protocol for detection of Tau_{rec}

- Coating of Tau_{rec} Roboscreen 441 in the differently treated Eppendorf tubes for 24 h at 4°C; c= 100 ng/mL, V= 100 µL, PBS at pH= 7.4
- Coating of Tau_{rec} from the tubes (stored for 24h under point 1) at RT over night, V_{Taurec}= 12.5 µL + 12.5 µL sample dilution + 75 µL conjugate 1 (Innogenetics kit, 1/100 dilution)
- Washing of strips 4 times with washing solution from the kit, 1/25 dilution 400 µL. Add conjugate 2 (Innogenetics kit) in the 1/100 dilution and distribute 100 µL per well. Incubate 30 min at RT
- Washing of strips 4 times and add TMB in 1/100 dilution (Innogenetics kit); distribute 100 µL per well and incubate for 25 min at RT in the dark
- Add 100 µl of stop solution (2N H_2SO_4)

2.4.1.4 "Sandwich" ELISA protocol for detection of TauPHF from CSF

- Coating of Tau PHF in non- treated and treated tubes at 4°C for 24h ; (V= 50 µL, dilution of CSF in PBS is 1/250)
- Coating of T46 antibody at 37°C for 2 h in coating buffer (pH= 9.4) on untreated PP (Neuroscreen) strips; (V= 50 µL, c= 2µg/mL)
- Washing of strips with 0.05% Triton in PBS (3 times, 200 µL) and saturation with PBS- Triton (0.05%)
- Washing of strips with 0.05% Triton in PBS (3 times, 200 µL) and coating with TauPHF (stored for 24 h under point 1) at 37°C during 2h
- Washing of strips and coating of Ac_d (Innogenetics Kit) at 37°C for 30 min; (V= 50 µL, c= 1/100)
- Washing of strips and addition of Strep-HRP (Innogenetics Kit) at RT for 30 min; (V= 50 µL, c= 1/100)
- Washing of strips and addition of TMB (Innogenetics Kit) at RT in dark for 30 min; (V= 50 µL, c= 1/100)
- Addition of H_2SO_4 (V= 50 µL, c= 2N) and plate reading at 450 nm

2.4.1.5 "Sandwich" ELISA protocol for detection of Tau_{tot} from CSF

- Coating of CSF (LCR 0911191055755LYS) in the untreated and treated Eppendorf Tubes for 24 h at 4°C; V= 100 µL,
- Coating of CSF from the tubes (stored for 24h under point 1) at RT over night, V_{CSF}= 25 µL + 75 µL conjugate 1 (Innogenetics kit, 1/100 dilution: 30 µL of conj 1 + 3 mL of conj. dilution)
- Washing of strips 4 times with washing solution from the kit, 1/25 dilution 400 µL. Add conjugate 2 (Innogenetics kit) in the 1/100 dilution and distribute 100 µL per well. Incubate 30 min at RT
- Washing of strips 4 times and add TMB in 1/100 dilution (Innogenetics kit); distribute 100 µL per well and incubate for 25 min at RT in the dark
- Add 100 µl of stop solution (2N H_2SO_4)
- Read plates at 450 nm

2.4.1.6 "Sandwich" ELISA protocol for detection of Aβ-42 from CSF

- Coating of CSF (LCR 0911191055755LYS) in the untreated and treated Eppendorf Tubes for 24 h at 4°C; V= 100 µL,
- Coating of CSF from the tubes (stored for 24 h under point 1) at RT over night, V_{CSF}= 25 µL + 75 µL conjugate 1 (Innogenetics kit, 1/100 dilution: 30 µL of conj 1 + 3 mL of conj. dilution). Incubate 1h at RT
- Washing of strips 5 times with washing solution from the kit, 1/25 dilution 400 µL. Add conjugate 2 (Innogenetics kit) in the 1/100 dilution and distribute 100 µL per well. Incubate 30 min at RT
- Washing of strips 5 times and add TMB in 1/100 dilution (Innogenetics kit); distribute 100 µL per well and incubate for 30 min at RT in the dark

- Add 50 µl of stop solution (0.9N H_2SO_4)
- Read plates at 450 nm

2.4.1.7 "Sandwich" ELISA protocol for detection of α-syn

- Storage of α-syn in untreated and treated Eppendorf tubes for t= 0 to 3 months at the T= -20ºC and 4ºC at V= 100 µL
- Coating of detection antibody C211 diluted 1:200 with 200 mM $NaHCO_3$/0.02%NaN_3, pH= 9.6. Incubated over night at 4 ºC in 100 µL per well; (V= 100 µL)
- Washing with PBS buffer/ 0.05% Tween 20® (4 times, V= 200 µL) and blocking with 2.5% Gelatin in 200 µL PBS buffer. Incubated for 2h at 37 ºC; (V= 100 µL)
- Washing with PBS buffer / 0.05% Tween 20 (4 times, V= 200 µL) and addition of 100 µL antigen diluted in PBS buffer. Incubated for 2 h at 37 ºC; (V= 100 µL)
- Washing with PBS buffer / 0.05% Tween 20 (4 times, V= 200 µL) and addition of primary antibody FL -140 diluted to 1:1000 in PBS buffer + 2.5% of gelatine. Incubated for 2 h at 37 ºC; (V= 100 µL)
- Washing with PBS buffer / 0.05% Tween 20 (4 times, V= 200 µL) and addition of secondary antibody anti-rabbit-HRP diluted to 1:10000 in PBS buffer + 2.5% of gelatine. Incubated for 1 h at 37 ºC; (V= 100 µL)
- Washing with PBS buffer / 0.05% Tween 20 (4 times, V= 200 µL) and addition of SureBlue TMB solution from KPI, V= 100 µL. Incubate for 30 min at RT
- Addition of H_2SO_4 (V= 100 µL per well), c= 0.6 N (0.31 M)
- Read absorbance immediately at 450 nm

3 Results and discussion: Surface modification and analyses

3.1 Hydrophobic modification of polymeric surfaces through one-step CF_4 plasma treatment

The goal of this study is to obtain surfaces with minimal surface energy that will be potentially able to resist the adsorption of selected proteins [18].The CF_4 plasmas are known to be a source of different atomic and molecular radical species (F, CF, CF_2 and CF_3) in their ground, excited or ionized states. As the temperature of electrons in used plasma corresponds to the dissociation energy of most molecules and as the probability for recombination of neutral atoms comparing to the neutralisation of charged species is very low, the main species that will react with the surface are the neutral atoms and molecules [173]. The fluorine molecular species (CF, CF_2 and CF_3) are acting as building blocks by substituting the hydrocarbon bonds, while on the other side F atoms can react either as subsistent or etch the material [67]. Therefore it is very important to monitor the presence of reactive species in the plasma phase as a function of disharge parameters, accounting for the discharge power and the gas flow, corresponding to the pressure in the reactor chamber. The presence of excited species in the plasma phase was monitored by optical emission spectroscopy, while their relative ground state concentrations were estimated by actinometry [174].

In the next step the surface energy was measured by the contact angle method, where a drop of ultrapure milliQ water was deposited to the surface of substrates treated at different conditions, varying power, pressure and time of treatment. This method was also used for determining the surface stability with time under N_2 and air. The relative elemental composition of treated samples and their chemistry was determined by X-ray photoelectron spectroscopy (XPS). In the final step the optimally treated samples (exhibiting strongest hydrophobic character) were chosen and their surface charge was measured by zeta potential method, while the changes in the surface roughness and morphology were evaluated by atomic force microscopy (AFM).

3.1.1 Characterization of the plasma phase

In order to determine the species present in plasma phase the discharge was created either without any input of source gas at the ultimate pressure or with the addition of CF_4 gas. The flow of gas varied between 5 and 40 sccm, corresponding to the pressure between 1.4×10^{-2} and 3.9×10^{-2} mbar, while the power was adjusted from 10 to 100 W. Before each experiment the reactor chamber was pumped for at least half and hour with the intention to acquire the ultimate pressure in the order of magnitude 1×10^{-5} mbar. The optical emission spectra of plasma phase without and with inlet of source gas are presented in the Figures 35 and 36, respectively.

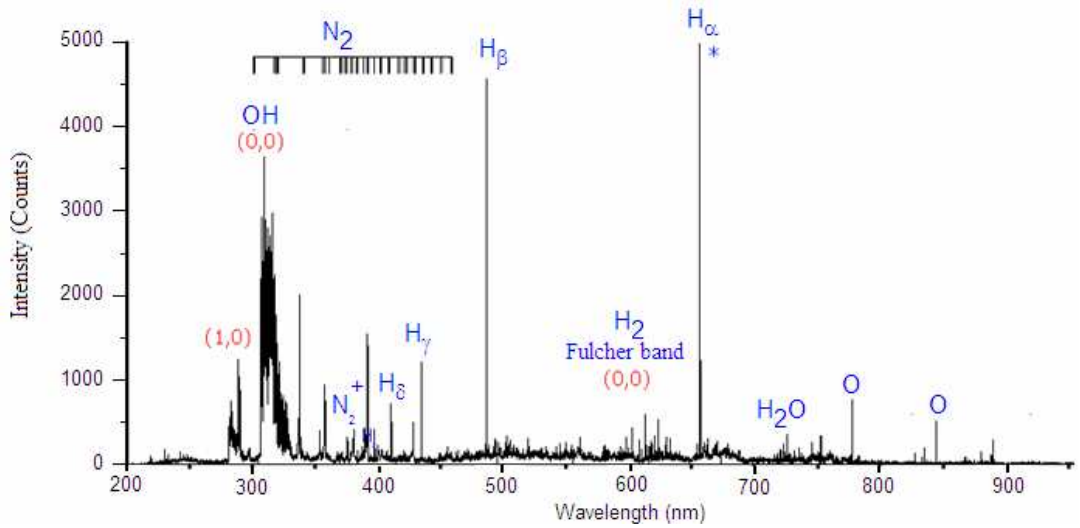

Figure 35: OES spectrum at discharge power of 50W at ultimate pressure (p= 2×10^{-5} mbar).

Figure 35 presents an optical emission spectrum monitored at base pressure, p= 2×10^{-5} mbar. The spectrum is composed of bands corresponding to transition of OH at 309.1 nm ($A^2\Sigma^+\rightarrow X^2\Pi$), hydrogen Balmer lines, and oxygen lines at 777.7 and 844.8 nm corresponding to $3p^5P\rightarrow 3s^5S^0$ and $3p^3P\rightarrow 3s^3S^0$ transitions respectively. This spectrum matches well to typical water plasma spectra presented by several authors [175]. There are also many bands between 300 and 450 nm that are correlated to different transitions of nitrogen molecules [176].

An optical emission spectrum of CF_4 plasma is presented in Figure 36. This spectrum is composed of a large continuum in UV part, between 200 and 400 nm, corresponding to the emission continuum of CF_2^+ ion. Several bands between 240 and 300 nm are attributed to different vibrational transitions of CF_2 radicals. Principal lines observed at 246, 249 and 252 nm are ascribed to the vibrational transition of CF_2 molecule from A (0, ν_2, 0) to X (ν_1, ν_2, 0). The emission of CF is observed between 200 and 250 nm, corresponding to the transitions $A^2\Sigma\rightarrow X^2\Pi$ and $B^2\Delta\rightarrow X^2\Pi$ [66]. Additional molecular bands are much weaker and overlap with continuum. Strong lines in UV correspond to the N_2 second positive band and traces of N_2^+ can be also observed.

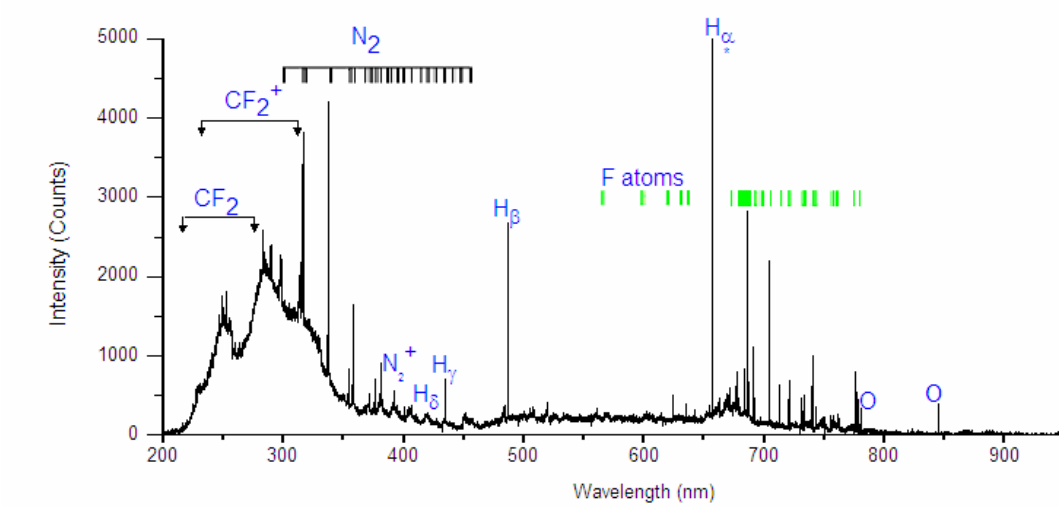

Figure 36: OES spectra at discharge power of 50 W and CF_4 flow of 40 sccm (p= 3.9×10^{-2} mbar).

There is a presence of weak oxygen atomic lines at 777.2 and 844.4 nm and of Balmer series of hydrogen lines as well. Atomic emission is dominated by F atom with many lines from 560 nm to 780 nm. The major atomic fluorine line emissions in this region are $^2P_0 \longrightarrow {}^2P$ (at 703.7, 712.8 and 720.3nm), $^2S_0 \longrightarrow {}^2P$ (at 731.0, 733.3 and 733.9nm), $^4P_0 \longrightarrow {}^4P$ (at 742.6, 755.3, 757.3 and 760.7 nm) and $^4D \longrightarrow {}^2P$ (at 775.5 and 780.1 nm). The presence of CF_3 band can not be confirmed due to the overlapping with CF_2 emission continuum between 230 and 300 nm. There exist many reports about the presence or absence of CF_3 emission lines in CF_4 plasma discharge [177,178]. Nevertheless, the optical emission spectra of CF_4 plasma strongly depend on the ultimate pressure at which experiments are performed. Therefore, optical emission spectra, especially in the UV region differ substantially among individual discharges, causing the statements to be often contradictory.

In plasma reactor the change of discharge parameters such as power and flow of gas will influence the density of radicals in the plasma phase. The conversion of radical concentration in the plasma is not necessarily the same as the change of intensity in the optical emission spectra. For this reason a quantitative evaluation of the species concentration (actinometry) can be employed. The basic principle is the addition of a low concentration of noble gas such as argon (usually bellow 5%) to the source gas, considering that this amount of gas will not change the characteristics of plasma. In our study the actinometry was performed with the addition of 2 % of argon gas to 98% of main gas-tetrafluoromethane. The lines studied with actinometry were the F line at 703.3 nm, CF line at 202.4 nm and CF_2 line at 251.6 nm, while the argon lines used were the one at 750.4 nm for the determination of relative ground concentration of F atoms and 416.4 nm for the determination of ground concentration for CF and CF_2 molecules.

The evolution of different excited species (I_x/I_{Ar}) as a function of RF discharge power is shown in Figure 37 and as a function of inlet gas concentration in Figure 38. Whatever was the concentration of the gas or the power of discharge, the main radicals present in the plasma were CF_2 molecules and F atoms. It can be seen in Figure 37 that the density of atomic F is increasing until the power reaches 60 W and afterwards remains constant, while the concentration of CF_2 radical has the opposite tendency and decreases with power. The drop becomes more pronounced for the power exceeding 60 W. The concentration of CF radicals is negligible comparing to F and CF_2 radicals and remains constantly low with the change of power or gas flow. Presence of such strong CF_2 and F emission lines indicates that CF_4 molecule is just partially dissociated under present

plasma conditions. Otherwise also CF emission lines would be much higher. The increase of power thus causes a linear growth of fluorine species in comparison to CF_x radicals. In the plasma, electrons gain energy directly from the electric field and loose energy by collisions with the particles. Therefore, electrons with certain energy will govern the rate of ionization, dissociation and excitation process of the source gasses or precursors in the plasmas. The increase in power increases the electron density, which as a consequence causes a higher dissociation of CF_4 gas [179].

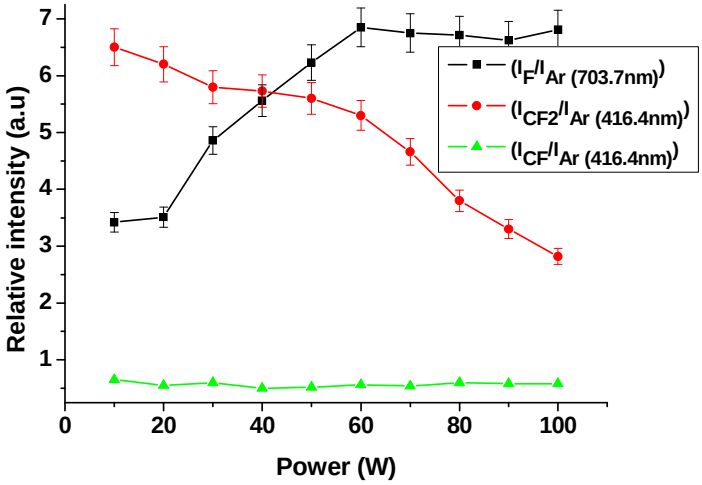

Figure 37: Evolution of relative intensities of F, CF and CF_2 lines as a function of discharge power (flow= 40 sccm, p= 3.9×10^{-2} mbar).

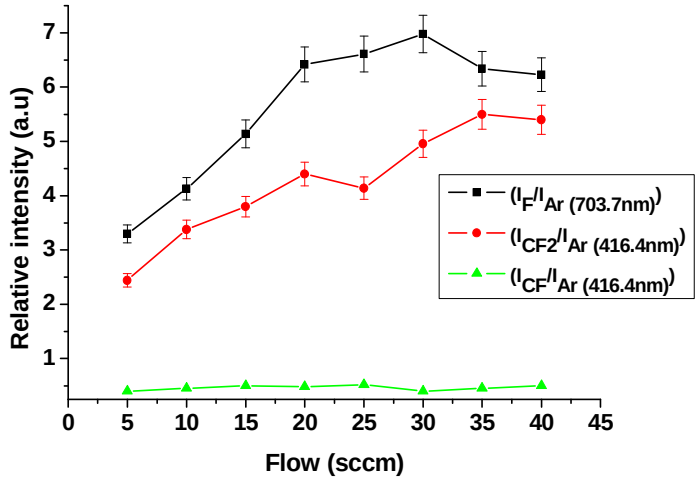

Figure 38: Evolution of relative intensities of F, CF and CF_2 lines as a function of gas flow at P= 50W; p= 8.2×10^{-3} mbar (5 sccm) to 3.9×10^{-2} mbar (40 sccm).

Results in Figure 38 indicate that the relative intensity of fluorine species is higher than of CF_2 radicals. But in the same time, they have the same tendency; higher the flow of gas, higher is the density of radicals. The concentration of F radicals grows until the flow of 30 sccm is reached, forming a plateau and slightly drops afterwards, while the concentration of CF_2 species is slowly increasing all the way to the final flow of 40 sccm. Therefore, the probability for higher formation of F and CF_x radicals also increases with the amount of gas inserted to the discharge chamber, but only just certain level. At very high density of source

gas, the electron free path is shorter. Consequently electrons can not gain enough kinetic energy from the field (can not be accelerated enough) leading to lowered rate of dissociation. Results have shown that the amount of F and CF_2 species is strongly dependant on the flow of the gas and the power of discharge.

3.1.2 Characterization of modified surfaces; determination of the hydrophobic properties

The goal of this preliminary study was to identify the plasma parameters that would allow us to attain surfaces with minimal free energy. In the next step the examination of ageing effect on the treated surfaces was performed. The stability of surfaces with time is important because their performance for biomedical applications is required in a longer period of time. The polypropylene plates were treated in CF_4 discharge under varying power, pressure and time of treatment. The contact angles were measured with a drop of ultrapure miliQ water (3 μL) around 1 min after the treatment. The base pressure at the beginning of the experiments was around 2×10^{-5} mbar. The ageing of the surfaces was followed under air and nitrogen atmosphere at room temperature for 1 month.

3.1.2.1 Influence of discharge power on the wettability of modified surfaces

Figure 39 presents the effect of discharge power on hydrophobization of the samples. To study the influence of the input power, the flow was fixed to 40 sccm and the time of treatment to 7 min. The power varied in the range of 10 to 100 W. Results showed that at low powers the surface energy starts to decrease and reaches the minimum value at 50 W, corresponding to a contact angle of 132°. On the other hand, when a higher power than 50 W is employed, the contact angle starts decreasing again reaching the value of 121° at 100 W.

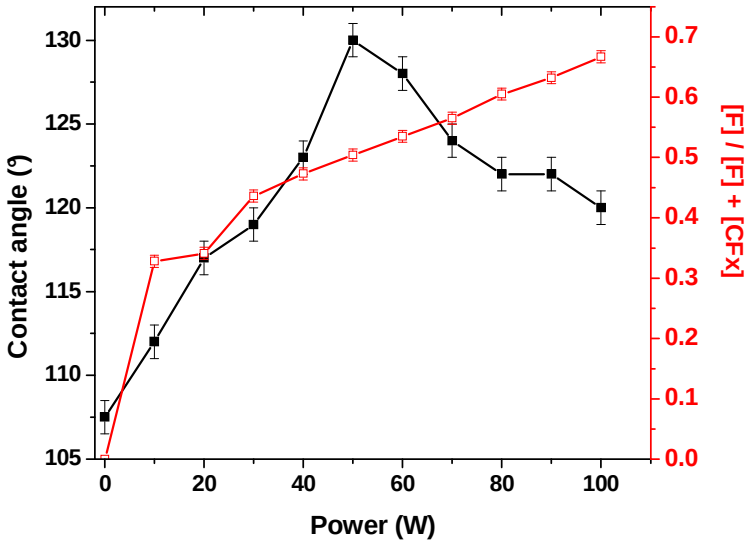

Figure 39: Effect of discharge power on water contact angles of CF_4 treated PP plates (black curve) and on relative concentration of fluorine species in the discharge obtained from actinometry measurements (red curve).

If we compare the contact angle results with actinometry measurements (Figure 39; black and red lines), the contact angle measurements show maximum at 50 W, while the percentage of F atoms linearly increases from 32% to 68% with the increase of power from 10 and 100 W. The highest contact angle is obtained when the plasma phase is composed from approximately 50% of fluorine atoms. As mentioned before, the fluorine atoms can act as etching agents or contribute to the substitution reactions. Therefore, it seems that a balance in gas composition exists, where the optimized hydrophobization (deposition vs. etching) can be realized. It can be seen in Figure 37 as well, that at P= 45 W, there is a switch at which F atoms become main species in the plasma phase comparing to CF and CF_2 radicals. When the power employed is less than 50 W, technically the balance between F atoms and fluorinated species is in favour of deposition comparing to etching, even though the relative amount of radicals responsible for fluorination seems to be too low.

3.1.2.2 Influence of pressure on the wettability of modified surfaces

Influence of gas flow on surface energy and gas composition is presented in Figure 40. The power was fixed to 50 W and time of treatment to 7 min. The results indicate that the water contact angle on treated samples almost linearly depends on the gas flow. For small flows, lower than 15 sccm, the contact angles on the treated samples are even lower than on the untreated due to the degradation and oxidation effect. The untreated sample possesses a water contact angle equal to 107.5°, while samples treated at 10 and 15 sccm of CF_4 gas have the angles of 74° and 98° respectively. The highest contact angle is obtained at the highest flow (40 sccm), reaching the value of 132°.

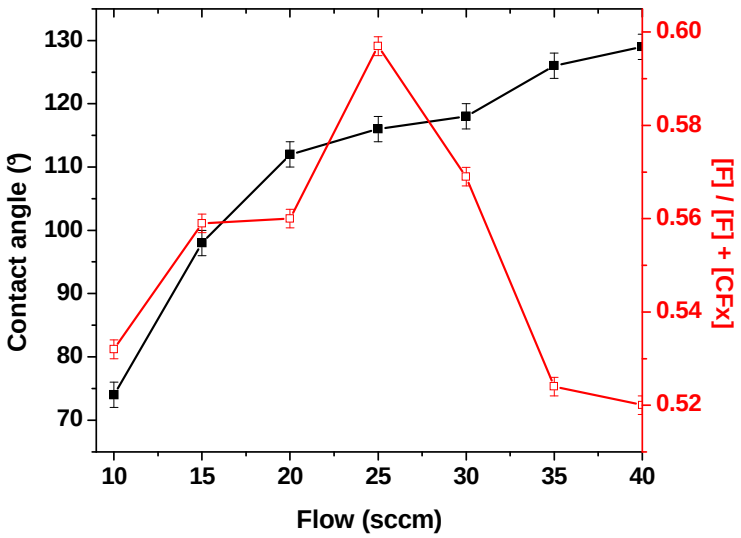

Figure 40: Effect of pressure (gas flow) on water contact angles of CF_4 treated PP plates (black curve) and on relative concentration of fluorine species in the discharge obtained from actinometry measurements (red curve).

The actinometry measurements (Figure 40, red line) demonstrate that the percentage of fluorine in the discharge varies between 52 % and 60 %. There is a maximum at 25 sccm indicating that at this pressure the prevalence of fluorine species is the highest. With the flow increasing further, the relative F concentration in the plasma phase rapidly decreases and

reaches minimum between 35 sccm and 40 sccm, corresponding to 52% of F in the discharge. As in the investigation of power influence, we came to the same conclusion, namely that for optimal hydrophobization of our substrates the amount of atomic fluorine in the plasma discharge should be around 50%.

3.1.2.3 Influence of treatment time on the wettability of modified surfaces

In Figure 41, we report the variation of contact angle with time for two different gas flows (20 and 40 sccm) at a constant discharge power of 50 W, where the time of treatment varied between 0 and 10 min. For the two flows, the optimal time was reached when the lowest surface energy is obtained; i.e. 7 min. However, it can be seen that the degree of hydrophobization for lower flows is almost negligible comparing to the untreated sample, while for higher flows there is a notable difference. Contact angle measurement on the untreated sample gave 107.5°, while the maximal contact angle after around 7 minutes, at a flow of 20 sccm is 114° at a flow of 20 sccm and 132° at a flow of 40 sccm. For higher gas flows, no matter how long the treatment time was, the level of hydrophobization was superior. It can be also noticed that at low gas flows, the measured contact angle initially decreases below the one of the untreated sample (102°). After 3 min of treatment, it starts increasing again and reaches its maximum after 7 min. Longer treatments lead to a decrease of contact angle for around 10° between 8th and 10th minute.

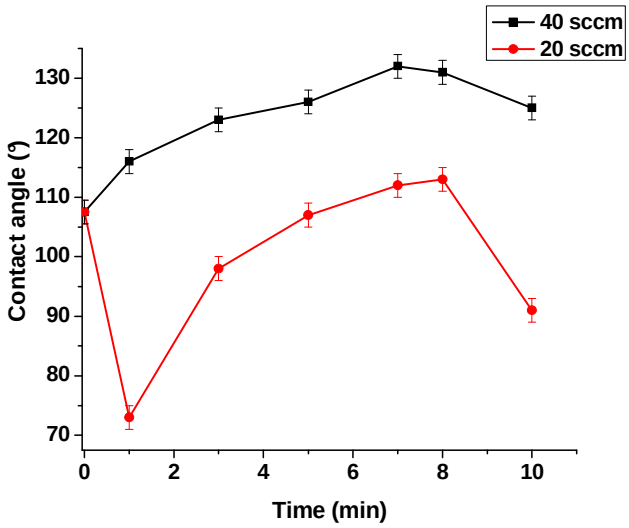

Figure 41: Effect of time of treatment on water contact angles of CF_4 treated PP plates (black curve at 40 sccm (p=3.9×10^{-2} mbar) and red curve at 20 sccm (p=2.4×10^{-2} mbar); P= 50 W.

The growth of hydrophobic character and relative concentration of fluorine species with gas flow was reported by several authors [65]. They were observing peak evolution either with actinometry or mass spectrometry measurements. The amount of CF_x species was reported to be negligible below the flow of 20 sccm, where it starts to increase linearly with the flow. When the flow was superior to 20 sccm, as well the relative amount of fluorine containing species started to increase linearly with power. The growth of water contact angle with gas flow is reported for different polymer substrates, while the increase of power provided diverse results [66]. In some cases the surface energy obtained minimum at certain power and in the others there was a sharp increase in water contact angles at higher powers. These differences were explained mostly by surface roughness, namely when substrates

possess the roughness below 10 nm contact angles varied between 110° and 130°, while at rough substrates it is possible to obtain completely superhydrophobic surfaces exhibiting contact angles practically up to 180° [61, 67].

3.1.2.4 Ageing effects on the plasma-fluorinated surfaces

Plasma treated polymer surfaces have often been observed to go under substantial changes in their surface properties and chemistry with time. This ageing is usually ascribed to two fundamental processes: post-plasma oxidation and surface adaptation [180].

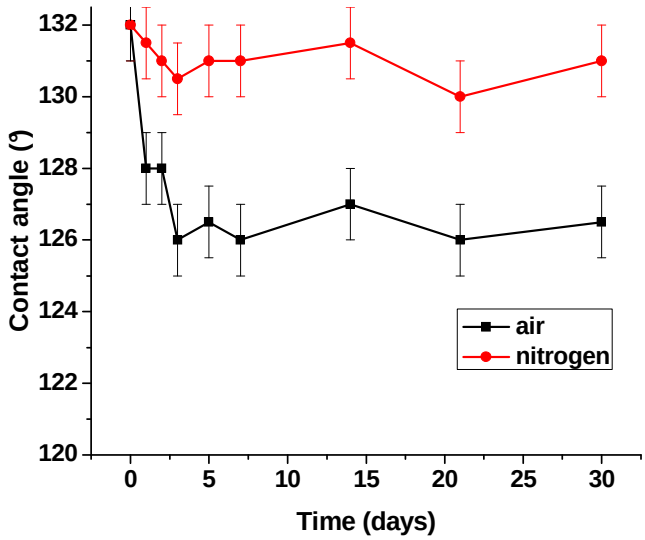

Figure 42: Contact angle measurements on the CF_4 treated PP plates in a month period stored under air (black curve) and nitrogen (red curve).

Figure 42 is showing the results of contact angle measurements that were carried out continuously for a month, in order to determine the ageing of CF_4 plasma treated substrates under air and nitrogen atmosphere. The results are indicating that there is no or negligible ageing of the treated samples (even after one month) under nitrogen atmosphere and a slight decrease of water contact under air. The change in the contact angle reached around 5° in the first few days and after this it remains stable. Partial lost of hydrophobicity in the case of samples stored under air can be attributed to the post-oxidation reactions of free radicals, created on the surface after plasma treatment with in-diffusing atmospheric oxygen that was observed several authors [181]. The negligible ageing of CF_4 plasma treated substrates is not surprising, as both air and nitrogen are considered as hydrophobic medium; consequently the surface rearrangement does not take place. These reorientations of polymer chains from the surface to the bulk occur due to the interfacial energy differences between the polymer and its environment, therefore bigger changes are expected in the case of polar surface modifications.

3.1.3 Characterization of the chemical composition of modified surfaces

The chemical composition of untreated polypropylene plates and CF_4 plasma-treated plates was obtained by XPS analyses. Several samples were prepared at different discharge conditions, which are specified in Table 5. Sample 1 is a virgin PP plate, whereas samples 2 to 9 present plasma modified PP plates. The discharge power (P) was changed in the range between 20 W and 100 W, the treatment time (t) between 1 min and 15 min and the gas flow (Φ) between 10 sccm to 40 sccm.

The elemental surface composition obtained from the low resolution XPS spectra of untreated and CF_4 plasma treated samples with corresponding water contact angle measurements is gathered in Table 5. It can be observed that the untreated sample is mainly composed of carbon, 94.0%, and a small concentration of oxygen, 4%. There was also a small amount of impurities observed on the surface (Si, S) that are not gathered in the table. For samples treated with CF_4 plasma the relative concentration of C falls down to 44.3 % and the concentration of F rises up to 46.2 %.

Table 5: Description of samples, surface composition in at.% and contact angle values.

Sample : P (W), t (min), Φ (sccm)	C (%)	O (%)	F (%)	Al (%)	F/C	O/C	Contact angle (°)
1. (0,0,0)	94.0	4.1	/	/	/	0.04	107.5
2. (50,7,10)	47.4	11.5	35.1	3.3	0.74	0.24	74
3. (50,7,20)	47.3	9.7	38.6	2.3	0.82	0.21	112
4. (50,7,30)	45.2	7.7	44.3	1.7	0.98	0.17	121
5. (50,7,40)	46.1	6.4	46.2	0.8	1.00	0.14	132
6. (20,7,40)	54.2	6.7	38.6	0.3	0.71	0.12	117
7. (100,7,40)	44.3	8.7	42.5	3.0	0.96	0.20	119
8. (50,15,40)	49.9	9.9	39.1	1.2	0.78	0.20	117
9. (50,1,40)	53.1	8.4	36.1	0.0	0.68	0.16	113

3.1.3.1 Influence of treatment time on the surface chemistry

The variation of contact angle and F/C ratio as a function of treatment time is presented in Figure 43.a. After just 1 min of treatment, the concentration of fluorine remarkably increased from 0 % to 36.1%, which corresponds to F/C ratio 0.68 and the contact angle of 113°. The highest F/C ratio equal to 1.00 was attained after 7 min of treatment, where the water contact angle (Θ) reached 132°. After 15 min of treatment, the F/C ratio again decreased to 0.78, accounting for approximately 20% lower degree of sample fluorination comparing to the sample treated at optimal conditions; the Θ dropped back to 117°. The effect can be ascribed to the higher degree of impurities (O, Al) observed on the surface (Table 5). The comparison of contact angle evolution and the XPS results shows that there is a clear correlation between the incorporation of fluorine functional groups and contact angle values (Figure 43). Graph contact angle vs. F/C ratio (Figure 43.b) can be decomposed to two linear parts; below the F/C ratio of 0.7 where the hydrophobization rate is very slow and above this value, where a sharp increase of contact angle with augmentation of fluorine species is observed.

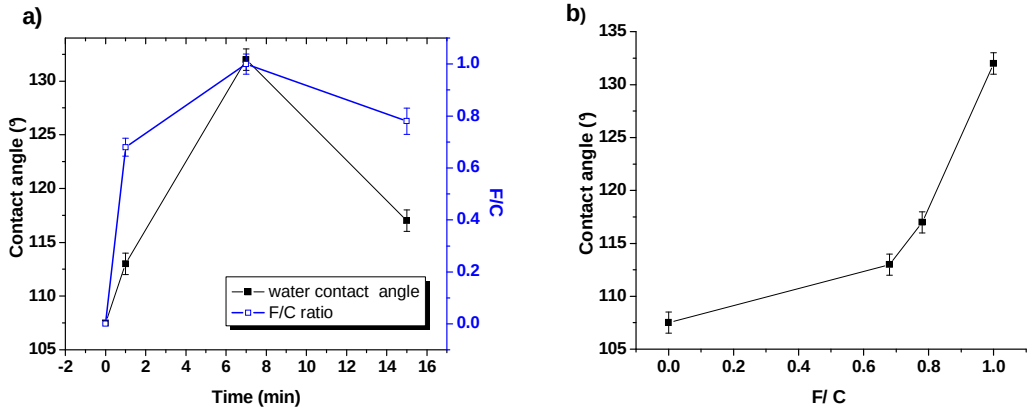

Figure 43: a) Variation of the contact angle and F/C ratio as a function of treatment time (P= 50 W, Φ= 40 sccm) and b) contact angle as a function of fluorination ratio.

3.1.3.2 Influence of discharge power on the surface chemistry

The effect of the RF power on the hydrophobization and on the extent of fluorination is demonstrated in Figure 44.a. Results show that the water contact angle and F/C ratio are growing with increase of power up to 50 W where they both reach maximum. The degree of fluorination at these conditions is 1.00 and corresponds to the contact angle value of 132°. A further increase of discharge power leads to important decrease of contact angle (for 13°), even though the F/C ratio stays approximately the same (Figure 44.b).

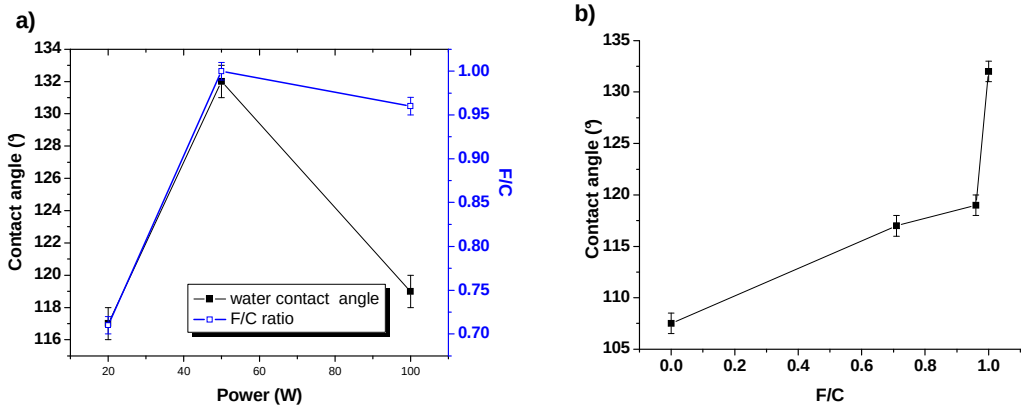

Figure 44: a) Variation of the contact angle and F/C ratio as a function of discharge power (t= 7 min, Φ= 40 sccm) and b) contact angle as a function of fluorination ratio.

If we refer to the results from low resolution XPS analyses (Table 5) we see that the main difference between the conditions is the amount of impurities on the surface, in the form of aluminium and oxygen. These functionalities are known to have relatively high surface energy which could assist to the difference in the surface energies of the two samples compared. On the other hand the OES studies showed that above the P= 45 W the atomic fluorine species prevail in the discharge and probably the etching process removes partially fluorine from the surfaces. More information about functional groups on the surface at high power conditions will be provided by high resolution XPS analyses.

3.1.3.3 Influence of pressure on the surface chemistry

The influence of gas flow on the evolution of the contact angle and the F/C ratio is shown in Figure 45.a. Both, F/C ratio and contact angle are increasing with the gas flow. Already at 10 sccm (p= 1.4×10^{-2} mbar) the degree of fluorination increases from 0 to 0.74 and after this point grows progressively up to the relative F/C ratio 1. What can be noticed is that even though the F/C ratio increased substantially at 10 sccm, the water contact angle became even inferior to the non-treated sample (Figure 45.a). As this F/C ratio was sufficient to observe hydrophobic surfaces at different times and power (Figures 43 and 44) the reason for such a small contact angle should lay elsewhere. The difference in elemental composition on these samples (Table 5, samples 2-5) show a clear correlation between the amount of aluminium and oxygen impurities on the surface. This phenomenon will be discussed in detail later in the chapter (page 65).

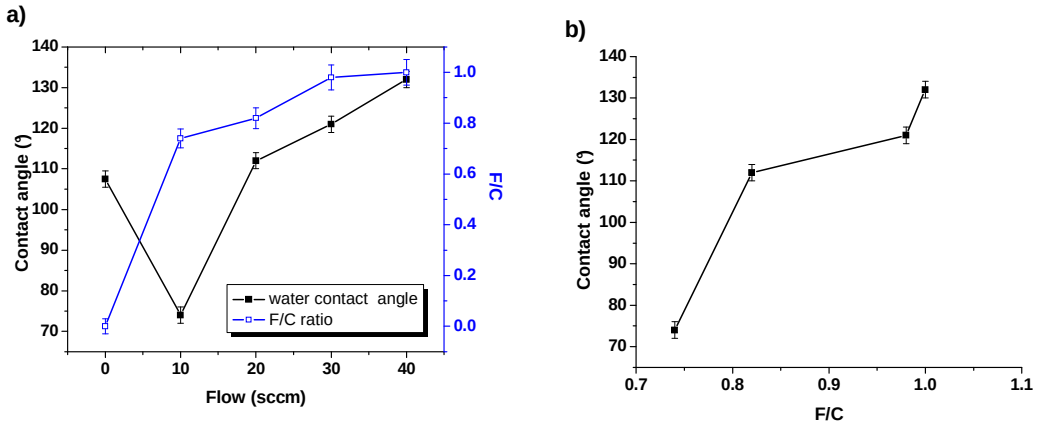

Figure 45: a) Variation of the contact angle and F/C ratio as a function of gas flow; (t= 7 min, P= 50 W) and b) contact angle as a function of fluorination ratio.

Theoretically the relative concentration of fluorine should be 66.7%. Despite the fact that this value is not reached it can not be stated that the surface is not highly covered with the fluorine functional groups. It should be noted that the contact angles are controlled by the few outermost layers of polymer materials, whereas the analyzing depth for C 1s photoelectrons in XPS analyses is estimated at about 8.5 nm (3λ sin 45°= 8.5 nm at λ= 4) [182].

Next to the relative elemental concentration of treated samples, it is important to determine the nature of the chemical bonds introduced by the plasma treatment. The formation of new functional groups on the surface was determined from high resolution C 1s XPS spectra, presented in Figure 46. The description of the samples with possible peak assignments and their percentages are gathered in Table 6.

The C 1s peak of untreated PP consists of two peaks, a major one at 285.0 eV belonging to the C-C/C-H (C1) bond and a smaller one at 286.7 eV corresponding to the bond C-O (C2), Figure 46.a. The C-C/C-H bonds belong to the backbone of polypropylene $(-CH_2-CH(CH_3)-)_n$, while the low quantity of C-O bonds can be ascribed to impurities in the polymer itself. After plasma treatment, four new peaks appear (C3-C6) that are assigned to the $\underline{C}F$/ $\underline{C}HF-CH_2$/ $\underline{C}=O$ (288.2 eV), $\underline{C}F-CF_n$ (289.7 eV), $\underline{C}F_2$ (291.6 eV) and $\underline{C}F_3$ (293.6 eV) functional groups [183]. There is also a big increase of C2 peak, primarily due to the formation of $\underline{C}$-CF bond; Figure 46.b.

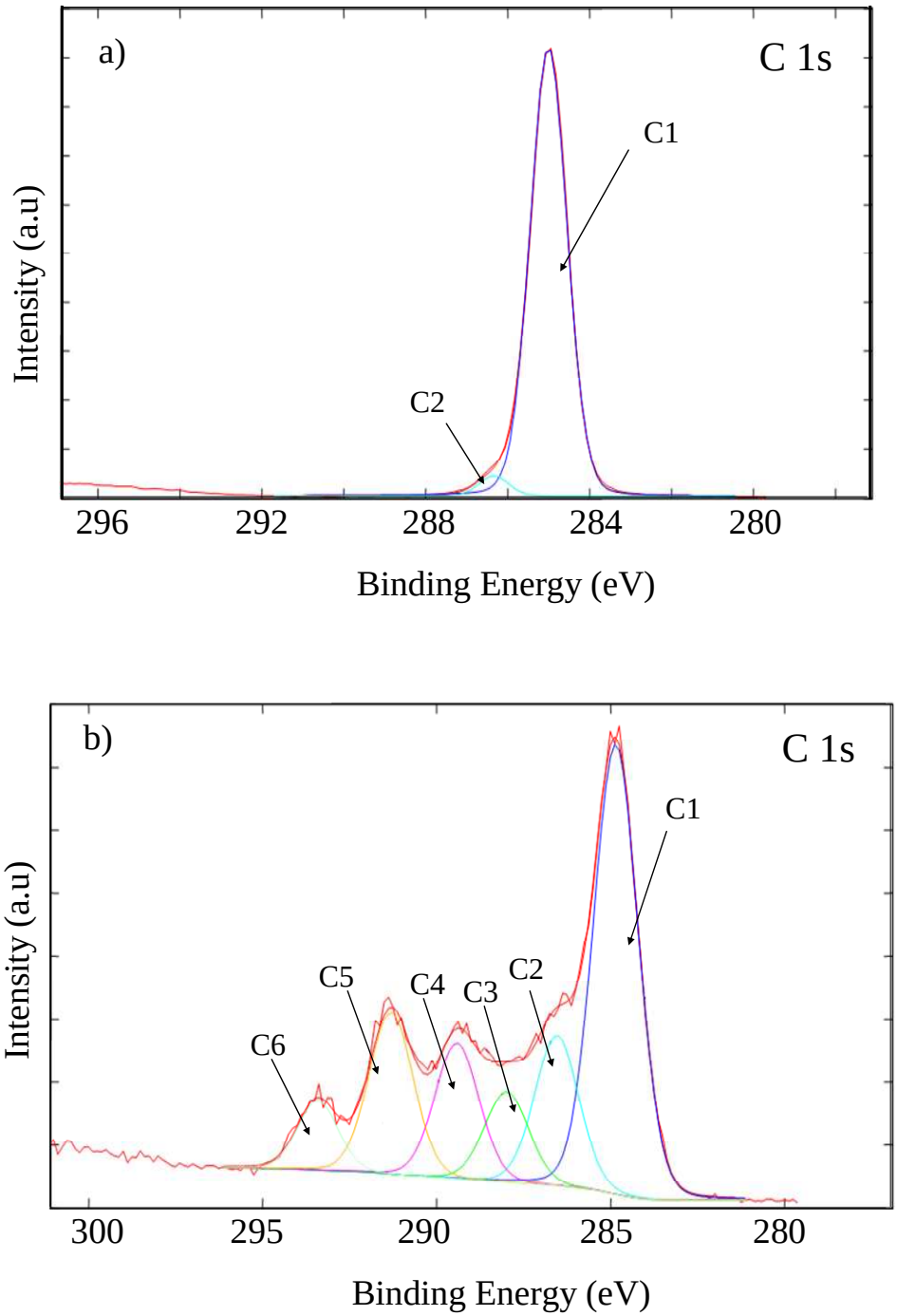

Figure 46: High resolution C 1s spectra of a) untreated PP sample and b) PP treated with CF_4 plasma; P= 50 W, t= 7 min and flow= 40 sccm ($p=3.9\times10^{-2}$ mbar).

The relative proportion of all functional groups is growing with the gas flow (samples 2-5). The relative amount of CF functional groups is hard to determine, because C2-C4 peaks are superimposed by oxygen containing functional groups (Table 6). However, it can be seen that at the flow of 40 sccm, the relative amount of CF_2 and CF_3 functional groups reaches maximum, there was 3% more of CF_3 groups and 11% of CF_2 fuctional groups found on the surface. A comparison of samples (5-7) treated in CF_4 plasma (t =7 min, flow = 40 sccm) at a variable power between 20-100 W produced a relative increase of CF_2 and CF_3 functional groups until the power of 50 W, for 4 % and 1.1 %

respectively. Over and below this power, the concentration of CF_2 and CF_3 peaks decreased and reached similar values at either 20 or 100 W. At the same time, the higher the power of discharge was, higher was the relative amount of CF species observed on the surface. Considering the optical emission, contact angle and low resolution XPS studies, we can presume that at higher power there is partial removal of fluorine groups from the surface, which are later replaced by oxygen functionalities under exposal to atmosphere. Therefore at a medium power there is less CF species and more CF_2 and CF_3, which are responsible for higher degree of fluorination.

The progression of the relative amount of the fluorinated species with time can be seen in the Table 6, samples 5, 8 and 9. The relative concentrations of CF_2 and CF_3 functional groups have the same tendency; their concentration grows until around 7 min (for 5.5 % and 1.5 % respectively) and after it starts decreasing. However, the amount of CF_2 functional groups is still higher after 15 min (12.4 %) of treatment than after 1 min (9.9 %). The same conclusion can be drawn for CF functional groups, with the difference to CF_2 species, their relative concentration does not reach maximum at 7 min, but keeps increasing with longer treatment times.

Table 6: Relative concentrations of carbon functionalized groups derived from the C 1s spectra obtained on the PP samples treated with CF_4 plasma

Component Energy (eV)	**C1 (%) 285.0 eV**	**C2 (%) 286.7 eV**	**C3 (%) 288.2 eV**	**C4 (%) 289.7 eV**	**C5 (%) 291.6 eV**	**C6 (%) 293.6 eV**
Possible assignment	C-C/C-H	C-O/C-CF	CF/ C=O CHF-CH2	CF-CF_n	CF_2	CF_3
Sample: P (W) t(min),Φ(sccm)						
1. (0,0,0)	97.9	2.1	0	0	0	0
2. (50,7,10)	62.0	15.1	8.4	7.4	4.6	2.5
3. (50,7,20)	52.4	17.8	9.5	8.7	7.7	3.9
4. (50,7,30)	50.0	13.7	8.1	10.6	12.0	5.6
5. (50,7,40)	42.7	14.3	8.7	12.9	15.4	6.1
6. (20,7,40)	55.4	12.6	6.8	9.4	11.3	4.6
7. (100,7,40)	45.3	16.9	10.4	10.9	11.5	5.0
8. (50,15,40)	48.2	14.0	9.9	11.6	12.39	4.0
9. (50,1,40)	54.5	13.5	9.0	8.8	9.9	4.4

Let us first consider the type of reactions happening in the gas chamber. The electron temperature is only a few eV. Average electrons are therefore likely to excite CF_4 molecules to a variety of electronic, vibrational and rotational states but cannot dissociate or ionize the molecules. Only the fastest electrons are capable of dissociation, let alone ionization. The lowest dissociation energy is found for the reaction $CF_4 \rightarrow CF_3 + F$. Since the electron temperature in our plasma is rather low, this reaction probably prevails. Apart from it, dissociation like $CF_3 \rightarrow CF_2 + F$ seems quite possible, but is definitely less probable. The final concentrations of CF_x molecules should decrease in the following way: CF_4, CF_3, CF_2, CF, C. The concentration of F atoms should be a bit higher than the concentration of CF_2 and CF_3 molecules. These radicals are primarily reacting through a hydrogen substitution mechanism with the surface (ex. $C_xH_y + CF_z \rightarrow C_xH_{(y-1)}F_z$).

As seen from results above, the relative proportion of impurities in the form of O and Al increases on the surface when higher power is employed or/and with longer treatment times and decreases with higher flow of gas. In order to explain these effects we will first address the optical emission spectrum presented in the Figure 35, which is revealing some interesting

features. Besides the fact that the predominant radiative radicals at ultimate pressure are H, OH, O and N_2 it is interesting that these radicals are also visible in spectra obtained in CF_4 plasma (Figure 36). Although the partial pressure of water vapour is very low during the system feeding with CF_4 the concentration of the impurity radicals remains substantial. The ultimate pressure is about $2x10^{-5}$ mbar. This is probably also the upper limit of the water vapour partial pressure at experiments with CF_4. It is known that plasma facilitates desorption of gases from the chamber walls so the partial pressure of water vapour may be increased after turning on the discharge.

On the other hand, a constant flow of CF_4 facilitates pumping of the impurity gases what should cause continuous decreasing of the water vapour partial pressure during experiments with CF_4. In any case, the concentration of impurities in CF_4 is well below 1%. The richness of the spectra presented in Figures 35 and 36 is explained by collision phenomena in gaseous plasma. The dissociation energy of CF_4 is 12.6 eV, while the ionization energy of CF_4 is about 16 eV [184], which is much higher than the dissociation energy of water vapour or OH molecules, which is at about 5 and 4 eV, respectively. Although the concentration of water molecules is rather low, the concentration of O and H radicals is substantial, due to a high probability of their formation during inelastic collisions with electrons, metastable CF_4^* molecules and CF_3^+ ions. In the first approximation we can conclude that water vapour gets fully dissociated in CF_4 plasma. If the partial pressure of H_2O molecules is $4x10^{-5}$ mbar, the resultant density of neutral oxygen atoms is $n = p/kT = 1x10^{18}$ m^{-3}. The resultant flux of O radicals on the sample surface is $j = ¼\ n\ v = 1.5x10^{20}$ $m^{-2}s^{-1}$. Neutral oxygen atoms may cause oxidation of the polypropylene sample. Although the reaction probability is far from 1 [185], the oxidation can be pretty intense after several seconds, let alone minutes, of plasma treatment. This effect explains the formation of the oxygen rich functional groups on the surface of our samples. Namely, as shown by numerous authors, exposure of organic materials to O radicals causes formation of O-rich surface functional groups [186-188].

On the other hand, CF_4 plasma is also rich in CF_x radicals as well as F atoms. As shown by other authors [64-68], the exposure of polymer materials to such radicals causes fluorination of the surface layer of samples. Unfortunately it is difficult to estimate the absolute value of the F and CF_x radicals in our plasma. Still, it is reasonable to predict about 1 % of dissociation fraction of CF_4 molecules what would give an F radical density of about $5x10^{18}$. The density of oxygen and fluorine atoms in our plasma is therefore roughly of the same order of magnitude. There should be a competition for binding to the surface of the sample. The potential barrier for the oxidation of organic materials is somehow lower than potential barrier for the fluorination. The final concentration of the O and F functional groups should therefore depend on the type of polymer and concentration of different reactive species in the plasma. A higher concentration of F radicals would facilitate higher hydrophobicity of the samples. This is confirmed by XPS results summarized in Table 5 as well as the results of the contact angle measurements in Figures 39-41.

Finally, we should address to the appearance of smaller quantities of Al on the surface, which is attributed to the sputtering of the powered electrode. Since the density of CF_4 molecules in the chamber is much larger than the density of CF_3 molecules and F atoms (let alone CF_2 and CF molecules), and since the ionization energy of CF_4 molecules is smaller than the ionization energy of CF_3 and F, it can be expected that the CF_4^+ ions will prevail. The ions are accelerated in the DC sheath and bombard the powered electrode with the kinetic energy of about 200 eV. As soon as an ionized molecule reaches the electrode surface it is dissociated to atoms. On the average, each atom takes about a fifth of the CF_4^+ ion kinetic energy, i.e. about 40 eV. Most of this energy is spent for heating of the electrode and a smaller fraction is spent on the sputtering. The ion density in unperturbed plasma is around $1x10^{16}m^{-3}$ and this means that the resultant flux of CF_4^+ ions onto the electrode surface would be about $1x10^{18}$ m^{-2} s^{-1}. Therefore the concentration

of Al, although low, is probably due to (extremely weak) sputtering of the powered electrode made from aluminium. The sputtering yield will depend on the flux of ions onto the powered electrode, the type of ions and the kinetic energy and all three parameters will depend on the discharge power. This can not be avoided in capacitively coupled RF discharges at low pressures; nevertheless it could be minimized by coating of electrode by thin film of Teflon, which should be in a good thermal connection to the powered electrode.

3.1.4 Characterization of the surface charge of plasma-fluorinated surfaces

Acid-base properties of untreated and CF_4 treated polypropylene were evaluated by measuring zeta potential towards the pH of $1{,}7\times 10^{-3}$ M NaCl buffer solution (Figure 47). The plasma treatment was performed at optimal conditions where substrates exhibited strongest hydrophobic character; P= 50 W, p= 3.9×10^{-2} mbar and t= 7 min.

The ζ (pH) curve for the untreated PP sample shows a typical curve of non-polar polymer surfaces. The absence of plateau indicates that there are no dissociable acid or base groups present on the surface. Namely, the origins of the charge at polymer surface with a contact with electrolyte solutions is attributed to the dissociation of the acidic or basic surface groups and the preferential adsorption of cations or anions in competition to the water adsorption. The anions adsorb stronger in neutral 1:1 electrolytes, and for this reason the zeta potential is negative for most of the polymer surfaces [188]

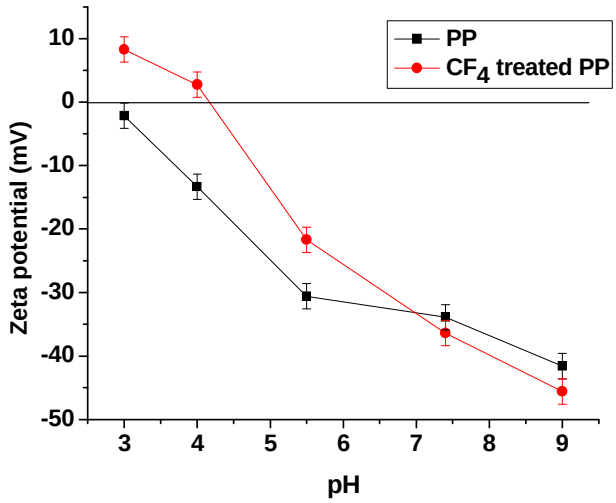

Figure 47: Zeta potential measurements vs. pH for untreated PP (black curve) and CF_4 plasma treated PP (red curve).

As shown in Figure 47, plasma treatment shifts the isoelectric point (IEP) to lower pH values. This shift suggests that the treated surface has more acidic character than the untreated polypropylene surface. Normally CF_4 has no acid-base character by Brønsted effect, because it can not react as either hydrogen donor or acceptor. There are several actors that could lead to these properties: increase of oxygen and aluminium functional groups on the surface (Table 5, sample 5) and very probably due to the fact that samples are negatively charged towards the plasma in the discharge chamber. Namely, samples were visibly

electrostatic when removed from the plasma chamber and the charge stayed on the surface if there was no artificial drainage of the charge from the surface.

3.1.5 Characterization of the surface morphology

The morphology and roughness of untreated and CF_4 plasma-treated surface was analyzed by atomic force microscopy. The height and 3D AFM images of untreated PP sample are shown in Figure 48. The sample does not exhibit any special topography features on the surface. There are only a few grain like structures observed with heights between 45 nm and 115 nm. These are probably the inorganic additives used in the polymer production. Nevertheless, their density is much too low to influence the surface roughness. The average surface roughness measured over 10 × 10 µm area was 2.8 ± 0.1 nm.

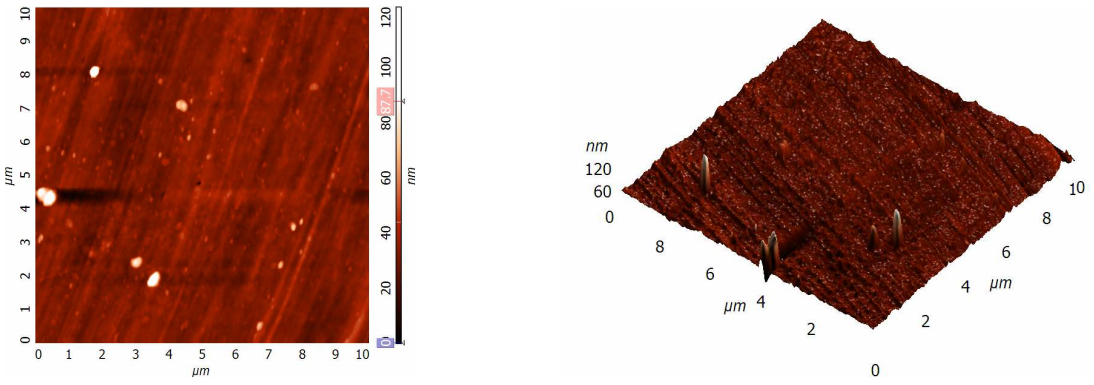

a) b)

Figure 48: AFM images of untreated PP plate; a) height and b) 3D image.

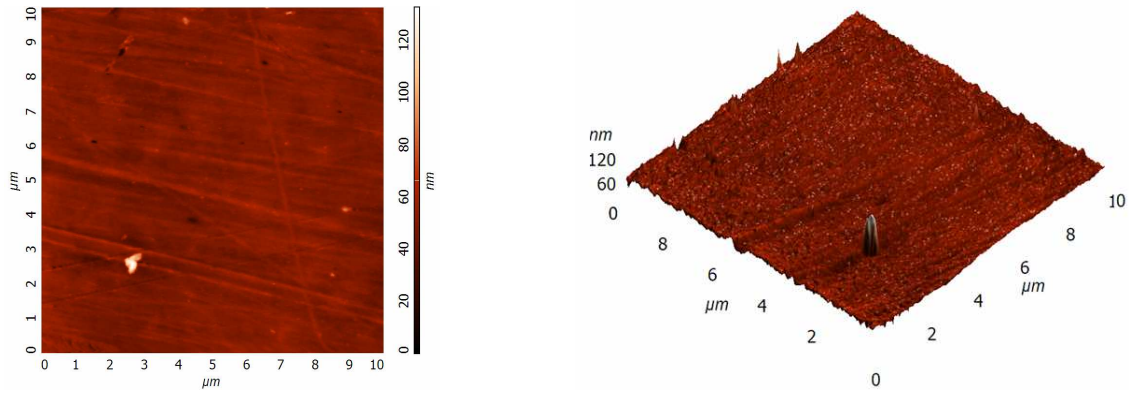

a) b)

Figure 49: AFM images of CF_4 treated PP plate; a) height and b) 3D image.

After CF_4 plasma treatment there was no noticeable difference observed, even though the sample was submitted to bombardment with fluorine radicals for 7 min (Figure 49). The average surface roughness measured over 10 × 10 µm area was 2.4 ± 0.1 nm. The slight smoothening of surface could be due to the removal of imbedded particles from the polymer matrix or simply due to the fact that the surface is rather inhomogeneous at this scale and the imaging was taken on the clearer part. The height of impurities remained the same. The changes in surface roughness after plasma treatment are mostly caused by chemical erosion with atoms and/or physical erosion by ions in plasma. Usually amorphous parts are removed

much faster than the crystalline counterparts and by this a surface topography can be created [189,190]. As analyzed polymers are amorphous and possess initially very low or no crystalline phase, there is no preferential etching detected and thus there are no special features observed after the plasma treatment.

This absence of surface roughness on our polypropylene plates is a good indicator why superhydrophobic character could not be attained. Several authors have reported that the F/C ratio is not the main evidence for highly hydrophobic surfaces [64, 65]. They have shown that the contact angles on the same type of polymer substrate treated with CF_4 plasma reached the value of 125º or 175º solely due to the difference in surface roughness. The F/C ratio gained from XPS analyses was even lower in the case of superhydrophobic surface. Interesting results were reported as well for the hydrophobization of samples that were pre-treated by oxygen plasma in order to assure the adequate surface roughness. In the next step these substrates were functionalized by CF_4 plasma treatment and superhydrophobic character was obtained [68].

Summarizing the one-step CF_4 plasma treatment results, we can say that the optical emission study coupled with contact angle measurements and XPS analyses gave us valuable data: if we want to obtain an optimal balance between surface functionalization and surface etching the relative amount of atomic fluorine species in the discharge towards the molecular CF_x species should be around 50 %. These conditions are obtained at maximal gas flow of 40 sccm, moderate power of 50 W and treatment time of 7 min. Presence of impurities on the surface (O, Al) was more evident at higher powers, longer treatment times and lower gas flow. Their existence was ascribed to the post-oxidation reactions, reactions of impurities in the discharge chamber (mainly water vapour) and to the weak sputtering of powered electrode made of aluminium. AFM imaging allowed us to confirm that the surface roughness on our substrates was not important enough to ascent from highly hydrophobic to superhydrophobic surfaces.

3.2 Hydrophilic modification of polymers through two-step treatment: Plasma activation and polymer grafting

In the following study the goal is to activate the polypropylene surfaces in order to initiate the grafting of desired polymer or polymer containing material. The activation itself was performed by helium plasma treatment. Helium plasma was used for the abstraction of hydrogen from C-H bond on the polymer surface where free radicals form. These radicals can after interact to form cross-links, unsaturated groups, react with incoming oxygen or act as initiators for subsequent polymer grafting [82]. The polymer grafting technique is used to chemically bond two or more types of molecules having different configurational and/or constitutional features.

The radical species present in the plasma phase were observed by optical emission spectroscopy, while the efficiency of activation and surface chemistry were monitored by wettability measurements and XPS analyses. In the next step activated substrates were immersed into pure polymer solution of poly (N-isopropylacrylamide) (PNIPAM) or into PNIPAM solution containing surfactant (cetyl trimethylammonium bromide (CTAB) or Polyoxyethylene (20) sorbitan monolaurate (Tween 20®)). The immersion was carried out at different concentrations, polymer to surfactant molar ratios and plasma parameters in order to study how the experimental conditions influence the polymer grafting. Surfaces were analyzed by contact angle method, XPS analyses, zeta potential measurements and the surface imaging was obtained by AFM analyses.

3.2.1 Fist step: Activation of substrates by helium plasma

3.2.1.1 Helium plasma characterisation

Typical optical emission spectrum of helium plasma is presented in Figure 50. The ultimate pressure before the inlet of gas was 2 x10^{-5}mbar. The power during experiments was changed between 10 and 100 W, while the flow varied from 10 sccm to 90 sccm, related to the pressure between 2.8×10^{-4} and 1.2×10^{-1} mbar. Spectra were obtained about 30 s after plasma ignition.

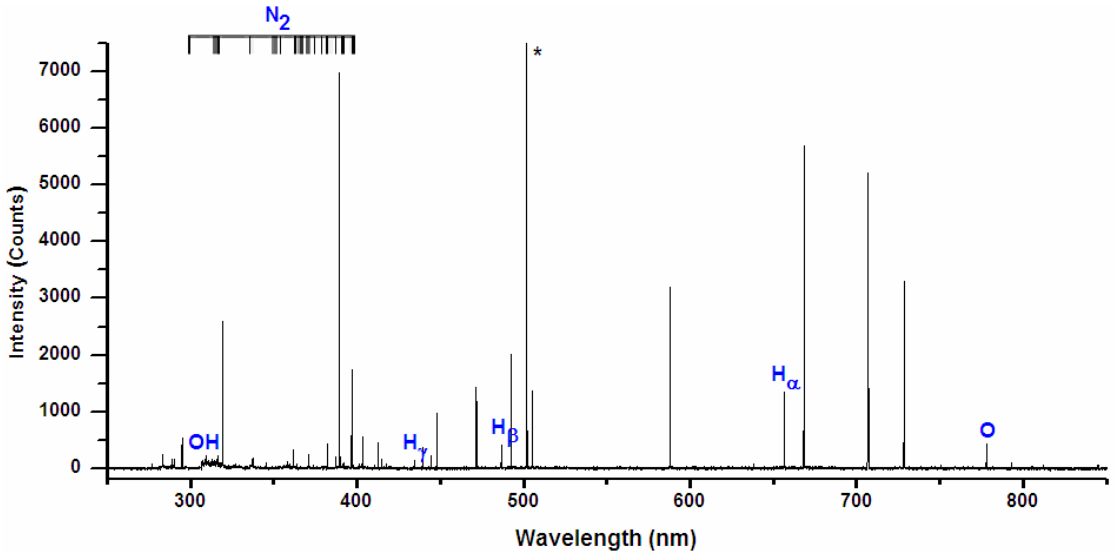

Figure 50: OES spectra of He plasma (P= 70 W, flow= 30 sccm and p= 1.5×10^{-2} mbar).

In the UV region (between 250 nm and 400 nm) there are typical He emission lines observed with some additional nitrogen and OH peaks as main impurities in the plasma phase. The helium lines are not marked on the spectrum and correspond to all additional lines throughout the spectrum that are not identified. The helium spectra are known to be very rich and contains up to 2440 emission lines with different relative intensities [191]. For this reason we needed to monitor the plasma at very short acquisition times in order to be able to observe other excited species next to helium that are present in the plasma phase. As a consequence lots of the He emission lines are hidden in the background. In the visible region between 400 nm and 700 nm, we observed two types of peaks corresponding to He and the others to H_α, H_β, H_γ, H_δ Balmer lines. Above the 700 nm the emission lines belong mainly to He radicals with a peak at 777.7 nm accorded to oxygen $3p^5P \rightarrow 3s^5S^0$ transition.

The evolution of oxygen (777.7 nm), nitrogen (337.6 nm) and helium (504.8 nm) emission lines as a function of flow is shown in Figure 51.a. Discharge power during measurements was fixed to 70 W. The amount of He and impurities grows linearly with flow, however for the helium slope is more important and reached maximum at the flow equal to 70 sccm.

In the Figure 51.b are presented optical emission lines of helium and impurities as a function of power at constant gas flow of 30 sccm, corresponding to the pressure 1.5×10^{-2} mbar. Until the power of 50 W, the amount of impurities stayed relatively low and constant. After this power they have started increasing and reached maximum at 80 W. The same evolution was observed for He emission lines; however the relative amount of He emission lines towards the impurities was higher at elevated powers.

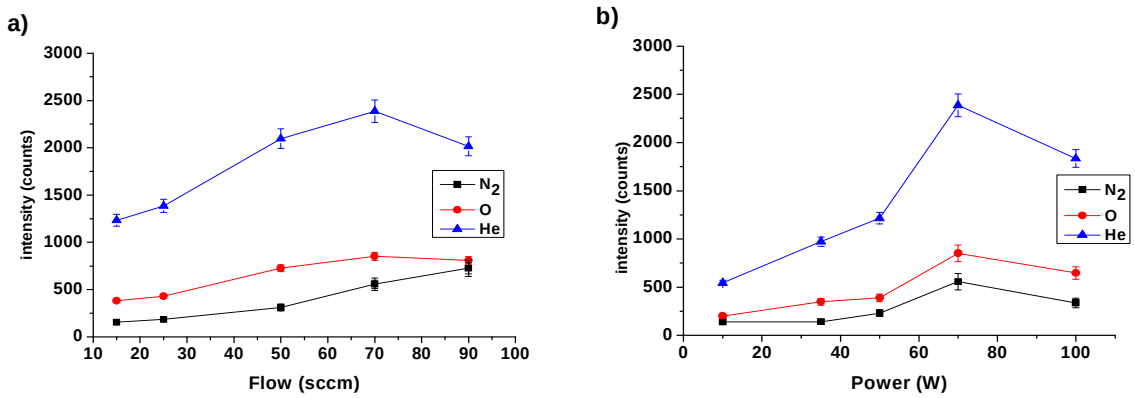

Figure 51: Intensity of He, O and N_2 lines as a function of a) gas flow (P= 70 W, p= 2.8×10^{-4} - 1.2×10^{-1} mbar) and b) discharge power (Φ= 30 sccm, p= 1.5×10^{-2} mbar).

3.2.1.2 Characterisation of the activated surface, determination of hydrophilic properties

The goal of this part of experiments was to determine the plasma condition parameters that would allow us to attain the surface with maximal free energy. The polypropylene plates were treated in He discharge under different power, pressure and treatment time. The contact angles were measured with a drop of ultrapure milliQ water (3 μL) around 1 min after the treatment. The base pressure at the beginning of the experiments was around 2×10^{-5} mbar. The ageing of the surfaces was followed under air at room temperature for 2 weeks.

3.2.1.2.1 Influence of pressure on the wettability of modified surfaces

Influence of gas flow on surface energy and gas composition is presented in Figure 52. For this purpose the power was fixed at 75 W and time of treatment to 1 min. The results are indicating that the water contact angle on treated samples very slightly increases, for 5°, with pressure until the flow of 70 sccm (p= 7.5×10^{-2} mbar). Above this flow the contact angle starts to rise quite substantially and reaches the value of 32° at 90 sccm (p= 1.2×10^{-1} mbar).

The optical emission measurements of He line intensity as a function of pressure is shown in the Figure 52.a. Until the flow of 70 sccm the intensity of He lines grew with the gas flow, followed by a slight drop of intensity. If we compare this to the contact angle measurements it seems that they rise with gas flow- higher quantities of helium radical species. Figure 52.b is suggesting that the relative intensity of He lines I(He)/ I(He+O+N_2) toward the impurities is falling with flow, which is rather contradictory from what we presumed before about the presence of impurities in plasma phase and their importance in surface activation. What needs to be taken into account is that the helium plasma is extremely rich with metastable species which excite the impurities in the plasma by different inelastic collisions. Therefore the atomic concentration of the impurities in the excited states can not be exactly correlated to their quantity in the ground state.

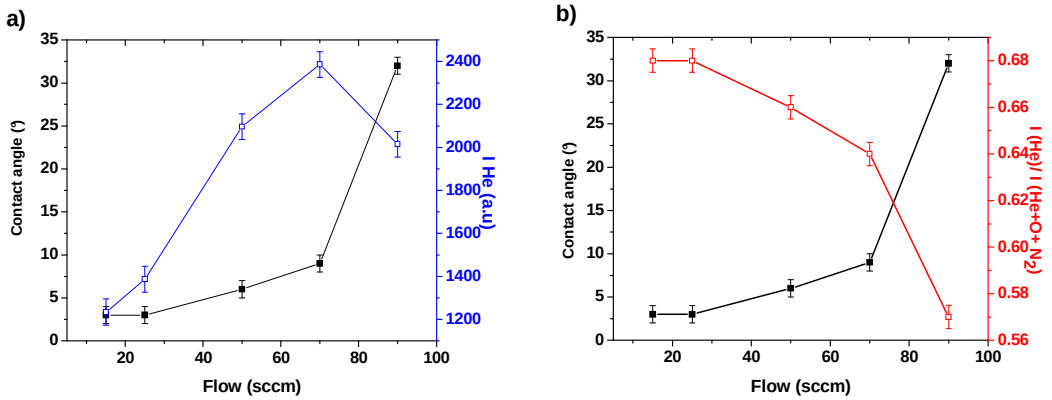

Figure 52: Effect of pressure (gas flow) on water contact angles of He plasma treated PP plates vs. a) He intensity lines and b) relative intensity of He line toward impurities (He/ He+O+N_2) obtained from optical emission spectroscopy.

3.2.1.2.2 Influence of discharge power on the wettability of modified surfaces

In order to evaluate the change of contact angle as a function of power, plasma conditions were fixed as follows: a gas flow to 30 sccm, and a treatment time to 1 min. The power varied in the range between 10 W and 100 W. Results in Figure 53 are showing that there is rather linear decrease of water contact angles with increasing discharge power up to 100 W. At these parameters, so called superhydrophilic conditions were obtained. The term superhydrophilicity was introduced to describe the complete spreading of water or liquid on substrates, although the definition has not been clarified yet and the unrestricted use of these terms sometimes stirs controversy, especially from the roughness point of view [192].

The comparison of results between contact angle measurements and optical emission spectroscopy indicate that higher helium intensity leads to higher activation of the surface. The intensity of He lines grows with power until around 70 W and after slightly decreases. It should be mentioned that at such low gas flow the reflected power at 100 W can reach up to 20 W, which could explain the drop of He intensity lines. As well with higher power the electron temperature decreases, therefore the ionization of He gas (Ei= 26.8 eV) [191] could be more difficult. Contrary to the results obtained by gas flow measurements, present study showed that higher He emission intensity leads to higher activation of the surface. This controversy suggests us that the He radicals are probably not the only species responsible for

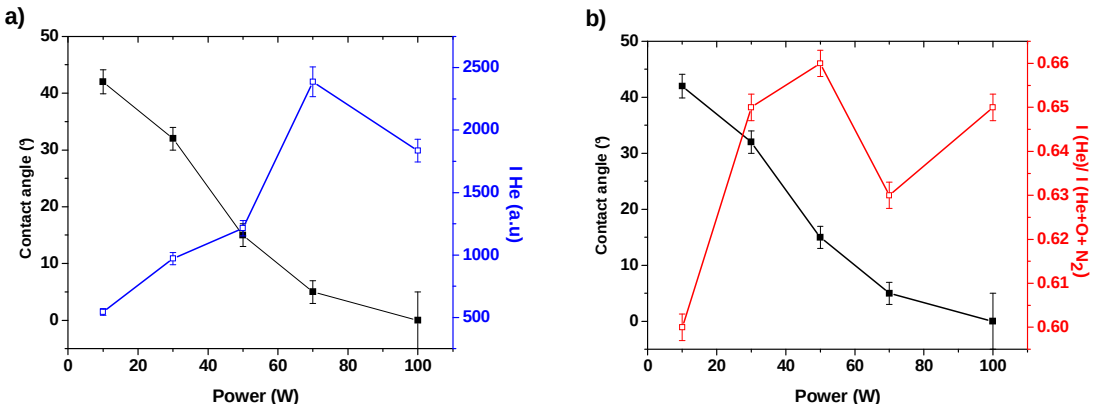

Figure 53: Effect of power on water contact angles of He plasma treated PP plates vs. a) He intensity lines and b) relative intensity of He line toward impurities (He/ He+ O+ N_2) obtained from optical emission spectroscopy.

Figure 53.b is showing a local minimum of relative intensity of He lines towards the impurities at 70 W, even though the contact angle keeps decreasing with power. At this point it must be said that the contact angle measurements at this power were often different, ±5º, probably due to the disturbance with reflected power. For this reason the power chosen for the future experiments was 70 W, where the plasma was stable and there was no reflected power.

3.2.1.2.3 Influence of treatment time on the wettability of modified surfaces

The evolution of contact angle with the time of treatment from 0 min to 3 min was established at following plasma conditions; P = 75 W and flow = 30 sccm, Figure 54. The decrease of contact angle until 1 min is very important, from 107.5° to 7° and then, between 1 min and 3 min it drops for few more degrees and becomes immeasurably low.

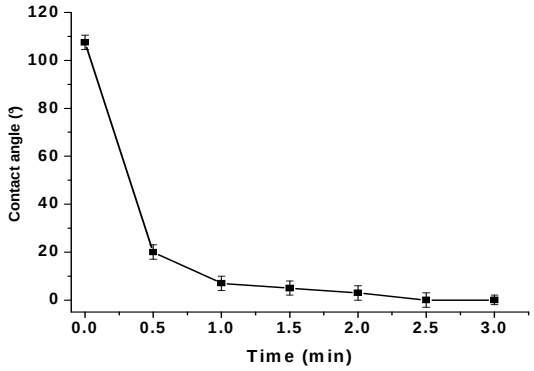

Figure 54: Effect of treatment time with helium plasma on water contact angle.

3.2.1.2.4 Ageing effects on the plasma-activated surfaces

Figure 55 is showing the ageing effect of He treated PP plates at optimal conditions when exposed to air. The ageing is very important in the first few hours after the plasma treatment and completely stabilizes after 4 days of exposal to air, where it reaches the value of 32°. Of our great interest is the ageing in a short time, up to 5 min, because we need to assure that the intended reactive groups are present on the plasma activated surface for the covalent immobilization of a polymer layer. Typical time needed between the plasma activation and surface grafting for our experiments is around 30 and 60 s. The contact angle measurements show little ageing affects in first minutes, therefore we can predict that there are still great amounts of free radical species present on the surface at the time of grafting reaction.

It can be said on generally that the ageing of plasma-grafted surfaces is caused by internal and external factors. Internal factors (entropy, interfacial enthalpy, glass transition temperature (Tg), crystallization and crosslinking density) influence the mobility of polymer chains, while external factors (oxidations, hydrolysis, radiation and temperature) are provided by the environment. The most important factor in helium plasma-treated samples are the post-oxidation reactions with free radicals which are followed by the surface adaptation. These chain reorientations are driven as a response to interfacial energy difference between the plasma-treated polymer surface and its

environment. As air is considered to be hydrophobic medium (compared to water) the polar groups on the surface tend to burry themselves in the bulk of the polymer until the equilibrium is reached [42]. Helium plasmas are often used for forming crosslinking and it was reported that under the condition that their density is important enough they can restrict to some point the surface mobility and adaptation. However the results communicated are diverse [193]. There is no general rule for ageing and it depends strongly on the type of plasma, substrate and ageing conditions.

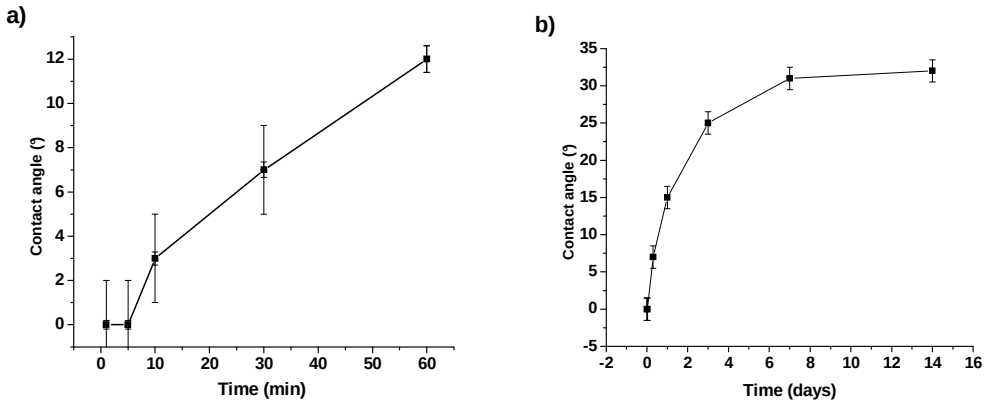

Figure 55: Contact angle measurements on the He treated PP plates stored under air; a) short time storage (up to 1 h), b) long time storage (up to 2 weeks).

3.2.1.3 Characterisation of the activated surface, determination of hydrophilic properties

The chemical composition of the untreated and He plasma treated plates was obtained by XPS analyses. Treated samples were stored under air for two weeks before they were analysed. Several samples were prepared at different discharge conditions, which are specified in Table 7.

Table 7: Elemental composition of samples (at. %).

Sample conditions: P (W), **t** (min), Φ (sccm)	**C (%)**	**O (%)**	**Al (%)**	**O/C**	**Contact angle (°)**
1. (0,0,0)	95.0	5.0	/	0.053	107.5
2. (75,1,15)	70.1	17.9	1.7	0.255	5
3. (75,1,30)	71.8	18.8	1.5	0.262	7
4. (75,1,50)	73.6	19.4	1.1	0.264	12
5. (75,1,80)	75.9	19.25	0.8	0.254	27
6. (20,1,30)	76.3	18.4	0.6	0.238	52
7. (100,1,30)	68.7	22.1	2.2	0.322	3
8. (75,0.5,30)	75.4	18.3	0.9	0.242	34
9. (75,3,30)	65.6	23.2	2.8	0.353	0

Sample 1 is a virgin PP plate, whereas samples 2-9 are plasma-modified PP plates. The discharge power (P) was changed in the range between 20 W and 100 W, treatment time (t) between 0.5 min and 3 min and the gas flow (Φ) between 15 sccm to 80 sccm. The elemental surface composition obtained from the low resolution XPS spectra of untreated and He plasma-treated samples is gathered in Table 7. There was also a small amount of impurities (Si, S, N) present on the surface that are not added to the table.

3.2.1.3.1 Influence of treatment time on the surface chemistry

The untreated sample 1 is composed mainly of carbon with a small percent of oxygen groups. After He plasma treatment (samples 2-9), the O/C ratio increases on all samples. There is also appearance of impurities in the form of aluminium, with relative concentration up to 2.8%.

The highest amount of oxygen, 23.2% or highest O/C ratio (0.353) is observed on the sample that was exposed to plasma for the longest treatment time (Table 7). The longer treatment time seems to enable a creation of higher amount of free radicals on the surface through hydrogen abstraction that consequently react with the oxygen from the atmosphere or can form crosslinking and unsaturated groups. These conditions correspond to immeasurably low water contact angle (Figure 56). The comparison of contact angle evolution and the XPS results (Figure 56.a) shows a correlation between the maximal incorporation of oxygen functional groups and ultimate surface energy with time. If we superimpose the two curves we can see the linear correlation between contact angle and O/C ratio with time, where at the O/C ratio of 0.32, the signs of surface saturation with oxygen functionalities appear (Figure 56.b).

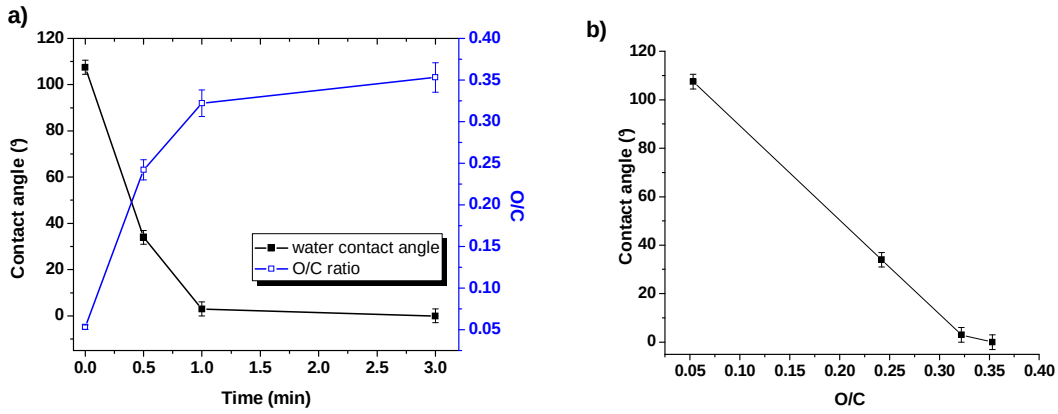

Figure 56: a) Variation of the contact angle and O/C ratio as a function of treatment time (P= 75 W, Φ= 30 sccm) and b) contact angle as a function of O/C ratio.

3.2.1.3.2 Influence of discharge power on the surface chemistry

The influence of discharge power on surface oxidation is quite abundant (Table 7). The O/C ratio at 100 W is 0.322, which is much larger than the O/C ratio at 75 W (0.262) or 20 W (0.238). The relative concentration of impurities is also much more pronounced with higher power (samples 3, 6 and 7); the amount Al increased by 1.6 % at 100 W comparing to the sample treated for the same time and flow at the power of 20 W.

The effect of the RF power on oxygen incorporation and substrate activation is demonstrated in Figure 57.a. The water contact angle is falling progressively with power input, while interestingly the O/C ratio at 20 W is not much lower than at 75 W. Optical emission studies showed that at 80 W the intensity of He lines reaches maximum while the relative intensity of He towards the oxygen impurities reaches minimum. Second thing that can be noticed as well is that there are higher amounts of aluminium impurities present on the surface at elevated powers. Results of contact angle measurement as a function of O/C ratio (Figure 57.b) are suggesting that at O/C ratio around 0.25 the surface starts to be saturated with oxygen functional groups.

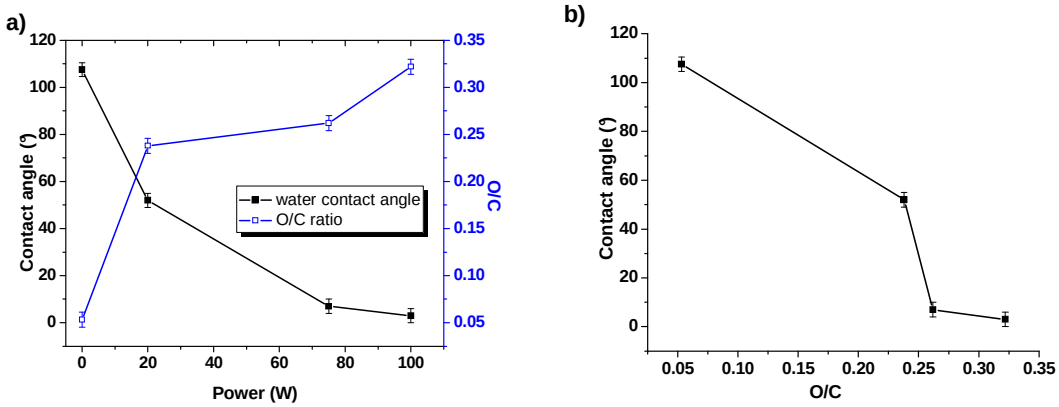

Figure 57: a) Variation of the contact angle and O/C ratio as a function of discharge power (t= 1 min, Φ= 30 sccm) and b) contact angle as a function of O/C ratio

3.2.1.3.3 Influence of pressure on the surface chemistry

The influence of gas flow on the evolution of the water contact angle and the O/C ratio is shown in Figure 58. The contact angle is increasing with gas flow (the oposite tendency to He emission lines), while the O/C ratio remains rather unchanged (Figure 58.a).

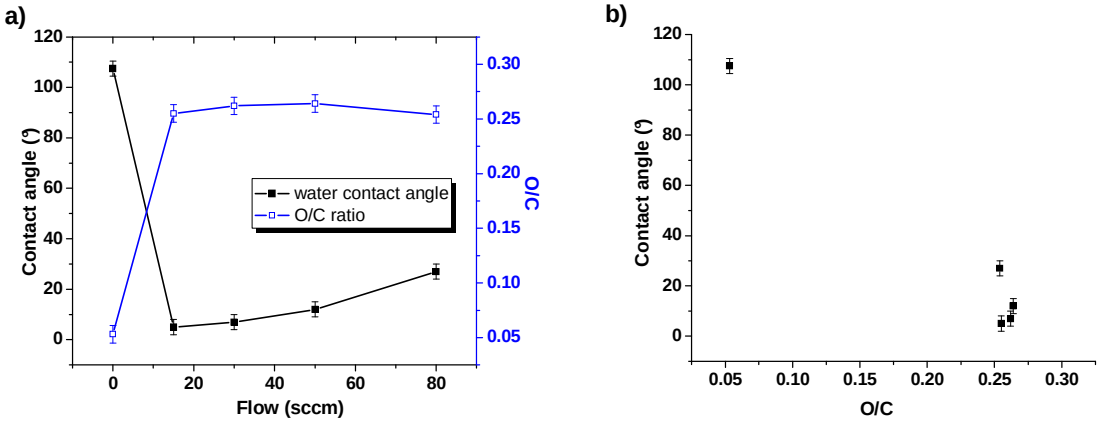

Figure 58: a) Variation of the contact angle and O/C ratio as a function of gas flow; (t= 1 min, P= 75 W) and b) contact angle as a function of O/C ratio.

In parallel with CF_4 plasma treatment the amount of aluminium on the surface decreases with increased gas flow (Table 7). In helium plasmas the ions have much lower mass and the sputtering coefficient is much lower than for CF_3^+ and similar heavy ions. The Al concentration in Table 7, however, is not much lower to those in Table 5. The dilemma can be explained by Penning ionization in He plasmas, namely electrons in plasma excite He atoms into the triplet states that are metastable. On the other hand the ionization fraction is at least an order of magnitude lower than the concentration of impurity gases in the He plasma. Taking this into account, it can be concluded that the concentration of heavy ions that are able to cause sputtering in He plasma at low gas flows is almost the same as in CF_4 plasma.

A high resolution C 1s spectrum was measured in order to provide some information about the functional groups on the surface of the untreated and treated samples. A characteristic C 1s spectrum of helium treated sample is presented in Figure 59. Relative concentrations of different functional groups on the surface of the samples after treatment are gathered in Table 8.

Table 8: Relative concentrations of carbon functionalized groups derived from the C 1s spectra obtained on the PP samples treated with He plasma.

Component Energy (eV)	**C1 (%) 285.0 eV**	**C2 (%) 286.7 eV**	**C3 (%) 288.2 eV**	**C2+ C3 (%)**
Possible assignment	C-C/C-H	C-O	C=O	
Sample P(W), t (min), Φ (sccm)				
1. (0,0,0)	98.2	1.8	/	1.8
2. (75,1,15)	81.9	14.0	4.1	18.1
3. (75,1,30)	81.2	14.2	4.6	18.8
4. (75,1,50)	79.8	15.1	5.1	20.2
5. (75,1,80)	82.2	13.3	4.5	17.8
6. (20,1,30)	81.7	14.3	4.0	18.2
7. (100,1,30)	79.6	15.3	5.1	21.1
8. (75,0.5,30)	80.1	15.1	4.8	19.8
9. (75,3,30)	78.0	16.6	5.4	21.9

The untreated sample is composed of mainly one peak C1 at 285.0 eV, corresponding to C-C/C-H bonds and a smaller one C2 at 286.7 eV belonging to single C-O functional groups (Table 8). After plasma treatment a new peak appears C3 at 288.1 eV, ascribed to C=O double bond (Figure 59, Table 8). At the same time the relative amount of C-O functional increase with treatment, up to 16.6 % comparing to the 1.7% for the untreated sample.

Samples have similar composition after treatment at all conditions and as expected those that were exposed longer to plasma treatment have slightly higher amount of C-O and C=O functional groups (2%). Relative concentration of groups with single bonds is 3 times higher than the amount of double bonds, around 15% and 5% respectively. These functional groups are caused mainly by post-oxidation reactions of free radicals with air and partially through oxidation reactions with the impurities (mostly water vapour) that are heaped up in the reactor chamber.

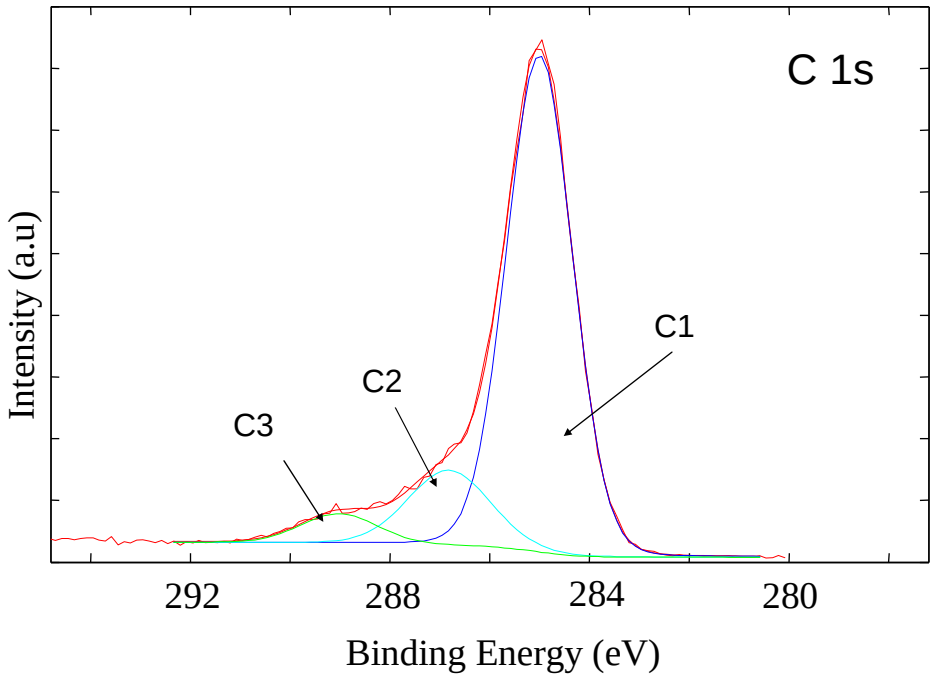

Figure 59: High resolution C 1s spectrum of He treated PP sample; P= 75 W, t= 1 min and flow= 30 sccm ($p=1.5\times10^{-2}$ mbar).

The results above have shown that superhydrophilic polypropylene surfaces can be obtained as long as we provide high discharge power (>75 W), low flow (< 30 sccm) and the treatment time superior to 2.5 min. At these conditions the XPS analyses showed the highest amount of both oxygen and aluminium atoms on the surface. Nevertheless it is hard to distribute the influence of each component on the formation of superhydrophilic surface and therefore further analyses should be undertaken on this topic. What needs to be mentioned at this point is that by using noble gasses such as helium, the formation of extremely reactive free radicals on the surface occurs. These free radicals abruptly react with the atmosphere or the liquid to which they are exposed to. Therefore the contact angles that were measured immediately after the plasma treatment probably show better insight into the phenomena than the XPS analyses that were performed approximately 2 weeks after the treatment. In this time the ageing of samples was already severe, the contact angle increased form immeasurably low to approximately 30º (Figure 55.b).

3.2.2 Polymer grafting onto plasma-activated surface

After the helium plasma treatment step the activated samples were taken from the discharge chamber and immersed into three different types of polymer or polymer containing solutions at altered experimental conditions. Surfaces were analyzed by contact angle measurements, XPS analyses, zeta potential method, while their topography was examined by AFM imaging.

3.2.2.1 Characterisation of the modified surfaces, determination of the hydrophilic properties

The surface energy of samples was calculated from the contact angle measurements of three different liquids (ultrapure milliQ water, diiodomethane and glycerol) using the Fowkes and Owens- Wendt method:

$\gamma_l (1+\cos\Theta) = 2 (\gamma_s^d \gamma_l^d)^{1/2}$ and $\gamma_l (1+\cos\Theta) = 2 (\gamma_s^d \gamma_l^d)^{1/2} + 2 (\gamma_s^p \gamma_l^p)^{1/2}$

where γ stands for surface energy, Θ for contact angle and the indexes s and l indicate the solid and liquid respectively. The exponents d and p present dispersive and polar components of the surface energy. The surface energies of different liquids are gathered in Table 9.

Table 9: Surface energies of different liquids used for contact angle measurements.

Liquid	γ_l (mJ/m^2)	γ_l^d (mJ/m^2)	γ_l^p (mJ/m^2)
Water	72.8	21.8	51.0
Diiodomethane	50.8	49.5	26.4
Glycerol	63.4	37	1.3

3.2.2.1.1 Grafting of PNIPAM

3.2.2.1.1.1 Optimisation of grafting parameters

In order to optimize the grafting parameters of PNIPAM, the solutions were prepared in different range of concentrations, between 0.001 g/L and 10 g/L. Helium plasma-treated polypropylene plates (P= 75 W, flow= 30 sccm and t= 3 min) were immersed into aqueous polymer solutions for 2 h at room temperature. The time between completed plasma activation and immersion was less than one minute. After that samples were taken from the liquid, rinsed with distilled water and dried under laminar flow at room temperature over night. The contact angles on dried samples were measured with 3 µL drop of water and 1.5 µL drop of diiodomethane (Figure 60.a). In the next step the solution concentration was fixed at 2 g/L and the time of immersion (at same plasma parameters) varied between 5 min and 300 min (Figure 60. b).

Figure 60.a is showing an evolution of contact angles with the concentration of polymer solution. The contact angle with diiodomethane remained the same for all concentrations while the water contact angle measurements showed a dynamic curve. The point at c= 10^{-8} g/L should be noted that it corresponds to the plasma-activated PP substrate immersed into distilled water solution as a reference for 2 h, because the concentration of polymer is in logarithm scale it could not be set to zero. It can be seen that the changes on the surface begin to happen between the concentration of 0.01 g/L and 0.05 g/L and become stable in the range of concentrations between 0.5 g/L and 10 g/L, corresponding to the water contact angle around 10°. In the Figure 60.b is shown the change of contact angle with time of immersion in PNIPAM solution that was prepared at the concentration of 0.5 g/ L. For short treatment times, less than 10 min, the contact angle value exceeds 30°, which corresponds to

the value of helium plasma-activated sample stored in water. Above 15 min of immersion stable surfaces are obtained with the contact angles approximately 10°. The contact angle with diiodomethane did not change with immersion time and remained at a value of 55°.

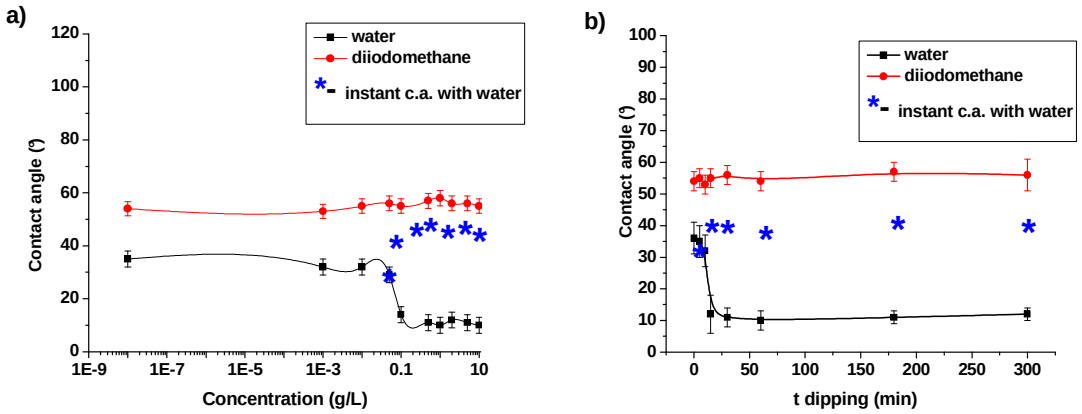

Figure 60: Contact angle measurements on PNIPAM treated substrates as a function of a) concentration b) dipping time. The * present the measurement of water contact angle instantly after drop deposition.

These contact angles were measured when the water contact angle stopped spreading over the surface, typically between 3 s and 5 s after their deposition. The blue stars on the Figure 60 present the Θ that was measured instantly (with the camera) after drop deposition, where the values corresponded to around 40-45°. The dynamism of the surface could be explained by specific properties of PNIPAM polymer. The NIPAM monomer is composed of hydrophobic part (carbon backbone and dimethyl groups) and hydrophilic amid part. For this reason, dried grafted samples probably expose their hydrophobic parts towards the air, because the air is considered to be hydrophobic medium (compared to water). When these chains come in contact with water, the structural rearrangements happen where hydrophilic parts get exposed to the water and hydrophobic parts burry themselves into the bulk. From these measurements it can be concluded that the polymer was successfully grafted on our substrates and if we want to obtain stable freely fluctuating chains the concentration should be around 0.5 g/L. The total surface energy measured at these conditions was calculated by Fowkes method and corresponds to 72.1 mJ/m^2, where polar part presents 58 mJ/m^{2}and apolar 13.6 mJ/m^2. The Θ used for the calculation of surface energy was at 10°. We have taken into account rather this contact angle than the one measured instantly due to the fact that these samples will be used in aqueous medium for further applications and are therefore of our prime interest.

PNIPAM is a very well known thermosensitive polymer with the lower critical solution temperature (LCST) temperature between hydrophilic and hydrophobic state at around 32°C [105]. At room temperature the WCA values reported by several authors varied between 40° and 65°. The extent of transition above the LCST temperature depends strongly on grafting conditions and the size of polymer chains. For example it is possible that there is no transition or extremely weak transition observed with augmentation of temperature above LCST. This was mainly attributed to the fact that the polymer chains were too short. On the other side the transitions even up to the Θ of 90° were reported, corresponding to the water contact angle value of apolar C-H chains found in polymers like polypropylene or polyethylene [109].

The absence of temperature transition was also present on our supports. There could be several reasons; firstly it could be due to the small molar mass of PNIPAM molecule

(20000-25000 g/mol), secondly the grafting of polymers by plasma activation method did not exhibit typical brush regime, due to the extremly large number of active sites in short distances that can react non-specifically with polymer backbone or side chain functional groups or finally the water spreading over the surface (dilution of hydrophilic chains) is energetically more favourable than the temperature induced hydrophobic transition. Namely the spreading of the water drop on modified substrates occurred even at elevated temperatures as high as 60°C.

The change of water contact angle on PNIPAM grafted sample with time is shown in Figure 61. It can be seen that there is a rapid drop of contact angle from 40º to 13º in the first two seconds after the deposition and after it starts to stabilise and reaches the final contact angle of 10 º.

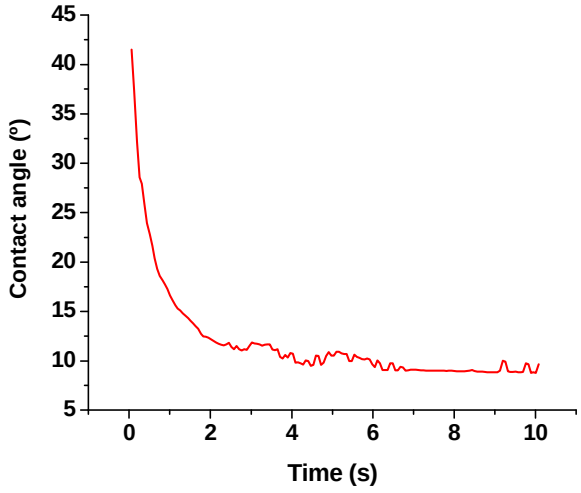

Figure 61: Water contact angle as a function of deposition time on PNIPAM grafted surface.

3.2.2.1.1.2 Influence of plasma treatment time on PNIPAM grafting

With the intention to study the influence of plasma parameters on PNIPAM grafting the activation of substrates by helium plasma was done at P= 75 W and flow 30 sccm while the time of treatment varied between 0 and 180 s. The solution concentration was fixed at 0.5 g/L and the time of immersion to 2 h. The surface energy parameters provided by contact angle measurements are gathered in Table 10.

Table 10: Surface energy of PP films grafted with PNIPAM at different plasma activation times.

Method/ Time He (s)	**Fowkes**			**Owens- Wendt**	
	γ_{tot} (mJ/m^2)	γ_s^d (mJ/m^2)	γ_s^p (mJ/m^2)	γ_s^- (mJ/m^2)	γ_s^+ (mJ/m^2)
PP virgin	34.8	34.7	0.1	0.0	0.1
0	35.1	23.4	11.8	27.6	1
10	69.4	18.4	51.0	111.3	2.4
30	69.4	17.9	51.5	110.0	2.4
60	69.8	17.8	52.0	109.5	2.4
180	72.1	19.1	52.9	110.0	1.2
180*	53.8	22.3	31.6	60.3	0.1

The total surface energy of samples increased from 34.8 mJ/m^2 up to 72.1 mJ/m^2 due to the incorporation of polar functional groups onto the surface. The surface energy parameters marked by asterix (*) at 180 s correspond to the Θ measured instantly after the deposition, before the substrate had opportunity to stabilize.

It can be seen that even a very short plasma activation time of 10 s enables high grafting yield of PNIPAM. Contrary, without plasma pre-treatment there is a very low incorporation of PNIPAM molecules and the total energy is similar to the one of virgin PP. The distinction between dispersive and polar component however showed that there were some changes that happened on the surface. The same information is obtained from the Owens-Wendt method where the basic component increased from 0.0 mJ/m^2 to 27.6 mJ/m^2 for PNIPAM grafted substrate without plasma pre-treatment respectively to the virgin PP sample.

On all other surfaces activated by He plasma there is a considerable increase of basic component. This is in a good correlation with the PNIPAM properties, because amides are basic molecules that possess pKa around 30 for *N*,*N*-dimethylacetamide (CH_3CONMe_2, where Me = CH_3). Interestingly there is not much difference in surface energy parameters between the samples that were activated by helium plasma just for 10 s and the ones activated for 180 s, even though that their surface energy varied substantially.

3.2.2.1.2 Grafting of MIX I

MIX I is standing for the mixed solution of Poly (N-isopropylacrylamide) (PNIPAM) polymer and cetyltrimethylammonium bromide (CTAB) surfactant. Preparation of solutions is explained in experimental section (2.1.2) and their molar ratios are indicated before each experiment. The mixture of polymer and surfactant was done in order to obtain surfaces with desired functional properties, concerning functional groups, charge and topography. The choice of CTAB was made due to the fact that recombinant prion protein possesses very high isoelectric point (pI=9.8) and therefore at working conditions (pH=7.4) the protein will be partially positively charged and potentially repelled (electrostatically) from the positively charged surface provided by CTAB.

3.2.2.1.2.1 Optimisation of grafting parameters

In the first part of this study, the influence of polymer and surfactant concentration on the surface energy parameters was evaluated. The samples were activated by He plasma (P= 75 W, flow= 30 sccm and t= 1 min) and immediately immersed into solutions at various concentration ratios between polymer and surfactant. Either concentration of PNIPAM (C_p) was fixed at 0.5 g/L and concentration of CTAB (C_c) was changed between 0.1 and 2 mM or the concentration of CTAB was fixed at 1 mM and the concentration of PNIPAM changed between 0.02 and 2 g/L. The preparation of solutions is described in the experimental part. The surface free energy components determined by contact angle measurements are gathered in Table 11.

The results are showing that there is no or very small effect of polymer to surfactant ratios on the total surface energy (γ_{tot}) measured by Fowks method (Table 11). The notable difference is observed just with the sample that was immersed into pure surfactant solution, resulting in a total surface energy 62.3 mJ/m^2 with 21.1 mJ/m^2 belonging to dispersive part and 41.2 mJ/m^2 to the polar component. The CTAB discloses higher apolar properties towards PNIPAM, which is in a good agreement with their chemical composition.

Table 11: Surface energy of PP films grafted with MIX I at different molar ratios of polymer and surfactant; where $C_{PNIPAM=}$ C_p (g/L) and C_{CTAB}= C_c (mM).

Method/ Solution;	Fowks			Owens- Wendt	
	γ_{tot} (mJ/m^2)	γ_s^d (mJ/m^2)	γ_s^p (mJ/m^2)	γ_s^- (mJ/m^2)	γ_s^+ (mJ/m^2)
C_P= 0.5; Cc= 0.0	69.8	17.8	52.0	109.5	2.4
C_P= 0.5; Cc= 0.1	68.2	17.9	50.3	78.2	0.0
C_P= 0.5; Cc= 0.2	67.7	16.3	51.4	68.5	0.6
C_P= 0.5; Cc= 1.0	67.5	16.6	50.9	61.5	0.1
C_P= 0.5; Cc= 2.0	65.4	15.5	49.9	50.5	2.5
C_c= 1.0; Cc= 0.02	66.7	18.8	47.4	53.5	2.1
C_c= 1.0; Cp= 0.2	67.3	17.2	50.1	61.1	1.0
C_c= 1.0; Cp= 0.5	68.2	17.9	50.3	68.2	0.0
C_c= 1.0; Cp= 2.0	70.3	17.3	50.0	83.3	0.0
C_c= 1.0; Cp= 0.0	62.3	21.1	41.2	40.3	2.4

On the other hand it can be clearly seen that the addition of surfactant to the polymer solution vigorously influences the surface basic component (γ_s^-, Figure 62). The basic character of CTAB (40.3 mJ/m^2) is much lower than the one of PNIPAM (109.5 mJ/m^2). Just a small addition of surfactant, much below the CMC at 1 mM, results in a severe drop of surface basic component. The drop is most pronounced until the addition of 0.2 mM of CTAB and keeps decreasing less radically after this concentration (Figure 62.a). When the surfactant solution is kept at 1 mM and PNIPAM is added the γ_s^- increases since the PNIPAM concentration of 0.01 g/L and starts to stabilize at c= 0.5 g/L. MIX I has a γ_s^- value between pure polymer and surfactant, 61.5 mJ/m^2, indicating that we have accomplished to graft both of the components onto the surface. By this relatively simple method, we can control the surface energy and its acid-base character.

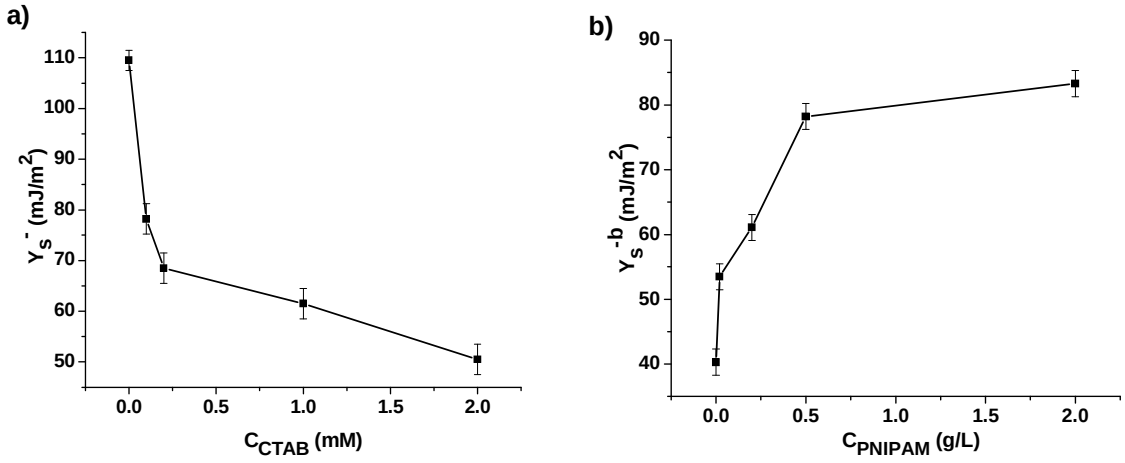

Figure 62: Influence of a) CTAB addition to polymer solution and b) PNIPAM addition to surfactant solution on the basic character of the surface.

3.2.2.1.2.2 Influence of plasma treatment time on MIX I grafting

The influence of plasma treatment time on MIX I grafting was done at different plasma activation times, between 0 s and 180 s, where flow was equal to 30 sccm and the power

of discharge 75 W. The concentration of PNIPAM solution was fixed at 0.5 g/L, concentration of CTAB to 1 mM and the time of immersion to 5 h.

Table 12: Surface energy of PP films grafted with MIX I at different plasma activation times.

Method/ Time He (s)	Fowkes			Owens- Wendt	
	γ_{tot} (mJ/m^2)	γ_s^d (mJ/m^2)	γ_s^p (mJ/m^2)	γ_s^- (mJ/m^2)	γ_s^+ (mJ/m^2)
PP virgin	34.8	34.7	0.1	0.0	0.1
0	31.1	28.5	2.6	4.32	0.0
10	69.7	15.9	53.9	63.9	1.0
30	69.0	16.5	52.5	65.9	0.1
60	67.5	16.6	50.9	61.5	0.1
180	67.1	15.2	51.8	66.6	0.5

Table 12 is showing the variation of the surface energy of PP films after grafting with MIX I at different plasma activation times. The total surface energy of the untreated sample increased from 34.8 mJ/m^2 up to 69.7 mJ/m^2 for treated samples respectively. Surfaces that were not activated by He plasma and immersed into MIX I solution show a very low grafting density. The polar component increased just for 2.5 mJ/m^2, apolar decreased for 6.2 mJ/m^2 and basic component for 4.32 mJ/m^2. The basic component of treated surfaces was on average around 65 mJ/m^2. For all treatment times the contact angle measurement results did not indicate any special differences between the grafted surfaces.

3.2.2.1.3 Grafting of MIX II

MIX II is standing for the mixed solution of poly(N-isopropylacrylamide) (PNIPAM) polymer and polyoxyethylene (20) sorbitan monolaurate (commercially also known as Tween 20®) surfactant. Details on solution preparation are described in experimental part. As mentioned before for MIX I, the mixture was done in order to obtain surfaces with desired functional groups, charge and topography. Tween 20® was chosen because the non-fouling surfaces are known to often possess neutral polar functional groups with high degree of hydration [194].

3.2.2.1.3.1 Optimisation of grafting parameters

With a purpose to examine how different concentration of polymer and surfactant impact the surface energy and potential basic-acidic character, He plasma-activated samples (P= 75 W, flow= 30 sccm and t= 3 min) were immersed into solutions with different concentration ratios between PNIPAM and Tween 20®. The concentration of PNIPAM (C_p) was fixed at 0.5 g/L and mass fraction of Tween 20® (W_T) in the distilled water varied between 0.01 % and 0.1 %. After that the concentration of Tween 20® was fixed at 0.05 % and concentration of PNIPAM changed between 0.02 and 2 g/L. The surface free energy components determined by contact angle measurements are gathered in Table 13.

The total surface energy (γ_{tot}) between the samples did not change substantially, approximately up to 7 mJ/m^2 between samples. The pure surfactant has a polar energy γ_s^p= 41.3 mJ/m^2 and the pure polymer γ_s^p= 58.5 mJ/m^2, whereas their mixture has a values in between the two, averagely around 45.0 mJ/m^2. Therefore the addition of Tween 20® to the

PNIPAM solution gives rise to the dispersive component (γ_s^d), while the polar component (γ_s^p) and basic character of the surface decrease. The decrease of polarity with surfactant incorporation is due to the long hydrocarbon chains, while in the PNIPAM backbone each monomer possesses a polar amid group. These dimethylamide functional groups have the pKa around 30, while the big surfactant head of Tween 20® is composed of larger amount of ether, ester and alcohol groups, which pKa's are around 40-50, 20-30 and 16-18 respectively.

Table 13: Surface energy of PP films grafted with MIX II at different molar ratios of polymer and surfactant; where $C_{PNIPAM=}$ C_p (g/L) and C_{Twee20}= W_T (%).

Method/ Solution;	Fowkes			Owens- Wendt	
	γ_{tot} (mJ/m^2)	γ_s^d (mJ/m^2)	γ_s^p (mJ/m^2)	γ_s^- (mJ/m^2)	γ_s^+ (mJ/m^2)
C_P= 0.5; Wt= 0.0	72.1	13.6	58.5	110.0	1.2
C_P= 0.5; W_T= 0.01	67.7	22.2	45.5	73.0	0.1
C_P= 0.5; W_T= 0.02	69.7	21.9	47.8	77.9	0.1
C_P= 0.5; W_T= 0.05	66.8	23.4	43.5	63.9	0.0
C_P= 0.5; W_T= 0.10	71.0	25.5	45.4	54.4	0.1
W_c= 0.05; **Cp= 0.02**	68.0	27.6	40.4	61.4	0.0
W_c= 0.05; **Cp= 0.2**	72.2	25.8	46.4	74.9	0.1
W_c= 0.05; **Cp= 0.5**	66.8	23.4	43.5	73.9	0.0
W_c= 0.05**; Cp= 2.0**	70.7	25.5	45.4	77.9	0.1
W_c= 0.05; **Cp= 0.0**	74.2	32.9	41.3	50.1	0.1

Figure 63.a presents the influence of surfactant addition to 0.5g/L PNIPAM polymer solution on surface basicity. The basic character of PNIPAM substrates is progressively decreased by addition of Tween 20®, from 109.5 mJ/m^2 corresponding to PNIPAM down to 54.4 mJ/m^2 when 0.10% of surfactant is added. This value is quite close to the γ_s^- of Tween 20®, assimilated to 50.1 mJ/m^2.

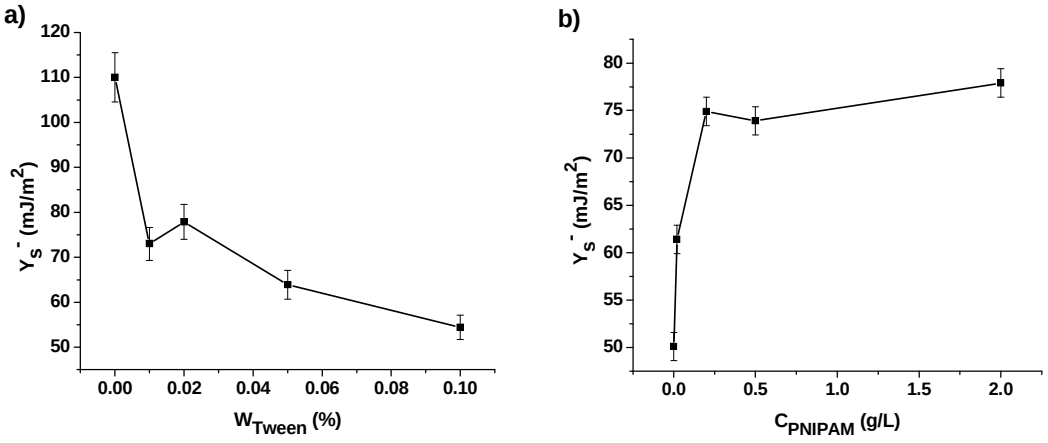

Figure 63: Influence of a) CTAB addition to polymer solution and b) PNIPAM addition to surfactant solution on the basic character of the surface.

When the surfactant solution is kept at 0.05 % and PNIPAM is added, the γ_s^- increases since the PNIPAM concentration of 0.01 g/L and starts to stabilize at c= 0.2 g/L. Even though the concentration of PNIPAM keeps increasing the γ_s^- does not change substantially, indicating a strong influence of surfactant in a wide range. MIX II has a

basic value between pure polymer and surfactant, around 70 mJ/m^2, indicating the presence of both components on the surface. In the two studies, values of surface energy obtained in the case of surfactant addition to polymer are coherent and stable. Contrary to this, when PNIPAM was added to surfactant solution the values were not that clear. It could be due to the micellization of surfactant solution before the polymer was added.

3.2.2.1.3.2 Influence of plasma treatment time on MIX II grafting

The substrates were activated by helium plasma at P= 75 W and flow 30 sccm and the time of treatment varied between 0 and 180 s. The concentration of PNIPAM solution was fixed at 0.5 g/L and concentration of Tween 20® to 0.05%. The immersion of the activated substrates was done for 5 h.

Table 14: Surface energy of PP films grafted with MIX II at different plasma activation times

Method/ Time He (s)	**Fowkes**			**Owens- Wendt**	
	γ_{tot} (mJ/m^2)	γ_s^d (mJ/m^2)	γ_s^p (mJ/m^2)	γ_s^- (mJ/m^2)	γ_s^+ (mJ/m^2)
PP virgin	34.8	34.7	0.1	0.0	0.1
0	29.7	28.6	1.2	2.8	0.1
10	67.0	24.4	42.6	88.7	1.9
30	68.5	18.5	50.0	85.4	0.3
60	67.0	24.4	42.6	82.0	1.0
180	66.8	23.4	43.5	73.9	0.0

The results are presented in Table 14. Analogous to PNIPAM and MIX I grafting, the time does not seem to affect much the extent of total surface energy or its basic-acid properties. When the surface was not activated the difference became important. The grafting is inhibited and there is almost no difference in surface energy components between the virgin PP sample and the virgin PP sample immersed into MIX II solution. This information is indicating that there is an extremely low grafting yield without plasma pre-treatment and that activation is necessary in order to obtain successful grafting of polymer-surfactant complex on our substrates.

3.2.2.1.4 Ageing of grafted samples

The ageing of PNIPAM, MIX I and MIX II grafted samples under atmosphere at room temperature was monitored up to two months. This time was chosen due to the fact that long time stability of the surfaces is required for bio-application reasons. All samples were prepared after 3 min of activation by helium plasma and immersed into a) PNIPAM solution at c= 0.5 g/L, b) MIX I solution at C_{PNIPAM}= 0.5 g/L and C_{CTAB}= 1mM and c) MIX II solution at C_{PNIPAM}= 0.5 g/L and $W_{Tween20}$= 0.05%. The results in Figure 64 are attesting for the sample stability in the period of at least two months.

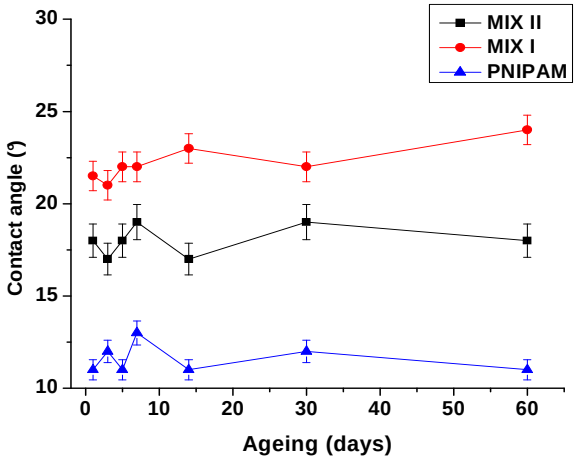

Figure 64: Ageing of PNIPAM, MIX I and MIX II grafted samples under air in the period of two months.

3.2.3 Characterisation of the chemical composition of grafted surfaces

The surface chemistry of polypropylene plates grafted with PNIPAM, MIX I and MIX II was examined by XPS analyses. The extent of polymer and/or polymer containing surfactant solutions was followed as a function of helium plasma treatment time, which was varied between 0s and 180 s. The activation was done at discharge power 75 W and gas flow 30 sccm. The treated supports were also alternatively washed with buffer (PBS) solution and water in order to ensure that the grafted layers were stable.

3.2.3.1 Grafting of PNIPAM

PNIPAM solutions for XPS study of grafted supports were prepared at the concentration of 0.5 g/L. The immersion time of plasma activated PP substrates in these solutions was fixed to 2 h. The information about the surface chemistry was obtained from the XPS high resolution C 1s and N 1s scan (Figures 65.a and 65.b respectively). Relative concentrations of different functional groups on the surface of the samples are gathered in Table 15.

The C1 peak at 285.0 eV corresponds to C-C/C-H bonds, C2 peak at 286.4 eV to C- N/C-O and C3 at 287.7 eV is indicative of C=O functional groups. The amount of C-C/C-H bonds decreased from 97.2% down to 70.5 % for the samples that were exposed to helium plasma for the longest time. On the other side the peaks C2 and C3 increased to 14.6 % and 14.8 % respectively. Theoretically for PNIPAM molecules, the C 1s peak should posses 66.7% of C1 peak and 16.7% of C2 and C3 peaks, under the condition that they belong strictly to the N-C and C=O bond respectively. Nevertheless it is hard to distinguish and decompose the C2 peak, C-N and C-O bonds, because their binding energies are too close at 285.9 eV for C-N and at 286. 5 eV for C-O. Analogously can be said for the C3 peak, which could belong to either C=O/O-C-O bonds at 287.7 eV and N-C=O at 288.1 eV. The N 1s peak at 399.9 eV (Fig. 65.b) is assigned to N-C/N-C=O functional groups.

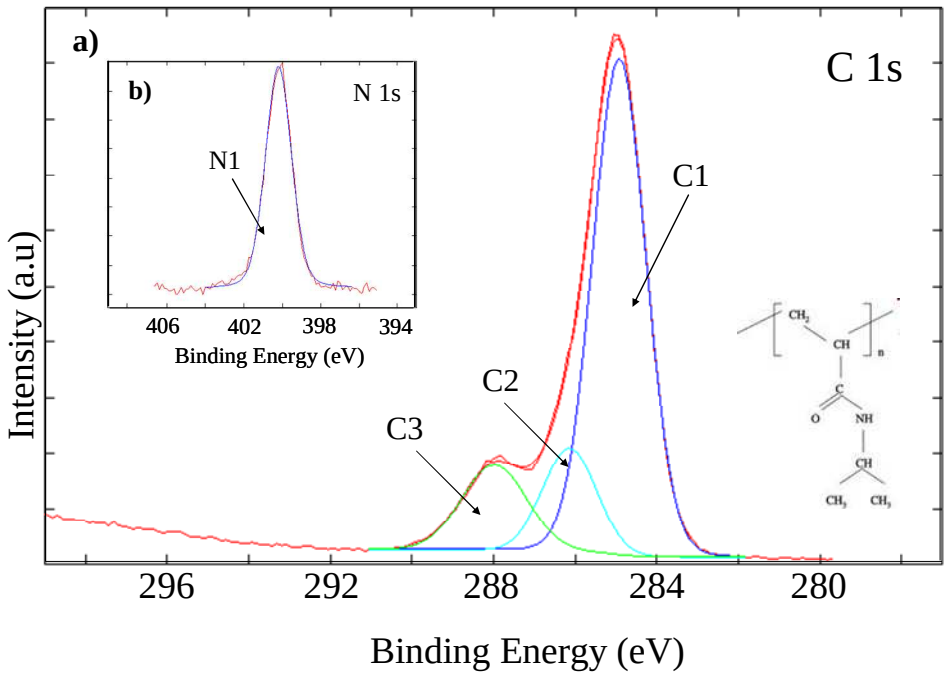

Figure 65: High resolution a) C 1s and b) N 1s spectra of PNIPAM grafted on helium activated PP plates (P= 75 W, flow= 30 sccm and t= 3 min; $t_{dipping}$= 2 h and c= 0.5 g/L).

The results in Table 15 suggest that there is a great difference of functional group distribution between the samples as a function of plasma activation time, adversely to the surface energy measurements. Higher plasma treatment times lead to lower the relative amount of C2 peak and increase the C3 peak composed of double C=O/C=O-N functional groups found in PNIPAM. In another way the percentage of polar groups on the surface remained practically the same no matter how long the pre-treatment time was, but their chemical nature is different. Absence of pre-irradiation gives coherent results with contact angle measurements, indicating that the grafting yield of polymer was extremely low. The results are showing that there was the highest incorporation of PNIPAM chains on surfaces that were pre-treated with plasma for the 180 s, where the Θ on activated samples was immeasurably low. The difference between PNIPAM treated samples with and without washing in buffer solution (Table 15, samples 180 s* and 180 s respectively) is insignificant, indicating the strong covalent attachment of grafted layers.

Table 15: Decomposition of C 1s peaks of untreated and PNIPAM-grafted samples with assigned functional groups and their relative concentrations at different He activation times. The * stands for the sample washed with buffer solution.

Component Energy (eV)	**C1 (%) 285.0 eV**	**C2 (%) 286.4 eV**	**C3 (%) 287.7 eV**	**C2+C3/ ΣC1+C2+C3**
Possible assignment	C-C/C-H	C-O/ C-N	C=O/ N-C=O	
PP	97,2	2,8	/	2.9 %
PNIPAM 0 s	88.2	8.2	3.6	11.8 %
PNIPAM 10 s	72.0	22.5	5.5	28.0 %
PNIPAM 60 s	70.0	18.8	7.2	26.0 %
PNIPAM 180 s	70.5	14.6	14.8	29.4 %
PNIPAM 180 s*	68.5	16.6	14.9	31.5%

3.2.3.2 Grafting of MIX I

MIX I solutions for XPS analyses were prepared at the C_{PNIPAM}= 0.5 g/L and C_{CTAB}= 1 mM. The immersion of plasma-activated PP substrates in these solutions was fixed to 5 h. Additionally CTAB solution alone was prepared at 1 mM in order to compare sample properties. The chemical composition of treated samples derived from high resolution C 1s spectra is gathered in Table 16. The C 1s and N 1s high resolution peaks of PNIPAM, CTAB and MIX I grafted after 180 s of helium pre-treatment are presented in Figures 65, 66 and 67 respectively.

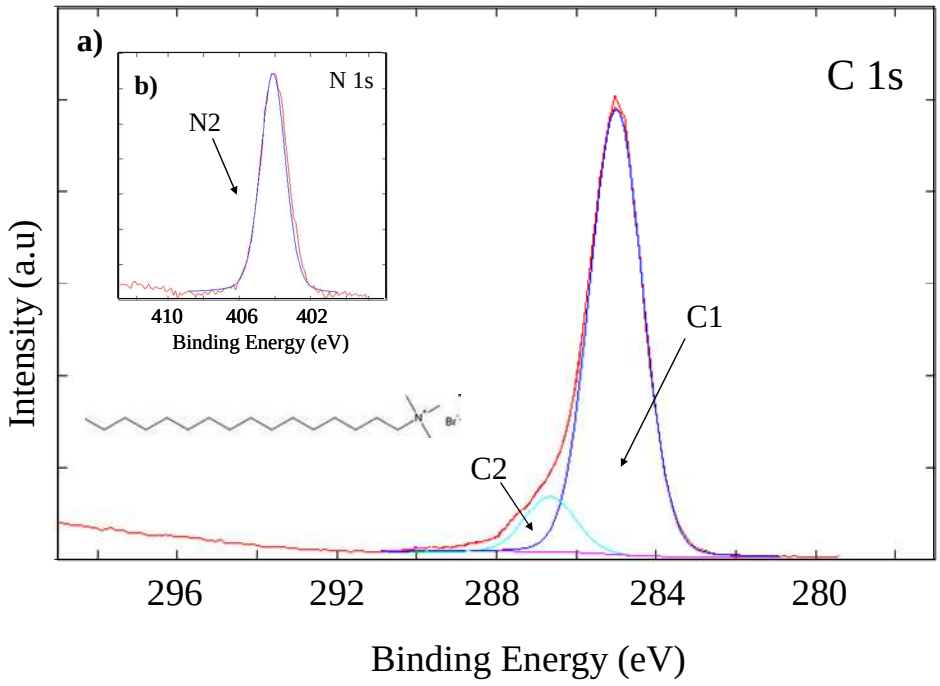

Figure 66: High resolution a) C 1s and b) N 1s spectra of CTAB grafted on helium activated PP plates (P= 75 W, flow= 30 sccm and t= 3 min; $t_{dipping}$= 5 h and C_{CTAB}= 1 mM).

Figure 66.a is showing a high resolution spectra of CTAB with two peaks, a major one (C1) at 285.0 eV ascribed to C-C/C-H functional groups and a smaller one at 286.4 eV corresponding to C-N/C-O functionalities. The N2 peak at 402.5 eV corresponds to charged nitrogen group functionalities as found in surfactant (Figure 66.b). Namely, CTAB is cationic surfactant, composed of long hydrocarbon chain and N^+ $(CH_3)_3$ Br^- head.

MIX I (Figure 67) spectrum corresponds to both individual spectra of polymer and surfactant (Figure 65 and Figure 66). There is an appearance of C3 peak, in comparison to sole surfactant, due to the incorporation of PNIPAM. Nevertheless, the relative amount of C=O/N-C=O functional groups was smaller in comparison with a pure PNIPAM polymer. Moreover the N 1s peak of MIX I is composed of two sub-peaks N1 at 399.1 eV and N2 at 402.5 eV, belonging to amid group of PNIPAM and positively charged nitrogen of CTAB. This data are indicating that the surface is composed of both- polymer and surfactant.

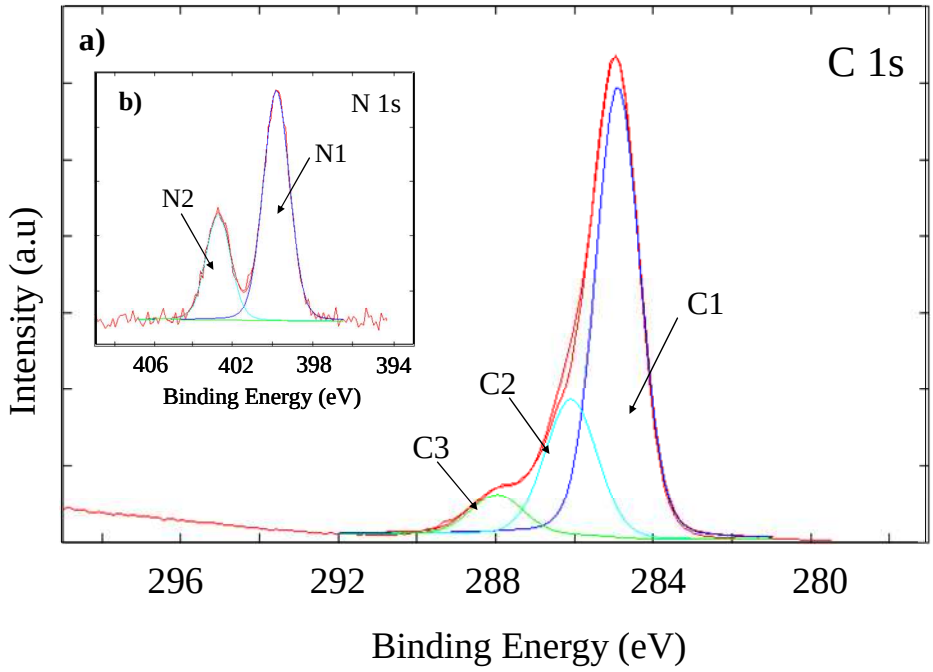

Figure 67: High resolution a) C 1s and b) N 1s spectra of CTAB grafted on helium activated PP plates (P= 75 W, flow= 30 sccm and t= 3 min; $t_{dipping}$= 5 h; C_{CTAB}= 1 mM and C_{PNIPAM}=0.5g/L.

Table 16: Decomposition of C 1s peaks of untreated and MIX I grafted samples with assigned functional groups and their relative concentrations at different He plasma-activation times. The * stands for the sample washed with buffer solution.

Component Energy (eV)	**C1 (%) 285.0 eV**	**C2 (%) 286.4 eV**	**C3 (%) 287.7 eV**	**C2+C3/ ΣC1+C2+C3**
Possible assignment	C-C/C-H	C-O/ C-N	C=O/ N-C=O	
PP	97,2	2,8	/	2.80 %
MIX I 0 s	92.7	7.3	/	7.30 %
MIX I 10 s	77.2	14.5	8.3	22.8 %
MIX I 60 s	75.6	15.7	8.6	24.3 %
MIX I 60 s*	74.4	16.8	8.5	25.3%
MIX I 180 s	73.0	16.9	10.1	27.0 %
PNIPAM 180 s	70.5	14.6	14.8	29.4 %
CTAB 60 s	88.1	12.0	/	12.0 %

The results in Table 16 are showing various things. First the untreated polypropylene plate immersed into polymer/surfactant solution exhibited very little change in the surface functional groups. The same conclusion was drawn from contact angle measurements. The amount of polar functional groups on the surface increases with pre-treatment time. Contrary to PNIPAM polymer where C2 peak was decreasing with treatment time and C3 increasing, there is an augmentation of both (C2 and C3) peaks in MIX I grafted samples, corresponding to the C-O/C-N and N-C=O/C=O functional groups respectively. The results are confirming the presence of both components (PNIPAM and CTAB) on the surface. Consistently with PNIPAM results, there were no denoting changes observed on the MIX I treated surface after washing them in buffer solution.

3.2.3.3 Grafting of MIX II

MIX II solutions for XPS analyses were prepared at the C_{PNIPAM}= 0.5 g/L and $W_{Tween20}$= 0.05%. The immersion of plasma activated PP substrates in these solutions was fixed to 5 h. Additionally pure Tween 20® solution was prepared at 0.05% for grafting. The high resolution C 1s spectra gave information about the surface chemistry of grafted polymers. The corresponding functional groups are gathered in Table 17, while C 1s and N 1s spectra of Tween 20® and MIX II are shown in Figures 68 and 69 respectively.

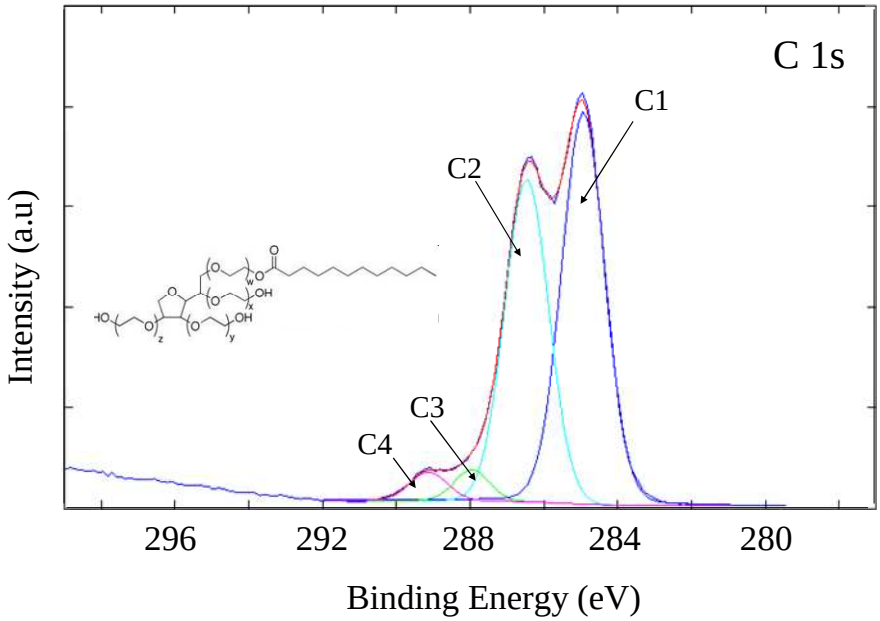

Figure 68: High resolution C 1s spectrum of Tween20 grafted on helium activated PP plates (P= 75 W, flow= 30 sccm and t= 3 min; $t_{dipping}$= 5 h and $W_{Tween20}$= 0.05%).

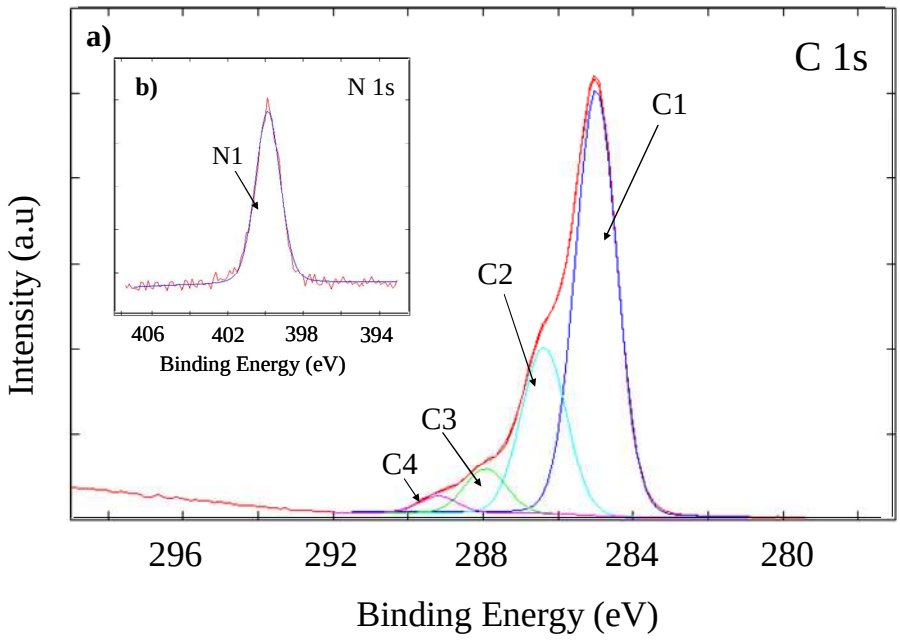

Figure 69: High resolution a) C 1s and b) N 1s spectra of MIX II grafted on helium activated PP plates (P= 75 W, flow= 30 sccm and t= 3 min; $t_{dipping}$= 5 h; $W_{Tween20}$= 0.05% and C_{PNIPAM}=0.5g/L).

The C 1s peak of Tween 20® is showing a markedly high C2 peak, which corresponds to the single C-O bonds. Looking at the chemical formula of Tween 20® (Figure 68), it can be seen that the big polar head is composed from a large number of ether bonds. There is also a C3 peak observed at 287.7 eV of double C=O bonds and additional component was identified; C4 at 289.0 eV ascribed to COOR bonds (Figure 68). After the addition of PNIPAM to surfactant the C 1s spectra changes quite substantially and there is an appearance of N 1s peak that is not observed in the Tween 20® surfactant (Figure 69). Furthermore the decrease of the C2 and C4 components and increase C1 and C3 are also observed. These results confirm the presence of both PNIPAM and Tween 20® components on the surface.

The grafting of MIX II without the plasma activation, lead to practically same functional groups and concentrations as found on the untreated polypropylene. The relative amount of C2 peak grows with the plasma activation time. The relative increase of C2 peak at 180 s is 23% in comparison to the non-activated sample. As the surfactant used in MIX II is composed of a large hydrophilic head and the PNIPAM insertion reaches 20% of C-O/C-N functional groups, the high amount of C2 peak (26.5%) presents an evidence of high surfactant incorporation on the surface. The sample washing in buffer solution brought unessential changes in the surface composition, confirming strong chemical bonding between the substrate and grafted molecules.

Table 17: Decomposition of C 1s peaks of untreated and MIX II grafted samples with assigned functional groups and their relative concentrations at different He activation times. The * stands for the sample washed with buffer solution.

Component Energy (eV)	**C1 (%) 285.0 eV**	**C2 (%) 286.4 eV**	**C3 (%) 287.7 eV**	**C4 (%) 289.0 eV**	**C2+C3+C4/ ΣC1+C2+C3+C4**
Possible assignment	C-C/C-H	C-O/ C-N	C=O/ N-C=O	COOH/ COOR	
PP*	97,23	2,77	/		
MIX II 0 s	96.6	3.4	/	/	3.40 %
MIX II 10 s	71.7	19.3	7.5	1.5	28.3%
MIX II 60 s	69.0	24.5	4.2	2.3	31.0 %
MIX II 180 s	64.9	26.5	6.4	2.15	35.1 %
MIX II 180 s*	64.8	24.3	7.2	3.7	35.2%
PNIPAM 180 s	70.5	14.6	14.8	/	29.4 %
TWEEN 20 180 s	51.80	42.1	3.1	3.0	48.2 %

3.2.4 Characterisation of the surface charge of grafted surfaces

The zeta potential measurements were investigated on different polymer surfaces in 1.7×10^{-3} M NaCl solution at varying pH values. First surfaces examined were the virgin PP sample and a PP sample treated with helium plasma for either 1 min or 3 min. The second set of samples were the substrates grated with PNIPAM, MIX I and MIX II as well after 1 min of helium plasma-activation or 3 min of activation. The zeta potential measurements were made in the period of few days after surface activation and/or grafting (Figure 70).

The untreated PP sample has typical ζ- pH plots of non-polar polymers. The isoelectric point of a virgin substrate is at pH= 4.5, which is in a very good agreement with other authors [195]. The shift of IEP to lower pH is usually evidence for acidic functional groups on the surface and was observed for all treated surfaces. As we know our surfaces

possess basic character and there is stronger adsorption of anions in neutral electrolytes, we will rather consider the potential relatively among the treated surfaces. The zeta potential measurements at pH= 7.4 and 9.6 from zeta plots for different treatments are summarized in the Table 18 together with the contact angle measurements and XPS results. The two pH chosen are the ones we are most interested in for a further study of biological samples.

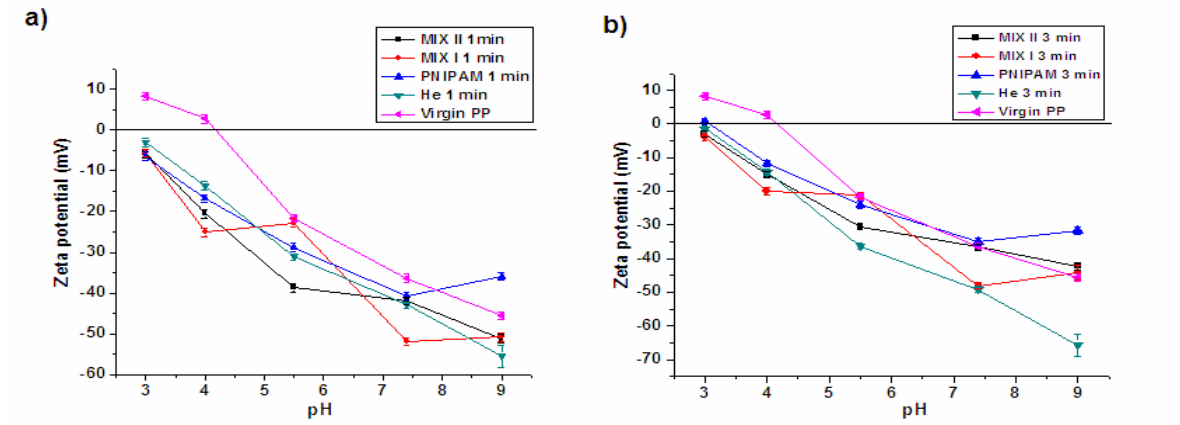

Figure 70: Zeta potential measurements on helium plasma pre-treated samples for a) 1 min and b) 3 min and grafted with PNIPAM, MIX I and MIX II.

Let us first compare the effect of plasma treatment time on zeta potential. For all the grafted samples the potential is higher at shorter plasma treatment time of 1 min. It could be said that these surfaces are less basic, corresponding to lower incorporation of polymer/ surfactant functional groups which was also suggested by XPS study. Contrary to grafted samples, the activated sample shows smaller basic character after prolonged treatment time, coherently with increased O/C ratio. MIX I is the only sample that reached a plateau, suggesting that the surface contained acid or basic functional groups were completely dissociated. Indeed, MIX I is the only sample that contains a surface charge from CTAB; $(C_{16}H_{33})N^{+}(CH_3)_3Br^{-}$.

Table 18: Surface parameters (zeta potential, basic energy and N/C ratio) of virgin PP sample and He plasma-activated samples for one and three minutes grafted with PNIPAM, MIX I and MIX II.

Treatment	ζ(mV); pH=7.4	ζ (mV); pH=9.6	γ_s^{-b} (mJ/m^2)	γ_s^{+b} (mJ/m^2)	N/C (%)
PP virgin	-36.4	-45.6	0.0	0.1	/
He 1min	-42.7	-55.5	46.4	1.5	/
He 3 min	-49.1	-65.6	44.9	1.6	/
PNIPAM 1 min	-40.7	-37.9	109.5	2.4	0.063
PNIPAM 3 min	-35.0	-32.7	110.0	1.2	0.103
MIX I 1 min	-51.9	-50.8	61.5	0.1	0.058
MIX I 3 min	-48.0	-44.0	66.6	0.5	0.041
MIX II 1 min	-41.9	-51.2	82.0	1.0	0.020
MIX II 3 min	-36.6	-42.3	73.9	1.0	0.042

If the three methods are compared, PNIPAM exhibits most basic character by all methods. Because of the greater electro-negativity of oxygen, the carbonyl (C=O) possesses stronger dipole than the N-C bond. The presence of a C=O dipole and, to a lesser extent the N-C dipole, allows amides to act as H-bond acceptors. The N/C XPS ratio was chosen because of the basic character of amino groups. The basic character

information provided by contact angle and zeta potential analyses suggest that MIX II is more basic than MIX I, while the XPS measurements point out the contrary. The higher N/C ratio of MIX I does not take into account that the nitrogen groups of MIX II contain free electrons adversely to positively charged nitrogen of CTAB. For MIX II the zeta potential measurements suggest more basic character after 3 min of pre-treatment while the contact angle measurements propose the opposite.

The two methods are often not completely in agreement, because the acid-base properties measured by zeta potential are due to the dissociation of functional groups according to Brønsted theory, whereas the contact angle approach determines electron donor/acceptor according to Lewis. Another difference between the methods is that zeta potential measures (feels) the charge of the surrounding and not just exclusively surface charge like the contact angle method. The results of the three methods nicely overlap and methods are complementing each other.

3.2.5 Characterisation of the surface morphology

The morphology of polypropylene samples grafted by PNIPAM, MIX I and MIX II was analyzed by atomic force microscopy. AFM analysis allowed us to obtain 3D images of the surface and measure the average surface roughness.

3.2.5.1 Surface morphology of PNIPAM

The 2D AFM images of helium treated PP sample and He treated PP sample grafted with PNIPAM are presented in figures 71.a and 71.b respectively. Plasma activation was performed at P= 75 W, flow= 30 sccm and time of treatment 3 min. The PNIPAM solution for grafting was prepared at the c= 0.5 g/L. The helium activated sample presents smooth surface with the average surface roughness 3.1 ±0.1 nm, where the roughness was measured without a dust particle that can be seen in the left corner (Figure 71.a). After the PNIPAM grafting we obtained even smoother surface with the average surface roughness measured over 10 µm × 10 µm area 2.2 ±0.1 nm (Figure 71.b). The smoothing can most probably be ascribed to the formation of homogeneous polymer layer, that covered the stripes present on either untreated or plasma treated surfaces, arising from the polymer production.

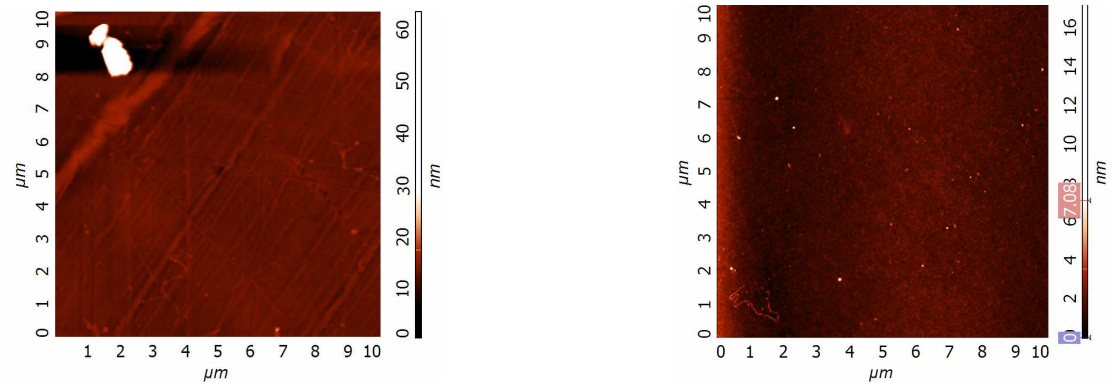

a) **b)**

Figure 71: AFM images of a) He treated PP support and b) He treated PP support grafted with PNIPAM.

3.2.5.2 Surface morphology of MIX I

The surface morphology measurement of MIX I grafted samples was composed of two parts. In the first part the study of MIX I grafting was performed at two different plasma activation times, 10 s and 60 s, at fixed mixing ratio: C_{PNIPAM}= 0.5 g/L and C_{CTAB}= 1 mM. For the reference pure CTAB (C= 1 mM) without added polymer was grafted on a substrate after 60 s of activation time. The AFM images over an area of 10 µm × 10 µm are shown in Figures 72-74.

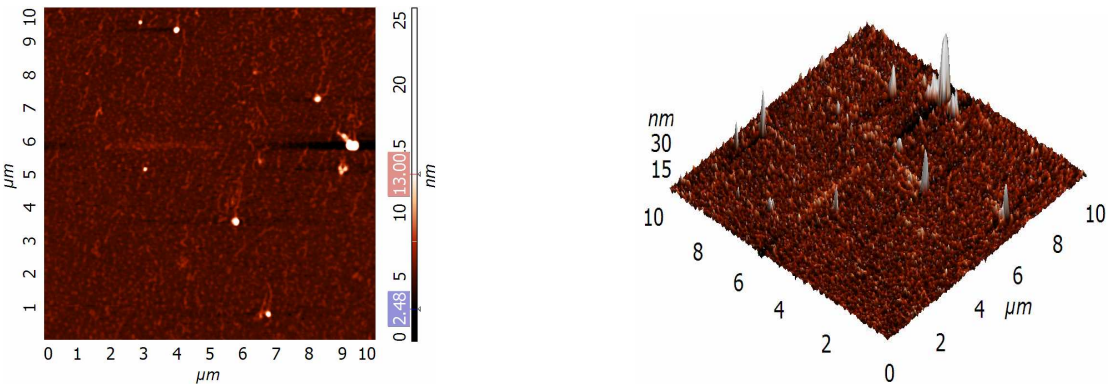

a) b)

Figure 72: a) 2D and b) 3D AFM images of MIX I over the area 10 µm × 10 µm grafted at t_{He}= 10 s. Sa= 3.1 ± 0.1 nm.

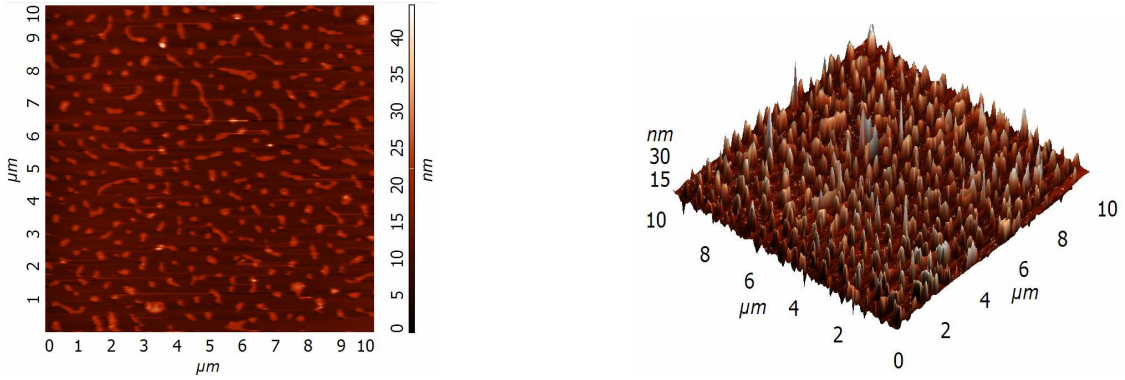

a) b)

Figure 73: a) 2D and b) 3D AFM images of MIX I over the area 10 µm × 10 µm grafted at t_{He}= 60 s. Sa= 6.4 ± 0.1 nm.

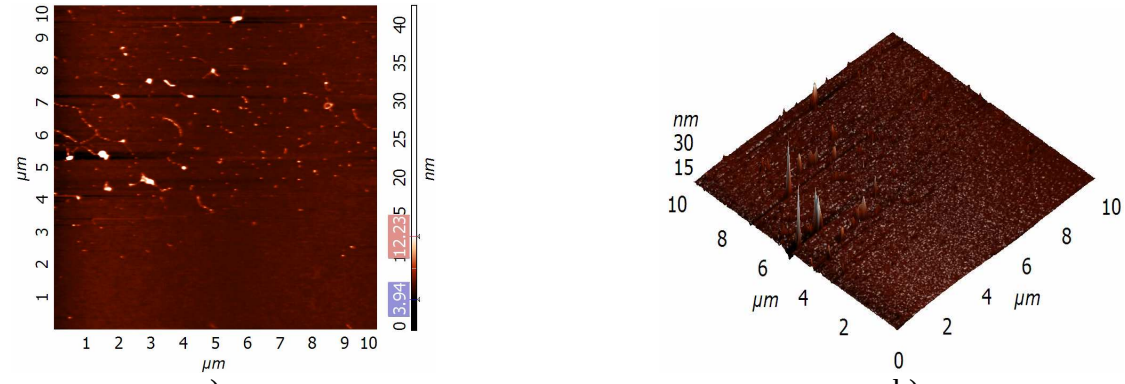

a) b)

Figure 74: a) 2D and b) 3D AFM images of CTAB over the area 10 µm × 10 µm grafted at t_{He}= 60 s; Sa= 2.9 ± 0.1 nm.

Figures 72 and 73 are showing the difference in surface morphology between the sample that was activated with helium plasma for 10 s and the one that was activated for 60 s. The surface treated for a short time exhibits hair like spread features all over the surface, with heights between 6 nm and 8 nm. There are as well some individual peaks observed with height around 23 nm. The average surface roughness of the sample is 3.1 ± 0.1 nm.

After prolonged plasma treatment time there was a noticeable difference observed (Figure 73). It seems that the increase of surface energy caused the aggregation of thinner lines and formation of relatively regular structures (however not completely separated) that have average diameter between 150 and 250 nm and height around 26 nm and average surface roughness Sa= 6.4±1 nm. The same height of peaks was observed for the few structures observed on sample treated for 10 s. Therefore we can presume that the aggregation started, just the surface energy was not important enough to reach final conditions. The structures on the surface are micelles formed between the surfactant and polymer. The evidence of mutual cooperation between polymer and surfactant on creation of mixed micelles is evident from the comparison between Figure 71 and Figure 74 where pure polymer and pure surfactant are grafted on the activated substrate.

In the next step the influence of polymer and surfactant concentration was examined. The substrates were activated by helium plasma for 60 s at P= 75 W and flow= 30 sccm. The solutions were prepared at four different surfactant concentrations: C_1~CAC, CAC<C_2<CMC, C_3~CMC, C_4> CMC. The detailed description of solutions is described in experimental part. The concentrations were calculated from the Isothermal calorimetric investigations published by other authors. Figure 75 is presenting the height images obtained by AFM measurements for the samples prepared at different concentration of surfactant to polymer ratio.

The grain like structures started appearing on the surface when the concentration of surfactant was approximately at the critical aggregation concentration, Figure 75.a. The average surface roughness over the 5 μm × 5 μm was 3.6 ± 0.1 nm. It can be seen through roughness analyses that the surface roughness increased in comparison to the PNIPAM or CTAB sample. The micelles on the surface have diameter between 100 and 200 nm and their height varies between 6 and 11 nm. This height is much lower than the one observed for higher concentrations of surfactants (around 25 nm). When the concentration further increased very regular and dense structures appeared, with a diameters around 80 nm (Figure 75.b). The peak heights increased to 15-25 nm and therefore the average surface roughness increased to 6.9 ± 0.1 nm.

Figure 75.c is showing the surface at the conditions where the concentration of CTAB in the polymer solution was around the CMC point. The average surface roughness of the surface is 4.6 nm, where the micelles that remained have a height of 15 nm and the size between 50 and 90 nm. The other filaments have the size between 4 nm and 6 nm. Above the CAC value the average surface roughness decreases back substantially to 2.4 nm. Now bigger aggregates with different shapes and sizes were formed, from small micelles with diameter about 50 nm to merged features with the sizes up to 400 nm.

For mixtures of ionic surfactants and non-ionic polymers the scattering techniques revealed that the structures of these complexes are surfactant aggregates formed around the polymer chain polymer and are often described as “necklace models”. These aggregates are typically smaller than the micelles of pure surfactant in aqueous solution. The theoretical size of CTAB is around 2.2 nm at it forms micelles with aggregation number between 75 and 120. Therefore we can say that the features observed by AFM imaging with small diameters between 50 and 100 nm belong to the mixed micelles, whereas for bigger micelles we can say that the aggregation of surfactant was favourable.

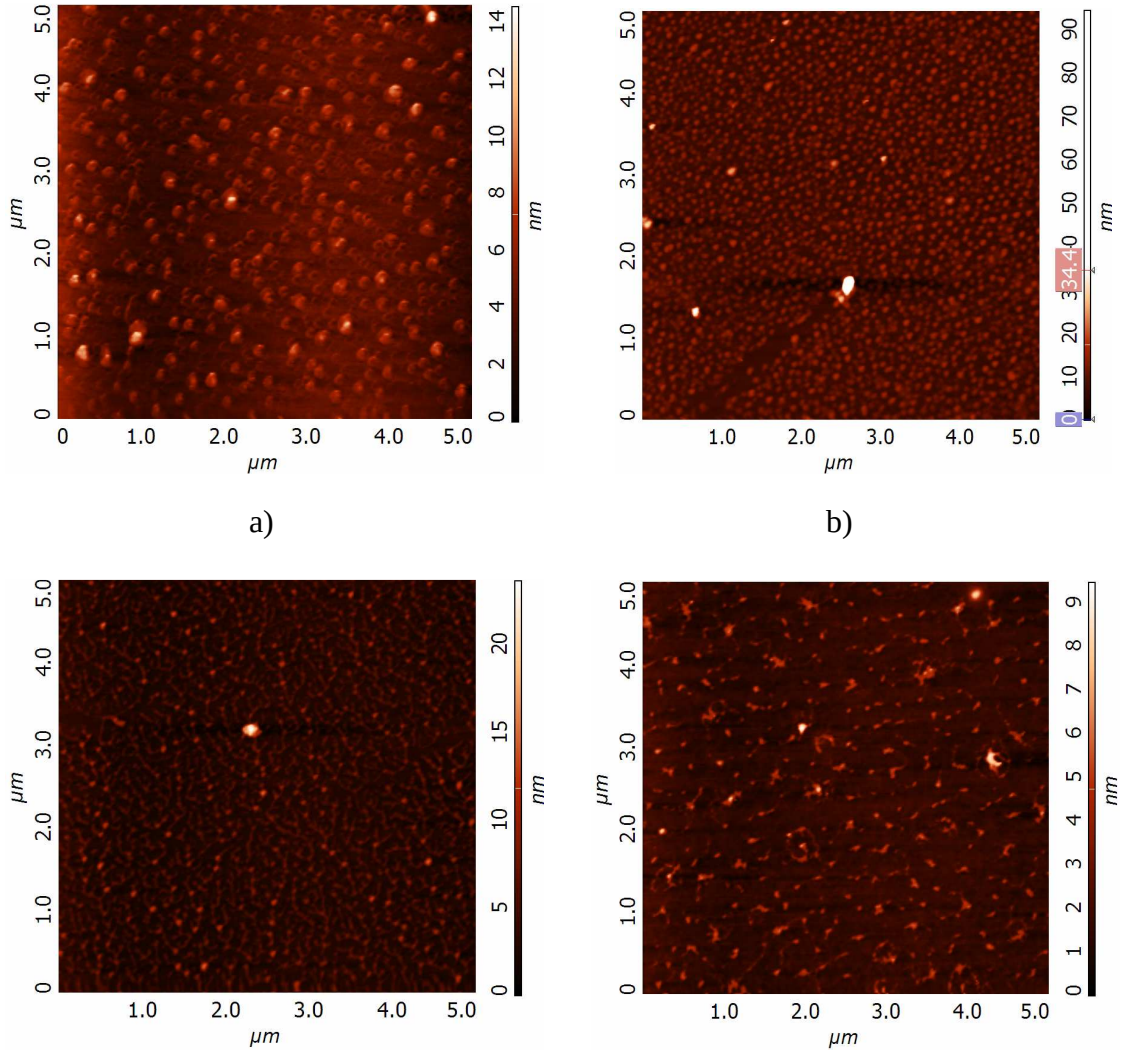

Figure 75: AFM images of MIX grafted samples at a) C_1~CAC, b) CAC<C_2<CMC, c) C_3~CMC and C_4> CMC.

The polymer bound surfactant aggregates start to form (in the solution) at so called critical aggregation concentration (CAC) which is lower than critical micelle concentration (CMC). The CAC in literature between the PNIPAM and CTAB was established to be 0.23 mM at 29ºC with the maximum of calorimetric curve at 0.5 mM, corresponding to highest number of surfactant bound to the polymer chain. The mechanism proposed was that the isopropyl group of PNIPAM incorporates to the surfactant aggregates, whereas more hydrophilic backbone shields the hydrocarbon/water interface. Further increase of surfactant concentration leads to decrease of calorimetric curve, indicating lower binding and reaches minimum. After with supplement of surfactant the enthalpy is increased again due to the favourable formation of free surfactant micelles than polymer-binding aggregates. The results of micellization in solution are in a very good agreement with formation of the mixed micelles on the grafted surfaces. It seems that micelles keep their shape even after grafting from the solution, providing that the surface energy and amount of free radicals on the surface are just right.

3.2.5.3 Surface morphology of MIX II

The surface morphology measurements of MIX II grafted samples as a function of plasma activation time, 10 s and 180 s, are shown over a surface area 10 µm × 10 µm in Figures 76 and 77 respectively. The immersion solution were prepared at C_{PNIPAM}= 0.5 g/L and $W_{Tween20}$= 0.05%, where immersion time was 5 h.

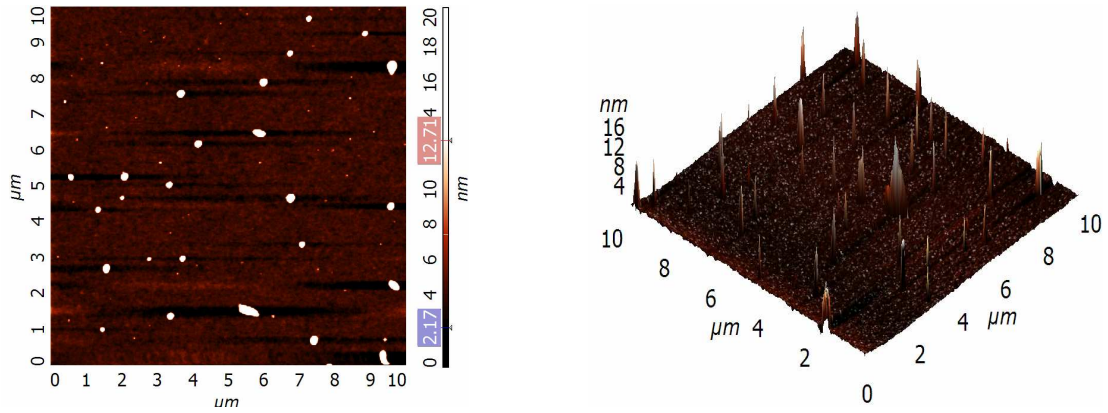

a) b)

Figure 76: a) 2D and b) 3D AFM images of MIX II over the area 10 × 10 µm grafted at t_{He}= 10 s

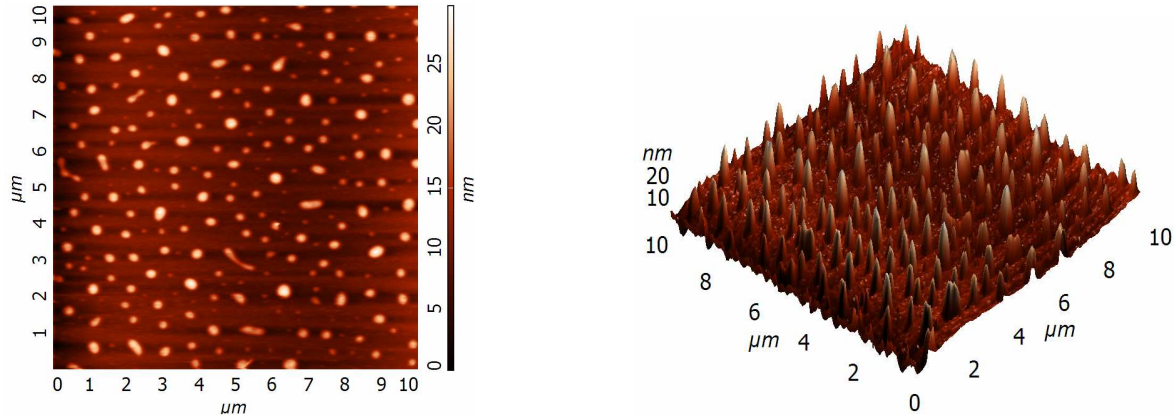

a) b)

Figure 77: a) 2D and b) 3D AFM images of MIX II over the area 10 × 10 µm grafted at t_{He}= 180 s

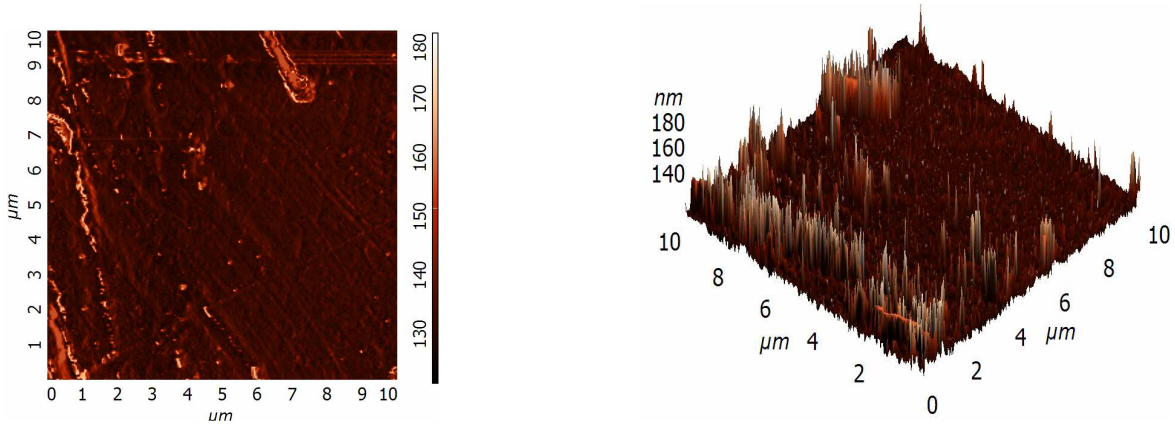

a) b)

Figure 78: a) 2D and b) 3D AFM images of Tween 20 over the area 10 × 10 µm grafted at t_{He}= 180 s

Figures 76 and 77 are showing the difference in surface morphology between the grafted sample that was activated with He plasma for 10 s and the one that was activated for 180 s. The short time activation leads to much lower extent of aggregate formation comparing to the sample that was pre-treated for 180 s (Figure 77). The average surface roughness over an area of 10 µm × 10 µm for sample activated for 10 s was 2.8 ± 0.1 nm. The height of the peaks on average is 12 nm and their diameter between 70 nm and 200 nm.

The increase of plasma activation time leads to increase of surface roughness and formation of regular structures. The height of the peaks now increased to 26 nm on average with sizes between 150 nm and 300 nm, resulting in a surface roughness Sa= 7.1 ±1 nm. The micelles are larger than the micelles obtained for MIX I due to the larger size of surfactant. The size of Tween 20® is approximately 8.5 nm, whereas its aggregation number is around 58. Figure 78 is an AFM image of the pure Tween 20® surfactant grafted on the surface after 180 s of plasma activation. A thick and smooth layer is formed with relatively high amount of irregularities on the surface, Sa= 3.6 ± 0.1 nm.

In the next step the influence of polymer and surfactant concentration was examined. The substrates were activated by helium plasma for 180 s at P= 75 W and flow= 30 sccm. The solutions were prepared at four different surfactant concentrations: C_1~CAC, CAC<C_2<CMC, C_3~CMC, C_4> CMC. The detailed description of solutions is described in experimental part.

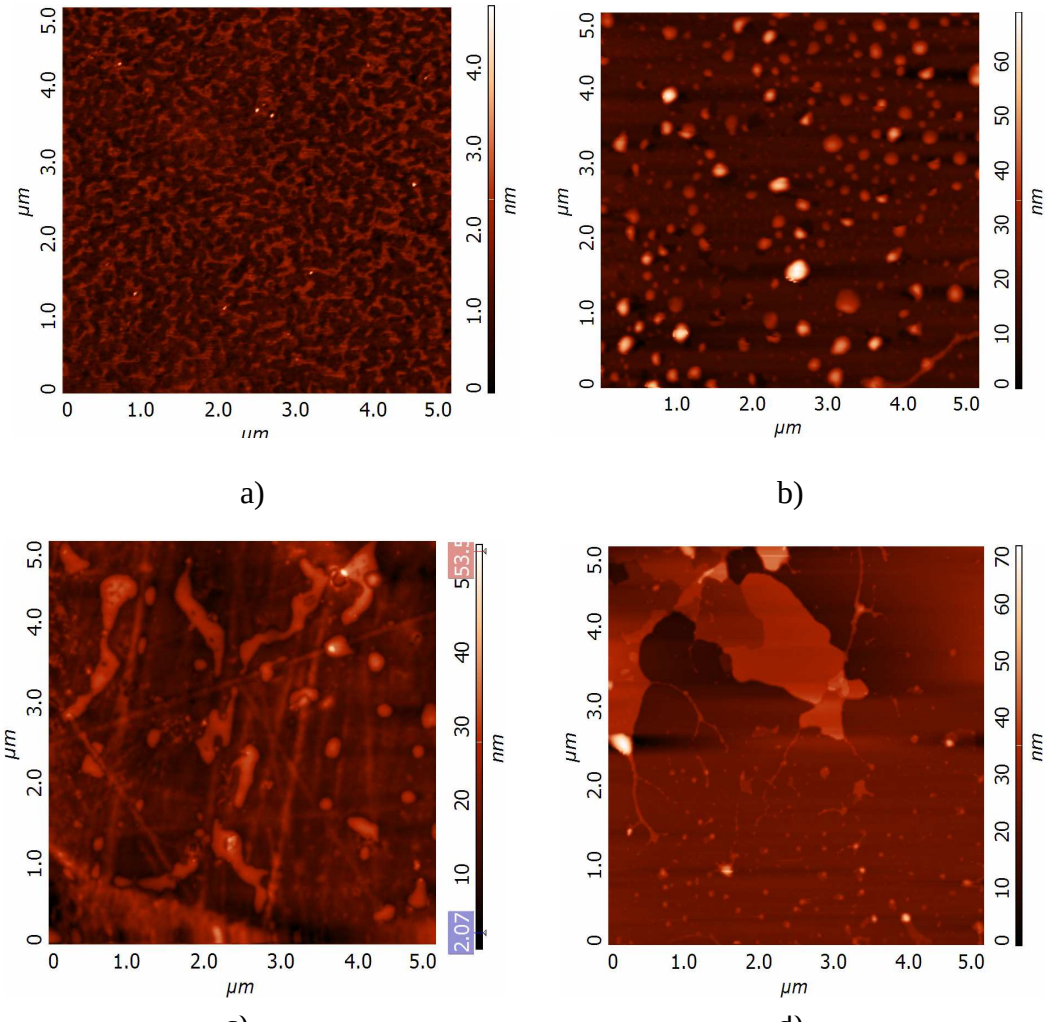

Figure 79: AFM images of MIX II grafted samples at a) C_1~CAC, b) CAC<C_2<CMC, c) C_3~CMC and C_4> CMC

As non-ionic surfactants like Tween 20® very weakly interact with PNIPAM we could not find the CAC values for the two components. The interaction of non-ionic surfactants and non-ionic polymers can be induced by incorporating hydrophobic moieties in order to strengthen the hydrophobic interaction between them. Therefore we have presumed as if PNIPAM was hydrophobically modified by slightly increasing the temperature of solution to 28ºC and calculated the approximate ratios.

Figure 79 is presenting the height images obtained by AFM measurements for the samples prepared at different surfactant to polymer ratios. Figure 79 is showing that grafting of MIX II is different than MIX I. Micelles are observed just on sample 79.b, where the concentration of surfactant was between the CAC and CMC. At very low concentration of surfactant, Figure 79.a, continues polygonal network structures were obtained with the height around 2 nm. The surface appears as the formation of micelles is in the progress; however the separation did not occur yet. Further increase of surfactant leads to the formation of mixed micelles with various sizes between 50 nm and 300 nm. Their height varies in the range from 30 nm to 60 nm (Figure 79.b). Average surface roughness on the area of 5 μm × 5 μm is 8.2 ± 0.1 nm. Figures 79.c and 79.d show appearance of big irregular plaques on the surface at elevated concentration of surfactant. These features could be probably prescribed to the viscosity of Tween 20®.

The addition of surfactant to polymer solution is always an exothermic process. Binding of surfactant to polymers will strongly depend on their molecular properties and are characteristic for each polymer surfactant mixture. It can be confirmed that morphological changes on the surface strongly depend on plasma parameters and polymer/ surfactant ratio, therefore for the desired application a fine tuning of the surface needs to be performed.

3.2.6 Conclusions

The surface energy measurements obtained by contact angle analyses did not show much influence on the surface characteristics of grafted samples with plasma pre- treatment time, even though the surface energy before the grafting varied between the samples. Contrary to this, the XPS analyses and AFM imaging showed that there was a great difference between the supports. This was explained by the fact that the grafting at all conditions introduced the polar functional groups on the surface, but their chemical nature was different. On the other hand if samples were not activated by plasma the yield of grafting was very low. The introduction of small concentration of surfactants to polymer solution rapidly and markedly changed (decreased) the basic character of pure polymer. This was observed by both, contact angle and zeta potential analyses. The basic character of the samples falls in the following order: PNIPAM> MIX II> MIX I, coherently with their molecular characteristics. The formation of nano-structured features on the grafted surfaces is strongly dependant on the plasma characteristics and as well the molar ratios used between the surfactant and the polymer. Therefore this technique presents a relatively simple method to control the surface characteristics (functional groups, surface charge, acid- base character and topography) for various applications, however fine tuning of conditions needs to be performed. These surfaces display high stability under atmosphere conditions in the period of at least two months.

4 Protein adsorption study and biological validation of modified supports

In the introduction we have exposed the problematic of protein adhesion on the storage tubes made of polypropylene. No matter what was the nature of the protein (recombinant, cellular or infectious) the adsorption was substantial. Therefore the interest is to preserve these proteins in the solution, especially the biomarkers found in the cerebrospinal fluid (CSF), that are used as an aid in diagnostics of various neurodegenerative diseases like Creutzfeldt–Jakob, Parkinson and Alzheimer disease.

The goal of the study presented in this chapter was to determine the surface characteristics, regarding surface energy components, functionalities and topography that lead to the lowest adsorption of these proteins. For this purpose in the first phase the Eppendorf tubes were treated with CF_4 plasma or grafted PNIPAM, MIX I and MIX II. Afterwards these tubes were subjected to various neurodegenerative agents in their native, recombinant or infectious forms for certain time and analyzed by classical ELISA (Enzyme-linked immunosorbent assay) protocols, optimized for each protein. These tests provided information about the amount of adsorbed and/ or recovered proteins from different tubes. In order to access to some additional details on the protein adsorption to modified supports, XPS and confocal microscopy analyses were performed in the presence of proteins.

In the second part the influence of storing conditions (temperature, time and pH) on the protein adsorption were considered. This was followed by the study of the plasma grafting parameters and polymer to surfactant ratio on protein adsorption, taking in mind that these factors markedly influence the surface properties (amount of functionalities, roughness and nano-topography) and therefore very likely their interactions with proteins. Finally, some general conclusions about the influence of surface properties on protein adsorption will be drawn.

4.1 Evaluation of the non-fouling properties of treated supports by direct and "sandwich" ELISA tests

For the following experiments the Eppendorf tubes were treated either with CF_4 plasma or pre-treated with helium plasma and grafted with PNIPAM, MIX I or MIX II. The CF_4 plasma treatment was performed at conditions where the surface energy had the lowest value (P= 50 W, Φ= 40 sccm and t= 7 min; Chapter 3.1). At these conditions the F/C ratio reached 1.00 and the water contact angle 132º.

The other lot of Eppendorf tubes was activated by helium plasma (P= 70 W, Φ= 30 sccm) for 60 s when MIX I was grafted and for 180 s when immersion was done in the PNIPAM or MIX II solutions. The PNIPAM solution was prepared at c= 0.5 g/L (N/C= 0.10, Θ= 10º), MIX I at c_{PNIPAM}= 0.5 g/L and c_{CTAB}= 1 mM in 1:1 volume ratio (N/C= 0.06, Θ= 23º) and MIX II at c_{PNIPAM}= 0.5 g/L and $W_{Tween20}$®= 0.05% in 1:1 volume ratio (N/C= 0.04, Θ= 17º). Immersion lasted 2 h for PNIPAM and 5 h for MIX I and MIX II. Afterwards Eppendorf tubes were emptied, washed with distilled water and dried under laminar flow at ambient temperature.

I have performed the biological analyses under a frame of European project Neuroscreen in three different laboratories: ULG (Centre de Recherche sur les Protéines Prion, Université de Liège), CHUL (Hospices Civils de Lyon) and L-UNI (Lancaster University). Each laboratory is specialized for certain type of diseases; therefore the protocols used for the following analyses were optimized by each laboratory and are detailed in experimental section.

Essentially all proteins (with exception of α-syn that was stored for longer time) were put into untreated and treated Eppendorf tubes and stored for 24 h at 4ºC. At the same time a reference sample was made, where protein was stored in untreated PP tube and immediately frozen at -80ºC. This sample stayed frozen for 24 h and analysed in parallel with samples that stayed for 24 h at 4ºC. From now on, this will be referred to as a $\tau_{15(-80ºC)}$ sample, which will correspond to 100% of the protein recovery. The index 15 stands for 15 minutes needed from the time the sample is unfrozen and analysed. After 24 h the ELISA tests were performed either on the tubes (direct ELISA) and/or on the supernatant ("sandwich" ELISA) corresponding to amount of the protein adsorbed or recovered from the tubes respectively.

4.1.1 Evaluation of the non-fouling properties of treated supports by direct and "sandwich" ELISA tests during the storage of recombinant proteins: $PrPrec_{hum}$, Tau_{rec} and α-syn

The recombinant human prion protein ($PrPrec_{hum}$) was diluted in PBS buffer at pH=7.4 and stored in untreated and treated Eppendorf tubes at the concentration of 1μg/mL. The tubes were stored at 4ºC for 24 h, while one untreated tube was put to -80 ºC ($\tau_{15(-80ºC)}$) for 24 h. After this time proteins were taken from the tubes and deposited on the strips pre-coated with capture antibodies and analysed with "sandwich" ELISA test. Alongside the ELISA tests were performed directly on the Eppendorf tubes. The results of direct and "sandwich" ELISA tests are presented in Figure 80. The red column is showing the amount of protein adsorbed on the Eppendorf tubes, while the yellow column presents the amount of recovered protein in supernatant. The optical density results were normalised

towards the sample stored at -80ºC ($\tau_{15(-80ºC)}$), corresponding to 100% of the protein. The improvement of treatment towards the untreated PP tube that was stored for 24 h at 4ºC are written above the column in red colour ($\eta_{(PP)}$).

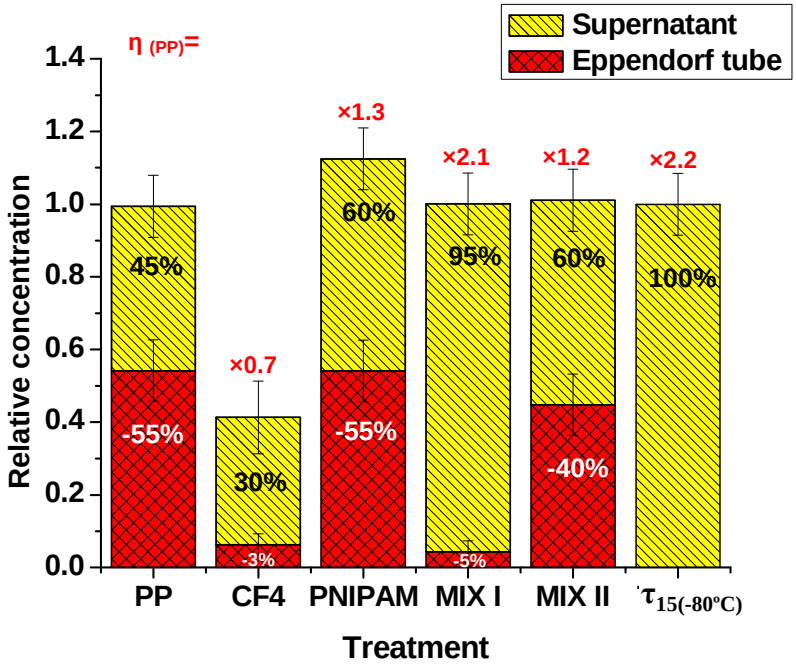

Figure 80: Optical density measurements of direct (red) and "sandwich" (yellow) ELISA test on $PrPrec_{hum}$ stored for 24h at 4ºC; ($\tau_{15(-80ºC)}$) is sample stored in PP frozen at -80ºC for 24 h.

The average measurements obtained by several experiments are indicating that around 55% of the initial amount of proteins was lost due to the adsorption on the untreated polypropylene tubes after 24 h of storage. In the case of fluorinated tubes (by CF_4 plasma) an unusual phenomena can be observed. In one way the amount of protein adsorbed is very close to the background as if practically no protein was adsorbed and on another hand just 30 % of the protein was detected in the remaining solution. The hydrophobic surfaces are known to cause irreversible adsorption of proteins due to the spreading of hydrophobic core of the protein over the surface, resulting in irreversible unfolding of the proteins [196]. The deformation of the protein monolayer is enabling the formation of the second layer resulting in a high loss of proteins from the solution. The growth of third layer on the other hand is normally prevented due to the low affinity of proteins among themselves. Nevertheless, the formation of thick protein layer can cause the burring of the recognition sites of the protein to the bulk and as a consequence they can not be accessed and recognized by the antibodies, leading to the false negative signal of protein presence on the tubes. Therefore the 70% of the protein that was not detected was most probably adsorbed on the tubes and not identified due to the above mentioned reasons. Another reason next to the hydrophobicity could be the presence of small quantities of aluminium on the walls of Eppendorf tubes, as the proteins and other biomolecules possess relatively high affinity towards the metals.

On the other hand the experiments performed on PNIPAM treated tubes gave too high signal. In one way the direct ELISA test indicate that 55% of the protein was adsorbed to the tubes, while the "sandwich" ELISA test is showing that there was 60% of the protein recovered from the solution. We need to realise that the data about the protein recovered from the supernatant are exact and the difference comes from the proteins adsorbed on the Eppendorf tube. If we look at the scheme of direct ELISA test (Chapter 2.4) we see that it

is composed of several steps: first the protein is coated in the tubes, than the surface is blocked with BSA (in the case of $PrPrec_{hum}$), afterwards the detection antibody coupled with HRP is added. Finally TMB is added that reacts with HRP which gives colourful reaction indicating the presence of the protein on the surface. Presuming that the surface was not blocked well with BSA, the parasite interactions between the PNIPAM grafted surface and the antibody/HRP or TMB can occur, leading to the false augmentation of the signal on Eppendorf tubes. The repelling properties of PNIPAM towards BSA below the LCST have been reported by several authors [197]. For this reason we have performed XPS analyses on the treated surfaces exposed to BSA solution, in order to affirm or invalidate their interaction. Indeed the results showed that there was no adhesion of BSA observed on PNIPAM grafted plates and will be presented more in detail in Chapter 4.2.1. Anyhow, the recovery of protein from PNIPAM treated tubes remains close to the untreated tubes, which is not adequate from the application aspect.

Similarly to PNIPAM, relatively high adsorption (around 40%) of $PrPrec_{hum}$ was observed on the MIX II treated surface as well. Adversely to all other tubes, MIX I showed a very low adsorption (5%) and very high recovery (95%) of the protein. In other words, there was 2.1 times more protein preserved in the MIX I treated tubes compared to the untreated PP tubes at the same storage conditions. These results are attesting to a high improvement in performance of Eppendorf tubes, under the condition that an appropriate treatment is applied.

All the results presented are the outcome of several experiments that were performed during the three years of experiments. This means that the proteins were provided from different sources and that the tubes were prepared independently for each experiment, leading to repetitive statistical results.

The results of Tau_{rec} storage are presented in Figure 81. Protein was diluted in PBS buffer solution to the c= 100 pg/mL and stored for 24 h at 4ºC. After 24 h the supernatant from these tubes was examined by “sandwich” ELISA tests, giving us just the results about the amount of recovered protein from the solution.

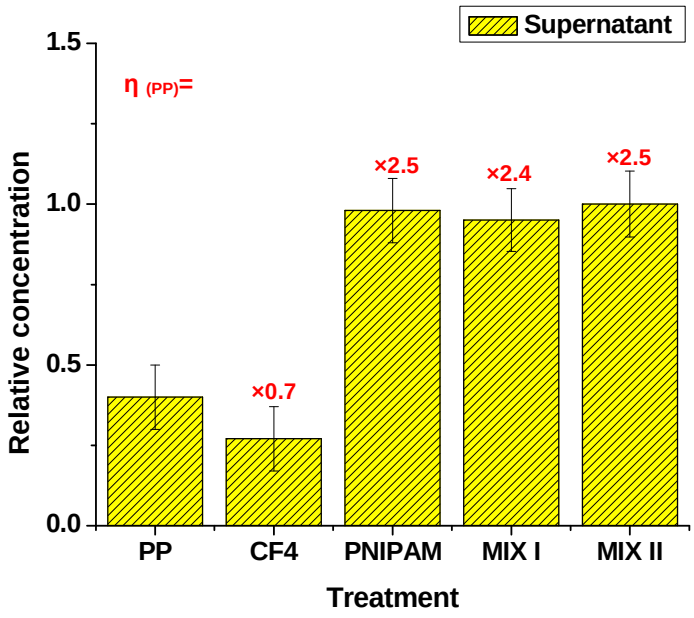

Figure 81: Optical density measurements of “sandwich” ELISA test on Tau_{rec} stored for 24 h at 4ºC.

The tests were not performed directly on the tubes due to two reasons: on one hand the laboratory working with Tau protein (CHUL) is focused on the study of the supernatant and on the other hand as tests are extremely expensive just the "sandwich" ELISA is used because it gives much more accurate results and is more sensitive than direct ELISA test. One more point needs to be mentioned; for this experiment we did not have a frozen sample at -80ºC ($\tau_{15(-80ºC)}$), therefore we can not quantify the amount of adsorbed protein. Nevertheless, we can compare the values obtained on treated tubes towards the untreated PP sample, which will give us the relative value how much more of the protein was recovered from the treated tubes than from the untreated tube. For this reason the percentages are not put in the columns, but the relative improvement is written above them ($\eta_{(PP)}$).

For the fluorinated Eppendorf tubes, as before, the loss of protein is high. On the other hand there are around 2.5 times more proteins that remained in the solution comparing to untreated PP tubes for all hydrophilically modified samples. It seems that the Tau_{rec} protein is rather unselective towards the PNIPAM, MIX I or MIX II treatments.

The storage results of monomeric recombinant α-syn over 1 month period are shown in Figure 82. The storage in the untreated tube resulted in approximately 65% loss of protein, similarly to MIX I and CF_4 treatments. On the other hand PNIPAM treated Eppendorf tubes preserved relatively high amount of α-syn (85%) even after storage of 1 month. In other words, we detect 2.4 times more protein when stored in PNIPAM compared to the virgin PP tube. Unfortunately the results of storage on MIX II are not available. There were several experiments performed on monomeric recombinant alpha-synuclein in ULG and CHUL laboratories, however due to its high aggregation properties we could not attain repetitive results. At this attempt we have tried different protein providers, different capture and detection antibodies, blocking agents and protocols, in spite of that, the consistency of results was not sufficient. Alpha-synucleins have no organised structure which makes them especially prompt to form big aggregates and for this reason the detection is usually done with the precipitated oligomeric form.

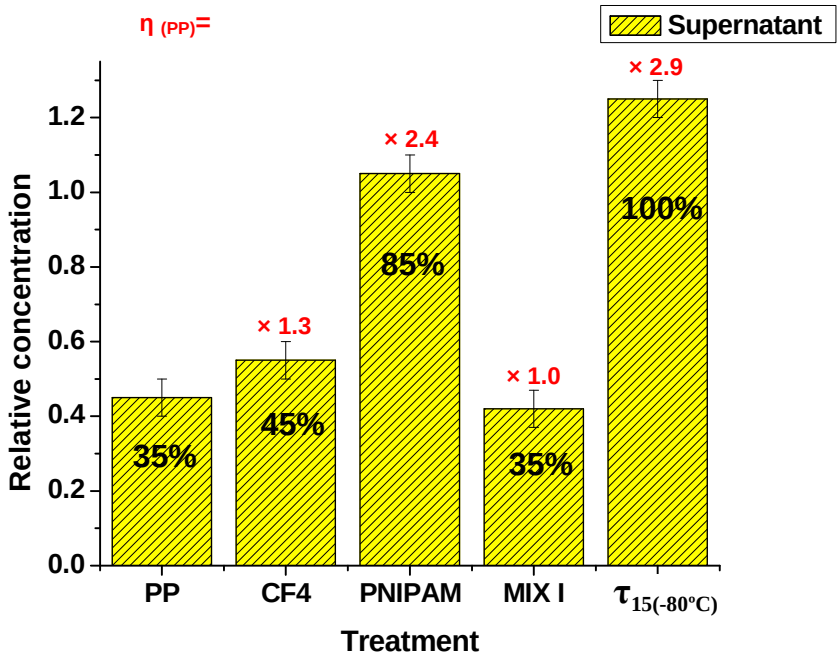

Figure 82: Optical density measurements of "sandwich" ELISA test on α-syn stored for 1 month at 4ºC; ($\tau_{15(-80ºC)}$) is sample stored in PP frozen at -80ºC for 1 month.

4.1.2 Evaluation of the non-fouling properties of treated supports by direct and "sandwich" ELISA tests during the storage of proteins from CSF: TauPHF, Tau_{tot} and Aβ-42

In the next part of experiments the cerebrospinal fluid (CSF) of a patient was stored for 24 h at 4ºC. The CSF itself contains approximately 0.3% of various plasma proteins, or 15 to 40 mg/dL. From this fluid the recovery of neurodegenerative agents was monitored by "sandwich" ELISA protocols. The protocols are described in detail in experimental part.

The optical density measurements of PrPc in CSF and $PrPrec_{hum}$ spiked in CSF are shown in Figure 83. By spiked we mean that the recombinant prion protein was added in the c= 50 ng/mL to the CSF of a patient. The biomedical studies [198] have shown that the level of total prion protein in CSF of humans affected by different neurological diseases is significantly reduced. For this reason it is very important to ensure that the reduction of total prion protein is not a consequence of protein adsorption onto the walls of Eppendorf tubes. The loss of PrPc reaches the value around 40% when stored in untreated Eppendorf tube for 24 h. On the other hand the recovery results of prion protein storage in PNIPAM treated tubes is much higher, around 85% of the protein remained in the solution. Even better results are obtained for CSF stored in MIX II modified Eppendorf tubes, there was no lost of PrPc observed. Comparing to the untreated PP tubes, there was around 1.6 times more of the protein preserved with MIX II treated tubes.

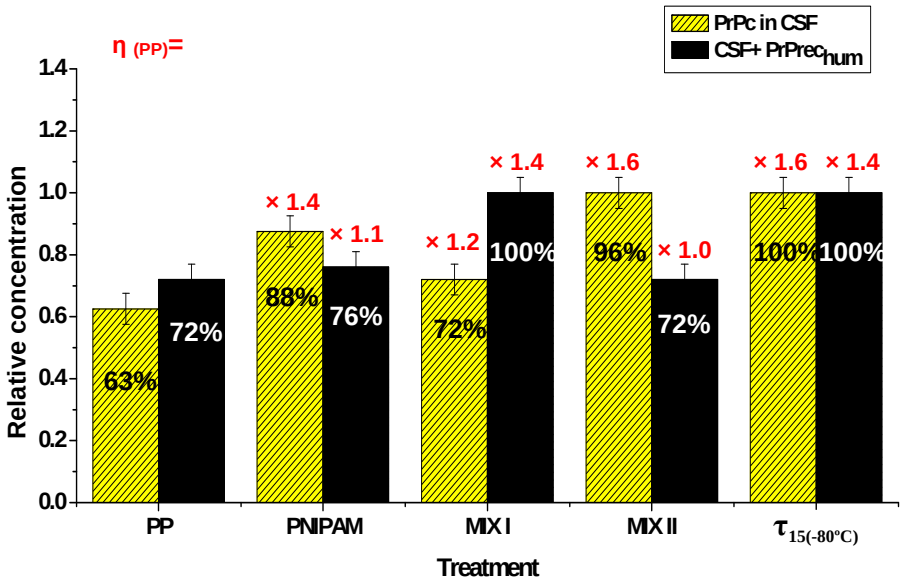

Figure 83: Storage of CSF (yellow) and CSF spiked with $PrPrec_{hum}$ (black) in modified Eppendorf tubes for 24 h at 4ºC and detected for PrP protein.

In the Figure 83, the black columns are presenting the storage results of CSF spiked with $PrPrec_{hum}$. Whether the $PrPrec_{hum}$ was stored in a single buffer solution or in the matrix (CSF), there was a high adsorption of recombinant prion protein observed on the PNIPAM and MIX II and extremely low on MIX I treated Eppendorf tubes. This is indicating a strong affinity of the recombinant form of prion protein towards the PNIPAM and MIX II and low affinity towards MIX I, which is completely opposite as observed for PrPc.

Figure 84 is showing ELISA "sandwich" results for the storage of cerebrospinal fluid (CSF) for 24 h at 4ºC. The CSF was tested for Tau total, hyperphosphorylated Tau (TauPHF) and Aβ-42 peptide. These three biomarkers are present in the CSF and are often used for the diagnostics of Alzheimer's disease [199]. Patients that have developed the disease posses higher amount of total Tau and phosphorylated Tau in their CSF, while the amount of Aβ-42 peptide decreases.

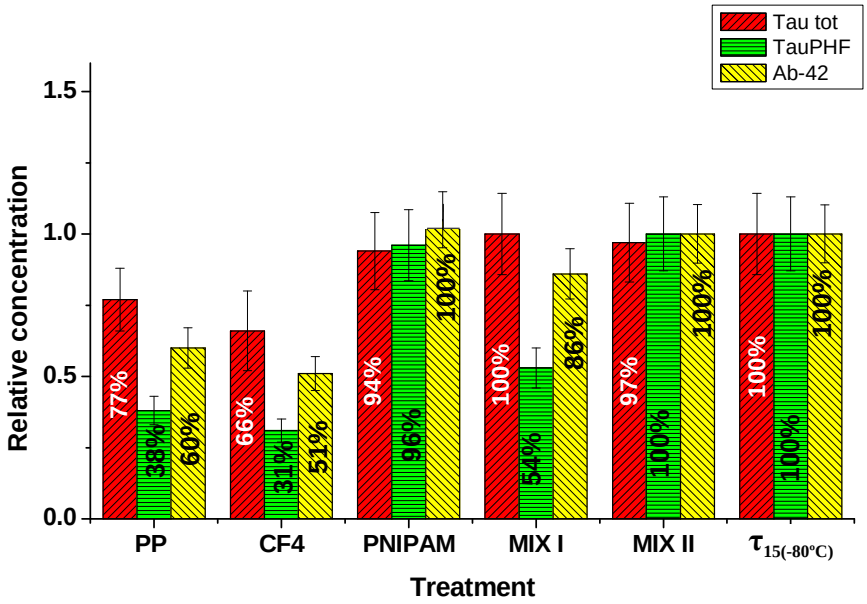

Figure 84: Storage of CSF in different Eppendorf tubes for 24h at 4ºC; recovery of Tau total (red), TauPHF (green) and Aβ-42 (yellow).

The quantity of total Tau protein in CSF decreased for around 20% in untreated and CF_4 treated tubes, while the protein concentration remained practically unchanged for all hydrophilically treated surfaces. Similar results were obtained for recombinant Tau protein.

The hyperphosphorylated Tau and amyloid Aβ-42 have comparative tendencies towards the supports. There was no visible adsorption observed for the two proteins on PNIPAM and MIX II treated Eppendorf tubes. In comparison with the untreated tubes, a remarkable increase of detected TauPHF protein (×2.6) is attained. Furthermore the amount of Aβ-42 peptide is 1.6 times higher when CSF was stored in PNIPAM and MIX II, compared to the virgin PP tubes. For Aβ-42 peptide stored in MIX I modified tubes, the recovery results are relatively good, there was around 85 % of the protein that stayed in the supernatant, while for TauPHF protein the loss was more important (46%).

The surface properties of treated supports are gathered in Table 19, whereas the recovery values for each protein can be found in Table 20. The recovery of Tau_{rec} is referred to the untreated Eppendorf tubes, while the recovery of the rest of the proteins corresponds to the initial value of the fresh sample. Table 20 contains the basic properties of proteins as well, where AA stands for number of amino acids, pI to isoelectric point and HP/HB to hydrophilic or hydrophobic character respectively.

Table 19: Table of basic surface properties (surface energy components, zeta potential and XPS measurements) of untreated and treated samples.

	PP virgin	PNIPAM	MIX I	MIX II
γ_{tot} (mJ/m^2)	34.8	72.1	67.5	66.8
γ_s^d (mJ/m^2)	34.7	19.1	16.6	23.4
γ_s^p (mJ/m^2)	0.1	52.9	50.9	43.5
γ^{b+} (mJ/m^2)	0	110.0	61.5	73.9
ζ (pH=7.4) (mV)	-36.4	-35.0	-51.9	-36.6
O/C	0.05	0.29	0.20	0.31
N/C	0.0	0.10	0.06	0.04
Rms (nm)	2.8	2.2	6.4	7.1

Table 20: recovery data for stored proteins in PBS and CSF relatively to the fresh sample and basic properties of studied proteins; asterix (*) marks the relative recovery of Tau_{rec} in PBS towards the untreated Eppendorf tube and / stands for non determined results.

	PP virgin	PNIPAM	MIX I	MIX II	Protein properties
Recovery in PBS (%)					size (AA), pI, Hydrophilicity
$PrPrec_{hum}$	45 %	60 %	95 %	60 %	218, 9.8, HP
Tau_{rec}	/ *	+ 150 % *	+ 150 % *	+ 150 % *	441,6.5-8.5,/
α- syn	35 %	85 %	30 %	/	140,4.7, HP
Recovery in CSF (%)					
PrPc	60 %	85 %	70 %	95-100 %	/, 5-8, /
Tau_{tot}	80 %	95 %	100 %	95 %	/, /, /
Tau PHF	40 %	100 %	55 %	100 %	/, 5.5-6.5,/
Aβ-42	60 %	100 %	85 %	100 %	42,5.5,HB

The $PrPrec_{hum}$ has an extremely good recovery when stored in MIX I treated tubes. The first statement that can be made is that the surface should possess hydrophilic character in order to be repellent for $PrPrec_{hum}$. Nevertheless, that does not exclude PNIPAM and MIX II treated surfaces that were shown to adsorb relatively high amounts of recombinant prion protein. If surface properties of MIX I are compared to MIX II and PNIPAM, few differences can be observed. Firstly, MIX I has the lowest dispersive component, γ_s^d= 16.6 mJ/m^2, whereas the dispersive components of PNIPAM and MIX II are 19.1 mJ/m^2 and 23.4 mJ/m^2 respectively. Therefore, the dispersive component falls in the same order as $PrPrec_{hum}$ adsorption on MIX II>PNIPAM>MIX I.

Secondly, MIX I possesses the lowest basic character and O/C ratio from the hydrophilically treated surfaces. In conclusion, the importance of the charge at working conditions (pH=7.4) is most important on MIX I treated surfaces and corresponds to the value of ζ(7.4)= -51.9 mV, while the zeta potential on both PNIPAM and MIX II is just around -35 mV. This factor seems to be of a great importance, most probably due to the fact that the isoelectric point of $PrPrec_{hum}$ is very high (pI= 9.8) which means that at working conditions the protein is becoming less charged and more prone to aggregate. It

is known [200] that the highest protein adsorptions are observed when the net surface charge of a protein is zero, therefore the highly charged surface as found in MIX I ($\zeta(7.4)$= -51.9 mV) seems to induce the electrostatic repulsion between the protein and the surface.

The recombinant Tau protein is relatively large molecule composed from 441 amino acids and presents an isoelectric point between 4.7 and 6.9. The recovery of Tau protein was improved on all hydrophilic surfaces and did not show any specific selectivity among them. On the other hand α-syn is a small protein (140 amino acids) with pI=4.7. The recovery of recombinant α-syn gave relatively good results with PNIPAM treatment, 85% of the protein was preserved even after 1 month of storage. The size of proteins has a very important effect Namely the amount of amino acids between proteins vary severely, meaning that some proteins will have large amount of patches that are attracted to a certain surface. On another hand these proteins are subjected to constant change of conformations that occur in picoseconds range, leading to higher amount of aggregation for certain proteins.

In contrary, the lost of the protein on untreated and MIX I treated tubes was substantial, 65% in the case of untreated tubes and 70% on the tubes treated with MIX I. Considering the surface, PNIPAM has much more basic character than other treatments and also the highest total surface energy and low surface roughness. As α-syn is small, the surface roughness could play an important role in α-syn adsorption, but unfortunately there are no results available for MIX II to confirm this hypothesis. Comparing the three proteins, it could be said that the higher the pI of a protein is, less basic and more charged should be the surface in order to repel the protein in question.

The recovery of proteins from CSF is showing quite opposite results to the recovery of recombinant proteins stored in PBS. The cellular prion protein is now adsorbed in highest quantities onto the MIX I treated tubes, followed by PNIPAM treatment, whereas the signal of the CSF stored in MIX II remained unchanged in comparison to the fresh sample. This alteration could be due to the lower isoelectric point of the PrPc (pI= 5-8) comparing to the pI of $PrPrec_{hum}$ at 9.8.

The adsorption study from a single component solution clearly showed that the proteins with lower pI are repelled better from surfaces with higher basic character and O/C ratio. The recovery of TauPHF and Aβ-42 peptide from CSF is extremely high with PNIPAM and MIX II treatment as there was no lost of proteins observed after 24 h of storage. On the other hand, MIX I was subjected to relatively strong protein adsorption, the amount of TauPHF adsorbed was 45%, while less adsorption of Aβ-42 was observed. The difference between the two proteins is that Aβ-42 peptide is highly hydrophobic. It seems that different types of Tau protein have higher affinity for the surfaces with lower hydrophobic character, O/C ratio and important surface charge.

The results above showed that there are important differences in results obtained from a single-component recombinant protein solution and a complex multi-component solution like CSF. One reason is that the properties of the native, recombinant and infectious form of proteins differ substantially and secondly there is probably a preferential adsorption of non-degenerative proteins present in the plasma phase to the Eppendorf tubes, leaving the desired proteins intact in the solution. Namely a very important factor in a complex solution is mass transfer towards the surface, which will depend on the concentration of individual protein in the solution and is inversely correlated to its molecular weight. The smaller proteins with high concentrations will come to the surface first and are replaced afterwards with larger proteins having higher affinity for the surface. The studied neurodegenerative agents have relatively small masses in comparison to the other proteins from the plasma [201], so the replacement effect is highly probable. As MIX II is working extremely well for the recovery of all proteins from CSF even though their properties vary, we expect strong affinity of other plasma proteins towards the MIX II.

4.2 Evaluation of the non-fouling properties of treated supports by physicochemical characterization of surfaces after protein contact

For the below mentioned experiments the polypropylene plates were treated either with CF_4 plasma or pre-treated with helium plasma and grafted with PNIPAM, MIX I or MIX II. The conditions used for treatments were the same as for the biological validation test presented in the previous chapter. In the following step, different neurodegenerative proteins ($PrPrec_{hum}$, Tau_{rec} and α-syn) and blocking agent (BSA) were spread over the surface and left at room temperature for 2 h. The concentration of neurodegenerative recombinant proteins for the following experiments was 50 ng/mL, whereas the mass fraction of BSA was set to 3%. As it was mentioned in the previous section (4.1.1) the results between the direct and "sandwich" ELISA test were not coherent for PNIPAM and CF_4 treatments. For this reason the tests with BSA were done in order to obtain some additional information about the ability of BSA to block differently modified surfaces. We have supposed that the PNIPAM has a low affinity towards the BSA and because of this, the surface could not be blocked sufficiently, triggering the parasite interactions of other molecules used for the detection (HRP, TMB) with the surface. This could lead to a false positive signal on the tube, as if the protein was present. After immersion in protein solution, the plates were rinsed with distilled water and dried under laminar flow. On these supports, XPS and confocal microscopy analyses were performed in order to attain some supplement information and compare the results to biological validation ELISA tests.

4.2.1 Chemical characterization of treated surfaces exposed to protein solution

The high resolution C1s XPS spectra of untreated sample (PP), CF_4 plasma treated, PNIPAM, MIX I and MIX II grafted samples that were exposed to different protein solutions are shown in Figure 85. The corresponding peak assignments are gathered in Table 21 and Table 22.

Table 21: Decomposition results of high resolution C 1s peaks of hydrophobically treated samples exposed to protein solution with belonging functional groups and O/C ratio.

Component Energy (eV)	**C1 285.0**	**C2 286.7**	**C3 288.2**	**C4 289.7**	**C5 291.6**	**C6 293.6**	**O/C**
Possible assignment	C-C/C-H	C-O, C-F	O-C=O	CF-CF_n	CF_2	CF_3	
PP+CF_4	42.7	14.3	8.7	12.9	15.4	6.1	0.14
PP+ CF_4+ BSA	41.9	13.5	7.8	14.3	15.6	6.9	0.13
PP+ CF_4+PrPrec	61.9	9.5	6.7	7.4	10.3	4.2	0.16
PP+ CF_4+Taurec	44.6	13.7	7.9	13.5	15.1	5.2	0.13
PP+ CF_4+α-syn	39.4	13.9	8.1	14.5	16.7	7.4	0.11

Table 22: Decomposition results of C 1s peaks of untreated and hydrophilically treated samples exposed to protein solution with belonging functional groups and O/C ratio.

Component Energy (eV)	**C1 (%) 285.0 eV**	**C2 (%) 286.4 eV**	**C3 (%) 287.7 eV**	**C4 (%) 289.1 eV**	**O/C**	**N/C**
Possible assignment	C-C/C-H	C-O, C-N	C=O, N-C=O	O-C=O		
PP	97.2	2.8	/	/	0.05	/
PP+BSA	52.4	27.4	20.2	/	0.30	0.23
PP+PrPrec	98.1	1.9	/	/	0.04	/
PP+Taurec	92.3	4.9	2.8	/	0.14	0.03
PP+α-syn	95.6	3.2	1.1	/	0.10	/
PNIPAM	69.5	17.1	13.4	/	0.29	0.10
PNIPAM + BSA	70.1	16.4	13.5	/	0.28	0.09
PNIPAM+PrPrec	70.5	20.6	6.6	2.3	0.26	0.05
PNIPAM+Taurec	71.2	16.6	12.2	/	0.28	0.07
PNIPAM+α- syn	64.3	22.6	13.1	/	0.36	0.05
MIX I	80.6	13.7	5.7	/	0.20	0.06
MIX I + BSA	56.0	24.4	17.6	2.0	0.25	0.21
MIX I + PrPrec	83.4	12.2	4.2	/	0.18	0.04
MIX I + Taurec	83.5	13.2	3.3	/	0.19	0.05
MIX I + α-syn	85.5	9.7	2.8	1.9	0.22	0.02
MIX II	60.2	30.6	6.6	2.5	0.31	0.04
MIX II + BSA	59.1	20.8	19.8	/	0.28	0.23
MIX II + PrPrec	73.1	18.6	6.2	2.2	0.29	0.03
MIX II + Taurec						
MIX II + α-syn	64.9	25.2	7.1	2.8	0.47	/

Let us first consider the adhesion of the blocking agent (BSA) to the untreated and treated surfaces. The hydrophobically treated support (CF_4) showed no significant change in the chemical composition (Table 21) upon exposure of the surface to the BSA solution. This could happen either due to the low adsorption of BSA at shorter times of exposure or, more likely, because of the low wettability of the surface that disallowed a homogenous spreading of the protein across the support. Namely the XPS analyses the surface in the spot area of 400 μm, while the size of the sample was 1 cm × 1 cm. Therefore there exists a probability that we did not manage to analyse the area on which the proteins were spread. Adversely, the exposure of virgin PP substrate to BSA solution brought big changes in surface composition (Table 22, Figure 85.a). The C1 peak at 285.0 eV that corresponds to C-C/C-H bonding decreased from 97.2 % to 52.4%, while the C2 peak (C-O/C-N) increased from 2.8% to 27.4%. At the same time new peak at 287.7 eV appeared belonging to C=O/N-C=O functionalities. Consequently there was a big increase of O/C and N/C ratio for 0.25 and 0.23 respectively. These data are indicating an extremely high adsorption of BSA to the untreated polypropylene surface.

For the hydrophilically modified surfaces the PNIPAM treated supports showed complete resistance towards the BSA. There was no change of the surface chemical composition before and after the exposition of PNIPAM plate to the BSA solution (Table 22, Figure 85.b). This result confirms the inadequate surface blocking as proposed before and possibility of foreign interactions of the surface with HRP labelled detection antibody or TMB. Highly noticeable changes can be seen for the attachment of BSA to the MIX I and

MIX II treated surfaces (Table 22).The C1 peak of MIX I decreased from 80.6% to 65.0%, while C2 and C3 peaks increased from 13.7% to 24.4 % and 5.7% to 17.6% respectively. A new C4 peak with relative intensity of 2% also appeared. Adsorption of BSA to MIX II treated supports decreased the C2 peak from 30.6% to the 20.8% and increased the C3 peak from 6.6% to 19.8%. There was also a disappearance of C4 peak, corresponding to O-C=O bonding. The adsorption of BSA is very strong on all supports except PNIPAM (and CF_4). As the N/C ratio of all supports that strongly interacted with BSA is around 0.23 and the diameter of BSA (6.4 nm) corresponds to analytical depth of XPS, it can be said that the BSA completely covered and therefore blocked these surfaces.

In the next step we will consider the attachment of neurodegenerative proteins to either hydrophilic or hydrophobic surfaces. The XPS results of recombinant protein adsorption on hydrophobically (CF_4) treated plates are shown in Table 21. There was a remarkable increase of C1 peak observed at 285.0 eV (19.8%) for $PrPrec_{hum}$ adsorbed on the fluorinated plates in comparison with the plates that were not exposed to protein solution. At the same time the relative concentration of C2-C5 peaks, belonging to different fluorinated functional groups decreased quite substantially, suggesting high adsorption of $PrPrec_{hum}$ on the plates. The same was observed by ELISA tests, confirming the high affinity of $PrPrec_{hum}$ for hydrophobic supports. Oppositely, there were no significant changes in the surface chemistry of the fluorinated surfaces exposed to Tau_{rec} and α-syn protein solutions. Unfortunately, the available amount of proteins was limited and as mentioned before for BSA, it prevented the homogenous spreading of protein across the substrate due to the extremely low surface energy of fluorinated supports. Therefore it can not be said that the adsorption did not occur (as the biological validation tests showed the contrary), but rather that the scanned surface area with XPS was not sufficiently large and well positioned. The XPS results will be compared after with confocal microscopy imaging, where the samples can be scanned over an area as large as 1 cm × 1 cm by simple manipulation of the sample position towards the imaging area.

The exposure of PNIPAM grafted sample to tau_{rec} protein solution did not result in change of surface chemistry composition indicating no or negligible adsorption of this protein to the surface (Figure 85.b). Immersion of PNIPAM treated plates into α-syn solution showed very small changes in surface functionalities, the C2 (C-O/C-N) peak increased for 4% suggesting a small adsorption of α-syn to the surface. On the other hand the adsorption of $PrPrec_{hum}$ from gave rather important decrease of C3 peak (C=O, N-C=O) for 7% and a new peak (C4) appeared at 289.1eV (O-C=O). The results are confirming stronger attachment of prion protein to PNIPAM surface comparing to α-syn, as was already suggested by biological validation results.

The adsorption of all neurodegenerative proteins to the MIX I treated supports is very low and can not be deducted from the high resolution C1s spectra (Figure 85.c). However if we look at peak composition in Table 22, it is possible to see that α-syn adsorbed to MIX I treated surfaces. Namely, C2 and C3 peaks decreased comparing to MIX I treated sample (for 4% and 2.4% respectively) and a formation of C4 peak occurred (1.9%). There was also an increase of C1 peak for 4.9%, corresponding to C-C/C-H functional groups.

Contrary to MIX I, MIX II high resolution C 1s spectra show extremely attractive surface upon protein adsorption. All proteins with exception of Tau_{rec} adsorbed substantially (Figure 85.d). This confirms the biological validation test performed on recombinant proteins. The adsorption of $PrPrec_{hum}$ on MIX II caused a high decrease of C2 peak (10%) suggesting that a big amount of recombinant prion protein was adsorbed on the surface even though the concentration of protein was very low (50ng/mL). Likewise for the $PrPrec_{hum}$ adsorption, the α-syn adsorption results in the drop of C2 peak, however less severely (5.4%). From these results we can conclude that MIX II possesses a higher affinity towards the $PrPrec_{hum}$ than towards the α- syn. On the other hand, the contact of MIX II plates with Tau_{rec} solution

did not bring any visible changes in surface composition, proposing its neutrality toward the Tau protein. It is interesting to compare the behaviour of recombinant forms of protein towards the natural forms found in CSF. Adversely to recombinant forms of proteins in PBS, MIX II showed remarkably high recovery of different types of proteins from CSF as shown by biological validation tests.

Regrettably the XPS analyses could not be performed on proteins from the CSF, taking into account that it is composed of a large variety of different proteins. The XPS results are in a good agreement with biological tests for hydrophilic supports, while for hydrophobic treatments homogeneous spreading of proteins was hindered by the low surface energy of supports, therefore the interpretation of these results needs to be taken cautiously.

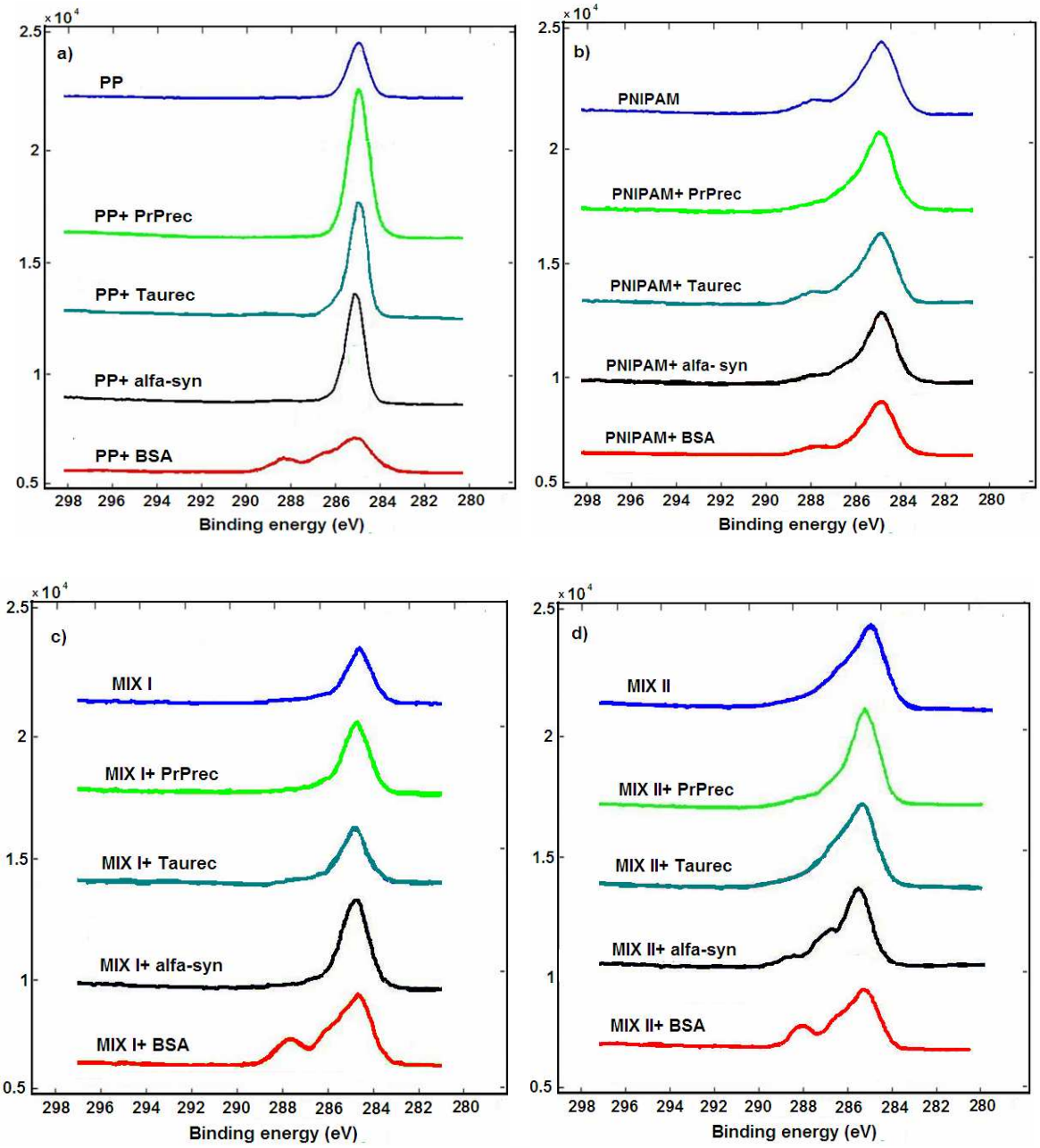

Figure 85: Comparison of high resolution C1s spectra of untreated PP sample and untreated PP sample dipped in protein solutions: BSA, $PrPrec_{hum}$, Tau_{rec} and α-syn.

4.2.2 Visualization of surfaces exposed to protein solution

The confocal microscopy technique allows visualization of proteins by fluorescence and was employed to obtain some complementary information on the protein adsorption. The untreated and treated surfaces (CF_4, PNIPAM, MIX I and MIX II) were exposed to different protein solutions ($PrPrec_{hum}$, Tau_{rec} and α-syn) coloured with rhodamine. The volume fraction of rhodamine in PBS buffer was 0.5%, where the concentration of proteins was set to c= 50 ng/mL. In the next experiment untreated and treated surfaces were immersed into rhodamine solution in the absence of proteins in order to ensure that the fluorescence of the surface correspond just to the presence of proteins and not to the interaction of rhodamine with the treated surfaces. The time of immersion for both experiments was 2 h. After this step, all surfaces were dried over night under laminar flow at room temperature.

Images obtained by confocal microscopy analysis are presented in Figure 86. It needs to be mentioned that images corresponding to the rhodamine interaction with substrate (experiment two, without protein) are not presented here. The images shown in figure 86 present just the fluorescence that was caused by adsorbed proteins, where the background caused by rhodamine interaction with treated surfaces was already subtracted.

Let us first consider the adsorption of prion protein. Coherently with the ELISA results, the lowest adsorption of prion protein was observed on the MIX I treated surface (red square). The adsorption of $PrPrec_{hum}$ on PNIPAM shows rather high amount of proteins present on the surface that are covering it extremely homogeneously in comparison to other surfaces. Virgin PP and CF_4 treated surfaces are showing large aggregates, while MIX II treated surface seems to induce oligomerization of proteins and formation of closed structures in the form of rings. In our experiment proteins were exhibited to ambient temperature under air, which could explain the aggregates observed on the surface. If we compare the amount of prion protein adsorbed between the treatments, it seems that they drop in an order: CF_4>PNIPAM~MIX II>PP>MIX I. This is in a good agreement with results obtained by biological tests.

The amount of Tau_{rec} adsorption was very low for all hydrophilic surfaces (green squares), whereas PP and CF_4 show high surface coverage with proteins. Finally the α-syn adsorption presents a formation of interesting branched features on the surfaces, indicating an extremely high protein oligomerization. The lowest adsorption of α-syn was observed on PNIPAM treated samples, consistent with the immunology test.

The confocal pictures presented were chosen from several measurements on different areas. It needs to be mentioned that the surface is extremely inhomogeneous towards the protein solution; namely there are some areas with large aggregates and on the other side practically nothing could be observed on them. The great inhomogeneity comes from the fact that the proteins were simply spread over the surface and not immersed into the protein solution. Nevertheless, there is a very good agreement between the biological validation tests and confocal microscopy results.

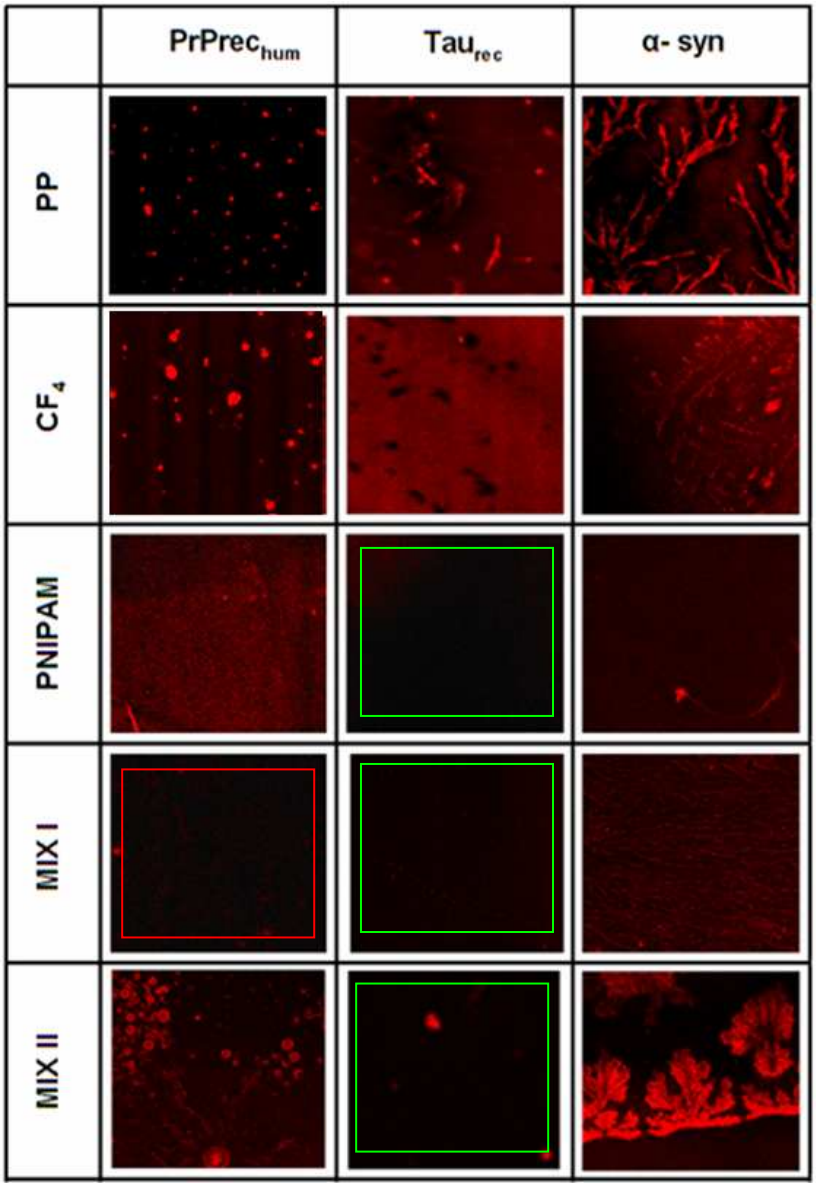

Figure 86: Confocal microscopy images: influence of surface properties on adsorption of PrPrec$_{hum}$, Tau$_{rec}$ and α-syn.

4.3 Influence of storage conditions on protein adsorption

The origins of protein-surface interactions are found in different intermolecular forces, thermodynamics and entropically based interactions such as hydrophobic interactions, conformational entropy and restricted mobility. In addition the adsorption depends on the intermolecular forces within the protein molecules, which may lead to the change in their conformation. This is strongly influenced by solution chemistry (pH, T, ionic strength, addition of various molecules) and can be used to control the adsorption process.

In order to study how some of these factors influence the protein behaviour several experiments were made. In the first, part the influence of protein concentration, storage time and temperature on the adsorption of PrPrec$_{hum}$ onto the hydrophobically modified surfaces was studied. Afterwards, the influence of long time storage (3 months) on adsorption of α-syn to differently treated tubes was monitored at two different temperatures (- 20ºC and +

4ºC). Finally, the $PrPrec_{hum}$ and TauPHF were stored in different buffer solutions over night, where pH of the storage solutions varied between 5.5 and 9.8. All recovery measurements were done on supernatant by "sandwich" ELISA protocols.

4.3.1 Influence of concentration, time and temperature of storage on adsorption of $PrPrec_{hum}$ to hydrophobically modified surfaces

The Eppendorf tubes were treated by CF_4 plasma at P= 50 W, Φ= 40 sccm and t= 7 min. At these conditions maximal water contact angle on the surface was observed at 132º. The $PrPrec_{hum}$ solutions were prepared at two different concentrations; c_1= 50 ng/mL and c_2= 1µg/mL. These proteins solutions were stored in either virgin PP Eppendorf tubes or CF_4 plasma treated tubes at the V= 100 µL. A part of these samples was stored at -20ºC and the other part at 4ºC. In the next phase after 15 min half of the tubes were taken from the fridge at 4ºC and freezer at -20ºC and immediately analyzed by immunology tests. The second half of the samples was left in the cold and analyzed after 1 month.

The results of $PrPrec_{hum}$ short time storage in untreated and CF_4 treated tubes are shown in Figure 87. For the following results the optical density measurements were not normalised as for other graphs presented, due to the fact that these experiments were performed at different protein concentrations, temperature and time, making their presentation clearer if optical density is used. There was no sample that was stored at - 80ºC as a reference ($(\tau_{15(-80ºC)})$), therefore the results are presented quantitatively, but as relative improvement of treated tubes towards the virgin PP tubes ($\eta_{(PP)}$) at the same experimental conditions. The direct ELISA tests performed on the Eppendorf tubes (red columns) are showing slightly higher adsorption of prion protein on fluorinated tubes comparing to the untreated PP tubes for elevated concentrations (1µg/mL) of the protein. This was true for both temperatures, - 20ºC and + 4ºC.

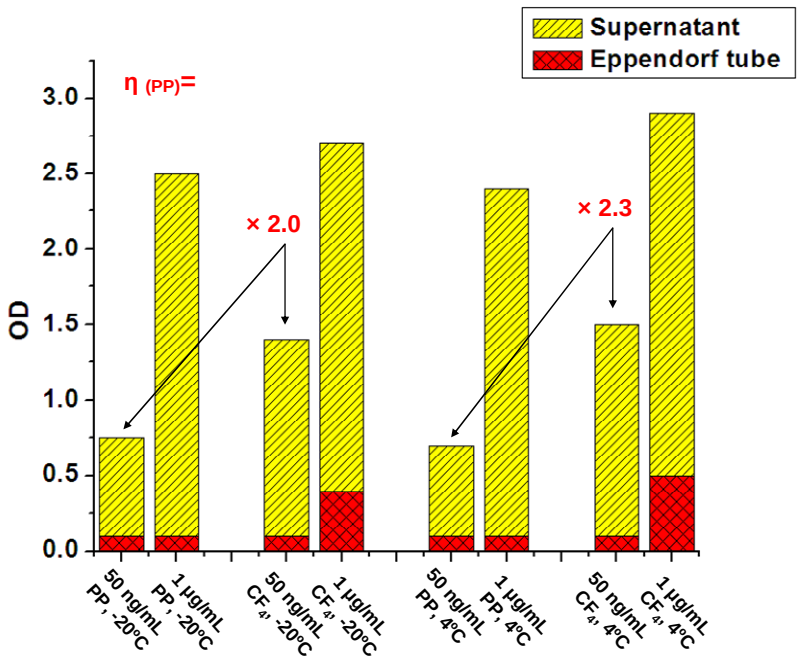

Figure 87: Storage of $PrPrec_{hum}$ for 15 min in untreated and CF_4 plasma treated Eppendorf tubes at different protein concentrations and temperatures.

On the other hand when proteins were stored at lower concentrations (50 ng/mL) the protein recovery (yellow columns) was twice higher when stored in CF_4 treated tubes in comparison to virgin PP tubes (× 2.3 at 4ºC). The adsorption to hydrophobic materials was reported to be stronger (and in higher quantities) in parallel to the materials with higher surface energy. However this is only partially true and strongly depends on the protein concentration. If the concentration of proteins in the solution is high enough that the mass transport is much faster than the rate of protein spreading and reorientation, more protein will be adsorbed on low energy surfaces. For diluted solutions the effect can be quite opposite what was also observed on our surfaces. This means for example, that the efficiency of the tubes used in laboratory for preparation of the samples could be improved by plasma fluorination, as the lost of protein is smaller comparing to the untreated PP tubes. The advantages of this technique are several: it is rather simple, extremely fast, and "clean" and moreover possesses sterilization abilities.

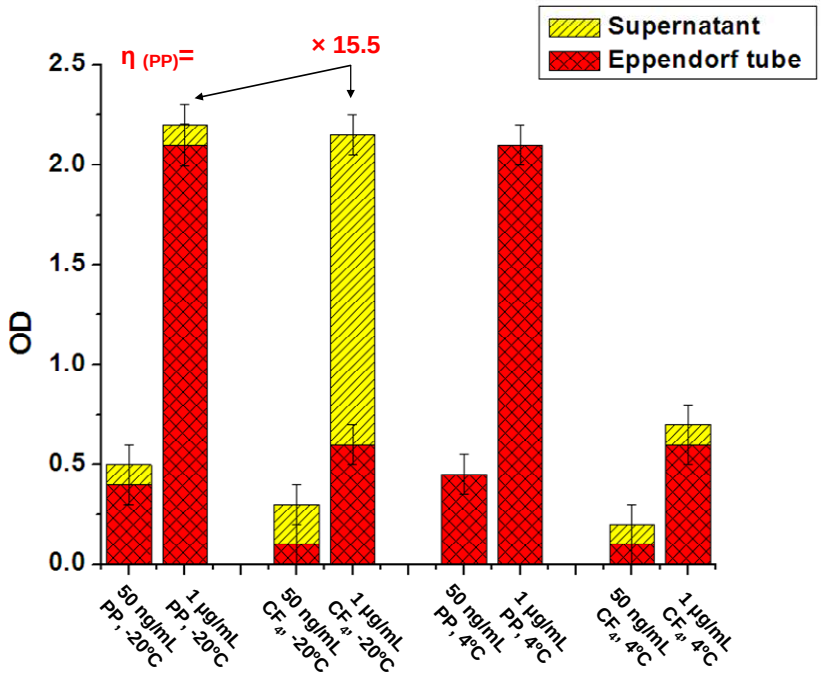

Figure 88: Storage of $PrPrec_{hum}$ for 1 month in untreated and CF_4 plasma treated Eppendorf tubes at different protein concentrations and temperatures.

The results of $PrPrec_{hum}$ storage over a period of one month in untreated and CF_4 plasma treated Eppendorf tubes at different protein concentrations and various temperatures are presented in Figure 88. First thing that can be observed is the complete loss of protein on untreated PP tubes at both temperatures and both concentrations. The $PrPrec_{hum}$ solution that was stored in CF_4 treated tubes at -20ºC on the other hand shows relatively high recovery of the protein. Comparing to the untreated tubes, the improvement is 1550 %. If we assimilate it to the samples that were stored just for 15 min, we can say that around 50% of additional protein was lost in this one month on CF_4 treated tubes at -20ºC. At 4ºC, the same phenomena was obtained as in the $PrPrec_{hum}$ storage over night at the same temperature (Chapter 4.1.1), namely there was no proteins detected on the Eppendorf tube or in the solution, which was explained by formation of protein double layer.

4.3.2 Influence of time and temperature of storage on adsorption of α-syn to modified surfaces

The recombinant α-syn was diluted in PBS buffer at pH= 7.4 and stored in differently treated Eppendorf tubes for 1 to 3 months at different temperatures (- 20ºC and +4ºC). The reference sample was analysed (($\tau_{15(-80ºC)}$), corresponding to 100% of the protein. The results of "sandwich" ELISA tests are presented in Figure 89.

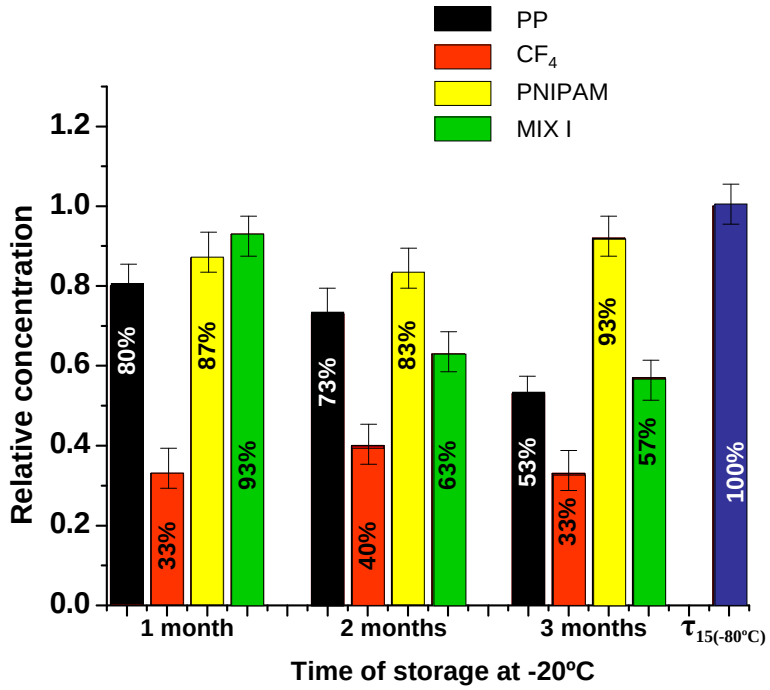

Figure 89: Storage of α-syn in a period from 1 to 3 months at -20ºC in untreated, CF_4 plasma treated and PNIPAM, MIX I grafted Eppendorf tubes.

The results are showing high adsorption of α-syn onto the CF_4 plasma treated Eppendorf tubes at -20ºC. The optical density is reduced by 67% already after one month of storage and does not change much with time afterwards. The adsorption of α-syn to the untreated and MIX I treated tubes progressively decreases with time, while for PNIPAM treated tubes there is initial drop of signal to 85% and afterwards the surface remained more or less stable in the period of three months. This could indicate that the protein is irreversibly adsorbed on PP and MIX I treated tubes, allowing a formation of double layer and further loss of biological material.

The optical density results of α-syn adsorption on the untreated and treated tubes at 4ºC over a period of three months is shown in Figure 90. This time a low recovery of protein on all treatments (except PNIPAM) happened already in a month. This is not surprising as the increase of temperature contributes to the change in enthalpy and system entropy, leading to spontaneous adsorption of the proteins. We have seen that no matter what was the temperature, the recovery of α-syn was the highest from the PNIPAM treated tubes. The lost of signal after 3 months of storage in PNIPAM tubes could be the correct result or the artefact, but unfortunately the experiments could not be repeated.

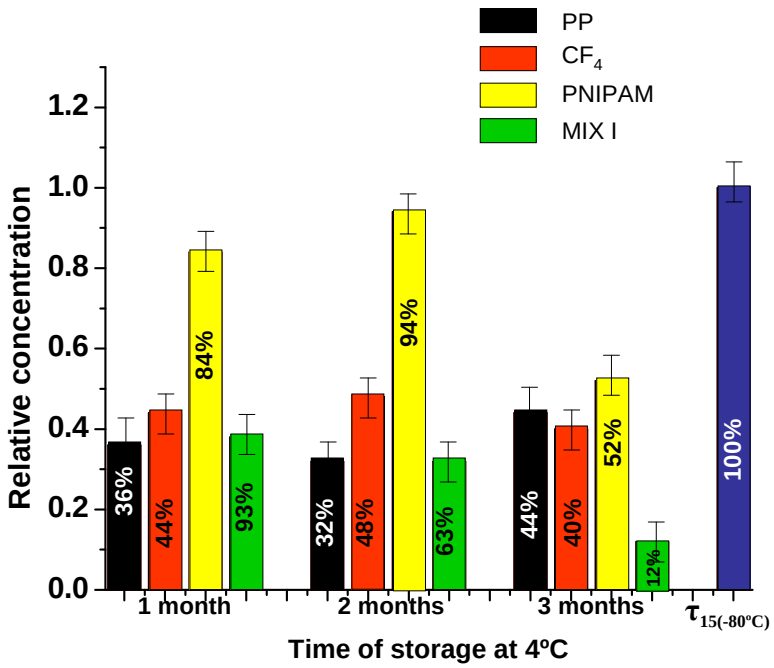

Figure 90: Storage of α-syn in a period from 1 to 3 months at +4ºC in untreated, CF_4 plasma treated and PNIPAM, MIX I grafted Eppendorf tubes.

4.3.3 Influence of the pH of storage buffer solutions on adsorption of $PrPrec_{hum}$ and Tau_{rec} on modified surfaces

The pH of the PBS buffer solution (pH=7.4) was adjusted to pH= 5.5 by addition of HCl and with addition of NaOH to pH= 9.6. $PrPrec_{hum}$ and Tau_{rec} proteins were diluted in the three different pH solutions mentioned above and stored for 24 h at 4ºC. The ELISA test results are presented in Figure 91 and Figure 92 for $PrPrec_{hum}$ and Tau_{rec} respectively.

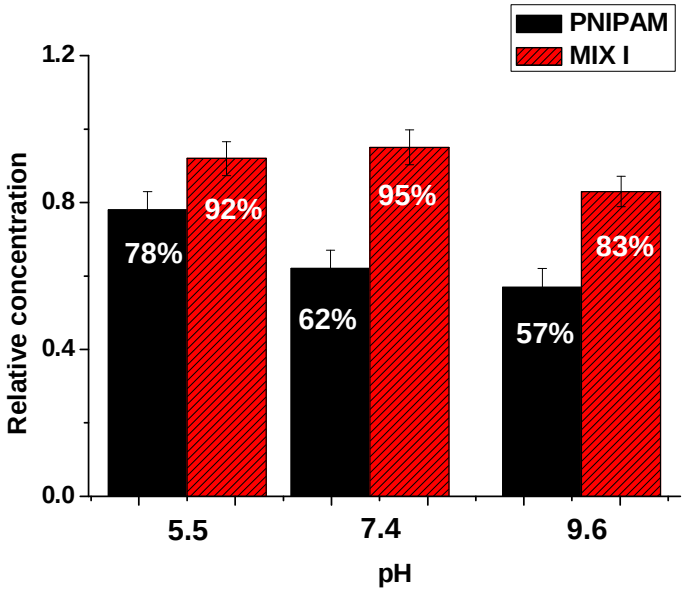

Figure 91: Influence of the pH on recovery of $PrPrec_{hum}$ from differently treated Eppendorf tubes.

Figure 91 is presenting the evolution of the $PrPrec_{hum}$ recovery curve as a function of pH. The standard conditions used for storing are at pH= 7.4. There was the highest amount of protein recovery at this pH for MIX I treated Eppendorf tubes, while PNIPAM showed 16 % improvement of recovery at lower pH. The adsorption of proteins at pH= 9.6 increased for both treatments with slightly different intensities among them. The alteration observed on MIX I treated surfaces is probably due to the partial neutralization of the positive charge of $R_4N^+Br^-$ molecule (CTAB) found in MIX I. The favourable conditions on PNIPAM treated tube at pH=5.5 could be ascribed to the insertion of charge enabling electrostatic repulsions.

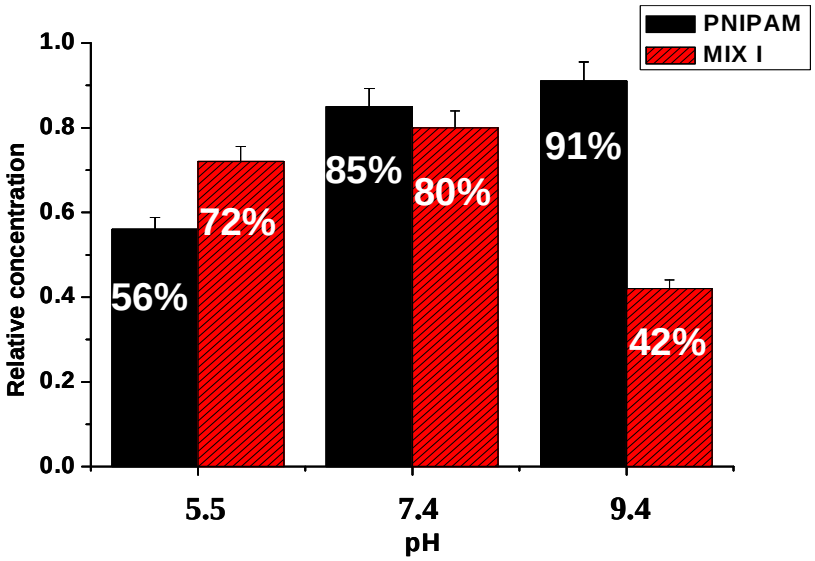

Figure 92: Influence of the pH on recovery of Tau_{rec} from differently treated Eppendorf tubes

The recovery of Tau protein from MIX I treatment showed best results at pH=7.4, while for pH= 9.6, a decrease in optical density signal is observed (Figure 92). This drop could be ascribed to the high difference in the surface charges at this pH. Namely, pI of the Tau_{rec} is somewhere between 4.7 and 6.9 that means that it would be more negatively charged at elevated pH, while the surface still contains partially positively charged functional groups.

Oppositely, the adsorption of Tau protein onto the PNIPAM treated tubes is lowest at most elevated pH. This could be explained by higher quantity of charge present at higher pH, decreasing the probability of protein aggregation.

For a number of proteins, the adsorption is maximized when solution pH is close to the isoelectric point of a particular protein [200]. This is related to the protein-solvent interactions becoming less favourable, and protein-protein interaction becoming less unfavourable when there is no net charge of the protein.

Generally when the solution environment becomes less hospitable to proteins they tend to adsorb and leave the solution. On the other hand, if the pH is far from the pI the electrostatic repulsions become more important and the proteins are retained in the solution. This is of course only true to certain pH levels, until the protein's stability is disrupted too severely.

4.4 Influence of surface properties on the protein adsorption

In the third chapter we indicated that the influence of plasma conditions and polymer to surfactant ratio influence strongly the final properties of the surface. The largest effects observed were on the chemical composition of the surface and especially on the surface topography. Therefore the Eppendorf tubes were activated by He plasma for 10 s, 60 s or 180 s and grafted with MIX I and MIX II. The concentration of PNIPAM was fixed to 0.5g/L, c_{CTAB}= 1mM and the $W_{Tween20}$= 0.05%. Afterwards PNIPAM was mixed with either CTAB or Tween 20® at different volume ratios. The treated tubes were exposed to $PrPrec_{hum}$ and TauPHF proteins for 24 h at 4ºC and tested with direct and/or "sandwich" ELISA tests. The ageing of the tubes was also tested, where the ELISA tests on $PrPrec_{hum}$ and Tau PHF storage were performed on Eppendorf tubes that were prepared 6 months before using.

4.4.1 Influence of surfactant to polymer ratio and plasma conditions on recovery of $PrPrec_{hum}$

The histograms of $PrPrec_{hum}$ adsorption as a function of plasma parameters and polymer to surfactant ratio are presented. Figure 93.a corresponds to MIX I treatment and the Figure 93.b to the MIX II treatment. The red columns are representing the amount of protein adsorbed on the surface and the yellow ones show the amount of protein recovered from solution. The results were not normalised due to the phenomena mentioned at the beginning of the chapter, where the concentration of proteins detected on the tubes and in the supernatant exceed 100%.

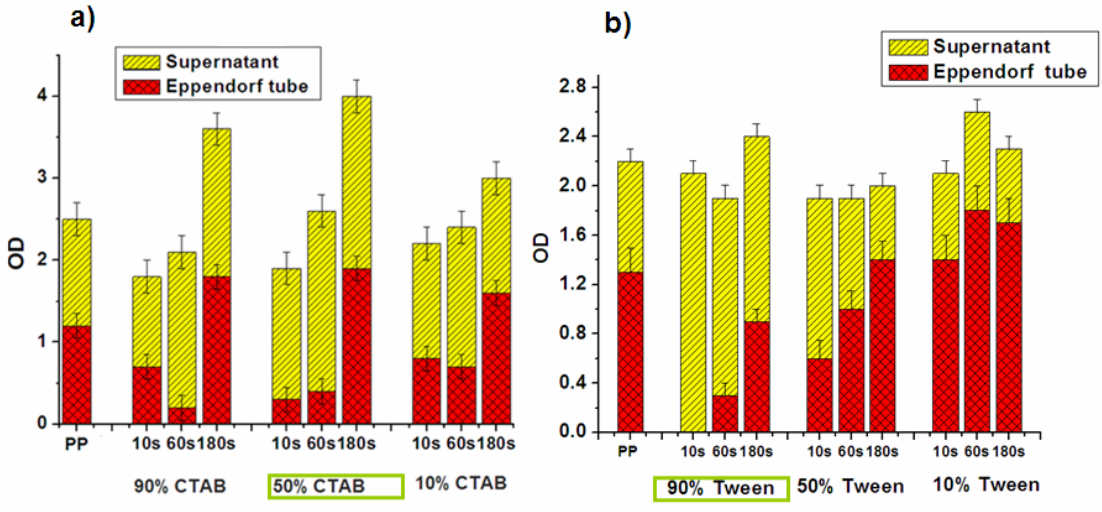

Figure 93: Optical density measurements on a) MIX I and b) MIX II treatments for the recovery of $PrPrec_{hum}$ as a function of plasma grafting conditions and polymer to surfactant ratio.

For the MIX I treatment (Figure 93.a), the higher value of surfactant seems to lead to a better recovery of $PrPrec_{hum}$. Even though that recovery of prion protein is rather high whether 90 % or 50% of surfactant was used, the results are still slightly better when the V_{PNIPAM}/V_{CTAB}= 1:1. The influence of plasma parameters is also important. Best results

were obtained with 60 s of plasma activation, while the prolonged treatment lead to extremely high signal on the Eppendorf tubes and at the same time relatively high recovery. As it was already seen with PNIPAM, a poor interaction between the blocking agents (BSA) caused artificial signal on the Eppendorf tubes due to the parasite interactions with streptavidin-HRP complex with the surface. Unfortunately, the information on BSA interaction with MIX I at these experimental conditions is not available, however there is a high probability that MIX I in this case has no or very little affinity towards BSA.

On the other hand, the adsorption of $PrPrec_{hum}$ on the MIX II (Figure 93.b) treated Eppendorf tubes gave much more regular behaviour. Longer treatment times and the high polymer concentrations result in higher adsorption of prion protein. All the previous tests presented on MIX II were performed at 50% of PNIPAM and 180 s of plasma pre-treatment time and as can be seen the conditions were not suitable for a good recovery of prion protein. With these test the perfect conditions were found (t=10 s, $V_{PNIPAM}/V_{Tween20}$= 1:9) at which no adsorption of $PrPrec_{hum}$ was detected.

4.4.2 Influence of surfactant to polymer ratio and plasma conditions on recovery of TauPHF

Figures 94.a and 94.b present the recovery of TauPHF as a function of plasma parameters and polymer to surfactant ratio on MIX I and MIX II treated tubes respectively. The measurements were done with “sandwich” ELISA test, where optical density values correspond to amount of protein that remained in the solution.

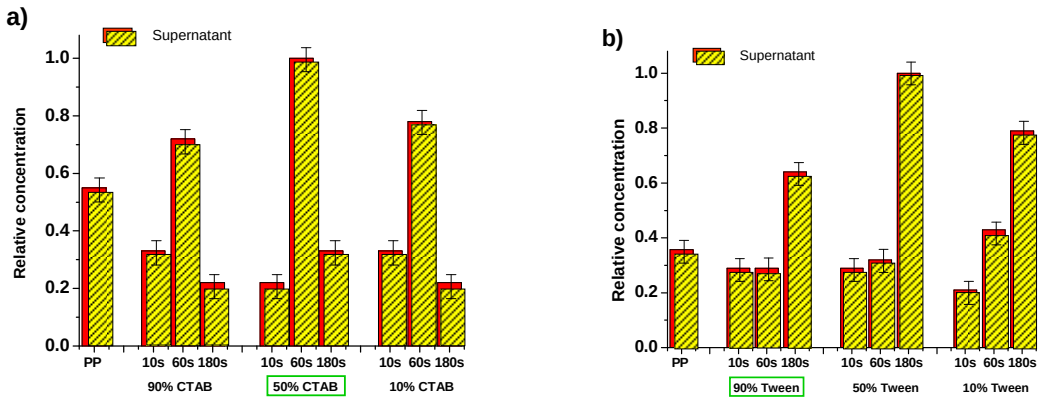

Figure 94: Optical density measurements on a) MIX I and b) MIX II treatments for the recovery of Tau_{rec} as a function of plasma grafting conditions and polymer to surfactant ratio.

The recovery of TauPHF from MIX I Eppendorf tubes showed best results for tubes that were pre-treated with He plasma for 60 s and grafted in the solution at the volume ratio V_{PNIPAM}/V_{CTAB}= 1:1. These are the same conditions that had the highest performance for $PrPrec_{hum}$ protein. The recovery of the TauPHF was 80% higher than in the untreated PP tubes. At all other conditions almost no protein was detected. Next to the plasma treatment time the concentration ratios had an influence on recovery as well, namely 33% more of the protein was detected at optimal conditions (50% of CTAB). Even though the recovery was improved quite remarkably, the loss of protein was still not negligible. If the

optical density values of best performing MIX I tube are compared to the MIX II optimal treatment (Figure 93.b), a big difference in the signal can be observed (ΔOD= 0.5). In other words 90% more of the protein remained in the solution in MIX II treated tubes comparing to MIX I treated tubes or 170 % more than in the virgin PP tubes.

The surface properties of MIX I and MIX II grafted supports as a function of plasma activation time are gathered in Table 23. The corresponding relative increase in the protein recovery for $PrPrec_{hum}$ and Tau_{rec} relatively to the untreated PP tubes are added to the last two columns. The lowest adsorption of prion protein was observed on MIX I surface that was pre-treated with He plasma for 60 s. At these conditions the O/C ratio and the surface potential were the highest, while the basic component reached the minimum. The AFM imaging showed that at these conditions regular nano-structured surface was obtained with average surface roughness of 6.4 nm. The AFM image of the sample pre-treated with helium plasma for 180 s and grafted with MIX I is not available, but it can be supposed that the visible structured features are present and are responsible for the difference from the short time activated sample recovery. Variations in the optical density between 60 s and 180 s pre-treatment times could be prescribed to lower basic character and slightly higher surface charge. The only plasma treatment condition that resulted in positive prion protein recovery for MIX II grafting was at 10 s of plasma activation time. If the surface properties of MIX I after 60 s and MIX II after 10 s of activation are compared, it could be said that the O/C ratio should be sustained preferably between 0.20 and 0.25 and more importantly the zeta potential should be extremely negative.

Table 23: Basic properties of grafted supports as a function of plasma treatment time and relative increase of concentration for $PrPrec_{hum}$ and Tau_{rec} towards the untreated tubes.

	O/C	**γ^- (mJ/m^2)**	**ζ (pH=7.4) (mV)**	**Sa (nm)**	**Rel. conc. (%) ($PrPrec_{hum}$)**	**Rel. conc. (%) (Tau_{rec})**
MIX I						
10 s	0.19	63.9	/	3.1	+ 23	-150
60 s	0.20	61.5	-51.9	6.4	+ 73	+ 80
180 s	0.19	66.6	-48.0	/	+ 61	- 67
MIX II						
10 s	0.26	88.7	/	2.8	+ 37	- 25
60 s	0.30	82.0	- 41.9	/	- 5	- 10
180 s	0.31	73.9	-36.6	7.1	- 35	+ 170

MIX II treatment reaches by far the highest value for Tau PHF recovery (+170%), when the plasma activation lasted 180 s. At these conditions extremely regular features were formed and the average surface roughness reached 7.1 nm. The O/C ratio reached 0.310 and the zeta potential decreased comparing to the Eppendorf tube that was treated for shorter times. MIX I treatment is able to decrease the Tau PHF adsorption for 80% comparing to the untreated tube when plasma pre- activation lasted 60 s. The similarities between the MIX I and MIX II treated surfaces that enable better recovery of Tau PHF are the highest O/C ratio and more importantly the regularity of the structured surface. Nonetheless, the performance of MIX I treated tube is relatively poor towards the MIX II treated tube.

The surface properties of MIX I and MIX II as a function of polymer to surfactant ratio and the values of $PrPrec_{hum}$ and Tau_{rec} recovery are gathered in Table 24. The recovery of prion protein from the MIX I treated tubes as a function of concentration ratio is the highest when the n_{PNIPAM}/n_{CTAB} is 1:50. Additional supplement of either polymer or surfactant results in increased adsorption. In contrary, MIX II treated tubes work better for recovery of

prion protein when higher amount of surfactant was added. If we combine these results with the plasma treatment results we see that up to 125% better recovery can be achieved if short treatment time and high surfactant to polymer ratio is used. On the other hand the recovery of Tau PHF presents the best results in MIX I and MIX II treated tubes at the polymer to surfactant ratio of 1:50 and 1:25 respectively. At these conditions extremely regular surface features were formed. Further addition of surfactants to PNIPAM polymer causes much higher adsorption of the Tau PHF.

Table 24: Basic properties of grafted supports as a function of polymer to surfactant ratio and the relative increase of optical density for $PrPrec_{hum}$ and Tau_{rec} towards the untreated tubes.

Treatment ($n_{Polymer}/n_{Surfactant}$)	**γ^{b-} (mJ/m^2)**	**Sa (nm)**	**Rel. conc. (%) ($PrPrec_{hum}$)**	**Rel. conc. (%) (Tau_{rec})**
MIX I				
1/5	78.2	/	+ 31	+ 40
1/10	68.5	3.6	/	/
1/50	61.5	6.4	+ 73	+ 80
1/100	50.5	6.9	/	/
1/500	/	4.6	+ 46	+ 30
MIX II				
1/2.5	/	/	- 35	+ 120
1/10	77.9	/	/	/
1/25	63.9	7.1	- 35	+ 170
1/50	54.4	8.2	/	/
1/250	/	/	+ 50	+ 80

In conclusion, the results have shown that the plasma conditions and surfactant to polymer ratio influence substantially the protein adsorption, either through introducing different functionalities or through influencing the surface topography. As the plasma activation time and surfactant to polymer ratio did not influence much the total surface energy and its polar and dispersive components, we can conclude that the surface potential and topography have much greater impact on the protein recovery. It seems that the surface that would repel the prion protein best should possess a high negative zeta potential, lower basic character and rather high O/C ratio. Tau PHF on the other hand was preserved the most when the surface roughness was very important and contained regular features. The zeta potential should be much smaller than for the prion protein as well, while high O/C ratio and moderate basic character seems to be desired.

4.4.3 Ageing of storage tubes and its influence on protein recovery

In order to observe the ageing effects on protein recovery the Eppendorf tubes were treated with PNIPAM, MIX I and MIX II and stored under air for 6 months. At the same time tubes were freshly prepared, stored under nitrogen and tested after one weak. The results of $PrPrec_{hum}$ and Tau PHF recovery are presented in Figure 95. For both experiments a sample was stored at -80ºC in the untreated PP tubes for 24 h ($\tau_{15(-80ºC)}$), that corresponds to 100% of the protein recovery.

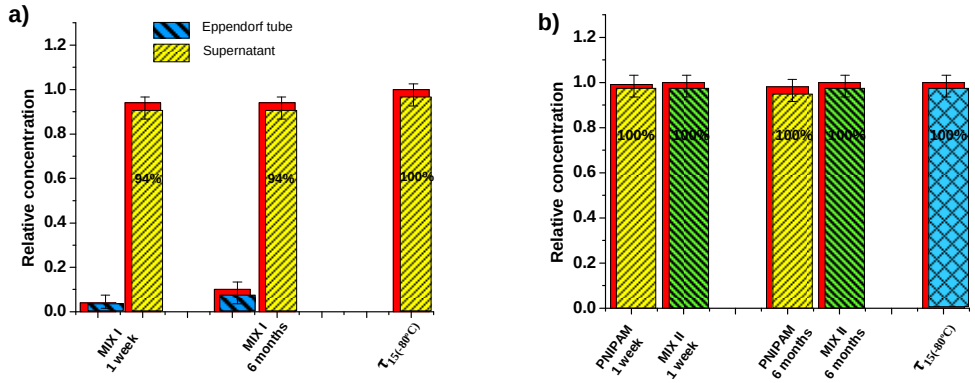

Figure 95: Recovery of a) $PrPrec_{hum}$ and b) Tau PHF stored for 24h at 4ºC in tubes that were treated either one week or 6 months before the analyses.

The results in Figure 95.a show that there is a slightly higher adsorption of $PrPrec_{hum}$ on MIX I treated tubes prepared 6 months before the analyses, however the recovery of the protein remains the same. The drop of the signal for 6 % is due to a low adhesion of prion protein to the MIX I treated Eppendorf tubes and not due to their ageing. There is no ageing observed on the PNIPAM and MIX II treated Eppendorf tubes for the recovery of Tau PHF (Figure 95.b). It can be concluded that the tubes possess stable treatments and can be used at least 6 months after they were produced. The stability of coatings is of a great importance for further applications.

4.5 Conclusions

Results of protein adsorption tests have shown that there is not just one factor responsible for protein interaction with the surface, but a mutual effect of different surface properties (charge, functional groups, acid- base character, nanostucturation), storage conditions (complexity of the solution, time, pH, temperature) and the properties of the protein itself (pI, size and hydrophobic/hydrophilic character). We have managed to attain no or negligible adsorption of all examined proteins on the Eppendorf tubes when storage was performed at 4ºC for 24 h. Despite the important amount of attempts, a unique surface treatment for all proteins could not be attained due to considerable variations of the protein properties. Nevertheless, few correlations between surface and protein properties were found:

- hydrophobic surfaces induced high adsorption of all neurodegenerative proteins
- $PrPrec_{hum}$ was recovered 95% from MIX I treatment and 100% for MIX II treatment (high surfactant ratio and short treatment time). The conditions needed for good recovery of prion protein (pI=9.8) are high negative zeta potential, low basic character and O/C ratio between 0.20 and 0.25
- Tau_{rec} stored in either PNIPAM, MIX I or MIX II showed 150% higher recovery relatively to untreated polypropylene tubes. The Tau_{rec} protein (pI=6.5-8.5) did not show any specificity towards all hydrophilic treatments
- α-syn (pI=4.7) was recovered 85% when stored in PNIPAM after 1 month at 4ºC or in other words relatively to the untreated tubes we have obtained 135% better recovery. The recovery results suggested that a surface should have small negative zeta potential, extremely basic character and smooth surface, probably due to its small size

- Storage of CSF in PNIPAM treated tubes showed 100% recovery for Tau PHF and Aβ-42 peptide, whereas when stored in MIX II it showed as well 95-100% recovery for PrPc indicating an importance of nanostructuration for recovery from multicomponent protein solutions
- For proteins with low pI, surfaces with higher basic character are desired with low negative zeta potential, while for proteins with high pI the situation is contrary
- An extremely precise coordination of surface properties is needed for high recovery of different neurodegenerative agents
- Treated tubes are very stable for a long time

5 General conclusions

In the presented work we were dealing with the development of new biocompatible surfaces that would be able to prevent the adhesion of specific neurodegenerative agents. These proteins were either in recombinant form as single component solutions in PBS or in the native and infectious forms found in complex multi-component solutions such as cerebrospinal fluid (CSF).

In the first part of this work we have shown that the interaction of reactive species found in CF_4 plasma lead to the incorporation of fluorine species on the polypropylene substrates, making them highly hydrophobic. By optimising the treatment parameters we have found, that if we want to obtain an optimal balance between surface functionalization and surface etching, the relative amount of atomic fluorine species in the discharge towards the molecular CF_x species should be around 50%. Presence of impurities on the surface (O, Al) was more evident at higher powers, longer treatment times and lower gas flow. Their existence was ascribed to the post-oxidation reactions, reactions of impurities (mainly water vapour) in the plasma phase with the substrate and due to the weak sputtering of the electrode. AFM imaging allowed us to see that the surface roughness on our substrates is not important enough to ascent from highly hydrophobic to super hydrophobic surfaces.

In the second part thin layers of polymer and polymer with small molecules were grafted on the surfaces pre-activated by helium plasma. At this step we have managed to obtain superhydrophilic properties of polypropylene supports, which opened an interesting field that should be further researched. The activation by helium plasma has shown to be a variable tool for the incorporation of free radicals on the surface that lead to covalent grafting of layers. The surface energy did not have much impact on the surface characteristics of grafted samples with plasma pre-treatment time, even though the surface energy before the grafting varied between the samples. In contrary, the XPS analyses and AFM imaging showed that there was a great difference between the substrates. This was explained by the fact that the grafting at all conditions introduced polar functional groups on the surface, but their chemical nature was different. On the other hand, if samples are not activated by plasma, the yield of grafting is very low. The introduction of small concentration of surfactants to polymer solution rapidly and markedly changed (decreased) the basic character of pure polymer. This was observed by contact angle analyses. The basic character of the samples falls in the following order: PNIPAM> PNIPAM-Tween 20®> PNIPAM-CTAB, coherently with their molecular characteristics. The formation of nano-structured features on the grafted surfaces was strongly dependent on the plasma characteristics and as well the molar ratios used between the surfactant and the polymer. Therefore this new method presents a relatively simple method to control the surface characteristics (functional groups, acid-base character and topography) for various applications, however fine tuning of conditions needs to be performed. These surfaces displayed high stability under atmosphere conditions in the period of at least two months.

In the third part the results between the proteins and modified surfaces were presented. It was shown that there was not just one factor responsible for protein interaction with the surfaces, but a mutual effect of different surface properties, storage conditions and the properties of the protein itself. We have managed to attain no or negligible adsorption of all examined protein on the Eppendorf tubes when storage was performed at 4ºC for 24 h.

Despite the important amount of attempts, the unique surface treatment for all proteins could not be attained due to considerable variations of the protein properties.

Nevertheless, few correlations between surface and protein properties were found:

1. $PrPrec_{hum}$ that possesses high pI (9.8) showed negligible or no adsorption onto the surfaces with high negative zeta potential, low basic character and O/C ratio between 0.20 and 0.25
2. Proteins with lower pI (Tau_{rec} and α-syn) on the other hand prefer lower zeta potential and higher basic character. Moreover the small α-syn was adsorbed less on the smooth surfaces with no particular surface morphologies.
3. Storage of CSF in MIX II treated Eppendorf tubes showed 100% recovery for all titrated biomarkers. These results indicated an importance of nano-structuration of the surface for the recovery of proteins from complex multicomponent solutions.
4. The surface roughness and nano-topography had an important role for all the stored proteins. It seems that highly ordered structures lead to lower adsorption of most of the proteins; however this observation is not straightforward, mostly due to the fact that other surface properties are altered at the same time. Therefore further work on this issue should be undertaken.

For the future experiments it would be also of a great interest to:

- monitor the kinetics of the neuro-protein adsorption to differently modified substrates by changing the solution properties
- monitor the behaviour of these proteins in the solution under different experimental conditions
- study long term storage at different temperatures
- construct di or tri-block copolymers with desired properties
- use the found parameters to prevent the attachment of cells and growth of biofilms
- adjust the parameters for improved protein and/or cell adhesion for various biomedical applications

6 Acknowledgements

The work presented in this manuscript was realized in the Plasma Laboratory (F4) Jožef Stefan institute and in the Laboratory Polymères, Colloïdes et Interfaces (PCI, UMR CNRS 6120) Université du Maine, France.

First and foremost, I would like to thank my advisors, Prof. Dr. Miran Mozetič and Dr. Fabienne Poncin-Epaillard for the guidance throughout my PhD, their time, ideas, stimulation and at the same time for leaving me great freedom and independence in the work orientation. I would also like to thank my co-advisor Ass. Prof. Dominique Debarnot for her assistance and advices. Furthermore, I extend my thanks to Dr. Karin Anselme, Ass. Prof. Uroš Cvelbar and Ass. Prof. Janez Kovač for agreeing to work as reporters of this document.

Such an interdisciplinary work could have never been conducted without the experts from other fields. Members of several groups have contributed immensely to my personal and professional time during the study. I wish to express my gratitude to Dr. Gilbert Legeay and Arnaund Coudreuse, Centre de Transfert de Technologie du Mans (CTTM) for financial, scientific and moral support. I would like to acknowledge the Centre de Recherche sur les Protéines Prion (CRPP) group, Dr. Benaissa El Moualij, Dr. Willy Zorzi, Dr. Ingrid Dupiereux, Dr. Olivier Thellin and Jean-Francois Thonnart, who always warmly welcomed me into their laboratory and helped me to learn, enjoy and profit from the whole experience with ELISA tests and prion proteins. Aforesaid goes as well to the team of Hospices Civils de Lyon (CHUL), Dr. Armand Perret-Liaudet, Dr. Isabelle Quadrio and Dr. Jérémie Seguin. The group gave me an insight into Tau protein and has been a source of open spirit and original ideas for various experiments. I would also like to thank the other teams that participated in the project who were a great pleasure to work with during the three years: Roboscreen from Leipzig, Charite from Berlin, L-UNI form Lancaster, MUW from Vienna and EUDICA from Annecy. I am also very grateful to Ass. Prof. Janez Kovač and Ass. Prof. Alenka Vesel from Jožef Stefan Institute for extensive XPS and AFM analyses, discussions and guidance. Regarding the optical emission analyses, I would like to deeply thank Dr. Slobodan Milošević, Institut za Fiziku Zagreb, for all the advice, discussions, help with result interpretation, his big generosity and hospitality.

I also express my sincere appreciation to all members of the laboratories in Slovenia and France. I will begin with Kristina Eleršič to whom I thank for always beeing ready to help, her good moral, brainstorming and fruitful conversations. I would also like to thank Dr. Aleksander Drenik, Dr. Ita Junkar, Tatjana Filipič, Ruža Bolte and Janez Trtnik for helping me in one way or another during my research. I will continue with my friends from the PCI ENSIM that allowed me to work in a good mood during the past three years: Dr. Caroline Mille with whom it was a great pleasure to work on the same project, Dr. Tiphaine Merian, Ass. Prof. Kateryna Fatyeyeva, Dr. Aissam Airoudj, Claudine Chahine, Naima Hachache, Houria and the others. I would also like to thank to our physicists: Dr. Charfeddine Mechri, Dr. Thomas Lavergne, Adil Ayouch, Jean-Baptiste Legland,

Mansour, Gwen, Nikolay, Ahmed, Mourad and others for numerous discussions from the plasma and quantum mechanics to every day life and for all the help during (lots of) informatics problems. Furthermore my gratitude goes to Dr. Aleksander Vrhovšek for his valuable advices and moral support. I can not forget my everyday friends, without whom I could not complete such work.

Last, but definitely not least, gratitude goes to my family that have always supported and believed in me.

7 References

[1] Hardy, J.; Allsop, D. Amyloid deposition as the central event in the aetiology of Alzheimer's disease. *Trends Pharmacol. Sci.* **12 (10),** 383 (1991).

[2] Shineman, D. W.; Fillit, H. M. Meeting the unique challenges of drug discovery for neurodegenerative diseases. *BMC Neurol.* **9(1),** I1 (2009).

[3] Spack, E. G.; Steinmetz, K. L. The basics of preclinical drug development for neurodegenerative disease indications: A review. *BMC Neurol.* **12(9),** S2 (2009).

[4] Shi, M.; Caudle, W. M.; Zhang, J. Biomarker discovery in neurodegenerative diseases: A proteomic approach: A review. *Neurobiology of Disease.* **35(2),** 157 (2009).

[5] http://www.sciencedaily.com/videos/2005/1210-detecting_alzheimers_early.htm **(**Accessed February 2011).

[6] Kepe, V.; Huang, S. C.; Small, G. W.; Satyamurthy, N.; Barrio, J. R. Visualizing pathology deposits in the living brain of patients with Alzheimer's disease. *Methods Enzymol*. **412,** 144 (2006).

[7] Gofflot, S.; El Moualij, B.; Zorzi, D.; Melen, L.; Roels, S.; Quatpers, D.; Grassi, J.; Vanopdenbosch, E.; Heinen, E.; Zorzi, W. Immuno-Quantitative Polymerase Chain Reaction: a new highly sensitive technology for detection and quantitation of prion protein. *J. Immunoassay*. **25(3)**, 241 (2004).

[8] Philipp, W.J.; Groth, D.; Giles, K.; Vodrazka, P.; Schimmel, H.; Feyssaguet, M.; Toomik, R.; Schacher, P.; Osman, A.A.; Lachmann, I.; Wear, A.; Arsac, J. N.; Prusiner, S. B. Transgenic mouse brains for the evaluation and quality control of BSE tests. *Biol Chem.* **338(3),** 349 (2007).

[9] Duda, J. E.; Giasson, B. I.; Mabon, M. E.; Lee, V. M. Y.; Trojanowski, J. Q. Novel antibodies to synuclein show abundant striatal pathology in Lewy body diseases. Annals of Neurology. 52(2), 205 (2002).

[10] Vladkova, T. Surface engineering for non-toxic biofouling control: A review. Journal of the University of Chemical Technology and Metallurgy. 42(3), 239 (2007).

[11] Perret-Liaudet, A.; Pelpel, M.; Lehmann, S.; Schraen, S.; Vanderstichele, H.; Quadrio, I.; Tholance, Y.; Zorzi, W.; Coudreuse, A. Sampling Tube, a Critical Factor in Alzheimer’s Disease Biomarker Standardization. *Alzheimer’s and Dementia*. **6(4),** 44 (2010).

[12] Dee, K. C.; Puleo, D. A.; Bizios, R. *An introduction to Tissue-Biomaterial Interactions* (John Wiley & Sons, Hoboken, New Jersy, 2002).

[13] http://www.zeusinc.com/UserFiles/zeusinc/Documents/Zeus_Biocompatibility.pdf (accessed February 2011)

[14] Ramakrishna, S., Mayer, J.; Wintermantel, E.; Leong, K.W. Biomedical applications of polymer-composite materials: A review. *Compos. Sci. Technol*. **61(9),** 1189 (2001).

[15] Leong, K.F.; Cheah, C.M.; Chua, C.K. Solid freeform fabrication of three-dimensional scaffolds for engineering replacement tissues and organs. *Bioaterials* **24 (13),** 2363 (2003).

[16] Wang, Z. G.; Wan, L. S.; Xu, Z. K. Surface engineerings of polyacrylonitrile-based asymmetric membranes towards biomedical applications: An overview. *J. Membr. Sci.* **304 (1-2),** 8, (2007).

[17] Andrade, J. D.; Hlady, V. Protein adsorption and materials biocompatibility. A tutorial review and suggested hypothesis. *Progress in Surface Science* **79**, 1 (1986).

[18] Poncin-Epaillard, F.; Legeay G. Surafce engineering of biomaterials with plasma techniques: A rewiev. *J. Biomater. Sci. Polymer Edition.* **14 (10),** 1005 (2003).

[19] Donlan, R. M. Biofilms: Microbial Life on Surfaces. *Emerg Infect Dis.* **8 (9),** 881 (2002).

[20] Vladkova, T. G. Surafce engineered polymeric biomaterials with improved biocontact properties: A review. *International Journal of polymer science.* ID 296094 (2010).

[21] Sin, D. C.; Kei H. L.; Miao X. Surface coatings for ventricular assist devices. *Expert Review of Medical Devices.* **6 (1),** 51 (2009).

[22] Hlady, V.; VanWagenen R. A.; Andrade J. D. *Surface and Interfacial Aspects of Biomedical Polymers* (Plenum Press, New York, 1985).

[23] Ykada, Y.; Suzuki, M.; Tamada Y. *Polymers as Biomaterials: Polymer surfaces possessing minimal interaction with blood components* (Plenum Press, New York, 1984).

[24] Gölander, C.G.; Jönsson, C.; Vladkova, T.; Stenius, P.; Eriksson, J.C. Preparation and protein adsorption properties of photopolymerized hydrophilic films containing N-vinylpyrrolidone (NVP), acrylic acid (AA) or ethyleneoxide (EO) units as studied by ESCA. *Colloids & Surfaces.* **21**, 149 (1986).

[25] Ma, H.; Hyun, J.; Stiller, P.; Chilkoti, A. "Non-Fouling" Oligo(ethylene glycol)-Functionalized Polymer Brushes Synthesized by Surface-Initiated Atom Transfer Radical Polymerization. Advanced materials. **16 (4),** 283 (2004).

[26] Beyer, D.; Knoll, W.; Ringsdorf, H.; Wang, J. H.; Timmons, R. B.; Sluka, P. Reduced protein adsorption on plastics via direct plasma deposition of triethylene glycol monoallyl ether. *J. Biomed.Mater. Res.* **36 (2),** 181 (1997).

[27] Coleman D.L .; Gregonis, D. E.; Andrade, J. D. Blood-materials interactions: the minimum interfacial free energy and the optimum polar/apolar ratio hypotheses. *Journal of Biomedical Materials Research.* **16 (4),** 381 (1982).

[28] Zhang, W.; Ji,J. H.; Zhang,Y.H.; Yan, Q.; Kurmaev, E. Z.; Moewes, A.; Zhao, J.; Chu, P.K. Effects of NH3, O-2, and N-2 co- implantation on Cu out- diffusion and antimicrobial properties of copper plasma- implanted polyethylene. *Appl.Surf.Sci.* **253 (22),** 8981 (2007).

[29] Cunliffe, D.; Smart, A.; Alexander, C.; Vulfson E. N. Bacterial Adhesion at Synthetic Surfaces. *Applied and Environmental Microbiology.* **65 (11),** 4995 (1999).

[30] Lydon, M. J.; Minett, T. W.; Tighe, B. J. Cellular interactions with synthetic polymer surfaces in culture. *Biomaterials.* **6 (6),** 396 (1985).

[31] Shin, H.; Jo, S.; Mikos, A. G. Biomimetic materials for tissue engineering. *Biomaterials*. **24 (24),** 4353 (2003).

[32] Chu, P. K. Enhancement of surface properties of biomaterials using plasma-based technologies. *Surface & Coatings Technology*. **201**, 8076 (2007).

[33] Nagaoka, S.; Akashi, R. Low friction hydrophilic surface for medical devices. *Journal of bioactive and compatible polymers*. **5 (2),** 212 (1990).

[34] Furuzono, T.; Sonoda, K.; Tanaka, J. A hydroxyapatite coating covalently linked onto a silicone implant material. *Journal of Biomedical Materials Research,* **56 (1),** 9 (2001).

[35] Mathieu, H. J.; Gao, X.; Chevolot, Y.; Balazs, D. J. Surface functionalization for biomedical applications. *Surface chemistry in biomedical and environmental science.* **2,** 145 (2006).

[36] Uyama, Y.; Kato, K.; Ikada, Y. Surface modification of polymer by grafting. Advances in polymer science. 137, 1 (1998).

[37] De las Heras Alarcón, C.; Pennadam, S. ; Alexander, C. Stimuli responsive polymers for biomedical applications: Crtitical review. *Chem. Soc. Rev*. **34,** 276 (2005).

[38] Bawa, P.; Pillay1, V.; Choonara, E. H.; du Toit, L. C. Stimuli-responsive polymers and their applications in drug delivery. *Biomedical materials*. **4 (2),** 022001 (2009).

[39] Schmaljohann, D. Thermo-and pH-responsive polymers in drug delivery. Advanced Drug Delivery Reviews. **58 (15),** 1655 (2006).

[40] D'agostino, R.; Favia, P.; Oehr, C.; Wertheimer, M. R. Plasma Processes and Polymers. *Plasma Processes and Polymers.* **1 (1),** 11 (2004).

[41] Desmet, T.; Morent, R.; De Geyter, N.; Leys, C.; Schacht, E.; Dubruel, P. Nonthermal Plasma Technology as a Versatile Strategy for Polymeric Biomaterials Surface Modification: A Review. *Biomacromolecules.* **10 (9),** 2351 (2009).

[42] Siow, K. S.; Britcher, L.; Kumar, S.; Griesser, H. J. Reactive Surfaces for Biomolecule Immobilization and Cell Colonization: A Review. *Plasma processes and*

polymers. **3**, 392 (2006).

[43] Tate, R. S.; Fryer, D. S.: Pasqualini, S.; Montague, M. F.; de Pablo, J. J.; Nealey P. F. Extraordinary elevation of the glass transition temperature of thin polymer films grafted to silicon oxide substrates. *Journal of Chemical Physics.* **115 (21),** 9982 (2001).

[44] Wertheimer, M. R.; Martinu, L.; Liston, E. M. *Plasma sources for polymer surface treatment* (Cornell University Press, London, 1982).

[45] Heberman, M. A.; Lichtenberg, A.J. *Principles of plasma discharges and materials processing.* (Wiley Interscience, New Yersey, 2005).

[46] Kurepa, M.; Čobić, B. *Fizika i tehnika vakuuma.* (Beograd, 1988).

[47] Mozetič, M. Značilnosti nizkotlačne šibkoionizirane plazme. *Vakuumist.* **17 (7),** 17 (1997).

[48] Vesel, A.; Junkar, I.; Cvelbar, U.; Kovac, J.; Mozetic, M. Surface modification of polyester by oxygen- and nitrogen-plasma treatment. *Surface and interface analyses.* **40 (11),** 1444 (2008).

[49] Hippler, R.; Pfau, S. S. M.; Schoenbach, K. H. *Low temperature Plasma Physics: fundamental aspects and applications.* (Wiley VCH, Berlin, 2001).

[50] Vesel, A.; Mozetic, M.; Zalar, A. XPS characterization of PTFE after treatment with RF oxygen and nitrogen plasma. *Surface and interface analyses.* **40,** 661 (2008).

[51] Auciello, O. *Ion bombardment modification of surfaces.* (Elsevier, Amsterdam, 1984).

[52] Morosoff, N.; Crist, B.; Bumgarner, M.; Hsu, T.; Yasuda H.

[53] Moss, S. J. Polymer degradation in reactive-gas plasmas. *Polymer Degradation and Stability*. **17 (3),** 205 (1987).

[54] Behnisch, J.; Friedrich, J.; Zimmermann, H. Topokinetics of the polyene formation in PVC films during treatment with non-oxidative plasma. *Acta Polymerica.* **42 (1),** 51 (1991).

[55] Ranby B.; Rabek, J.F. *Photodegradation, Photooxidation and Photostabilization of polymers, principles and applications.* (John Wiley, New York, 1975).

[56] Chatelier, R.C.; Xie, X.; Gengenbach., T. R.; Griesser, H. J. Quantitative Analysis of Polymer Surface Restructuring. *Langmuir*. **11 (7),** 2576 (1995).

[57] Morent, R.; De Geyter1, N.; Desmet, T.; Dubruel, P.; Leys, C. Plasma Surface Modification of Biodegradable Polymers: A Review. *Plasma Processes and Polymers.* (Article online February 2011 in advance of print).

[58] Svirachev, D. M.; Tabailov, N.A. Plasma treatment of polymer surfaces in different Gasses. *Bulg. J. Phys.* **32,** 22 (2005).

[59] Le Roux, D.J.; Paul, D.R. Preparation of composite membranes by a spin coating Process. *Journal of Membrane Science*. **74 (3, 4),** 233 (1992).

[60] Luscombe, C. K.; Li, H. W. ; Huck, W. T. S. ; Holmes, A. B. Fluorinated Silane Self-Assembled Monolayers as Resists for Patterning Indium Tin Oxide. *Langmuir*. **19 (13),** 5273 (2003).

[61] Fresnais, J.; Benyahia, L.; Chapel, J.P.; Poncin-Epaillard, P. Polyethylene ultrahydrophobic surface: synthesis and original properties. *Eur. Phys. J. Appl. Phys.* **26,** 209 (2004)

[62] Liu, T.; Dong, L.; Liu, T.; Yina, Y. Investigations on reducing microbiologically-influenced corrosion of aluminum by using super-hydrophobic surfaces. *Electrochimica Acta.* **55 (18),** 5281 (2010).

[63] Xiu, Y.; Zhang, S.; Yelundur, V. ; Rohatgi, A. ; Hess, D. W. ; Wong, C. P. Superhydrophobic and Low Light Reflectivity Silicon Surfaces Fabricated by Hierarchical Etching. *Langmuir*. **24 (18),** 10421 (2008).

[64] Shiu, J.Y.; Kuo, C. W.; Chen, P.; Mou, C. Y. Fabrication of Tunable Superhydrophobic Surfaces by Nanosphere Lithography. *Chem. Mater.* **16 (4),** 561 (2004).

[65] Poncin- Epaillard, F., Wang, W.; Ausserre, D.; Scharzenbach, W.; Derouard, D.; Sadeghi, N. Surface modification of hexatriacontane by CF_4 plasmas studied by optical emission and threshold ionization mass spectrometries. *Eur. Phys. J. AP*. **4,** 181 (1998).

[66] Airoudj, A.; Debarnot, D.; Beche, B.; Boulard, B.; Poncin- Epaillard, F. Improvement of the Optical Transmission of Polymer Planar Waveguides by Plasma Treatment. *Plasma processes and polymers*. **5 (3),** 275 (2008).

[67] Marais, S.; Metayer, M.; Labbe, M.; Valleto, J. M.; Alexandre, S. ; Saiter, J. M.; Poncin- Epaillard. F. Surface modification by low-pressure glow discharge plasma of an unsaturated polyester resin: Effect on water diffusivity and permeability. *Surface and Coatings Technology*. **122 (2, 3),** 247 (1999).

[68] Fresnais, J.; Chapel, J. P.; Benyahia, L.; Poncin- Epaillard, F. Plasma-Treated Superhydrophobic Polyethylene Surfaces: Fabrication, Wetting and Dewetting *Properties. Journal of adhesion science and technology.* **23 (3),** 131 (2009).

[69] Olde Riekerink, M. B.; Terlingen, J. G. A.; Engbers, G. H. M., Feijen, J. Selective Etching of Semicrystalline Polymers: CF_4 Gas Plasma Treatment of Poly(ethylene) *Langmuir.* **15 (14),** 4847 (1999).

[70] Coburn, J. W.; Winters, H. F. Plasma-Assisted Etching in Microfabrication. Annual *Review of Materials Science.* **13,** 91 (1983).

[71] d'Agostino, R.; Bruno, G.; Capezzuto, P.; Cramarossa, F. Mechanism of etching, polymerization and deposition in R.F. (radio frequency) discharges. *Pure Appl. Chem.* ***57*** **(9),** 1287 (1985).

[72] Vesel, A. Modification of polystyrene with a highly reactive cold oxygen plasma.

Surface and Coatings Technology. **205 (2),** 490 (2010).

[73] Drelich, J.; Chibowski, E. Superhydrophilic and Superwetting Surfaces: Definition and Mechanisms of Control. *Langmuir*. **26 (24),** 18621 (2010).

[74] Hofmann, S.; Csanyi, G.; Ferrari, A. C.; Payne, M. C.; Robertson, J. Surface Diffusion: The Low Activation Energy Path for Nanotube Growth. *Phys. Rev. Lett.* **95,** 036101 (2005).

[75] Garbassi, F.; Occhiello, E.; Polato F.; Brown, A. Surface effect of flame treatments on polypropylene. *Journal of material science.* **22 (4),** 1450 (1987).

[76] Hiroyuki, N.; Akira, J. Surface modification and metallization of fluorocarbon polymers by excimer laser processing. *Applied Physics Letters.* 63(25), 3527 (1993).

[77] Cvelbar, U.; Markoli, B.; Poberaj, C.; Zalar, A, Kosec, L. ; Spaić, S. Formation of functional groups on graphite during oxygen plasma treatment. *Applied surface science*. **253 (4),** 1861 (2006).

[78] Médard, N.; Soutif, N. C. J.; Poncin-Epaillard, F. Characterization of CO_2 plasma-treated polyethylene surface bearing carboxylic groups. *Surface and Coatings Technology*. **160 (2, 3),** 197 (2002).

[79] Short, R. D.; Steele, D. A. Testing the Hypothesis: Comments on Plasma Polymerisation of Acrylic Acid Revisited. *Plasma Processes and Polymers*. **7 (5),** 366 (2010).

[80] Poncin-Epaillard, F., Chevet, B.; Brosse, J. C. Modification of isotactic polypropylene by a cold plasma or an electron beam and grafting of the acrylic acid onto these activated polymers. *Journal of Applied Polymer Science*. **53 (10),** 1291 (1994).

[81] Debarnot, D.; Merian, T.; Poncin- Epaillard, F. Film Chemistry Control and Growth Kinetics of Pulsed Plasma-Polymerized Aniline. *Plasma chemistry and plasma Processing.* **31 (1),** 217 (2010)

[82] Tajima, S.; Komvopoulos, K. Surface Modification of Low-Density Polyethylene by Inductively Coupled Argon Plasma. *J. Phys. Chem. B.* **109 (37),** 17623 (2005).

[83] Hoffman, A. S. Surface modification of polymers: physical, chemical, mechanical and biological methods. *Macromol Symp.* **101,** 443 (1996).

[84] Zhao, B.; Brittain, W.J. Polymer brushes: surface-immobilized macromolecules. *Prog. Polym. Sci.* **25,** 667 (2000).

[85] Edmondson, S.; Osborne, V. L.; Huck, W. T. S. Polymer brushes via surface-initiated polymerizations. *Chemical Society reviews.* **33 (1),** 14 (2004).

[86] Zhou, F.; Huck, W. T. S. Surface grafted polymer brushes as ideal building blocks for “smart” surfaces. *Phys.Chem. Chem. Phys.* **8,** 3815 (2006).

[87] Voronov, A.; Shafranska, O. Dependence of thin polystyrene films stability on the thickness of grafted polystyrene brushes. *Polymer*. **44 (1),** 277 (2003).

[88] Advincula, R. Polymer brushes by anionic and cationic surface-initiated polymerization (SIP). *Advances in polymer science.* **197,** 107 (2006).

[89] Zhao, B.; Brittain, W. J.; Cheng, S. Z. D. AFM Study of Tethered Polystyrene-b-poly(methyl methacrylate) and Polystyrene-b-poly(methyl acrylate) Brushes on Flat Silicate Substrates. *Macromolecules.* **33 (23),** 8821 (2000).

[90] Minko, S. Grafting on Solid Surfaces: "Grafting to" and "Grafting from" Methods. *Polymer surfaces and interfaces*. DOI: 10.1007/978-3-540-73865-7_11, 215 (2008).

[91] Luzinov, I.; Minko, S.; Tsukruk, V. Adaptive and responsive surfaces through controlled reorganization of interfacial polymer layers. *Progress in Polymer Science*. **29 (7),** 635 (2004).

[92] Lupitskyy, R.; Roiter, J.; Tsitsilianis, C.; Minko, S. From Smart Polymer Molecules to Responsive Nanostructured Surfaces. *Langmuir.* **21 (19),** 8591 (2005).

[93] Liu, X.; Ye, Q.; Yu, B.; Liang, Y.; Liu, W. ; Zhou, F. Switching Water Droplet Adhesion Using Responsive Polymer Brushes. *Langmuir*. **26 (14),** 12377 (2010).

[94] Ayres, N.; Boyes, S. G.; Brittain, W. J. Stimuli-Responsive Polyelectrolyte Polymer Brushes Prepared via Atom-Transfer Radical Polymerization. *Langmuir.* **23 (1),** 182 (2007).

[95] Sidorenko, A.; Minko, S.; Schenk-Meuser, K.; Duschner, H.; Stamm, M. Switching of polymer brushes. *Langmuir.* **15,** 8349 (1999).

[96] Wu, D.; Yang, Y.; Cheng, X.;Liu, L.; Tian, J.; Zhao, H. Mixed Molecular Brushes with PLLA and PS Side Chains Prepared by AGET ATRP and Ring-Opening Polymerization. *Macromolecules.* **39 (22),** 7513 (2006).

[97] Motornov, M.; Minko, S.; Eichhorn, K. J. Nitschke, M.; Simon, F.; Stamm, M. Reversible tuning of wetting behavior of polymer surface with responsive polymer Brushes. *Langmuir.* **19,** 8077 (2003).

[98] Julthongpiput, D.; Lin, Y. S.; Teng, J., Zubarev, e. R.; Tsukruk, V. V. Y-Shaped Polymer Brushes: Nanoscale Switchable Surfaces. *Langmuir.* **19,** 7832 (2003). [99] Holmberg, K.; Jonsson, B.; Kronberg, B.; Lindman, B. *Surfactants and Polymers in Aqueous Solution.* (Wiley, Chichester, England, 2003)

[100] Shim, M.; Kam, N. W. S.; Chen, J.R.; Li, Y.; Dai, H. Functionalization of Carbon Nanotubes for Biocompatibility and Biomolecular Recognition. *Nano Letters.* **2 (4),** 285 (2002).

[101] Liu, H.; Xiao, H. Adsorption of poly(ethylene oxide) with different molecular weights on the surface of silica nanoparticles and the suspension stability. *Materials Letters.* **62,** 870 (2008).

[102] Sheu, M. S.; Hoffman, A. S.; Ratner, B. D.; Feijen, J.; Harris, J.M. Immobilization of polyethylene oxide surfactants for non-fouling biomaterial surfaces using an argon glow discharge treatment. *Journal of Adhesion Science and Technology.* **7 (10).** 1065 (1993).

[103] Tanaka, T.; Sato, E.; Hirokawa,Y.; Shunsuke Hirotsu,S.; Peetermans, J. Critical Kinetics of Volume Phase Transition of Gels. *Phys. Rev. Lett.* **55,** 2455 (1985)

[104] PNIPAM. http://fr.wikipedia.org/wiki/PNIPAM (Accessed February 2011)

[105] Okada, Y.; Tanaka, F. Cooperative Hydration, Chain Collapse, and Flat LCST Behavior in Aqueous Poly(N-isopropylacrylamide) Solutions. *Macromolecules.* **38 (10),** 4465 (2005).

[106] Wu, C.; Zhou, S. First Observation of the Molten Globule State of a Single Homopolymer Chain. *Phys. Rev. Lett.* **77**, 3053 (1996).

[107] Wu, C.; Zhou, S. Thermodynamically Stable Globule State of a Single Poly(N-isopropylacrylamide) Chain in Water. *Macromolecules.* **28 (15),** 5388 (1995).

[108] Halperin, A. Compression induced phase transitions in PEO brushes: the n-cluster Model. *The European physical journal B- Condensed matter and complex systems.* **3 (3),** 359 (1998).

[109] Plunkett, K. N.; Zhu, X.; Moore, J. S.; Leckband, D. E. PNIPAM Chain Collapse Depends on the Molecular Weight and Grafting Density. *Langmuir.* **22 (9),** 4259 (2006).

[110] Mizutani, A.; Kikuchi, A.; Yamato, M.; Kanazawa, H.; Okano, T. Preparation of thermoresponsive polymer brush surfaces and their interaction with cells. *Biomaterials.* **29 (13),** 2073 (2008)

[111] Ramirez- Fuentes, Y.S.; Bucio, E.; Burillo, G. Radiation-induced grafting of N - isopropylacrylamide and acrylic acid onto polypropylene films by two step Method. *Nuclear instruments & methods in physics research. Section B, Beam Interactions with materials and atoms.* **265 (1),** 183 (2007).

[112] Turana, E.; Demirci, W.; Caykara, T. Synthesis of thermoresponsive poly (N-isopropylacrylamide) brush on silicon wafer surface via atom transfer radical Polymerization. Thin Solid Films. **518 (21),** 5950 (2010).

[113] Wang, X.; McCord, M.G. Grafting of poly(N-isopropylacrylamide) onto nylon and polystyrene surfaces by atmospheric plasma treatment followed with free radical graft copolymerization. *Journal of Applied Polymer Science*. **104 (6),** 3614 (2007).

[114] Suzer, S.; Argun, A.; Vatansever, O.; Aral, O. XPS and water contact angle measurements on aged and corona-treated PP. *Journal of applied polymer science.* **74 (7),** 1846 (1999).

[115] Cheng, X.; Canavan, H. E.; Stein, M. J.; Hul, J. R.; Kweskin, S. J.; Wagner, M. S.; Somorjai, G. A.; Castner, D, G.; Ratner, B. D. Surface Chemical and Mechanical Properties of Plasma-Polymerized N-Isopropylacrylamide. *Langmuir*. **21 (17),** 783 (2005).

[116] Heinz, P.; Bretagnol, F.; Mannelli, I.; Sirghi, L. ; Valsesia, A. ; Ceccone, G. ; Gilliland, D. ; Landfester, K.; Rauscher, H.; Rossi, F. Poly(N-isopropylacrylamide) Grafted on Plasma-Activated Poly(ethylene oxide): Thermal Response and Interaction With Proteins. *Langmuir*. **24 (12),** 6166 (2008).

[117] Pan, Y. V.; Wesley, R.A.; Luginbuhl, R.; Denton, D. D.; Ratner, B. D. Plasma Polymerized N-Isopropylacrylamide: Synthesis and Characterization of a Smart Thermally Responsive Coating. *Biomacromolecules*. **2 (1),** 32 (2001).

[118] He, C.; Zhao, C.; Guo, X.; Guo, Z.; Chen, X.; Zhuang, X.; Liu, S.; Jing, X. Novel temperature- and pH-responsive graft copolymers composed of poly (L-glutamic acid) and poly(N-isopropylacrylamide). *Journal of Polymer Sience Part A: Polymer Chemistry.* **46 (12),** 4140 (2008).

[119] Rapoport, N. Physical stimuli-responsive polymeric micelles for anti-cancer drug delivery. *Progress in Polymer Science.* **32 (8, 9),** 962 (2007).

[120] Auditore-Hargreaves, K.; Houghton, R.L.; Monji, L.N.; Priest, J. H.; Hoffman, A. S.; Nowinski, R. C. Phase-separation immunoassays. *Clinical Chemistry.* **33 (9),** 1509 (1987).

[121] Cole, M. A.; Voelcker, N. H.; Thissen, H.; Griesse, H. J. Stimuli-responsive interfaces and systems for the control of protein–surface and cell–surface interactions: A review. *Biomaterials.* **30 (9),** 1827 (2009).

[122] De las Heras Alarcón, C.; Pennadam, S.; Alexander, C. Stimuli responsive polymers for biomedical applications. *Chemical Society Reviews.* **34 (3),** 276 (2005).

[123] Huber, D. L.; Manginell, R. P.; Samara, M. A.; Kim, B. I.; Bunker, B. C. Programmed Adsorption and Release of Proteins in a Microfluidic Device. *Science.* **301,** 352 (2003).

[124] Nakanishi, K.; Sakiyama, T.; Imamura, K. On the adsorption of proteins on solid surfaces, a common but very complicated phenomenon: A review. *Journal of Bioscience and Bioengineering.* **91 (3),** 233 (2001).

[125] Norde, W.; Haynes, C. A. Proteins at Interfaces II: Reversibility and the Mechanism of Protein Adsorption. *ACS Symposium Series.* **(602),** 26 (1995).

[126] Lundström, Models of protein adsorption on solid surfaces. *Progress in colloid and polymer science.* **70,** 76 (1985)

[127] Horbett, T. A. ; Brash, J. L. Proteins at interfaces: Current issues and future prospects. *ACS Symposium Series.* (1987).

[128] Karlsson, M.; Ekeroth, J.; Elwing, H.; Carlsson, U. Reduction of Irreversible Protein Adsorption on Solid Surfaces by Protein Engineering for Increased Stability. *The Journal of Biological Chemistry.* **280,** 25558 (2005).

[129] Yanrong, T.; Calonder, C.; Van Tassel, P. R. Protein adsorption: Kinetics and history dependence. *Journal of colloid and interface science.* **268 (1),** 1 (2003).

[130] Berg, J. M.; Tymoczko, J. L.; Stryer, L. *Biochemistry.* (W. H. Freeman and company, New York, 2002).

[131] Norde, W.; Anusiem, A. C. I. Adsorption, desorption and re-adsorption of proteins on solid surfaces. *Colloids and Surfaces.* **66 (1),** 73 (1992).

[132] Robertson, A. D. Intramolecular interactions at protein surfaces and their impact on protein function: A review. *Trends Biochem Sci.* **27 (10),** 521 (2002).

[133] Voet, D.; Voet, J.G.; Pratt, C. W. *Fundamentals of Biochemistry.* (John Wiley & Sons Inc.: New York, 2002).

[134] Chiti, F.; Dobson, C.M. Protein misfolding, functional amyloid, and human disease. *Annual Review of Biochemistry.* **75,** 333 (2006).

[135] Wertz, C. F.; Santore, M. M. Effect of Surface Hydrophobicity on Adsorption and Relaxation Kinetics of Albumin and Fibrinogen: Single-Species and Competitive Behavior. *Langmuir.* **17 (10),** 3006 (2001).

[136] Iwasaki, Y.; Nakabayashi, N.; Ishihara, K. *Proteins at solid-liquid interfaces. Nonbiofouling Surfaces Generated from Phosphorylcholine-Bearing Polymers.* (Springer-Verlag, Berlin Heidelberg, 2006).

[137] Malemsten, M. Formation of adsorbed protein layers. *J. Coll. Interface Sci*. **207,** 186 (1998).

[138] Malmsten, M. Van Alstine, J. M. Adsorption of poly(ethylene glycol) amphiphiles to form coatings which inhibit protein adsorption. *Journal of Colloid and Interface Science*. **177 (2),** 502 (1996).

[139] Karlsson, L. M. ; Schubert, M. ; Ashkenov, N. ; Arwin, H. Protein adsorption in porous silicon gradients monitored by spatially-resolved spectroscopic ellipsometry. *Thin solid films.* **455-456,** 726 (2004).

[140] Gray, J. J. The interaction of proteins with solid surfaces. *Curr. Opin. Struc. Biol.* **14,** 110 (2004).

[141] Latour, R. A. *Encyclopedia of Biomaterials and Biomedical Engineering: Biomaterials: Protein-Surface Interactions.* (Taylor & Francis, Washington, 2005).

[142] Andrade, J.D.; Hlady, V.; Wei, A.P. Adsorption of complex proteins at interfaces. *Pure & Appl. Chem.* **64 (11),** 1777 (1992).

[143] Hartvig, R. A.; van de Weert, M.; Østergaard, J.; Jorgensen, L.; Jensen, H. Protein Adsorption at Charged Surfaces: The Role of Electrostatic Interactions and Interfacial Charge Regulation. *Langmuir.* Article ASAP (2011).

[144] Haynes, C. A.; Sliwinsky, E.; Norde, W. Structural and electrostatic properties of globular proteins at a polystyrene-water interface. *Journal of colloid and interface Science.* **164 (2),** 394 (1994).

[145] Silva, R. A.; Urz, M. D.; Petri, D. F. ; Dubin, P. L. Protein Adsorption onto Polyelectrolyte Layers: Effects of Protein Hydrophobicity and Charge Anisotropy. *Langmuir.* **26 (17),** 14032 (2010).

[146] Ponche, A.; Bigerelle, M.; Anselme K. Relative influence of surface topography and surface chemistry on cell response to bone implant materials. Part 1: physico-chemical effects. *Proc. Inst. Mech. Eng. H.* **224 (12),** 1471 (2010).

[147] Anselme, K.; Ponche, A.; Bigerelle, M. Relative influence of surface topography and surface chemistry on cell response to bone implant materials. Part 2: biological aspects. *Proc. Inst. Mech. Eng. H.* **224 (12),** 1487 (2010).

[148] Lord, M. S.; Foss, M.; Besenbacher, F. Influence of nanoscale surface topography on protein adsorption and cellular response: A review. *Nano Today.* **5,** 66 (2010).

[149] Roach, P.; Eglin, D.; Rohde, K.; Perry, C. C. Modern biomaterials: bulk properties and implications of surface modifications: A review. *Journal of material science: Materials in medicine.* **18 (7),** 1263 (2007).

[150] Cai, K.; Bossert, J.; Jandt, K. D. Does the nanometer scale topography of titanium influence protein adsorption and cell proliferation? *Colloids and surfaces B: Biointerfaces.* **49 (2),** 136 (2006)

[151] Han, M.; Sethuraman, A.; Kane, R. S.; Belfort, G. Nanometer-Scale Roughness Having Little Effect on the Amount or Structure of Adsorbed Protein. *Langmuir.***19 (23),** 9868 (2003).

[152] Blanco, E. M. ; Horton, M. A.; Mesquida, P. Simultaneous investigation of the influence of topography and charge on protein adsorption using artificial nanopatterns. *Langmuir.* **24 (6),** 2284 (2008).

[153] Galli, C.; Coen, M. C.; Hauert, R. ; Katanaevc, V. L. ; Gröning, P.; Schlapbach, L. Creation of nanostructures to study the topographical dependency of protein Adsorption. *Colloids and Surfaces B: Biointerfaces.* **26 (3),** 255 (2002).

[154] Fournier, R.L. *Solute transport in biological systems. In Basic Transport Phenomena in Biomedical Engineering.* (Taylor & Francis, Philadelphia, 1999).

[155] Vroman, L.; Adams, A.L. Findings with the recording ellipsometer suggesting rapid exchange of specific plasma proteins at liquid/solid interfaces. *Surf. Sci.***16,** 438 (1969).

[156] Lee, W.K.; McGuire, J.; Bothwell, M. K. Competitive adsorption of bacteriophage T4 lysozyme stability variants at hydrophilic glass surfaces. *J. Colloid Interface Sci.* **269,** 251 (2004).

[157] Slack, S.M.; Horbett, T.A. *The Vroman effect: a critical review. In Proteins at Interfaces II. Fundamentals and Applications*. (ACS, Washington, DC, 1995).

[158] Fang, F.; Szleifer, I. Effect of Molecular Structure on the Adsorption of Protein on Surfaces with Grafted Polymers. *Langmuir.* **18 (14),** 5497 (2002).

[159] Halperin, A. Polymer Brushes that Resist Adsorption of Model Proteins: Design Parameters. *Langmuir.* **15 (7),** 2525 (1999).

[160] Hoffman, A. S. Non-Fouling Surface Technologies. *Journal of Biomat. Sci., Polymer Edition.* **10 (10),** 1011 (1999).

[161] Vladkova, T. G. Surface Engineered Polymeric Biomaterials with Improved Biocontact Properties: A review. *International Journal of Polymer Science*. (2010).

[162] Gong, P.; Grainger, D. W. Nonfouling surfaces: a review of principles and

applications for microarray capture assay designs. *Methods Mol Biol.* **381,** 59 (2007).

[163] Van de Vondele, S.; Vörös, J.; Hubbell, J. A. RGD-grafted poly-l-lysine-graft-(polyethylene glycol) copolymers block non-specific protein adsorption while promoting cell adhesion. *Biotechnology and Bioengineering.* **82 (7),** 784 (2003).

[164] Sofia, S. J.; Premnath, V.; Merrill, E. W. Poly(ethylene oxide) Grafted to Silicon Surfaces: Grafting Density and Protein Adsorption. *Macromolecules.* **31 (15),** 5059 (1998).

[165] Satulovsky, J.; Carignano, M. A.; Szleifer, I. Kinetic and thermodynamic control of protein adsorption. *Biophysics.* **97(16),** 9037 (2000).

[166] Ostuni, E.; Chapman, R. G.; Holmlin, R. E.; Takayama, S.; Whitesides, G. M. A Survey of Structure−Property Relationships of Surfaces that Resist the Adsorption of Protein. *Langmuir.* **17(18),** 5606 (2001).

[167] Ivanov, A. E.; Ekeroth, J.; Nilsson, L.; Mattiasson, B.; Bergenståhl, B.; Galaev, I. Y. Variations of wettability and protein adsorption on solid siliceous carriers grafted with poly(N-isopropylacrylamide). *Journal of Colloid and Interface Science.* **296 (2),** 538 (2006).

[168] Teare, D. O. H.; Barwick, D. C.; Schofield, W. C. E.; Garrod, R.P.; Beeby, P. A.; Badyal, J. P. S. Functionalization of Solid Surfaces with Thermoresponsive Protein-Resistant Films. *J. Phys. Chem. B.* **109 (47),** 22407 (2005).

[169] Carter, S.; Rimmer, S.; Rutkaite, R.; Swanson, L.; Fairclough, J. P. A. ; Sturdy, A. ; Webb, M. Highly Branched Poly(N-isopropylacrylamide) for Use in Protein Purification. *Biomacromolecules.* **7 (4),** 1124 (2006).

[170] Horwich, A. L.; Weissman, J. S. Deadly conformations-protein misfolding in prion disease. *Cell.* **89 (4),** 499 (1997).

[171] http://en.wikipedia.org/wiki/Alpha_synuclein. (Accessed February 2011).

[172] http://en.wikipedia.org/wiki/Tauopathy. (Accessed February 2011).

[173] Cvelbar, U.; Pejovnik, S., Mozetic, M.; Zalar, A. Increased surface roughness by oxygen plasma treatment of graphite/polymer composite. *Applied Surface Science.* **210 (3-4),** 255 (2003).

[174] Gottscho, R. A.; Miller., T. A. Optical techniques in plasma diagnostics. Pure & Appl. Chem. **56 (2),** 189 (1984).

[175] Kregar, Z.; Krstulović, N.; Vukelić, N. G.; Milošević, S. Space and time resolved optical emission spectroscopy characterization of inductively coupled RF water vapour plasma. *Journal of Physics D: Applied Physics*. **42 (14),** 5201 (2009).

[176] Lianzhu, Z.; Shuxia, Z.; Xiulan, M. Characterization of Nitrogen Glow Discharge Plasma via Optical Emission Spectrum Simulation. *Plasma Science and Technology*. **10 (4),** 455 (2008).

[177] D'Agostino, R.; Cramarossa, F.; Benedictis, S. Diagnostics and decomposition mechanism in radio-frequency discharges of fluorocarbons utilized for plasma etching or polymerization. *Plasma Chemistry and Plasma Processing.* **2 (3),** 213 (1982).

[178] Suto, M.; Washida, N. Emission spectra of CF_3 radicals. I. UV and visible emission spectraof CF_3 observed in the VUV photolysis and the metastable argon atom reaction of CF_3H. *The Journal of Chemical Physics.* **78 (3),** 1007 (1983).

[179] Huang, S.; Ning, Z. Y.; Xin, Y.; Di, X. L. Langmuir probe measurements in inductively coupled CF_4 plasmas. *Surface and Coatings Technology.* **200 (12, 13),** 3963 (2006).

[180] Murakami, T.; Kuroda, S. I.; Osawa, Z. Dynamics of Polymeric Solid Surfaces Treated with Oxygen Plasma: Effect of Aging Media after Plasma Treatment. *Journal of Colloid and Interface Science.* **202 (1),** 37 (1998).

[181] Hopkins, J.; Boyd, R. D.; Badyal, J. P. S. Plasma Fluorination versus Oxygenation of Polypropylene. *J. Phys. Chem.* **100 (16),** 6755 (1996).

[182] Narushim, K.; Tuchida, N.; Miyazaki, K. Surface characterization of plasma-modified poly(ethylene terephthalate) film surfaces. *Journal of Polymer Science Part B: Polymer Physics.* **42 (20),** 3727 (2004).

[183] Woodward, I.; Schofield, W. C. E.; Roucoules, E. V.; Badyal, J. P. S. Super-hydrophobic Surfaces Produced by Plasma Fluorination of Polybutadiene Films. *Langmuir.* **19 (8),** 3432 (2003).

[184] Kuroki, K.; Spence, D.; Dillon, M. A. Energy loss spectroscopy of CF4 at nonzero scattering angles. *J. Chem. Phys.* **96 (8),** 6318 (1992).

[185] Mozetic, M.; Vesel, A.; Ricard, A.; Babic, D.; Poberaj, I. A diagnostic method for real-time measurements of the density of nitrogen atoms in the postglow of an Ar-N_2 discharge using a catalytic probe. *J. Appl. Phys.* **97 (10),** 3308 (2005).

[186] Kim, K. S.; Lee, K. H.; Cho, K.; Park, C. E. Surface modification of polysulfone ultrafiltration membrane by oxygen plasma treatment. *Journal of Membrane Science*. **199 (1-2),** 135 (2002).

[187] Bhattacharya, S.; Datta, A.; Berg, J.M.; Gangopadhyay, S. Studies on surface wettability of poly(dimethyl) siloxane (PDMS) and glass under oxygen-plasma treatment and correlation with bond strength. *Journal of Microelectromechanical Systems*. **14 (3),** 590 (2005).

[188] Kihlman Øiseth, S.; Krozer, A.; Kasemo, B.; Lausmaa, J. Surface modification of spin-coated high-density polyethylene films by argon and oxygen glow discharge plasma treatments. *Applied Surface Science.* **202 (1-2),** 92 (2002).

[189] Poncin- Epaillard, F.; Brosse, J. C.; Falher, T. Cold Plasma Treatment: Surface or Bulk Modification of Polymer Films? *Macromolecules.* **30 (15),** 4415 (1997).

[190] Junkar, I.; Cvelbar, U.; Vsel, A.; Hauptman, N.; Mozetic, M. The Role of Crystallinity on Polymer Interaction with Oxygen Plasma. *Plasma Processes and*

Polymers. **6(10),** 667 (2009).

[191] http://physics.nist.gov/PhysRefData/ASD/lines_form.html (Accessed February 2011).

[192] Drelich, J.; Chibowski, E. Superhydrophilic and Superwetting Surfaces: Definition and Mechanisms of Control. *Langmuir*. **26 (24),** 18621 (2010).

[192] Favia, P.; Palumbo, F.; Stendardo, M. V.; D'Agostino, R. *Surface modification of polymeric biomaterials.* (Plenum Press, New York, 1996).

[193] Hower, J. C.; Bernards, M. T.; Chen, S.; Tsao, H. K.; Sheng, Y. J.; Jiang, S. Hydration of "Nonfouling" Functional Groups. *J. Phys. Chem. B.* **113 (1),** 197 (2009).

[194] Lameiras, F. S.; de Souza, A. L.; de Melo, V. A. R.; Nunes, E. H. M.; Braga, I. D. Measurement of the Zeta Potential of Planar Surfaces With a Rotating Disk. *Materials Research.* **11 (2),** 217 (2008).

[195] Lameiras, F. S.; de Souza, A. L.; de Melo, V. A. R.; Nunes, E. H. M.; Braga, I. D. Measurement of the Zeta Potential of Planar Surfaces With a Rotating Disk. *Materials Research.* **11(2),** 217 (2008).

[196] Benedek, K.; Dong, S.; Karger, B.L. Kinetics of unfolding of proteins on hydrophobic surfaces in reversed-phase liquid chromatography. *Journal of Chromatography* A. 317, 227 (1984).

[197] Shamim, N.; Hong, L.; Hidajat, K.; Uddin, M. S. Thermosensitive-polymer-coated magnetic nanoparticles: Adsorption and desorption of Bovine Serum Albumin. *Journal of Colloid and Interface Science*. 304(1), 1 (2006).

[198] Meyne, F.; Gloeckner, S. F.; Ciesielczyk, B.; Heinemann, U.; Krasnianski, A.; Meissner, B., Zerr, I. Total prion protein levels in the cerebrospinal fluid are reduced in patients with various neurological disorders. *J Alzheimers Dis*. 17(4), 863 (2009).

[199] Krolak-Salmon, P.; Seguin, J.; Perret-Liaudet, A.; Desestret, V.; Vighetto, A.; Bonnefoy, M. [Near a biological diagnosis of Alzheimer's disease and related disorders].*Rev Med Interne*. 29(10), 785 (2008).

[200] http://www.bjorksten.com/files/protein.pdf (Accessed February 2011).

[201] Josic, D.; Horn, H.; Schulz, P.; Schwinn, H.; Britsch, L. Size-exclusion chromatography of plasma proteins with high molecular masses. *Journal of chromatography*. 796(2), 289 (1998).

Index of Figures

Index of Tables

Appendix- List of publications and communications

Communications:

Vrlinic, T.; Mille, C.; Debarnot, D.; Coudreuse,A.; Legay, G.; Poncin- Epaillard, F. Development of new surfaces able to prevent the adsorption of specific neurodegenerative agents. ABioPlas, November 2010, Orléans, France.

Vrlinic, T.; Debarnot, D.; Legay, G.; Coudreuse,A.; Poncin- Epaillard, F. Creation of anti-biofouling materials through highly reactive plasma treatment and polymer grafting. Matériaux, October 2010, Nantes, France.

Vrlinic, T.; Debarnot, Poncin- Epaillard, F. Highly reactive plasma treatment and its applications; non-fouling surfaces for neurodegenerative agents. JED, June 2010, Nantes, France.

Vrlinic, T.; Mille, C.; Debarnot, D.; Poncin- Epaillard, F.; Mozetic, M.; Coudreuse,A.; Legay, G.; Zorzi, W.; El Moualij, B.; Quadrio, I.; Perret – Liaudet, A. *Creation of non-fouling surfaces for amyloid agents through plasma treatment and polymer grafting.* 3rd international conference on advanced plasma technologies, June 2010, Bohinjsko jezero, Slovenia.

Poncin- Epaillard, F. Mille, C.; Vrlinic, T.; Debarnot, D.; Legay, G.; Coudreuse,A. Plasma chemistry as a tool for designing new ELISA protocols. European Workshop on Biomaterials, Mai (2010), Iasi, Romania.

Vrlinic, T.; Debarnot, D.; Poncin- Epaillard, F.; Coudreuse,A.; Legay, G. Plasma chemistry as a tool for the preparation of anti-biofouling surfaces. GFP congres, November 2009, Le Mans, France.

Vrlinic, T.; Poncin- Epaillard, F.; Mozetic, M. Creation of anti-biofouling surfaces. Congres Bioadh09, November (2009), Le Mans, France.

Vrlinic, T.; Mille, C.; Debarnot, D.; Poncin- Epaillard, F. Plasma dans la Chimie. L'atelier du savoir du CNRS. La chimie dans le nanomonde : conception and function, October 2009, Saint Malo, France.

Poncin- Epaillard, F.; Vrlinic, T.; Mille, C.; Debarnot, D.; Legay, G.; Coudreuse, A. Control of the non-adhesion of specific proteins thanks to the plasma treatment onto polymers strips. 19th International symposium on Plasma chemistry, July 2009, Bochum, Germany.

Krstulovic, N.; Vujosevic, D.; Vratnica, Z.; Milosevic, S.; Cvelbar, U.; Elersic, K.; Junkar, I.; Drenik, A.; Vrlinic, T.; Mozetic, M.; Kovac, J. Optical emission

spectroscopy characterization of oxygen plasma during degradation of bacteria. 16th International Scientific Meeting on Vacuum Science and Technique, June 2009, Bohinj, Slovenia.

Vrlinic, T.; Poncin- Epaillard, F.; Kovac, J.; Mozetic, M. Surface fuctionalization of polypropylene with argon plasma created in capacitive coupled RF discharge. 16th International Scientific Meeting on Vacuum Science and Technique, June 2009, Bohinj, Slovenia.

Poncin- Epaillard, F.; Mille, C.; Vrlinic, T.; Debarnot, D.; Legay, G.; Coudreuse, A. Plasma treatments leading to surface properties regulation. Midem conference, Septembre 2008, Fiesa, Slovenia.

Poncin- Epaillard, F.; Mille, C.; Vrlinic, T.; Debarnot, D.; Legay, G.; Coudreuse, A. Exploration des traitements par plasma froid pour le contrôle de la bioadhésion d'un matériau. 10ème congrès SFP, Mai 2008, Paris, France.

Published articles:

Vrlinic, T.; Debarnot, D.; Legeay G.; Coudreuse A.; Zorzi, W.; El Moualij, B.; Mozetic, M.; Vesel, A.; Kovac, J.; Poncin-Epaillard. Elaboration of nano-structured grafted polymeric surface. *Journal of Colloid & Interface Science.* **362(2),** 300 (2011).

Vrlinic, T.; Mille, C.; Debarnot, D.; Poncin-Epaillard, F. Oxygen atom density in capacitively coupled RF oxygen plasma. *Vacuum.* **83**, 792 (2009).

Vrlinic, T.; Vesel, A.; Celbar, U.; Krajnc, M.; Mozetic, M. Rapid surface functionalization of poly(ethersulphone) foils using a highly reactive oxygen-plasma treatment. *Surf. Interface anal.* **39 (6)**, 476 (2007).

Cvelbar, U.; Mozetic, M.; Junkar, I.; Vesel, A.; Kovac, J.; Drenik, A.; Vrlinic, T.; Hauptman, N.; Klanjsek-Gunde, M.; Markoli, B.; Krstujovic, N.; Milosevic, S.; Gaboriau, F.; Belmonte, T. Oxygen plasma functionalization of poly(p-phenilene sulphide. *Applied surface science*. 253(19), 8669 (2007).

Articles in progress: (Publications under agreement of Neuroscreen consortium)

Vrlinic, T.; Debarnot, D.; Legay, G.; Coudreuse, A.; El Moualij, B.; Zorzi, W.; Perret-Liaudet, A.; Quadrio, I.; Mozetic, M.; Poncin- Epaillard, F. Non-adhesive behavior of new nanostructured PNIPAM surfaces towards specific neurodegenerative proteins.
(Submitted).

Vrlinic, T.; Debarnot, D.; Legay, G.; Coudreuse, A.; El Moualij, B.; Zorzi, W.; Perret-Liaudet, A.; Quadrio, I.; Mozetic, M.; Poncin- Epaillard, F. Are the interactions between neurodegenerative proteins and polymeric surfaces related to the hydrophilic and hydrophobic balance?
(Submitted).

Vrlinic, T.; Debarnot, D.; Legay, G.; Coudreuse, A.; El Moualij, B.; Zorzi, W.; Perret-Liaudet, A.; Quadrio, I.; Mozetic, M.; Poncin- Epaillard, F. Study of the solution conditions on the adhesion of neurodegenerative biomarkers.
(In progress).

Vrlinic, T.; Debarnot, D.; Legay, G.; Coudreuse, A.; El Moualij, B.; Zorzi, W.; Perret-Liaudet, A.; Quadrio, I.; Mozetic, M.; Poncin- Epaillard, F. Influence of surface grafting parameters on the yield of prion protein adhesion.
(In progress).